

Poly(vinyl alcohol) / Polyamide Thin-Film Composite Membranes

by

M. A. Elharati

*Thesis presented in partial fulfillment of the requirements for the degree of
Master of Science in Engineering (Chemical Engineering)*

at

Stellenbosch University



Processing Engineering Department

Faculty of Engineering

Supervisor: **Prof J. H. Knoetze**

Co-supervisor: **Prof R. D. Sanderson**

December 2009

DECLARATION

By submitting this thesis electronically, I declare that the entirety of the work contained therein is my own, original work, that I am the owner of the copyright thereof (unless to the extent explicitly otherwise stated) and that I have not previously in its entirety or in part submitted it for obtaining any qualification.

Signature.....

Date.....

Mohamed Ali Elharati

Copyright © 2009 Stellenbosch University

All rights reserved

Abstract

The aim of this study was to modify the surface of polyethersulfone (PES) ultrafiltration (UF) membranes to produce a more hydrophilic membrane by cross-linking poly(vinyl alcohol) (PVA) with sodium tetraborate ($\text{Na}_2\text{B}_4\text{O}_7 \cdot 10\text{H}_2\text{O}$) (SB) on the surface. Key preparation factors were identified as PVA molecular weight, concentrations of the PVA and SB, cross-linking reaction time, number of coatings and the mode of coating. The effect of these factors on the membrane performance (salt retention and permeate flux) is discussed. These PVA-SB membranes typically had 11.46% retention and 413.30 $\text{L/m}^2 \cdot \text{h}$ flux for a feed containing 2000 ppm NaCl (0.45 MPa, 20°C, 45 – 50 L/h). The coating was shown to be uniform and stable by Fourier transform infrared spectroscopy (FT-IR) analyses. Coating significantly increased hydrophilicity and a maximum flux increase of 500 $\text{L/m}^2 \cdot \text{h}$ was reached. Measurements showed a reduced water contact angle and this confirmed the obvious enhancement of surface hydrophilicity.

As a control, the role of the PVA base layer without cross-linking and the effects of its drying and heating on the water permeability of the PES-UF membrane were also studied, in order to ascertain maximum treatment conditions. Retention and permeate flux were determined (feed solution: 2000 ppm NaCl, applied pressure 0.45 MPa, 25°C, 45 – 50 L/h). It was found that the heating had the largest effect on the reduction of water permeability and therefore 50°C was the limit for treatment of this specific PES-UF membrane.

Thin-film composite (TFC) membranes were prepared by an interfacial polymerization (IP) reaction between a polyfunctional amine and tri- or di-functional carboxylic chloride and then evaluated for their reverse osmosis (RO) performance. The salt retention of the PVA-SB membranes was improved when covering the cross-linked PVA gel sub-layer with a polyamide (PA) layer. However, the permeate flux decreased to below 30 $\text{L/m}^2 \cdot \text{h}$ (2000 ppm NaCl, 1 – 2 MPa, 20°C, 45 – 50 L/h).

Two TFC membranes made from trimesoyl chloride (TMC) with *m*-phenylenediamine (MPD) or 2,6-diaminopyridine (DAP) exhibited retentions of 96.71% to 89.65% and fluxes of 10.93 to 27.91 $\text{L/m}^2 \cdot \text{h}$, depending on the type of diamine used, when tested with a 2000 ppm NaCl solution (2 MPa, 25°C, 45 – 50 L/h). Two TFC membranes made from a new 2,5-furanoyl chloride (FC) with MPD or DAP exhibited retentions of 34.22% to 58.54% and fluxes of 49.21 to 25.80 $\text{L/m}^2 \cdot \text{h}$, depending on the type of diamine used, when tested with a 2000 ppm NaCl solution (1 MPa, 25°C, 45 – 50 L/h).

Novel PVA-SB-DAP-FC membranes made from the DAP with FC had the highest hydrophilicity value and exhibited >58.54% NaCl retention and 25.80 $\text{L/m}^2 \cdot \text{h}$ flux, and 75.08% MgSO_4 retention and 34.75 $\text{L/m}^2 \cdot \text{h}$ flux, when tested with (2000 ppm feed, 1 MPa, 25°C, 45 – 50 L/h).

The effect of the chemical structures of the different amines and carboxylic chlorides used on the RO performances of the TFC membranes prepared by two amines reacting with TMC or FC, on the surfaces of the modified asymmetric PES-UF membranes, was investigated. FT-IR and water contact angle determination were used to characterize the chemical structure, morphology and hydrophilicity of the PA layers of the composite membranes.

The response surface methodology (RSM) was used to optimize the preparation conditions that had the largest effects on the RO performance of the PVA-SB-DAP-FC membranes. Good membrane performance could be realized particularly by manipulating three variables: DAP concentration, FC concentration and polymerization time (PT). The regression equation between the preparation variables and the performance of the composite membranes was established. Main effects, quadratic effects and interactions of these variables on the composite membrane performance were investigated.

The membranes were characterized in terms of pure water permeation (PWP) rate, molecular weight cut off (MWCO), solute separation and flux. Mean pore size (μ_p) and standard deviation (σ_p) of the membranes were determined using solute transport data. The results revealed that PVA-SB membranes have almost the same pure water permeation that PES-UF membranes have. The MWCO of the PES-UF membranes decreased from 19,000 to 13,000 Daltons when the membrane was coated with PVA.

Keywords: polyethersulfone ultrafiltration membrane, poly(vinyl alcohol), polyamide, thin-film composite membrane

Opsomming

Die doel van hierdie studie is die modifikasie van die oppervlakte van poliëtersulfoon ultrafiltrasie (PES-UF) membrane om meer hidrofiliese membrane te berei deur die kruisbinding van polivinielalkohol (PVA) met natriumtetraboraat ($(\text{Na}_2\text{B}_4\text{O}_7 \cdot 10\text{H}_2\text{O})$ (NaB) op die membraanoppervlakte. Sleutelfaktore in die bereidingsproses is geïdentifiseer, naamlik: PVA molekulêre massa, PVA en NaB konsentrasies, kruisbindingsreaksietyd, die aantal bestrykingslae, en die manier waarop die bestrykingslae aangewend is. Die invloed van hierdie faktore op die membraanontsouting en vloed is ondersoek, en word hier bespreek. Hierdie PVA-NaB membrane het die volgende tipiese resultate getoon: 11.46% ontsouting en $413.30 \text{ L/m}^2 \cdot \text{h}$ vloed (Kondisies: 2000 dpm NaCl oplossing, 0.45 MPa toegepaste druk, $20 \text{ }^\circ\text{C}$, vloeitempo 45–50 L/h). Die deklaag was uniform en stabiel, soos bepaal d.m.v. FTIR. Die aanwesigheid van die deklaag het die hidrofiliesiteit verhoog en 'n maksimum vloed van $500 \text{ L/m}^2 \cdot \text{h}$ is behaal. Die waterkontakhoek is ook gemeet; 'n laer waarde het 'n verbetering in die hidrofiliesiteit van die oppervlakte bevestig.

Die rol van die PVA basislaag, sonder kruisbinding (kontrole), en die effek van uitdroging en verhitting hiervan, is ook bestudeer, om sodoende optimale behandelingskondisies te bepaal. Membraanontsouting en vloed is bepaal (Kondisies: 2000 dpm NaCl oplossing, 0.45 MPa toegepaste druk, $25 \text{ }^\circ\text{C}$, vloeitempo 45–50 L/h). Verhitting het die grootste effek gehad op die afname in vloed. Daar is bevind dat 'n maksimum temperatuur van 50°C geskik is vir die behandeling van hierdie spesifieke PES-UF membraan.

Dunfilmsaamgestelde (DFS) membrane is berei d.m.v. 'n tussenvlakpolimerisasie-reaksie tussen 'n polifunksionele amien en 'n di- of tri-funksionele karbonielchloried, en daarna is die tru-osmose (TO) gedrag bepaal. Die ontsouting van die PVA-NaB membrane was hoër nadat die kruisgebinde PVA-jel sub-laag met 'n poliamied (PA) laag bedek is. Die vloed het egter afgeneem, tot onder $30 \text{ L/m}^2 \cdot \text{h}$ (Kondisies: 2000 dpm NaCl oplossing, 1–2 MPa toegepaste druk, $20 \text{ }^\circ\text{C}$, vloeitempo 45–50 L/h).

Twee DFS membrane is berei met trimesoëlchloried (TMC), naamlik met m-feniëldiamien (MFD) of 2,6-diaminopiridien (DAP). Afhangend van die diamien wat gebruik is, is die volgende ontsoutingsresultate en vloede verkry: 96.71% tot 89.65% en 10.93 tot $27.91 \text{ L/m}^2 \cdot \text{h}$ (Kondisies: 2 000 dpm NaCl oplossing, 2 MPa toegepaste druk, $25 \text{ }^\circ\text{C}$, vloeitempo 45–50 L/h). Twee DFS membrane is ook berei met 'n nuwe verbinding, 2,5-furanoëlchloride (FC), en MFD of DAP. Afhangend van die diamien wat gebruik is is die volgende ontsoutingsresultate en vloede behaal: 34.22% tot 58.54% en 49.21 tot $25.80 \text{ L/m}^2 \cdot \text{h}$ (Kondisies: 2000 dpm NaCl oplossing, 1 MPa toegepaste druk, $25 \text{ }^\circ\text{C}$, vloeitempo 45–50 L/h).

Die PVA-NaB-DAP-FC membrane het die hoogste hidrofiliesiteit getoon: 58.54% NaCl ontsouting en $25.80 \text{ L/m}^2 \cdot \text{h}$ vloed, en 75.08% MgSO_4 ontsouting en $34.75 \text{ L/m}^2 \cdot \text{h}$ vloed (2000 ppm NaCl oplossing, 1 MPa toegepaste druk, $25 \text{ }^\circ\text{C}$, vloeitempo 5–50 L/h).

Die invloed van die chemiese struktuur van die verskillende diamiene en karboksiesuurchloriedes wat gebruik is in die bereiding van die DFC membrane op die oppervlakte van die gewysigde PES-UF membrane is in terme van TO ondersoek. FTIR en kontakhoekbepalings is gebruik om die chemiese struktuur, morfologie en hidrofilisiteit van die PA lae van die saamgestelde membrane te bepaal.

Die eksperimentele oppervlakte ontwerp metode is gebruik om die bereidingskondisies vir die TO aanwending van die PVA-NaB-DAP-FC membrane te optimiseer. Goeie resultate is verkry deur die volgende veranderlikes te manipuleer: DAP en FC konsentrasies en die tydsduur van die polimerisasie. 'n Regressie-vergelyking tussen die bereidingsveranderlikes en die funksionering van die saamgestelde membrane is bepaal. Die volgende is ook ondersoek vir hul effek op die funksionering van die saamgestelde membrane: hoof-effekte, vierkantseffekte, en interaksie tussen veranderlikes.

Die eienskappe van die membrane wat bepaal is, is: deurlatingstempo van suiwer water (DSW), molekulêre massa-afsnypunt (MMAP), skeiding van opgeloste sout en vloed. Deurlating van opgeloste sout data is gebruik om gemiddelde poriegrootte (μ_p) en standaard afwyking (σ_p) van die membrane te bepaal. Resultate het getoon dat die PVA-NaB membrane amper dieselfde DSW gehad het as die PES-UF membrane. Die MMAP van die PES-UF membrane het afgeneem van 19,000 tot 13,000 Daltons na behandeling met PVA.

Sleutelwoorde: poliëtersulfoon-ultrafiltrasiemembraan, poli(vinielalkohol), poliamied, dunfilm-saamgestelde-membraan

To Mom and Dad

Acknowledgements

I would like to express my sincere gratitude to my research supervisor **Prof J. H. Knoetze**, for his guidance, enthusiasm, encouragement, help, supervision and patience through out this study. I am gratefully indebted to my co-supervisor **Prof R.D. Sanderson**, director of the Institute of Polymer Science, University of Stellenbosch, for a limitless supply of ideas, advice, and enthusiasm, encouragement and for the opportunity to undertake this study.

I would like to thank **Dr. W. Weber**, for his assistance and time so generously and patiently given to the chemical side of the project and for the many fruitful discussions. I also wish to express my deepest appreciation to **Dr. I. Goldie**, my mentor, for his persistent guidance, and the friendly and patient manner in which he advised and assisted me in numerous ways during this study.

Thank you so much **Prof E. P. Jacobs**, whose extensive knowledge of membrane research, development, and applications was, and still is, a source of inspiration to many students in this field. I am also very grateful to **Dr. Margaret Hurdall**, for her help with the editing, and her friendliness and patience throughout my years of study at the Institute.

Appreciation is also extended to the Faculty of Engineering, graduate students, and staff of the Chemical Engineering department for their assistance during my studies here. All the staff and students at the Institute of Polymer Science, thank you so much for your help and friendship. I would particularly like to thank **Deon Koen** for his valuable suggestions, help and friendship during my study.

I wish to thank **The Bureau of Research and Development in Libya**, for financial support for this research and **University of Stellenbosch**.

Finally, I am indebted to **my parents and my friends** whose support, understanding and encouragement have made all this possible. I dedicate this dissertation to them.

M.A. Elharati

TABLE OF CONTENTS

<i>DECLARATION</i>	<i>II</i>
<i>ABSTRACT</i>	<i>III</i>
<i>ACKNOWLEDGEMENTS</i>	<i>VIII</i>
<i>TABLE OF CONTENTS</i>	<i>IX</i>
<i>LIST OF FIGURES</i>	<i>XII</i>
<i>LIST OF TABLES</i>	<i>XV</i>
<i>LIST OF ABBREVIATIONS</i>	<i>XVI</i>
<i>LIST OF SYMBOLS</i>	<i>XX</i>
CHAPTER 1	1
INTRODUCTION AND OBJECTIVES	1
1.1 INTRODUCTION	2
1.2 STRUCTURE OF THE RESEARCH (RESEARCH APPROACH)	3
1.3 RESEARCH OBJECTIVES	3
1.3.1 <i>POLYETHERSULFONE ULTRAFILTRATION (PES-UF) MEMBRANES</i>	<i>4</i>
1.3.1.1 Characterization of the polyethersulfone (PES-UF) support.....	<i>4</i>
1.3.1.2 Effect of the heating and drying on the polyethersulfone (PES-UF) support.....	<i>4</i>
1.3.2 <i>POLY(VINYL ALCOHOL)-SODIUM TETRABORATE (PVA-SB) MEMBRANES</i>	<i>4</i>
1.3.2.1 Membrane fabrication.....	<i>4</i>
1.3.2.2 Membrane evaluation.....	<i>4</i>
1.3.2.3 Membrane characterization.....	<i>4</i>
1.3.3 <i>POLY(VINYL ALCOHOL) / POLYAMIDE (PVA-SB-PA) MEMBRANES</i>	<i>4</i>
1.3.3.1 Membrane fabrication.....	<i>4</i>
1.3.3.2 Membrane evaluation.....	<i>4</i>
1.3.3.3 Membrane characterization.....	<i>4</i>
1.3.4 <i>MEMBRANE CHARACTERIZATION IN TERMS OF SOLUTE TRANSPORT</i>	<i>5</i>
1.3.5 <i>OPTIMIZATION OF THE AQUEOUS SOLUTION USED TO PREPARE NANOFILTRATION MEMBRANES USING RESPONSE SURFACE METHODOLOGY</i>	<i>5</i>
1.4 OUTLINE OF THE THESIS	5
1.5 REFERENCES	5
CHAPTER 2	7
HISTORICAL AND THEORETICAL BACKGROUND	7
2.1 INTRODUCTION	8
2.2 MEMBRANE SYSTEMS	8
2.2.1 <i>ULTRAFILTRATION</i>	<i>9</i>
2.2.2 <i>REVERSE OSMOSIS (RO) AND NANOFILTRATION (NF)</i>	<i>12</i>
2.2.3 <i>MEMBRANE CONFIGURATIONS</i>	<i>14</i>
2.3 POLYETHERSULFONE MEMBRANES	16
2.4 POLY(VINYL ALCOHOL) AND POLY(VINYL ALCOHOL) MEMBRANES	16
2.4.1 <i>REACTIONS OF POLY(VINYL ALCOHOL) WITH BORIC ACID AND BORATE SALT SYSTEMS</i>	<i>21</i>
2.5 POLYAMIDE MEMBRANES	25
2.6 POLY(VINYL ALCOHOL) / POLYAMIDE MEMBRANES	27
2.7 REFERENCES	29
CHAPTER 3	40
MEMBRANE FABRICATION, CHARACTERIZATION AND EVALUATION	40
3.1 INTRODUCTION	41

3.2	CHARACTERIZATION OF POLYETHERSULFONE ULTRAFILTRATION MEMBRANES	41
3.2.1	<i>MATERIALS</i>	41
3.2.2	<i>THE EFFECT OF HEATING AND DRYING ON POLYETHERSULFONE ULTRAFILTRATION (PES-UF) MEMBRANES</i>	41
3.2.2.1	Drying	41
3.2.2.2	Heating	41
3.2.2.3	Morphology	42
3.3	POLY(VINYL ALCOHOL)-SODIUM TETRABORATE (PVA-SB) MEMBRANES	42
3.3.1	<i>MATERIALS</i>	42
3.3.2	<i>EXPERIMENTAL PROCEDURES</i>	42
3.3.2.1	Solution preparation	43
3.3.2.2	Membrane fabrication	43
3.4	POLY(VINYL ALCOHOL) / POLYAMIDE (PVA-SB-PA) MEMBRANES	43
3.4.1	<i>MATERIALS</i>	43
3.4.2	<i>EXPERIMENTAL PROCEDURES</i>	44
3.4.2.1	Solution preparation	44
3.4.2.2	Membrane fabrication	44
3.5	MEMBRANE CHARACTERIZATION	45
3.5.1	<i>FOURIER TRANSFORM INFRARED (FT-IR) SPECTROSCOPY</i>	45
3.5.2	<i>SCANNING ELECTRON MICROSCOPY (SEM)</i>	46
3.5.3	<i>CONTACT ANGLE MEASUREMENT</i>	46
3.6	MEMBRANE EVALUATION	48
3.6.1	<i>MATERIALS</i>	48
3.6.2	<i>EQUIPMENT</i>	48
3.6.2.1	Flat sheet test cells plant	48
3.6.2.2	Experimental procedures	48
3.6.3	<i>EVALUATION CRITERIA</i>	49
3.7	REFERENCES	49
CHAPTER 4		50
RESULTS AND DISCUSSION OF INITIAL INVESTIGATION		50
4.1	INTRODUCTION	51
4.2	CHARACTERIZATION OF POLYETHERSULFONE ULTRAFILTRATION MEMBRANES	51
4.2.1	<i>EFFECT OF DRYING ON THE PURE WATER PERMEATION (PWP) RATE OF THE POLYETHERSULFONE (PES-UF) SUPPORT</i>	52
4.2.2	<i>EFFECT OF HEATING ON THE PURE WATER PERMEATION (PWP) RATE OF THE POLYETHERSULFONE (PES-UF) SUPPORT</i>	52
4.2.3	<i>EFFECT OF DRYING AND HEATING ON THE PURE WATER PERMEATION (PWP) RATE OF THE POLYETHERSULFONE (PES-UF) SUPPORT</i>	52
4.3	EVALUATION OF POLY(VINYL ALCOHOL)-SODIUM TETRABORATE (PVA-SB) MEMBRANES	54
4.3.1	<i>EFFECT OF POLY(VINYL ALCOHOL) LAYER WITHOUT CROSS-LINKING</i>	54
4.3.2	<i>EFFECT OF POLY(VINYL ALCOHOL) MOLECULAR WEIGHT</i>	55
4.3.3	<i>EFFECT OF POLY(VINYL ALCOHOL) CONCENTRATION</i>	57
4.3.4	<i>EFFECT OF SODIUM TETRABORATE CONCENTRATION</i>	59
4.3.5	<i>EFFECT OF CROSS-LINKING REACTION TIME</i>	61
4.3.6	<i>EFFECT OF THE NUMBER OF COATINGS</i>	62
4.3.7	<i>EFFECT OF THE MODE OF COATING</i>	63
4.4	EVALUATION OF POLY(VINYL ALCOHOL) / POLYAMIDE (PVA-SB-PA) MEMBRANES	64
4.4.1	<i>EFFECT OF THE USE OF TRIMESOYL CHLORIDE WITH TWO DIFFERENT DIAMINES</i>	65
4.4.2	<i>EFFECT OF THE USE OF 2,5-FURANOYL CHLORIDE WITH TWO DIFFERENT DIAMINES</i>	65
4.5	MEMBRANE CHARACTERIZATION	68
4.5.1	<i>CONTACT ANGLE ANALYSIS</i>	68
4.5.2	<i>FOURIER TRANSFORM INFRARED (FT-IR) ANALYSIS</i>	72
4.6	REFERENCES	74
CHAPTER 5		75

OPTIMIZATION OF THE FABRICATION CONDITIONS FOR NANOFILTRATION MEMBRANES USING RESPONSE SURFACE METHODOLOGY.....	75
ABSTRACT.....	76
5.1 INTRODUCTION.....	76
5.2 RESPONSE SURFACE METHODOLOGY.....	77
5.3 EXPERIMENTAL.....	78
5.3.1 MATERIALS.....	78
5.3.2 MEMBRANE FABRICATION.....	79
5.3.3 MEMBRANE EVALUATION.....	79
5.3.4 EXPERIMENTAL DESIGN.....	79
5.4 RESULTS AND DISCUSSION.....	80
5.4.1 ANALYSIS OF VARIANCE.....	80
5.4.2 EFFECT OF PROCESS VARIABLES ON MEMBRANE PERFORMANCE.....	83
5.4.3 COMPARISON OF PREDICTED AND ACTUAL EXPERIMENTAL VALUES.....	90
5.5 CONCLUSIONS.....	93
5.6 REFERENCES.....	95
CHAPTER 6.....	97
MEMBRANE CHARACTERIZATION IN TERMS OF SOLUTE TRANSPORT USING UV SPECTROPHOTOMETRY AND GRAVIMETRY METHODS.....	97
ABSTRACT.....	98
6.1 INTRODUCTION.....	98
6.2 THEORETICAL BACKGROUND.....	99
6.2.1 MEMBRANE CHARACTERIZATION BASED ON SOLUTE TRANSPORT DATA.....	99
6.2.2 STOKES RADIUS OF POLYETHYLENE GLYCOL (PEG).....	100
6.3 EXPERIMENTAL.....	101
6.3.1 MATERIALS.....	101
6.3.2 CREATION OF CALIBRATION CURVES (CONCENTRATION VS. ABSORBANCE) OF POLYETHYLENE GLYCOL (PEG) OF DIFFERENT MOLECULAR WEIGHTS.....	101
6.3.3 ULTRAFILTRATION MEMBRANE EVALUATION.....	102
6.3.3.1 Procedure for the UV spectrophotometry method.....	103
6.3.3.2 Procedure for the gravimetry method.....	103
6.4 RESULTS AND DISCUSSION.....	103
6.4.1 CALIBRATION CURVES OF POLYETHYLENE GLYCOL (PEG) OF DIFFERENT MOLECULAR WEIGHTS.....	103
6.4.2 MEMBRANE CHARACTERIZATION BASED ON THE ULTRAVIOLET (UV) SPECTROPHOTOMETRY METHOD.....	104
6.4.2.1 Pure water permeation (PWP) rate.....	104
6.4.2.2 Molecular weight cut-off (MWCO) profiles.....	105
6.4.2.3 Mean pore size and pore size distribution.....	105
6.4.3 MEMBRANE CHARACTERIZATION BASED ON THE GRAVIMETRY METHOD.....	107
6.4.3.1 Molecular weight cut-off (MWCO) profiles.....	107
6.4.3.2 Mean pore size and pore size distribution.....	108
6.5 CONCLUSIONS.....	110
6.6 REFERENCES.....	110
CHAPTER 7.....	112
CONCLUSIONS AND RECOMMENDATIONS.....	112
7.1 CONCLUSIONS.....	113
7.2 RECOMMENDATIONS FOR FUTURE RESEARCH.....	114
APPENDIXES.....	116
APPENDIX A: FOURIER TRANSFORM INFRARED (FT-IR) SPECTRA.....	117
APPENDIX B: ULTRAVIOLET SPECTRA OF POLYETHYLENE GLYCOL (PEG) OF DIFFERENT MOLECULAR WEIGHTS.....	120
APPENDIX C: CALIBRATION CURVES OF POLYETHYLENE GLYCOL (PEG).....	124
APPENDIX D: MEMBRANE MORPHOLOGY.....	128
APPENDIX E: UNCLER MAGNETIC RESONANCE (NMR) SPECTRA.....	130

LIST OF FIGURES

Figure 1-1: Structure of the proposed research	3
Figure 2-1: Schematic representation of a two-phase system separated by a semipermeable membrane(based on [4])	9
Figure 2-2: Schematic representation of the phenomena of osmosis and reverse osmosis (RO) (based on [4]).....	12
Figure 2-3: Molecular structure of polyethersulfone (PES)	16
Figure 2-4: Schematic illustration of an interfacial polymerization (IP) reaction (based on [126])	26
Figure 2-5: Schematic of a thin-film composite (TFC) RO membrane and the chemical structure of an aromatic polyamide thin-film layer (based on [127])	26
Figure 3-1: Schematic describing the cross-linking process used to prepare poly(vinyl alcohol)-sodium (PVB-SB) membranes	44
Figure 3-2: Photograph of the sealed chamber used in photoacoustic (PAS) cell.....	45
Figure 3-3: Contact angle measurements: (a) principle, (b) experimental setup	47
Figure 3-4: Diagram of a flat sheet test cell plant.....	49
Figure 4-1: Effect of operating pressure on the RO performance of polyethersulfone ultrafiltration (PES-UF) support	51
Figure 4-2: Effect of drying time on the pure water permeation rate of the polyethersulfone ultrafiltration (PES-UF) support	52
Figure 4-3: Effect of heating on the pure water permeation rate of the polyethersulfone ultrafiltration (PES-UF) support	53
Figure 4-4: Effect of drying and heating on the pure water permeation rate of the polyethersulfone ultrafiltration (PES-UF) support	53
Figure 4-5: Effect of the poly(vinyl alcohol) coating layer on the performance of polyethersulfone ultrafiltration (PES-UF) support: (a) Flux, (b) Retention	55
Figure 4-6: Effect of poly(vinyl alcohol) molecular weight on the performance of poly(vinyl alcohol)-sodium tetraborate (PVA-SB) membranes: (a) Flux, (b) Retention.....	56
Figure 4-7: Effect of poly(vinyl alcohol) concentration on the performance of poly(vinyl alcohol)-sodium tetraborate (PVA-SB) membranes: (a) Flux, (b) Retention (first trial)	58
Figure 4-8: Effect of poly(vinyl alcohol) concentration on the performance of poly(vinyl alcohol)-sodium tetraborate (PVA-SB) membranes: (a) Flux, (b) Retention (second trial)	59
Figure 4-9: Effect of sodium tetraborate concentration on the performance of poly(vinyl alcohol)-sodium tetraborate (PVA-SB) membranes: (a) Flux, (b) Retention.....	60
Figure 4-10: Effect of cross-linking reaction time on the performance of poly(vinyl alcohol)-sodium tetraborate (PVA-SB) membranes: (a) Flux, (b) Retention	61
Figure 4-11: Effect of the number of coatings on the performance of poly(vinyl alcohol)-sodium tetraborate (PVA-SB) membranes: (a) Flux, (b) Retention	62
Figure 4-12: Effect of the mode of coating on the performance of poly(vinyl alcohol)-sodium tetraborate (PVA-SB) membranes: (a) Flux, (b) Retention	63
Figure 4-13: Effect of using trimesoyl chloride with different diamines on the performance of poly(vinyl alcohol)-sodium tetraborate-polyamide (PVA-SB-PA) membranes: (a) Flux, (b) Retention	66
Figure 4-14: Effect of using 2,5-furanoyl chloride with different diamines on the performance of poly(vinyl alcohol)-sodium tetraborate-polyamide (PVA-SB-PA) membranes: (a) Flux, (b) Retention ..	67
Figure 4-15: Contact angle values of polyethersulfone (PES-UF) support modified with poly(vinyl alcohol) of different molecular weights	68
Figure 4-16: Contact angle values of polyethersulfone (PES-UF) support modified with poly(vinyl alcohol) of different concentrations	69
Figure 4-17: Contact angle values of polyethersulfone (PES-UF) support modified with sodium tetraborate of different concentrations.....	69
Figure 4-18: Contact angle values of polyethersulfone (PES-UF) support modified using different cross-linking reaction times	70
Figure 4-19: Contact angle values of polyethersulfone (PES-UF) support modified using different number of coatings	70
Figure 4-20: Contact angle values of polyethersulfone (PES-UF) support modified with different of modes of coating	71

Figure 4-21: Contact angle values of poly(vinyl alcohol)-sodium tetraborate (PVA-SB) membranes modified with trimesoyl chloride (TMC)	71
Figure 4-22: Contact angle values of PVA-SB poly(vinyl alcohol)-sodium tetraborate membranes modified with 2,5-furanoyl chloride (FC).....	72
Figure 4-23: FT-IR spectra of polyethersulfone (PES-UF), poly(vinyl alcohol)-sodium tetraborate (PVA-SB) and poly(vinyl alcohol)-sodium tetraborate-polyamide (PVA-SB-PA) membranes	73
Figure 5-1: Normal probability plot of residual for (a) Flux and (b) Retention	84
Figure 5-2: Plot of residual vs. predicted response for (a) Flux and (b) Retention	85
Figure 5-3: Response surface and contour plot indicating the effect of DAP concentration and FC concentration upon flux for a polymerization time 60 sec	86
Figure 5-4: Response surface and contour plot indicating the effect of DAP concentration and IP polymerization time upon flux for a FC concentration 0.60%.....	87
Figure 5-5: Response surface and contour plot indicating the effect of FC concentration and IP polymerization time upon flux for a DAP concentration 1.5%	88
Figure 5-6: Response surface and contour plot indicating the effect of DAP concentration and FC concentration upon retention for a polymerization time 60 sec.....	89
Figure 5-7: Response surface and contour plot indicating the effect of DAP concentration and IP polymerization time upon retention for a FC concentration 0.60%	91
Figure 5-8: Response surface and contour plot indicating the effect of FC concentration and IP polymerization time upon retention for a DAP concentration 1.5%.....	92
Figure 5-9: Flux, predicted values by response model against the experimental data.....	94
Figure 5-10: Retention, predicted values by response model against the experimental data	94
Figure 6-1: Schematic representation of the creation of calibration curves (Concentration vs. Absorbance) of PEG of different molecular weights	102
Figure 6-2: Pure water permeation (PWP) rate of polyethersulfone (PES-UF) and poly(vinyl alcohol)-sodium tetraborate (PVA-SB) membranes.....	104
Figure 6-3: Molecular weight cut-off (MWCO) profile of polyethersulfone (PES-UF) and poly(vinyl alcohol)-sodium tetraborate (PVA-SB) membranes using ultraviolet (UV) method	105
Figure 6-4: Solute separation curve of polyethersulfone (PES-UF) and poly(vinyl alcohol)-sodium tetraborate (PVA-SB) membranes using ultraviolet (UV) method.....	106
Figure 6-5: Cumulative pore size distribution of polyethersulfone (PES-UF) and poly(vinyl alcohol)-sodium tetraborate (PVA-SB) membranes using ultraviolet (UV) method	107
Figure 6-6: Probability density function curve of polyethersulfone (PES-UF) and poly(vinyl alcohol)-sodium tetraborate (PVA-SB) membranes using ultraviolet (UV) method	107
Figure 6-7: Molecular weight cut-off (MWCO) profile of polyethersulfone (PES-UF) and poly(vinyl alcohol)-sodium tetraborate (PVA-SB) membranes using gravimetry method	108
Figure 6-8: Solute separation curve of polyethersulfone (PES-UF) and poly(vinyl alcohol)-sodium tetraborate (PVA-SB) membranes using gravimetry method.....	108
Figure 6-9: Cumulative pore size distribution of polyethersulfone (PES-UF) and poly(vinyl alcohol)-sodium tetraborate (PVA-SB) membranes using gravimetry method	109
Figure 6-10: Probability density function curve of polyethersulfone (PES-UF) and poly(vinyl alcohol)-sodium tetraborate (PVA-SB) membranes using gravimetry method	109
Figure A-1: FT-IR spectra of polyethersulfone (PES-UF), polyethersulfone / poly(vinyl alcohol) (PES / PVA), poly(vinyl alcohol)-sodium tetraborate (PVA-SB) membranes modified with poly(vinyl alcohol) (PVA) of different concentrations	117
Figure A-2: FT-IR spectra of polyethersulfone (PES-UF), polyethersulfone / poly(vinyl alcohol) (PES / PVA), poly(vinyl alcohol)-sodium tetraborate (PVA-SB) membranes modified with sodium tetraborate (SB) of different concentrations	117
Figure A-3: FT-IR spectra of polyethersulfone (PES-UF), polyethersulfone / poly(vinyl alcohol) (PES / PVA), poly(vinyl alcohol)-sodium tetraborate (PVA-SB) membranes modified with a different number of coatings	118
Figure A-4: FT-IR spectra of polyethersulfone (PES-UF), polyethersulfone / poly(vinyl alcohol) (PES / PVA), poly(vinyl alcohol)-sodium tetraborate (PVA-SB) membranes modified with different mode of coating	118
Figure A-5: FT-IR spectra of polyethersulfone (PES-UF), poly(vinyl alcohol)-sodium tetraborate (PVA-SB), poly(vinyl alcohol)-sodium tetraborate-m-phenylene diamine-trimesoyl chloride (PVA-SB-MPD-TMC) and poly(vinyl alcohol)-sodium tetraborate-2,6-diaminopyridine-trimesoyl chloride (PVA-SB-DAP-TMC) membranes	119
Figure A-6: FT-IR spectra of polyethersulfone (PES-UF), poly(vinyl alcohol)-sodium tetraborate (PVA-SB), poly(vinyl alcohol)-sodium tetraborate-m-phenylene diamine-2,5-furanoyl chloride (PVA-SB-MPD-	

FC) and poly(vinyl alcohol)-sodium tetraborate-2,6-diaminopyridine-furanoyl chloride (PVA-SB-DAP-FC) membranes.....	119
Figure B-1: Ultraviolet spectra of polyethylene glycol (PEG-1550).....	120
Figure B-2: Ultraviolet spectra of polyethylene glycol (PEG-2000).....	120
Figure B-3: Ultraviolet spectra of polyethylene glycol (PEG-4000).....	121
Figure B-4: Ultraviolet spectra of polyethylene glycol (PEG-6000).....	121
Figure B-5: Ultraviolet spectra of polyethylene glycol (PEG-10000).....	122
Figure B-6: Ultraviolet spectra of polyethylene glycol (PEG-12000).....	122
Figure B-7: Ultraviolet spectra of polyethylene glycol (PEG-20000).....	123
Figure B-8: Ultraviolet spectra of polyethylene glycol (PEG-35000).....	123
Figure C-1: Calibration curve of polyethylene glycol (PEG-1550).....	124
Figure C-2: Calibration curve of polyethylene glycol (PEG-2000).....	124
Figure C-3: Calibration curve of polyethylene glycol (PEG-4000).....	125
Figure C-4: Calibration curve of polyethylene glycol (PEG-6000).....	125
Figure C-5: Calibration curve of polyethylene glycol (PEG-10000).....	126
Figure C-6: Calibration curve of polyethylene glycol (PEG-12000).....	126
Figure C-7: Calibration curve of polyethylene glycol (PEG-20000).....	127
Figure C-8: Calibration curve of polyethylene glycol (PEG-35000).....	127
Figure D-1: Scanning electron microscopy (SEM) images of cross-section of polyethersulfone (PES-UF) membrane before and after drying and heating.....	128
Figure D-2: Scanning electron microscopy (SEM) images of the surface of a polyethersulfone (PES-UF) membrane before and after drying and heating.....	129
Figure E-1: ^1H NMR spectrum of 2,5-furanoyl chloride in CDCl_3	130
Figure E-2: ^{13}C NMR spectrum of 2,5-furanoyl chloride in CDCl_3	130

LIST OF TABLES

Table 2-1: Membrane separation processes [5].....	10
Table 2-2: Summary of ultrafiltration (UF), nanofiltration (NF) and reverse osmosis (RO) systems [4, 6, 9].....	15
Table 2-3: Qualitative comparison of various membrane modules [4, 6, 9].....	15
Table 2-4: General properties of poly(vinyl alcohol) (PVA) [3].....	18
Table 2-5: Development of poly(vinyl alcohol) (PVA) membranes [3, 44]	22
Table 2-6: Composition and RO performance of various polyamide (PA) membranes [2, 3, 27].....	28
Table 2-7: Comparison of solute retention data of NTR-7250HF, NTR-729HF and NTR-739HF membranes with that of cellulose acetate (CA) membranes [27].....	29
Table 3-1: Classification of membranes prepared in this study	42
Table 3-2: Polyethersulfone ultrafiltration (PES-UF) membrane properties [1].....	42
Table 3-3: Experimental conditions used to study the effect of drying and heating of the polyethersulfone ultrafiltration (PES-UF) membrane	42
Table 3-4: Materials used in the fabrication of poly(vinyl alcohol)-sodium tetraborate (PVA-SB) membranes.....	43
Table 3-5: Materials used in the fabrication of poly(vinyl alcohol)-sodium tetraborate-polyamide (PVA-SB-PA) membranes.....	44
Table 3-6: Materials used in the evaluation of membranes	48
Table 4-1: Typical conditions used to fabricate poly(vinyl alcohol)-sodium tetraborate (PVA-SB) membranes.....	54
Table 4-2: Aqueous and organic solutions used for the fabrication of PVA-SB-PA membranes.....	64
Table 4-3: Basic conditions used in the fabrication of PVA-SB-PA membranes	65
Table 4-4: Possible assignments of IR peaks in the spectra of the polyethersulfone (PES-UF), poly(vinyl alcohol)-sodium tetraborate (PVA-SB) and poly(vinyl alcohol)-sodium tetraborate- polyamide (PVA-SB-PA) membranes.....	73
Table 5-1: The variable factors investigated and levels in the experimental design.....	80
Table 5-2: Design layout and experimental results	80
Table 5-3: Analysis of variance of the regression model for flux.....	82
Table 5-4: Analysis of variance of the regression model for retention	82
Table 5-5: Comparison of the predicted and the actual experimental values	93
Table 6-1: Mean pore size (μp), standard deviation (σp) and molecular weight cut-off (MWCO) of polyethersulfone (PES-UF) and poly(vinyl alcohol)-sodium tetraborate (PVA-SB) membranes calculated from the solute separation curve using ultraviolet (UV) method.....	106
Table 6-2: Mean pore size (μp), standard deviation (σp) and molecular weight cut-off (MWCO) of polyethersulfone (PES-UF) and poly(vinyl alcohol)-sodium tetraborate (PVA-SB) membranes calculated from the solute separation curve using gravimetry method	110

LIST OF ABBREVIATIONS

Å	-	Angstrom
AlCl ₃ .6H ₂ O	-	Aluminium chloride hexahydrate
AFM	-	Atomic force microscopy
Al ₂ O ₃	-	Aluminium oxide
ANOVA	-	Analysis of variance
BaCl ₂	-	Barium chloride
Ba(OH) ₂ .8H ₂ O	-	Barium hydroxide octahydrate
bar	-	Bar
CA	-	Cellulose acetate
Ca ⁺²	-	Calcium ion
CAM	-	Contact angle measurement
CCD	-	Centre composite design
Cl ⁻	-	Chloride ion
cm	-	Centimetre
CO ₃ ⁻²	-	Carbonate ion
CuSO ₄	-	Copper sulfate
CSA	-	(±)-Camphor-10-sulfonic acid (β)
°C	-	Degree Celsius
°C ⁻¹	-	Thermal expansion coefficient
Da	-	Dalton
DAP	-	2,6-diaminopyridine
DD	-	Diffusion dialysis
dF	-	Degree of freedom
DI	-	De-ionized water
DTA	-	Differential thermal analysis
ED	-	Electrodialysis
FC	-	2,5-Furanoyl chloride
FT-IR	-	Fourier Transform Infrared Spectroscopy
GA	-	Glutaraldehyde
g	-	Gram
GS	-	Gas separation
h	-	Hour(s)
H ₂ SO ₄	-	Sulfuric acid
HCHO	-	Formaldehyde
HCl	-	Hydrochloric acid
I ₂	-	Iodine
IA	-	Itaconic acid
IP	-	Interfacial polymerization

IPC	-	Isophthaloyl chloride
$K_2S_2O_8$	-	Potassium persulfate
$KCr(SO_4)_2 \cdot 12H_2O$	-	Potassium chromium sulfate
kg/m^3	-	Kilogram per cubic metre
KI	-	Potassium iodide
$kJ/kg \cdot K^\circ$	-	Kilojoules per kilogram Kelvin
kJ/mol	-	Kilojoules per mole
kPa	-	Kilopascal
kv	-	Kilovolt
L	-	Litre
L/h	-	Litre per hour
LiCl	-	Lithium chloride
Lmd	-	Litre per square metre day
$L/m^2 \cdot h$	-	Litre per square metre hour
LS	-	Light scattering
m	-	Metre
MA	-	Maleic anhydride
MC	-	Membrane contactor
MD	-	Membrane distillation
ME	-	Membrane electrolysis
MF	-	Microfiltration
$MgSO_4$	-	Magnesium sulfate
min	-	Minute(s)
mL	-	Millilitre
μL	-	Microlitre
MLR	-	Multiple linear regressions
mm	-	Millimetre
μm	-	Micrometer
MPa	-	Megapascal
MPD	-	m-Phenylenediamine
$\mu S/cm$	-	MicroSiemens per centimetre
MWCO	-	Molecular weight cut-off
Na^+	-	Sodium ion
$Na_2B_4O_7 \cdot 10H_2O$	-	Sodium tetraborate
NaCl	-	Sodium chloride
NC	-	Cube points
NA	-	Axial points
NO	-	Centre points
n_D^{25}	-	Refractive index at 25°C
NF	-	Nanofiltration
NMR	-	Nuclear magnetic resonance
nm	-	Nanometre

NaOH	-	Sodium hydroxide
Na ₂ S	-	Sodium sulfide
Na ₂ SO ₄	-	Sodium sulfate
NTU	-	Nephelometric turbidity units
-O-	-	Ether linkages in the backbone chain
OH	-	Hydroxyl group
OS	-	Osmotic pressure
PA	-	Polyamide
PAN	-	Polyacrylonitrile
PAS	-	Photoacoustic
PEG	-	Polyethylene glycol
PEI	-	Polyethyleneimine
PES	-	Polyethersulfone
PES / PVA	-	Code for membranes based on PES and PVA without cross-linked
pH	-	Negative decimal logarithm of hydrogen-ion concentration
PIP	-	Piperazine
ppm	-	Parts per million
PS	-	Polysulfone
PSSA	-	Polystyrene sulfonic acid
PT	-	Polymerization time
PV	-	Pervaporation
PVA	-	Poly(vinyl alcohol)
PVAc	-	Poly(vinyl acetate)
PVME	-	Polyvinylmethylether
PVA-SB	-	Code for membranes on PVA and SB
PVA-SB-PA	-	Code for membranes on PVA, SB and PA
P ₁ & P ₂	-	Pressure gauges
R ²	-	Regression line (correlation coefficient)
RH	-	Relative humidity
RO	-	Reverse osmosis
RSM	-	Response surface methodology
s	-	Second(s)
SA	-	Sodium alginate
SB	-	Sodium tetraborate
SD	-	Sedimentation and diffusion
SDI	-	Salt density index
SEM	-	Scanning electron microscopy
SLS	-	Sodium dodecyl sulfate
SO ₂	-	Sulfone groups
SSW	-	Synthetic seawater
TC	-	Temperature controller
TDI	-	Toluene diisocyanate

TEA	-	Triethylamine
TEM	-	Transmission electron microscopy
TFC	-	Thin-film composite
T _g	-	Glass transition temperature
T _m	-	Crystalline melting point
TMC	-	Trimesoyl chloride
TPC	-	Terephthaloyl chloride
UF	-	Ultrafiltration
UV	-	Ultraviolet
v	-	Volts
V ₁ & V ₂	-	Control valves
VP	-	Vapour permeation
Wt%	-	Percentage by weight
ZrO ₂	-	Zirconia
ZnCl ₂	-	Zinc chloride
%	-	Percentage

LIST OF SYMBOLS

a	-	Stokes radius of solute, m
A	-	Water permeability coefficient
A_0	-	Intercept in eq. 6.4
A_1	-	Slope in eq. in 6.4
B	-	Solute permeability coefficient
C_F	-	Solute concentration in the feed stream
C_P	-	Solute concentration in the permeate stream
C_w	-	Solubility of water in the membrane
D_{AB}	-	Diffusivity of macromolecules in a solution, m^2/sec
D_s	-	Diffusion coefficient of salt
d_p	-	Pore size of the membrane, nm
d_s	-	Solute diameter, nm
D_w	-	Diffusion coefficient of water
f	-	Solute separation, %
J	-	Permeate flux of the membrane, $L/m^2.h$
J_s	-	Solute flux
J_w	-	Water flux through the membrane
K	-	Boltzmann's constant
K_s	-	Membrane-solution partition coefficient
MW	-	Molecular weight of the polymer, kg/mol
H_p	-	Mean pore size of the membrane, nm
μ_s	-	Geometric mean diameter of solute, nm
PWP	-	Pure water permeation rate, $L/m^2.h$
Q	-	Volume of the permeate, L
R	-	Retention, %
R_g	-	Gas constant
S	-	Effective membrane area, m^2
T	-	Absolute temperature, $^{\circ}C$
V	-	Total volume of the permeate collected, L
V_w	-	Partial molar volume of water
W_1	-	Weight of empty glass dish, g
W_2	-	Weight of the glass dish plus sample, g
W_s	-	Weight of sample, g
X_i	-	Multiple variables
x_i	-	Coded value of the i th independent variable
X_i	-	Uncoded value of the i th independent variable
X_i^*	-	Uncoded i th independent variable at the centre point
y	-	Response

ΔC_s	-	Solute concentration difference across the membrane
ΔP	-	Applied pressure difference across the membrane
Δt	-	Permeate collection time, hour
ΔX	-	Effective membrane thickness
ΔX_i	-	Step change value
$\Delta \pi$	-	Osmotic pressure difference across the membrane
B_o	-	Constant coefficient
B_i	-	Linear coefficients
B_{ii}	-	Quadratic coefficients
B_{ij}	-	Second-order interaction coefficient
η	-	Solvent viscosity, Pa.s
$[\eta]$	-	Intrinsic viscosity of the polymer, m ³ /kg
σ_g	-	Geometric standard deviation about the mean diameter of the solute
σ_p	-	Geometric standard deviation of the membrane

Chapter 1

INTRODUCTION AND OBJECTIVES

1.1 INTRODUCTION

Over the past few decades, membrane science and technology has led to significant innovation in both processes and products, particularly appropriate for sustainable industrial growth. Membranes and membrane processes were first introduced as an analytical tool in chemical and biomedical laboratories, and they developed very rapidly into industrial products and methods with significant technical and commercial importance. Today, membranes are commercially used, on a large scale, to produce potable water from sea water and brackish water, to clean industrial effluents and recover valuable constituents, to concentrate, purify, or fractionate macromolecules from mixtures in the food and drug industries, and to separate gases or vapours in petrochemical processes [1, 2].

In the most general sense, a synthetic membrane is a barrier that separates two phases and restricts the transport of various chemical species in a rather specific manner. A membrane may be solid or liquid, homogeneous or heterogeneous, isotropic or anisotropic in its structure, it may be neutral, may carry positive or negative charges, or may be bipolar. A membrane can be a fraction of a micrometre or several millimetres thick. A membrane can be very complex in both structure and function [3]. Membranes for the separation of solutions and liquid mixtures may be distinguished on the basis of pore sizes as reverse osmosis (RO) below 1 nm, ultrafiltration (UF) 20 – 100 nm, and microfiltration (MF) 100 nm – 2 μm , although this classification is very arbitrary. Pore sizes of nanofiltration (NF) membranes are between those of RO and UF membranes [4].

Thin-film composite (TFC) membranes typically consist of a cross-linked aromatic polyamide (PA) formed in situ on the surface of a microporous support via interfacial polymerization (IP). TFC membranes have a thin and dense active layer that controls membrane performance (permeability and selectivity), and a much thicker porous substrate that provides mechanical support to the active layer. In order to achieve high values of permeability and selectivity, the active layer should be ultra-thin and hydrophilic [5].

Applications of the composite membranes are broadened by enhancing their performance as well as their chlorine resistance. Therefore, much effort in the area of TFC membranes has been centred on developing membranes that provide higher flux and selectivity either through (i) design and synthesis of new polymers for forming thin films of the RO membranes, or (ii) physical / chemical modification of the thin films. The chemical modification of diamines by the introduction of sulfonic acid [6] or carboxylic acid groups [7], or incorporation of various polymers, such as poly(vinyl alcohol) (PVA) and poly(vinyl phenol) to the aromatic PA have been employed to improve water permeability [5, 8]. These modifications have resulted in TFC membranes with enhanced water flux but, simultaneously, an accompanying (considerable) loss of salt rejection, or vice versa.

In the past, less emphasis has been focused on the fabrication of TFC membranes consisting of a polyethersulfone (PES) support membrane coated with a thin, cross-linked hydrogel PVA layer. Hydrogels provide smooth, hydrophilic surfaces, with minimal protein binding. They can also be easily manipulated in terms of thickness and the degree of cross-linking to fit desired TFC membrane needs. This study contributes to knowledge of the preparation, characterization and use of PVA and PA for the fabrication of PVA gel sub-layer and PVA / PA TFC membranes.

The preparation of asymmetric cellulose acetate (CA) membranes in the early 1960s by Loeb and Sourirajan is generally recognized as a pivotal moment for membrane technology. Even since the discovery of CA RO membranes, considerable efforts have been directed at the search for new and

improved polymers for the production of RO membranes. Later the concept of TFC membranes was developed and numerous chemical systems were tested to prepare TFC RO membranes; the most successful of which were those of the aromatic PAs and polyetherimides [5].

PVA is useful in practical investigations of functional polymers because it can be easily modified through its hydroxyl groups. PVA has a highly hydrophilic character, good film-forming properties and outstanding physical and chemical stability, and hence it is an excellent membrane material for preparation of hydrophilic UF and NF membranes [9].

Numerous techniques have been used to cross-link PVA and manufacture an ultra-thin film of cross-linked PVA, such as cross-linking by heat, radiation treatment or treatment with organic compounds. PVA and a diamine compound have been used together as the polymeric precursor for manufacturing the thin-film desalting barrier of a composite membrane. PVA RO membranes made by the Nitto Electric Industrial Company gave retentions of >90% and a water flux of 65 L/m².h [10]. PVA RO membranes with salt retentions of >98% and reasonable fluxes of 42 L/m².h have already been commercialized, such as the NTR-739HF and the NTR-7199 membranes of the Nitto Electric Industrial Company [11].

In this thesis, PVA was cross-linked by sodium tetraborate (SB) to insolubilize the PVA layer. In order to improve the salt retention properties of the PVA-SB membrane, TFC membranes were created by IP on the PVA-SB surface, using a selection of the following diamines and di- or tri-carboxylic acid chlorides: m-phenylenediamine (MPD); 2,6-diaminopyridine (DAP); 2,5-furanyl chloride (FC); and trimesoyl chloride (TMC). These membranes subsequently comprise a PA skin over a PVA gel sub-layer.

1.2 STRUCTURE OF THE RESEARCH (RESEARCH APPROACH)

Various membrane materials were investigated in this study. **Figure 1-1** illustrates the structure of the proposed research. The thesis work ultimately comprises two parts: one focuses on SB cross-linked PVA membranes and their RO performance and hydrophilicity properties, and the other on PVA-SB-PA membranes and the investigation of their RO performances and their hydrophilicity properties.

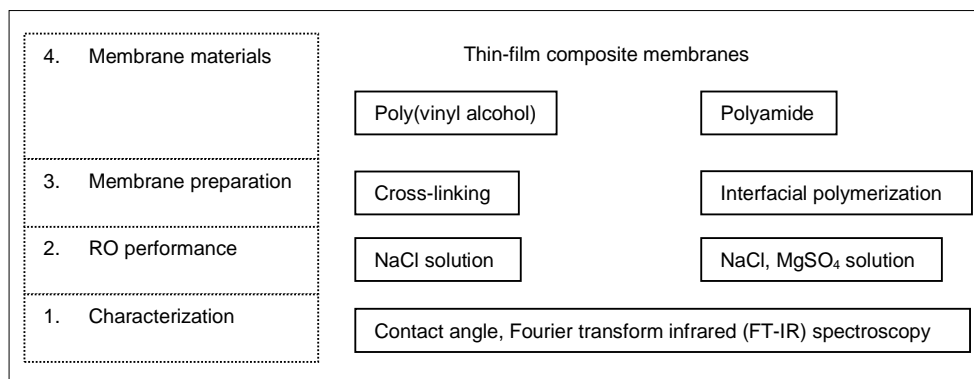


Figure 1-1: Structure of the proposed research

1.3 RESEARCH OBJECTIVES

The aim of the study was to fabricate TFC membranes by the cross-linking coating process, using PVA as precursor and SB as cross-linking agent. The fabrication of TFC membranes with high salt retention was not of primary importance in this thesis, and the emphasis was rather focused on the

synthesis of TFC membranes with high hydrophilicity and high flux. The objectives of the present study are given below under headings which refer to the main aspects investigated.

1.3.1 POLYETHERSULFONE ULTRAFILTRATION (PES-UF) MEMBRANES

1.3.1.1 Characterization of the polyethersulfone (PES-UF) support

To evaluate the PES-UF support, the retention of individual solutes (NaCl and MgSO₄) and the flux were determined.

1.3.1.2 Effect of the heating and drying on the polyethersulfone (PES-UF) support

To determine the limits of heating and drying procedures on the polyethersulfone support.

1.3.2 POLY(VINYL ALCOHOL)-SODIUM TETRABORATE (PVA-SB) MEMBRANES

1.3.2.1 Membrane fabrication

To investigate the effects of the numerous fabrication variables that influence the cross-linking coating process of PVA with SB, and then to determine their effects on the membrane properties.

1.3.2.2 Membrane evaluation

To evaluate the RO performance of PVA-SB membranes using a NaCl feed solution and to determine the effect of different operating pressures.

1.3.2.3 Membrane characterization

The hydrophilicity improvement of the membrane surface and the stability of the PVA-SB layer were to be confirmed through contact angle measurement (CAM) and Fourier transform infrared (FT-IR) analysis, respectively.

1.3.3 POLY(VINYL ALCOHOL) / POLYAMIDE (PVA-SB-PA) MEMBRANES

To improve the salt retention of PVA-SB membranes by the deposition of a PA skin on the insolubilized PVA gel sub-layer.

1.3.3.1 Membrane fabrication

To investigate the effect of the diamine and carboxylic acid chloride structure on membrane performance.

1.3.3.2 Membrane evaluation

To evaluate the PVA-SB-PA membranes for their RO performance in 2000 ppm NaCl and 2000 ppm MgSO₄ feed solutions at various pressures, and to compare the results with those of the PVA-SB membranes, without the PA skin.

1.3.3.3 Membrane characterization

The hydrophilicity improvement of the membrane surface and the stability of the PVA-SB-PA layer were to be confirmed through CAM and FT-IR analysis, respectively.

1.3.4 MEMBRANE CHARACTERIZATION IN TERMS OF SOLUTE TRANSPORT

To determine the molecular weight cut-off (MWCO) and pore size distribution of PES-UF and PVA-SB membranes.

1.3.5 OPTIMIZATION OF THE AQUEOUS SOLUTION USED TO PREPARE NANOFILTRATION MEMBRANES USING RESPONSE SURFACE METHODOLOGY

Response surface methodology (RSM) was used to optimize the preparation conditions that had large effects on the performance of the PVA / PA composite membranes.

1.4 OUTLINE OF THE THESIS

Chapter 1 includes an introduction to this research project and presents the objectives of the research. Chapter 2 presents a historical and theoretical background, including a description of various membrane technologies, the basic principles of membrane transport, a description of various methods for cross-linking PVA, the development of TFC membranes, and a brief review of the preparation of PA and PVA / PA membranes.

Experimental details of membrane fabrication, characterization and evaluation are presented in Chapter 3. The first part deals with the characterization of PES-UF membranes used as the substrate layer and an investigation of the effects of heat treatment and drying on the PES-UF membrane performance. This would help establish treatment limits. The second part deals with the cross-linking of PVA with SB to enhance the hydrophilicity of PES-UF membranes. The final part deals with experiments carried out to improve the salt retention properties of PVA-SB membranes by fabricating PVA-SB-PA membranes.

Chapter 4 focuses on the results obtained in the evaluation and characterization of the various types of membranes. In attempts to determine the effects of the respective parameters in the fabrication of the various types of membranes on the membrane performance, one parameter was varied at a time while the others were kept constant.

In Chapter 5, factorial experimental design was used to determine the main factors and optimal conditions for the PA layer. Chapter 6 focuses on the characterization of PES-UF and PVA-SB membranes in terms of their pure water permeation (PWP) rate, molecular weight cut-off (MWCO), solute separation and flux. Mean pore size (μ_p) and standard deviation (σ_g) of the membranes were determined using solute transport data. Chapters 5 and 6 are arranged in publication format, each with their own abstract, introduction, materials and methods, results and discussion, and conclusions section. The final chapter presents highlights important conclusions that can be made from the results obtained and recommendations for future work are made.

1.5 REFERENCES

- [1] Baker, R.W., *Membrane technology and applications*. Second ed., John Wiley & Sons Inc: California. 2004. p. 237-272.
- [2] Noble, R.D. and S.A. Stern, *Membrane separations technology: principles and applications*. First ed., Membrane Science and Technology Series, 2, Elsevier: Amsterdam. The Netherlands, 1995.

- [3] Mulder, M., *Basic principles of membrane technology*. First Ed., Kluwer Academic: Dordrecht. 1992.
- [4] Porter, M.C., *Handbook of industrial membrane technology*. First ed., Noyes Publications: New Jersey, U.S.A. 1990.
- [5] Petersen, R.J., *Composite reverse osmosis and nanofiltration membranes*. Journal of Membrane Science, 1993. 83: p. 81-150.
- [6] Zhou, Y., S. Yu, M. Liu, and C. Gao, *Polyamide thin-film composite membrane prepared from m-phenylenediamine and m-phenylenediamine-5-sulfonic acid*. Journal of Membrane Science, 2006. 270: p. 162-168.
- [7] Ahmad, A.L., B.S. Ooi, and J.P. Choudhury, *Preparation and characterization of co-polyamide thin-film composite membrane from piperazine and 3,5-diaminobenzoic acid*. Desalination, 2003. 158: p. 101-108.
- [8] Jian, S. and S.X. Ming, *Cross-linked PVA-PS thin-film composite membrane for reverse osmosis*. Desalination, 1987. 62: p. 395-403.
- [9] Finch, C.A., *Polyvinyl alcohol: properties and applications*, John Wiley and Sons: New York, 1973.
- [10] Kazuse, N., A. Iwama, and T. Shintani (*Nitto Electric Industrial Co., Ltd.*). March 1987, (Chemical Abstracts 106: 198245g).
- [11] Kawada, I., K. Inoue, Y. Kazuse, H. Ito, T. Shintani, and Y. Kamiyama, *New thin-film composite low pressure reverse osmosis membrane and spiral wound modules*. Desalination, 1987. 64: p. 387-401.

Chapter 2

HISTORICAL AND THEORETICAL BACKGROUND

2.1 INTRODUCTION

This background chapter will concentrate on various topics considered necessary for an understanding of the work previously done on membranes made from poly(vinyl alcohol) (PVA) and polyamides (PAs). It starts with an introduction to membrane systems including information on basic principles, commercial applications, and a comparison between the different membrane separation processes.

This is followed by the theory of the solution-diffusion mechanism, proposed by Lonsdale and co-workers, that governs species transport through the active layer [1]. The next section is about polyethersulfone (PES) ultrafiltration (UF) membranes. This is followed by a discussion of various reactions and methods that have been used to prepare water-insoluble symmetric and asymmetric PVA membranes.

A short section on PA membranes has been included, which describes the methods and materials used to make thin-film composite (TFC) membranes by interfacial polymerization (IP). A thorough review of this subject has been made in a PhD thesis by M.J. Hurndall [2] and a MSc thesis by D. Bezuidenhout [3]. Various commercial PA membranes are available that exhibit excellent salt retention properties, but they do not have PVA in their structure.

An insoluble PVA layer can be used as gel sub-layer in the preparation of low and high pressure reverse osmosis (RO) membranes. This will be discussed in Section 2.5. Nitto Denko (Nitto Electric Industrial Co.) in Japan was the most successful in combining the properties of PVA and PA by producing reverse osmosis (RO) and nanofiltration (NF) membranes consisting of an ultra-thin PA desalination layer over an insolubilized PVA gel sub-layer. Nitto Denko used monomeric amines, based on piperazine and piperazine-like derivatives, in the preparation of these membranes [3].

2.2 MEMBRANE SYSTEMS

Membranes are now being used for a variety of separations, e.g. particles from solution, salts from water, toxins from blood, and one gas from gas mixtures. Today, large scale membrane processes are used in a wide range of applications and the number of such applications is still growing. The first generation membrane processes are microfiltration (MF), ultrafiltration (UF), nanofiltration (NF), reverse osmosis (RO), electrodialysis (ED), membrane electrolysis (ME), diffusion dialysis (DD), and dialysis, and the second generation membrane processes are gas separation (GS), vapour permeation (VP), pervaporation (PV), membrane distillation (MD), membrane contactors (MC) and carrier mediated processes.

Passive transport through membranes occurs as a consequence of a driving force, and a difference in chemical potential seen as a gradient across the membrane driven by concentration, pressure, or by an electrical field. **Table 2-1** summarizes important membrane separation processes. These processes can be divided into three categories according to the driving forces involved in the separation. These membrane processes are based on different separation principles or mechanisms.

In spite of these differences all membrane processes have one thing in common, namely, the membrane. The membrane is the heart of every membrane process and can act as a permselective barrier or interface between two homogenous phases. **Figure 2-1** shows a schematic representation of membrane separation.

Phase 1 is usually presented as the feed or upstream side while phase 2 is presented as the permeate or downstream side. Therefore, the membrane has the ability to transport one component from the feed mixture more readily than any other component and this may occur via various mechanisms. The three processes UF, NF and RO will be discussed further.

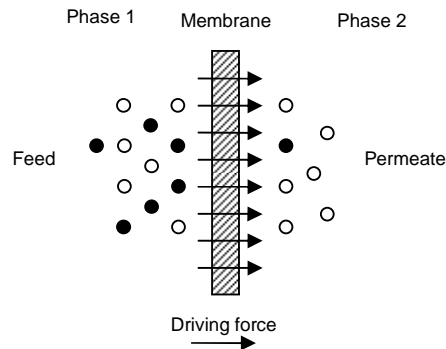


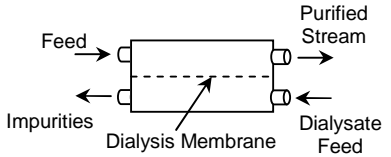
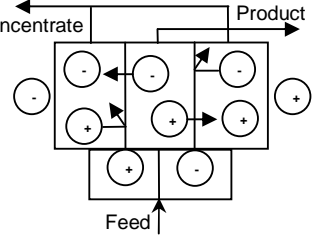
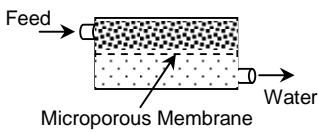
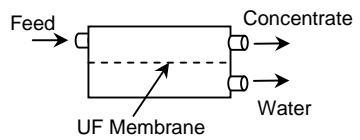
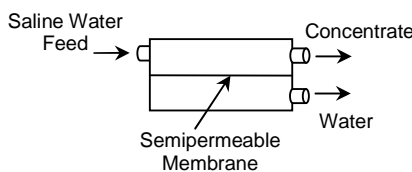
Figure 2-1: Schematic representation of a two-phase system separated by a semipermeable membrane(based on [4])

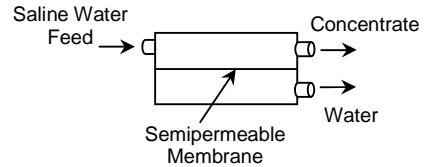
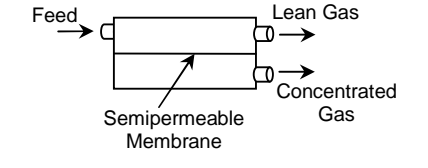
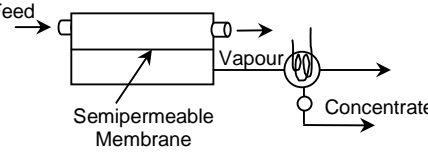
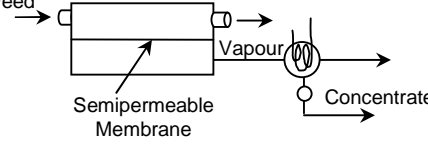
2.2.1 ULTRAFILTRATION

UF is a membrane process whose separation characteristics lie between those of NF and MF. UF and MF membranes can initially be considered as porous membranes whose retention is determined mainly by the size and shape of the solutes relative to the pore size of the membrane and where the transport of solvent is directly proportional to the applied pressure. UF membranes have pore diameters in the range 10 – 1000 Å. The thickness of the top layer of an UF membrane is generally less than 150 µm. UF membranes are typically used to filter dissolved macromolecules such as proteins and colloids from a solution, the lower limit being solutes with molecular weights of a few thousand Daltons. Another important consideration in UF is the ease with which the membranes foul and the ease with which they can be cleaned or, in some applications, sterilized.

Early UF membranes were made of cellulose acetate (CA), but later UF membranes were developed that have improved resistance to solvents, high and low pH and temperature, and oxidizing cleaning agents such as free chlorine. UF membranes have been prepared from a number of polymers other than CA namely, polycarbonate, polyvinyl chloride, polyamides, polysulfone (PS), PES, sulfonated polysulfone, polyvinylidene fluoride, polyimides, polyetherimides, copolymers of acrylonitrile and vinyl chloride, polyacetal, polyacrylates, polyelectrolyte complexes, and cross-linked PVA [4-6]. Inorganic (ceramic) materials, especially aluminium oxide (Al_2O_3) and zirconia (ZrO_2), have also been used for UF membranes [4, 6]. UF membranes are typically fabricated as follows: prepare a casting solution by dissolving the polymer in a suitable solvent, add one or more co-solvents or non-solvents, cast, quench in a non-solvent (usually water) and, optionally, anneal in water. These membranes have the characteristic skinned structure of the Loeb-Sourirajan membrane [7]. They can be characterized by different analytical techniques such as scanning electron microscopy (SEM), atomic force microscopy (AFM) and Fourier transform infrared (FT-IR) spectroscopy analysis [6, 8, 9]. UF membranes are usually characterized by their molecular weight cut-off (MWCO), based on the pore size distribution. UF membranes are often used as sub-layers in the preparation of composite membranes for RO, NF, GS and PV [8].

Table 2-1: Membrane separation processes [5]

Process	Concept	Materials passed	Driving force	Material retained
Dialysis		Ions and low-molecular weight organics (urea, etc.)	Concentration difference	Dissolved and suspended material with molecular weight > 1,000 Å.
Electrodialysis		Ions	Voltage, typically 1 – 2 v / cell pair	All non-ionic and macro-molecular species
Particle filtration		Water	Pressure difference	Suspended particles
Microfiltration		Water and dissolved species	Pressure difference, typically 0.068 MPa	Suspended material (silica, bacteria, etc.). Variable particle-size cut-off. Particles of diameter > 100 nm
Ultrafiltration		Water and salts	Pressure difference, typically 0.068 – 0.68 MPa	Biological, colloids, and macromolecules. Variable MWCO > 10 nm
Nanofiltration		Water and monovalent salts	Pressure difference, typically 0.68 – 1.38 MPa	Ionic divalent salts and small solutes. Particles of diameter > 1 nm

Process	Concept	Materials Passed	Driving Force	Material Retained
Reverse osmosis	 <p>Saline Water Feed → Semipermeable Membrane → Water, Concentrate</p>	Water	Pressure difference, typically 0.68 – 5.51 MPa	Virtually all suspended and dissolved material
Gas separation	 <p>Feed → Semipermeable Membrane → Lean Gas, Concentrated Gas</p>	Gases and vapours	Pressure difference, 0.1013 – 10.13 MPa	Membrane-selective permeable gases and vapours
Pervaporation*	 <p>Feed → Semipermeable Membrane → Vapour → Concentrate</p>	Less membrane selective liquids	Pressure difference	Membrane separation of liquids
Membrane distillation**	 <p>Feed → Semipermeable Membrane → Vapour → Concentrate</p>	Water	Heat / Temperature difference	Salts

* Pervaporation is a membrane distillation process that relies on the difference in partial pressures and on the change in the concentration on the membrane surface caused by membrane selective absorption of the liquids to be separated, and not on the pressure applied to the feed solution.

** Membrane distillation is a process that relies on the difference in temperature on the feed and on the sweep side of the membrane, where the water vapour is swept by a sweep gas and condensed.

The first synthetic UF membranes were prepared by Bechhold from collodion (nitrocellulose) [10]. Other important early works were by Zsigmondy and Bachmann [11], Ferry [12] and Elford [13]. The crucial breakthrough was the development of the anisotropic CA membrane by Loeb and Sourirajan in 1963 [7]. Michaels and co-workers [14] produced UF membranes from CA and many other polymers, including polyacrylonitrile copolymers, aromatic polyamides, PS and poly(vinylidene fluoride).

A vast number of laboratory-scale and industrial applications of UF have now been examined. The important applications of industrial UF today are in the areas of pollution control and the recovery of valuable by-products. Typical applications of UF membranes are concentrating proteins from milk whey, or recovery of colloidal paint particles from electrocoat paint rinse waters. Several hundred UF plants have now been installed around the world to process the rinse water, recycling the paint to the dip tank and permitting the purified rinse water to be reused. UF is now being introduced as a pre-treatment for RO units, especially in seawater desalination applications [4-6, 15].

2.2.2 REVERSE OSMOSIS (RO) AND NANOFILTRATION (NF)

RO and NF are considered as one process since the basic principles are the same. NF and RO are used when low molecular weight solutes, such as inorganic salts, or small organic molecules, such as glucose and sucrose, have to be separated from a solvent. NF and RO membranes can be considered as being intermediate between the open porous types of membranes (MF / UF) and dense nonporous membranes (PV / GS).

RO is a process in which an applied pressure is used to reverse the normal osmotic flow of water across a semipermeable membrane. **Figure 2-2** illustrates the osmotic phenomena. The membrane is permeable to the solvent (water) but not to the solute (salt). The normal water flow across a membrane is from the lower solute concentration solution to the higher solute concentration solution if the applied pressure is smaller than the osmotic pressure. At osmotic equilibrium, if a pressure (Δp) is applied to the concentrated solution just equal to the osmotic pressure difference between the two solutions ($\Delta\pi$), in this case, the water flow will stop (as shown in **Figure 2-2**). At higher pressure ($\Delta p > \Delta\pi$), water will flow from the concentrated solution to the dilute solution. The analogy of RO being the reverse of osmosis is therefore not strictly correct, and some authors prefer to use the term “hyper-filtration” to the more commonly used term.

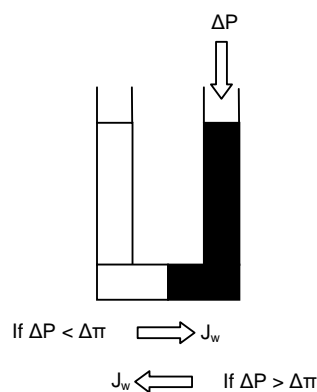


Figure 2-2: Schematic representation of the phenomena of osmosis and reverse osmosis (RO) (based on [4])

There are many theories for the transport mechanism of water across a RO membrane. The most accepted theory is the solution-diffusion mechanism proposed by Lonsdale and co-workers [1]. Solution-diffusion is generally accepted to govern species transport through the active layer. If it is assumed that no solute permeates through the membrane, then the effective water flow can be described by:

$$J_w = A (\Delta P - \Delta \pi) \quad (2.1)$$

where $(\Delta P = P_f - P_p)$ is the applied pressure difference, $(\Delta \pi = \pi_f - \pi_p)$ is the difference in osmotic pressure across the membrane. The f and p subscripts refer to the feed and the permeate sides, respectively. The water permeability coefficient A (hydrodynamic permeability coefficient) is a constant for a given membrane and comprises the following parameters:

$$A = \frac{D_w C_w V_w}{R_g T \Delta X} \quad (2.2)$$

where D_w is the diffusion coefficient of water, C_w is the solubility of water in the membrane, V_w is the partial molar volume of water, ΔX is the effective membrane thickness, R_g is the gas constant, and T is the absolute temperature. Water permeates through the semipermeable membrane by a solution-diffusion process because the water is much more soluble in the membrane than the salt is; it dissolves into the membrane and diffuses through the membrane under the applied pressure. The water flux through the membrane, J_w , can be represented by the equation:

$$J_w = \frac{D_w C_w V_w (\Delta P - \Delta \pi)}{R_g T \Delta X} \quad (2.3)$$

The solute flux, J_s , can be described by

$$J_s = B \Delta C_s \quad (2.4)$$

where ΔC_s is the solute concentration difference across the membrane ($\Delta C_s = C_f - C_p$) and B is the solute permeability coefficient. The solute permeability coefficient B is a function of the diffusivity and the distribution coefficient, as described by equation 2.5:

$$B = \frac{D_s K_s}{\Delta X} \quad (2.5)$$

where D_s is the diffusion coefficient of salt in the membrane and K_s is the partition coefficient of salt between the membrane and the solution. The permeation of salt through the membrane is also a solution-diffusion process, with the driving force being the concentration difference rather than the difference in pressure. The salt flux is then given by:

$$J_s = \frac{D_s K_s \Delta C_s}{\Delta X} \quad (2.6)$$

The selectivity of a membrane for a given solute is expressed by the retention coefficient:

$$R = 1 - \frac{C_p}{C_f} \quad (2.7)$$

Therefore, as the pressure increases the selectivity also increases because the solute concentration in the permeate decreases ($J_w \propto (\Delta P - \Delta \pi)$ and $J_s \neq (\Delta P - \Delta \pi)$). Taking into account that ($C_p = J_s / J_w$) and combining equations (2.3), (2.6) and (2.7), the retention coefficient can be written as:

$$R = \frac{A(\Delta P - \Delta\pi)}{A(\Delta P - \Delta\pi) + B} = 1 - \left\{ \frac{D_s K_s}{D_w C_w} \frac{R_g T}{V_w} \frac{(C_f - C_p)}{C_f} \frac{1}{(\Delta P - \Delta\pi)} \right\} \quad (2.8)$$

The pressures used in RO and NF are much higher than those used in UF. In contrast to UF to MF, the choice of material directly influences the separation efficiency through the constants A and B. In simple terms this means that the constant A must be as high as possible whereas the constant B must be as low as possible in order to obtain an efficient separation. In other words, the membrane (material) must have a high affinity for the solvent (mostly water) and a low affinity for the solute. This implies that the choice of material is very important because it determines the intrinsic membrane properties [4]. Equations 2.3, 2.6 and 2.8 indicate that the fluxes and retention depend upon D_w , C_w , D_s and K_s , which are intrinsic properties of the active layer material. In addition, whereas the fluxes are inversely proportional to the active layer thickness, ΔX , the retention is independent of ΔX . From the equations above it can be seen that when the applied pressure is increased the water flux increases linearly. The solute flux is hardly affected by the pressure difference; it is only determined by the concentration difference across the membrane. This means that the membrane thickness must be minimized in order to maximize the water flux but not so thin as to lead to the formation of defects [3, 4]. RO application may be classified as solvent purification or solute concentration processes. Most applications of RO are in the desalination of brackish water and especially seawater to produce potable water, and in the production of ultrapure water for the semiconductor industry. RO is also used in the food industry, the galvanic industry and the dairy industry [4].

NF membranes have a network structure that is more open than that of RO membranes. The retention of monovalent ions as Na^+ and Cl^- is much lower but the retention for bivalent ions such as Ca^{+2} and CO_3^{-2} is high. RO is the preferred process when a high retention for NaCl is required whereas the NF process is preferred for divalent and microsolite applications. The salt retention mechanism of NF membranes may involve one or more forces, namely, charge interaction, hydrated-ion size-exclusion, or dielectric interaction [3]. **Table 2-2** tabulates a summary of UF, NF and RO processes [4].

2.2.3 MEMBRANE CONFIGURATIONS

Large membrane areas are normally required to apply membranes on a commercial scale. The smallest unit into which the membrane area is packed is called a module. The module is the central part of a membrane installation. The development of the technology to produce low-cost membrane modules was one of the breakthroughs that led to commercial membrane processes in the 1960s and 1970s [6]. The earliest designs were based on simple filtration technology and consisted of flat sheets of membranes held in a type of filter press, the so called plate-and-frame modules. A number of module designs are possible, all of which are based on two types of membrane configuration: flat sheet and tubular. Plate-and-frame and spiral-wound modules involve flat sheet membranes whereas tubular, capillary and hollow fibre modules are based on tubular membrane configurations [4, 6, 8, 9].

Several types of membranes are available on the market today in a variety of commercial modules [5, 6, 15-17]. The advantages and disadvantages of the four commercial modules have been discussed in various papers [16, 18]. The choice of the module is mainly determined by economic considerations and the type of application. **Table 2-3** tabulates a qualitative comparison of various membrane modules [5, 6, 15].

Table 2-2: Summary of ultrafiltration (UF), nanofiltration (NF) and reverse osmosis (RO) systems [4, 6, 9]

	Ultrafiltration	Nanofiltration	Reverse Osmosis
Membrane type	Asymmetric porous	Composite	Asymmetric or composite
Membrane thickness	≈ 150 μm	Sub-layer ≈ 150 μm; top layer ≈ 1 μm	Sub-layer ≈ 150 μm; top layer ≈ 1 μm
Membrane pore size	≈ 1 – 100 nm	< 2 nm	< 2 nm
Driving force	Pressure (1 – 10 bar)	Pressure (10 – 25 bar)	Pressure: brackish water (15 – 25 bar) Pressure: seawater (40 – 80 bar)
Separation principle	Sieving mechanism	Solution-diffusion	Solution-diffusion
Membrane material	Polymer (e.g. polysulfone, polyacrylonitrile) Ceramic (e.g. zirconium oxide, aluminium oxide)	Polyamide (interfacial polymerization)	Cellulose triacetate, aromatic polyamide, and furfural alcohol (interfacial polymerization)
Main applications	Dairy (milk, whey, cheese making) Food (potato starch and proteins) Metallurgy (oil-water emulsions, electro paint recovery) Textile Pharmaceutical (enzymes, antibiotics, pyrogens) Automotive (electro paint) Water treatment, RO pre-treatment	Desalination of brackish water Removal of micropollutants Water softening Waste water treatment Retention of dyes (textile industry)	Desalination of brackish water Production of ultrapure water (electronic industry) Food industry (concentration of fruit juice and sugars) Dairy industry (concentration of milk)

Table 2-3: Qualitative comparison of various membrane modules [4, 6, 9]

	Tubular	Plate-and-frame	Spiral-wound	Capillary	Hollow fibre
Packing density	Low-----→Very high				
Investment	High-----→Low				
Fouling	Low-----→Very high				
Cleaning	Good-----→Poor				
Membrane replacement	Yes / No	Yes	No	No	No

2.3 POLYETHERSULFONE MEMBRANES

PES-UF membranes were selected as the porous substrates in the present study. These membranes have several desirable properties, such as good thermal stability (high heat resistance), excellent chemical resistance (high and low pH tolerance), and good mechanical properties. The main drawback of a PES membrane is its hydrophobicity, which often results in serious fouling when applied to water treatment and separation of bio-products. The molecular structure of PES is shown in **Figure 2-3**. It consists of phenylene ring structures connected by sulfone groups (SO_2) and ether linkages ($-\text{O}-$) in the backbone chain, to form a polymer.

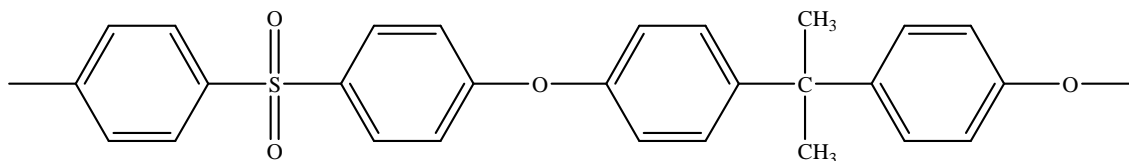


Figure 2-3: Molecular structure of polyethersulfone (PES)

Among the different membrane preparation techniques, asymmetric PES membranes are commonly prepared by diffusion induced phase separation (Zhang et al. [19]; Kim et al. [20]; Lin et al. [21]; Kastelan-Kunst et al. [22]; McHugh and Miller [23]). In this process a thin layer of the polymer, dissolved in an appropriate solvent, is cast on a suitable support and phase separation is induced by a non-solvent. This phase inversion can be achieved in several ways (Osmonics Inc. [24]; Van de Witte et al. [25]; Gelman Sciences Inc. [26]; Petersen et al. [27]), of which the immersion precipitation is the most efficient. Here, phase inversion is induced by immersing a film of the polymer solution in a bath containing a non-solvent. Both kinetics and thermodynamics play an important role during PES membrane formation. This has been extensively studied (Barth and Wolf [28]; Barton et al. [29]; Han et al. [30]; Han and Bhattacharyya [31]; Tkacik and Zeman [32]). Changing the preparation conditions influences both the kinetics and thermodynamics, resulting in a different membrane structure and subsequently a different membrane performance.

For example, an increase in the polymer concentration leads to a lower porosity of the membrane and hence to a lower water flux (Mosqueda-Jiminez et al. [33]; Barth et al. [34]). To increase the water flux, pore-forming agents, such as polyvinyl-pyrrolidone (Marchese et al. [35]; Han and Nam [36]), polyethylene glycol (Kim and Lee [37]) or an acid (Chaturvedi et al. [38]) can be added to the polymer solution. When, on the other hand, a volatile component like acetone is added to the polymer solution a denser top layer will develop, resulting in higher retentions (Barth et al. [34]).

2.4 POLY(VINYL ALCOHOL) AND POLY(VINYL ALCOHOL) MEMBRANES

Since the discovery of polymeric membranes a considerable amount of work has been carried out in search for new and improved polymers for membrane materials. PVA has been widely used in the manufacture of battery separators, pervaporation membranes and dialyzer diaphragms. The present study focuses on the modification of PES-UF membranes through cross-linking PVA with sodium tetraborate (SB), which has the ability to rapidly react with alcohol at ambient temperatures.

PVA is one of the most important water-soluble vinyl polymers. It is prepared by partial or complete hydrolysis of poly(vinyl acetate) (PVAc) [39]. The hydroxyl groups in PVA can form strong hydrogen bonds between intra- and intermolecular hydroxyl groups, which causes PVA to show high

affinity for water. The solubility of PVA in water depends on the degree of hydrolysis and the polymer chain length. However, to be used as separation membranes, PVA should be modified before use to offer long-term stability. Its chemical constitution and water solubility are however disadvantageous, often allowing degradation and elimination in the unmodified form. Chemical modification is a powerful tool for obtaining polymers with new properties and therefore increasing the scope of their applications [40]. **Table 2-4** summarizes some of the general properties of PVA.

PVA has a highly hydrophilic character, good film-forming properties and outstanding physical and chemical stability, and therefore is an excellent membrane material for the preparation of hydrophilic membranes. PVA is a useful material for the fabrication of RO membranes, based on its hydrophilic nature and its reactivity toward cross-linking reagents [40, 41].

In fact, considerable work has been carried out in the area of PVA RO composite membranes, where PVA or PVA copolymers were prepared as a selective skin layer of a composite RO membrane [3]. PVA is also used as a protective surface coating on top of composite membranes. Here its purpose is to enable to handle and fabricate the membranes into spiral-wound elements without causing damage to the ultra-thin barrier layer [27, 42]. PVA has been modified with different compounds, such as aldehydes, carboxylic acid, anhydrides, etc., to increase membrane selectivity. There are various possible ways to modify PVA for use in membranes, e.g.: copolymerization of vinyl acetate with hydrophobic monomers, followed by the hydrolysis of the acetate groups to form vinyl alcohol copolymers; and cross-linking and / or modification reactions via the hydroxyl groups of PVA.

A PVA solution is deposited or drawn onto a suitable surface, thereafter the polymeric film is precipitated from the solution by means of immersion in a suitable non-solvent. The membrane is, then insolubilized by reaction with any one of a number of reagents capable of cross-linking PVA. Membranes made by this process normally have a dense skin on one side, with the density and degree of cross-linking decreasing towards the other side of the membrane.

Reid and Spencer [43] were among the first to propose the use of cross-linked PVA for the fabrication of RO membranes. Jian and Ming [44] cross-linked PVA with dicarboxylic acids as cross-linking agents and sulfuric acid (H_2SO_4) as catalyst, at temperatures of 90 – 120°C. Dicarboxylic acids such as oxalic acid, malonic acid, succinic acid and citric acid can be used to cross-link PVA, resulting in a TFC membrane on PS as a support material. Results of IR spectra of PVA treated with oxalic acid and sulfuric acid, compared with those of untreated PVA, show new adsorption peaks appearing at 1750 cm^{-1} and 1200 cm^{-1} . Sulfuric acid is not only a catalyst but also a reactant. The effect of PVA concentration, cross-linking time and the number of carbon atoms in the diacid on the membrane performance was also investigated. Cadotte et al. [45] coated a PS support with an emulsion of PVAc dipped with sulfuric acid and formaldehyde, then heated it to 110°C to effect hydrolysis of the acetate groups, with concomitant cross-linking by formal linkages.

Fujimarki et al. [46] prepared TFC membranes from PVA by cross-linking with hexahydroxycyclohexane and sulfuric acid, and heating at 120°C for 10 min. Himeshima and Uemura [47] prepared a PVA composite membrane by cross-linking the PVA with divinyl sulfone at 70°C under alkaline conditions. Cadotte [48] prepared a version of a PVA composite membrane wherein the polymer was cross-linked by acetalization with a dialdehyde, catalyzed by phosphoric acid, and heat cured at about 100 to 110°C. An excess of phosphoric acid was used in the formulation, and served simultaneously as a catalyst and as a pore-former.

Table 2-4: General properties of poly(vinyl alcohol) (PVA) [3]

Type	Property	Value or description		Comments			Reference
Physical properties	Colour	White to ivory					[40]
	Storage stability	Indefinite		Dry storage			
	Light stability	Excellent					
	Density, kg/m ³	1270 – 1310		Increases with crystallinity			[49]
	Refractive Index, n_D^{25}	1.51 – 1.55					[41]
	Thermal expansion coefficient, °C ⁻¹	7 x 10 ⁻⁵ to 12 x 10 ⁻⁵		Temperature: 0 – 45°C			[50]
	Degree of crystallinity, %	0 – 50		Increases with heat treatment			
Thermal properties	Melting point, T _m , °C	230 – 267		Syndiotactic, Fully hydrolyzed			
	Melting point, T _m , °C	228 – 240		Atactic, Fully hydrolyzed			
	Melting point, T _m , °C	212 – 235		Isotactic, Fully hydrolyzed			
	Melting point, T _m , °C	180		87 – 89% hydrolyzed			[50]
	Glass transition temperature, T _g , °C	70 – 80		Various methods; Fully hydrolyzed			[40]
	Glass transition temperature, T _g , °C	58		87 – 89% hydrolyzed			
	Heat of fusion, kJ/mol	6.8 – 7.0					[51]
	Heat capacity, kJ/kg.K°	1.51					
Crystallographic data	Unit cell	Monoclinic					[51]
	Cell dimensions: A, Å	7.81					
	Cell dimensions: B, Å	2.52					
	Cell dimensions: C, Å	5.51					
	Cell dimensions: β, Å	91.7					
	Density, kg/m ³	1350		Crystalline regions			
		1291		Amorphous regions			
Barrier properties	Permeability, P, O ₂ , barrier	0.000001		RH = 0%			
	Permeability, P, O ₂ , barrier	0.0018		RH = 50%			
	Permeability, P, O ₂ , barrier	0.11		RH = 90%			
	Permeability, P, CO ₂ , barrier	0.042		RH = 75%			[52]
	Permeability, P, CO ₂ , barrier	0.052		RH = 84%			
	Permeability, P, CO ₂ , barrier	1.3		RH = 90%			
Viscosity / Molecular mass relationship	Mark-Houwink constants for dilute solutions in water, $\eta = KM^a$	K value	A value	Mol mass x 10 ⁴	Method	Temp, °C	
		20	0.76	0.6 to 2.1	OS	25	
		300	0.50	0.9 to 17	OS	25	
		140	0.60	1.0 to 7.0	SD	25	[51]
		66.6	0.64	0.6 to 16	OS	30	
		42.8	0.64	1.0 to 80	LS	30	
		45.3	0.64	1.0 to 80	LS	30	
Burning characteristics	Ease of ignition	Moderately difficult					
	Self extinguishing	Slowly					
	Flame character	Slightly smokey					
	Fumes	Brown					[52]
	Odour	Sweetish aldehyde odour					
	Behaviour on heating	Softens and chars					
	Residue	Black residue					
Degradation	Degradation products	Quantitatively yields water		Temp = 250 °C			
		Mainly water and ethanol		Temp = 250 °C			[51]
OS = Osmotic pressure		SD = Sedimentation and diffusion		LS = Light scattering		RH = Humidity	

Lang et al. [53] prepared TFC membranes by coating porous PS membranes with PVA and cross-linking its surface. Aldehydes, dialdehydes and malic acid were used as cross-linking agents. The effect of additives to the PVA solution, of solvents used for making PVA solutions, and alcohols used for the membrane post-treatment on the RO performance were investigated. The effects of PVA solution coating, drying and heat treatment on the water permeability were also studied without cross-linking.

Li and Barbari [54] spin coated PVA hydrogels onto regenerated cellulose membranes to form thin-gel composite UF membranes. The effect of hydrogel thickness and the degree of cross-linking on the pure water permeation (PWP) and UF flux were studied. Flux decreased with increasing hydrogel thickness. Na et al. [55] dynamically prepared anti-fouling PVA TFC membranes by passing an aqueous solution containing PVA, cross-linking agents and additives, through a porous substrate membrane at a specific pressure, followed by heat treatment and drying. The effects of PVA concentration, dynamic coating time, concentration of additives, cross-linking agent concentration, curing time and support membrane on the PWP and protein retention of the resultant membranes were studied.

NF composite membranes based on PVA and sodium alginate (SA) were prepared by coating PVA / SA (95/5 wt %) solutions on microporous PS supports. For the formation of a defect free thin active layer on a support, the PS support was multi-coated with a dilute PVA / SA blend solution. The PVA / SA active layer formed was cross-linked at room temperature using an acetone solution containing glutaraldehyde as cross-linking agent [56].

Peter and Stefan [57] prepared asymmetric PVA membranes, which were used to separate organic solvents and phenols from aqueous solutions by using dicarboxylic acid containing 2 – 10 carbon atoms. Other workers [58] found that insoluble membranes could be formed by heating PVA films containing 5 – 15% oxalic, maleic, fumaric or phthalic acid at 80 – 120°C for 2 h, where no loss in solubility was observed under the same conditions with malonic, succinic, glutaric, adipic, or salicylic acids.

Chen et al. [59] used formaldehyde as a cross-linking agent to prepared PVA RO membranes that had high NaCl retention but reasonably low water permeability. The membranes were made by spreading a 6 – 8% solution of PVA on Plexiglass plates, drying at room temperature, and heating at 120 – 200°C. The membranes were immersed in the formalization bath (consisted of 20% H₂SO₄, 20% Na₂SO₄, and 5 – 7% HCHO) at room temperature for 20 h; then the temperature was raised to the desired level 50 – 60°C for 1 – 2 h. This was to allow sufficient time for the reagents to penetrate the membranes as uniformly as possible. Chang [60] used formaldehyde as a cross-linking agent to prepare asymmetric PVA membranes and determined the permeabilities and fluxes of 54 mono and divalent anions and cations of sodium and chloride salts. Sodium salts of monovalent polyatomic anions gave higher retentions than those of monovalent monatomic anions. Higher retentions of divalent cations suggest that the membrane surface is negatively charged.

Peter and Stefan [61] used the reaction of PVA with dialdehydes to produce water-insoluble membranes. PVA membranes treated with glyoxal, glutaraldehyde and adipic aldehyde showed promising retention characteristics for phenol, Na₂S and, to a lesser extent, pyridine and ammonia [57, 61]. Peter and Stefan [57] used various ketones to insolubilize asymmetric PVA membranes produced by phase-inversion precipitation. The behaviour of membranes cross-linked by a variety of ketones

was investigated. The flux and phenol retention were found to be inadequate. The chemical stability of these and other asymmetric PVA membranes in various organic and inorganic solutions was also evaluated [3].

Dick and Nicolas [62] described the preparation of PVA membranes cross-linked with toluene diisocyanate (TDI). The influence of different preparation factors on the osmotic properties of the membranes was examined. The membranes showed good selectivity towards aqueous salt solutions (salt retention of 98% with water permeability coefficients of 2×10^{-7} to 5×10^{-7} cm²/s) and had better temperature and pressure stabilities than CA membranes. Their resistance to acid and alkaline hydrolysis was satisfactory.

Shang and Peng [63] prepared a modified PVA composite UF membrane with good water flux and anti-fouling performance by IP. The best fabrication conditions were: PVA 0.5 – 2% (wt), TDI 0.08 – 0.5% (vol), NaOH 0.2 – 0.4% (wt), SLS 0.8 – 1% (wt) and contact time 30 – 60 sec. The modified PVA composite UF membrane with a thin hydrophilic PVA layer had better anti-fouling performance than the PES support membrane.

Peroxidisulfates, such as potassium persulfate (K₂S₂O₈), have been widely used as initiators of aqueous vinyl polymerizations. Apart from being a source of free radicals, peroxidisulfates are known to be strong oxidizing agents in aqueous medium. The use of K₂S₂O₈ for the insolubilization of PVA membranes has been extensively studied by research groups at Stellenbosch University. Immelman et al. [64] prepared flat-sheet and tubular composite RO membranes by depositing aqueous solutions of PVA and K₂S₂O₈ on asymmetric poly(arylether sulfone) substrate membranes. The effects of several variables in the preparation reaction on the salt retention properties of these membranes have been discussed by Sanderson et al. [65] and Immelman et al. [64]. Bezuidenhout [3] studied the modification of PVA by reaction with potassium persulfate to form tolerant insoluble NF membranes on tubular PES-UF substrates.

Water-insoluble films of PVA have been successfully prepared by using radiation treatment, often involving the use of Co-60 as a gamma radiation source [66, 67]. The transport properties and chemical stability of these membranes have also been evaluated [68]. Various methods of insolubilization of PVA membranes, including radiation treatment, have been patented by Wydeven [69]. Miura [70] also described a novel method of producing PVA membranes by using radiation. These membranes showed good chemical resistance, mechanical strength, water permeability, durability and hydrophilic properties.

Heat treatment of PVA membranes is used to improve their selectivity but it causes a decrease in permeability. Wydeven [69] and Katz and Wydeven [71, 72] used heat treatment to make water-insoluble PVA membranes for RO desalination, using various procedures. Symmetric membranes were prepared by casting, air drying, and treating the membranes at various temperatures [73]. The retention of NaCl was good but the flux was very low. Asymmetric membranes, on the other hand, were made by heat-treating membranes that were precipitated in a complexing bath (CuSO₄). Their flux was very high [71].

Koyama et al. [73-75] prepared anionic composite membranes from mixtures of PVA and poly(styrene sulfonic acid), and by cross-linking them by heat treatment. They determined their RO performance for NaCl and various organic components.

Maleic anhydride can react with PVA by esterification, but can also be grafted onto PVA to form side chains [76]. After these reactions PVA contains double bonds and ion-dissociable groups, and hence cross-linking and ionic bonding can easily occur, thus increasing water resistance and improving the mechanical properties. Immelman et al. [77] prepared PVA membranes by insolubilization, and by cross-linking PVA with polymethyl vinyl ether-alt-maleic anhydride, either in the presence or absence of sulfuric acid.

Nitto Denko [78] prepared heat-resistant semipermeable membranes by first coating a microporous PTFE film with an aqueous solution of PVA and H_2SO_4 , heating the product, then coating with poly(acrylic acid), and reheating to $160^\circ C$. The membranes gave high NaCl retention. Sanderson et al. [65] and Immelman et al. [79] also used sulfuric acid to prepare insoluble RO membrane from PVA.

Tsuchihara et al. [80] studied the effects of added LiCl on the permeabilities of membranes that were prepared from blends of PVA and cyanoethylated PVA. Membranes with excellent chlorine stability were produced by cross-linking PVA with divinylsulfone and several of its derivatives [47]. Composite membranes exhibiting low NaCl retentions and high fluxes at low pressures were reported.

Ichimura and Watanabe [81] prepared photocrosslinkable PVA by reaction with styrylpyridinium and quinolinium salts containing formyl groups. Hirotsu et al. [82] prepared membranes for the separation of water/ethanol mixtures by using photochemically reactive PVA containing 1.18% N-methylstyrylpyridinium groups, a 5% solution of the modified polymer was coated on a porous CA membrane and cross-linked to yield membranes with good water / alcohol separation factors.

Metal salts have been used in a variety of ways in the production of PVA membranes [57, 61, 69, 71, 83-86]. The metal salts most commonly used in the fabrication of PVA membranes are $CuSO_4$, $ZnCl_2$, $KCr(SO_4)_2 \cdot 12H_2O$, $AlCl_3 \cdot 6H_2O$, $Ba(OH)_2 \cdot 8H_2O$, and ferric salts. **Table 2-5** lists the publication activity on RO membranes made with PVA.

2.4.1 REACTIONS OF POLY(VINYL ALCOHOL) WITH BORIC ACID AND BORATE SALT SYSTEMS

PVA has several unique features: it is water soluble, crystallisable, capable of hydrogen bonding, and forms ion complexes with various ions such as borate [87, 88], vanadate [89], and congo red [90, 91]. Polymer ion complexes have a wide range of applications. The structure and properties of PVA-borate complexes in alkaline media have been widely studied and theoretically interpreted by many authors [92-98]. The mechanism of the cross-linking reaction of the borate ion with PVA is believed to be a so-called "di-diol" complexation. The complex is formed between two diol units and one borate ion [96, 97]. Viscoelastic properties of PVA-borate gels prepared under alkaline conditions have been studied [99].

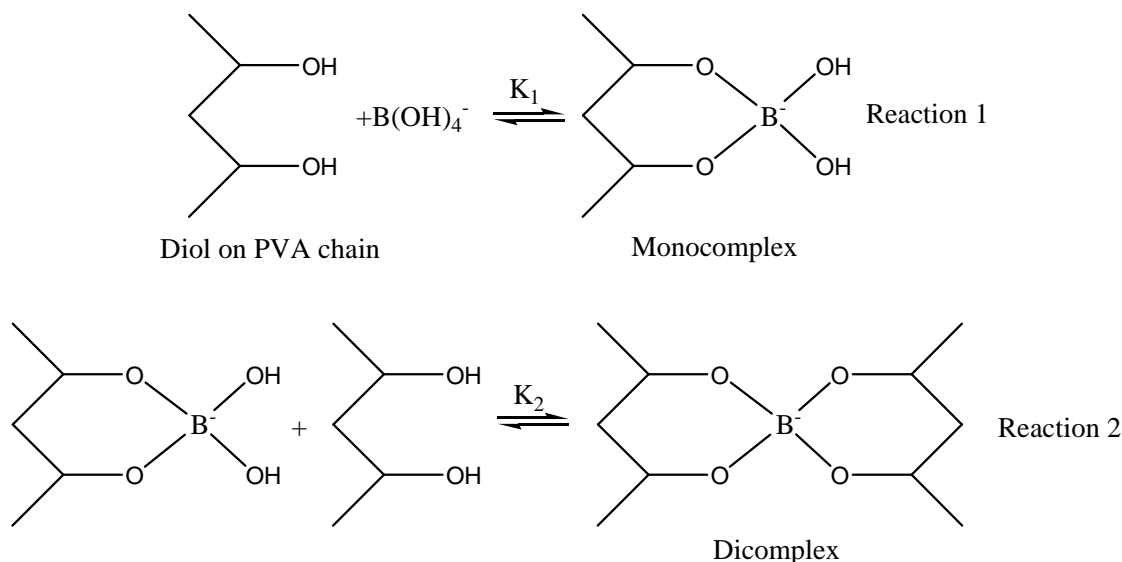
Ochiai et al. [87] and Kurokawa et al. [96] studied the viscosity behaviour of aqueous solutions of PVA with borate. They found that the viscosity was dependent on the boric acid, PVA and NaOH content. Shibayama et al. [100] also found a good proportional accordance between the intrinsic viscosity ratio of aqueous solutions of PVA with the borate ion and the equilibrium swelling ratio of gels.

Table 2-5: Development of poly(vinyl alcohol) (PVA) membranes [3, 44]

Year	Name	Treatment	Membrane performance				Reference
			Process	Conditions	Retention, %	Flux, Lmd	
1973	J.Y. Chen and W. Pusch	Formalization; dense film	RO, desalination	1000 ppm NaCl; 25°C; 4.2 MPa	92	3.3	[101]
1973	C.T. Chen et al.	PVA + Formaldehyde /H ₂ SO ₄ / Na ₂ SO ₄ / H ₂ O	RO, desalination	0.1 N NaCl, ; 25°C; 4.13 MPa	93 – 98	3.26 – 2.44	[59]
1975	Y. Nozawa and F. Higashide	Alkali bridging					[102]
1975	R. Dick and L. Nicolas	Diisocyanate	RO, desalination	35000 ppm NaCl, 28°C; 10 MPa	98	500	[62]
1976	S. Peter et al.	Cr ⁺³	RO, desalination	2000 ppm phenol; 25°C; 5 MPa	79	50	[84]
1976	S. Peter et al.	Boric acid, Cr ⁺³	RO, desalination	2000 ppm phenol; 25°C; 5 MPa	86	70	[84]
1977	T. Uragami and M. Sugihara	Alkali bridging					[103]
1977	S. Peter and R. Stefan	Cr ⁺³ ; GA	RO, desalination	2000 ppm phenol; 25°C; 5 MPa	95	30	[61]
1978	T. Uragami and M. Sugihara	Alkali bridging	UF	1% PEG 1000; 40°C; 5 MPa	40	30	[104]
1978	T. Uragami and M. Sugihara	Alkali bridging	UF	1% PEG 4000; 40°C; 5 MPa	100	28	[104]
1978	S. Peter and R. Stefan	Organic components; metal salts	RO, desalination	2000 ppm phenol; 25°C; 5 MPa	96	80	[105]
1980	K. Koyama et al.	PVA / PSSA + heat	RO, desalination	5000 ppm NaCl; 8 MPa	88 – 93	9 – 28	[73]
1980	Y. Kamiyama et al.	PVA + PIP + TMC + heat	RO, desalination	500 ppm MgSO ₄ ; 1.4 MPa	98	1250	[106]
1981	M. G. Katz and T. Wydeven	Heat treatment; asymmetric	RO, desalination	1800 ppm NaCl; 30°C; 7 MPa	83	560	[71]
1981	S. Peter and R. Stefan	Ketones	RO, desalination	2000 ppm phenol; 25°C; 5 MPa	73	100	[57]
1981	S. Peter and R. Stefan	Dicarboxylic acids	RO, desalination	2000 ppm phenol; 25°C; 5 MPa	74	60	[57]
1981	S. Peter and R. Stefan	Dialdehydes	RO, desalination	2000 ppm phenol; 25°C; 5 MPa	99	90	[57]
1981	M. G. Katz and T. Wydeven	Gamma radiation	RO, desalination	1000 ppm phenol; 25°C; 7 MPa	35	High	[107]
1981	R. W. Kormeyer and N.A. Peppas	PVA + GA / HCl / H ₂ O					[108]
1982	M. G. Katz and T. Wydeven	Heat treatment; symmetric	RO, desalination	1800 ppm phenol; 30°C; 7 MPa	78	30	[71]
1982	H. N. Chang	Formalization	RO, desalination	1800 ppm phenol; 25°C; 7 MPa	30	60	[60]
1982	T. Tsuchihara et al.	Cyanoethylation					[80]
1983	T. Wydeven et al.	CuSO ₄ ; heat treatment	RO, desalination			50	[69, 86]
1983	W. Ying	Boric acid, oxalic acid; Cr ⁺³	RO, desalination	3000 ppm phenol; 25°C; 5 MPa	90	5000	[109]
1983	W. Wojciak and A. Voelkel	Dicarboxylic acids					[58]
1983	NITTO	H ₂ SO ₄ + heat + PAN + heat	RO, desalination	5000 ppm NaCl; 4 MPa	96	420	[78]
1984	Y. Kazuse et al.	PVA + diamine + TMC	RO, desalination	500 ppm MgSO ₄	98	980	[110]
1985	W. Chiang and C. Hu	Maleic anhydride; heat					[76]

Year	Name	Treatment	Membrane performance				Reference
			Process	Conditions	Retention, %	Flux, Lmd	
1985	B. Gebben et al.	PVA + GA / HCl / H ₂ O	RO, desalination				[111]
1986	T. Uragami et al.	PVA + GA					[112]
1986	A. Higuchi and T. Lijima	PVA-co-IA					[113]
1986	Y. Kamiyama et al.	PVA + diamines + IPC / TMC	RO, desalination	500 ppm MgSO ₄	90–99	800–1250	[114]
1987	M. L. Brannon and N.A. Peppas	ZnCl ₂ ; GA		30 ppm theophylline		2.24	[83]
1987	T. Hirotsu et al.	Photochemical					[82]
1987	S. Jian and S.X. Ming	Dicarboxylic acids	RO, desalination	3500 ppm NaCl; 25°C; 4 MPa	95	120	[44]
1987	M. Miura	Gamma radiation					[70]
1987	Y. Kazuse et al.	PVA + PDA + TMC + heat	RO, desalination	2000 ppm NaCl; 25°C; 1 MPa	97	1000	[115]
1989	Y. Himeshima and T. Uemura	Divinylsulfone	RO, desalination	1500 ppm NaCl; 25°C; 0.75 MPa	15	330	[47]
1993	E. Immelman et al.	Sulfuric acid + heat	RO, desalination	2000 ppm NaCl; 25°C; 2 MPa	80	400	[65, 79]
1993	E. Immelman et al.	Persulfate + heat	RO, desalination	2000 ppm NaCl; 25°C; 2 MPa	60	650	[64, 65]
1993	E. Immelman et al.	PVA + PVME-alt-MA	RO, desalination	2000 ppm NaCl; 25°C; 2 MPa	60	600–900	[77]
1996	K. lang et al.	PVA + aldehyde or dialdehyde	RO, desalination	2000 ppm NaCl; 25°C; 1.724 MPa	90	120	[53]
1999	J. Jegal et al.	PVA + SA + GA	RO, desalination	1000 ppm PEG600, 25°C, 1.38 Mpa	95	1300	[56]
PEG = Polyethylene glycol		PIP = Piperazine	PDA = m-Phenylene diamine			TMC = Trimesoyl chloride	
PVA = Poly(vinyl alcohol)		MA = Maleic anhydride	IPC = Isophthaloyl chloride			IA = Itaconic acid	
PSSA = Polystyrene sulfonic acid		PVME = Polyvinyl methyl ether	PAN = Polyacrylonitrile			GA = Glutaraldehyde	

The PVA-borate cross-linking mechanism is divided into two reactions, i.e. mono-diol complexation (reaction 1) and a cross-linking reaction (reaction 2), as shown below [95, 96]



Once a borate ion is attached to a polymer chain (reaction 1), the polymer chain behaves as a polyelectrolyte unless the borate ion is removed from the chain. In this case, a significant contribution of electrostatic repulsion between mono-diol units is expected, resulting in expansion of the individual polymer chains.

In practical terms, the PVA-borax reaction may be used as the active component in low-cost, heavily filled, gellable water based systems for adhesives. Since gelation occurs immediately on contact, and is not reversible on heating, two-stage processes can be developed, where the polymer and the borax are applied separately and complex formation occurs on the substrate.

PVA forms complexes with boric acid and sodium borate (borax). Boric acid is presumed to form a mono-diol type bond, with borax forming a di-diol type bond [40, 116, 117]. It can be seen that the difunctional borax is more effective as a gelling agent than the monofunctional boric acid, as may be expected. It is also notable that the large molecules of polymer with a higher degree of polymerization more readily form gels at lower concentrations of the borax / boric acid additive [40, 118].

Sinton [88] studied the complexation chemistry of sodium borate with poly(vinyl alcohol). The cross-linked structure in the PVA-borax system was deduced by comparison of ^{11}B NMR spectra of the 2,4-pentanediol model system with that of the polymer system. Other model compounds studied were 1,5-pentanediol and 2,3-butanediol.

The viscosity behaviour of aqueous PVA-borax-NaCl systems was investigated by Ochiai et al. [87]. The intrinsic viscosity of PVA in borax solution increased with increasing borax concentration. In solutions containing both borax and NaCl, on the other hand, the viscosity decreased with increasing concentration of NaCl, and at high NaCl concentration phase separation was observed. In the absence of borax, the viscosity was nearly independent of the NaCl concentration. The results were interpreted in terms of a limited chain expansion due to charges and intrachain cross-links simultaneously introduced in the PVA chain when the chain was complexed with negatively charged tetrahedral borate ions.

Cheng and Rodriguez [116] studied the mechanical properties of borate cross-linked PVA gels. They found that H_3BO_3 does not introduce cross-links in PVA solutions, but that gelation does occur in the presence of cations, such as Na^+ .

Murakami et al. [117] studied the temperature-dependence of the viscosity of aqueous PVA-borax solutions. The intrinsic viscosity of aqueous PVA-borax solutions increased as the borax: PVA ratio increased, but it decreased as the temperature increased. The increase in intrinsic viscosity of PVA upon addition of borax may be due to an increase of the unperturbed dimensions of the PVA chain due to the complexation between borate and OH, and an increase in charge.

The mechanical and thermal properties of PVA cross-linked by borax were also investigated by Ochiai et al. [119]. Differential thermal analysis (DTA) curves for borax-cross-linked PVA showed that the polymer-borax complex was stable up to relatively high temperatures and that the crystalline structure of polymer chains decreased as the cross-link density increased. The temperature dependence of the mechanical properties also reflected the destructive effect of cross-linking on the crystalline structure and showed that the most highly cross-linked sample was a polymeric glass, up to the decomposition temperature. The cross-linked units did not crystallize and they immobilized the polymer chains.

Peter et al. [84] made asymmetric membranes by precipitating a complex of PVA and boric acid with acetone, redissolving the complex in an appropriate solvent, and drawing the solution onto a stainless steel plate. After being air dried and precipitated, the membranes were finally cross-linked by immersion in solutions containing polyvalent metal ions.

Borax can also be used for the preparation of dynamic membranes by the in-situ complexation of PVA membranes. Ying [109] prepared asymmetric dynamic membrane by pumping a PVA solution through a porous ceramic tube and then adding a solution of boric acid, oxalic acid and chromium salts to insolubilize the membrane thus formed. It was found that symmetric membranes could be obtained if the cross-linking agent was pumped through first, followed by the addition of the polymer.

Recently, Ma et al. [120] modified the surface of a PES UF membrane by an adsorption-cross-linking process of PVA with borax to enhance the antifouling. UF results showed that PVA modification caused a substantial but acceptable decrease in membrane flux. Results of fouling analysis, revealed a significant enhancement of the antifouling property, which was closely dependent on the PVA concentration and the cross-linking cycle. This is very interesting, as in the present study a similar system is used, but a better flux was obtained.

2.5 POLYAMIDE MEMBRANES

PA TFC membranes are prepared by IP reactions [6, 8, 9, 15, 27, 121]. IP has become a well-established and useful technique to prepare the dense, active top-layer of composite RO and NF membranes. Pioneering work on membrane preparation by IP was performed by Cadotte [122]. IP involves the polymerization of two reactive monomers dissolved in two immiscible solutions, respectively. The monomers can meet and react only at the interface of the solutions when the two solutions are brought into contact. As the condensation reaction continues, a polymer film is formed at the interface. The film is usually very thin because the growing interfacial polymer behaves as a barrier to diffusion of the two monomers, and the polymerization levels off at a limiting thickness, typically of the order of a micron or less. To provide durability to the fragile films the IP reaction is

frequently carried out on the surface of a microporous substrate, in which case the result is called a TFC membrane [123].

The composition, morphology and performance of interfacially polymerized membranes depends on several parameters, including the concentration of the reactants as well as their partition coefficients and reactivities, possible additives, solubility of the nascent polymer in the solvent phase, overall kinetics and diffusion rates of the reactants, presence of by-products, competitive side reactions, cross-linking reactions and post-reaction treatment [121, 124, 125]. The technique entails the application of an ultra-thin-film upon an asymmetric, porous support layer via an in-situ polymerization reaction occurring at the interface between two immiscible solvents containing reactive monomers (see **Figure 2-4**).

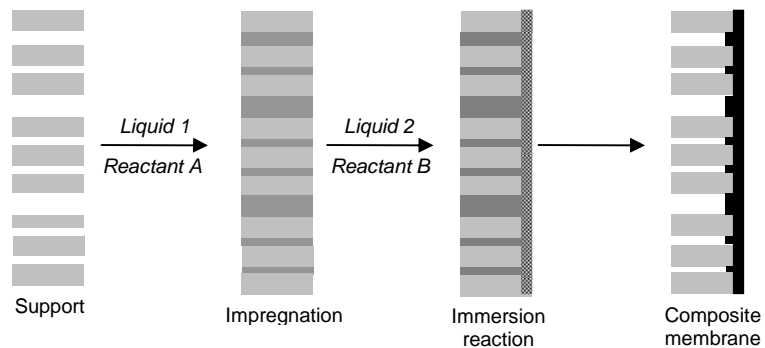


Figure 2-4: Schematic illustration of an interfacial polymerization (IP) reaction (based on [126])

A TFC membrane is a bi-layer film consisting of a thick, porous, non-selective support layer formed in a first process step with another ultra-thin selective barrier layer on top of it, formed in a second step. In TFC membranes the two layers are almost always different from one another in chemical composition and each individual layer can be optimized for its particular function. The active skin layer is the key component. It controls mainly the separation properties of the membrane, while the support layer gives the membrane the necessary mechanical properties. The selective layer of the TFC RO membrane comprises the partially cross-linked aromatic PA, as shown in **Figure 2-5**.

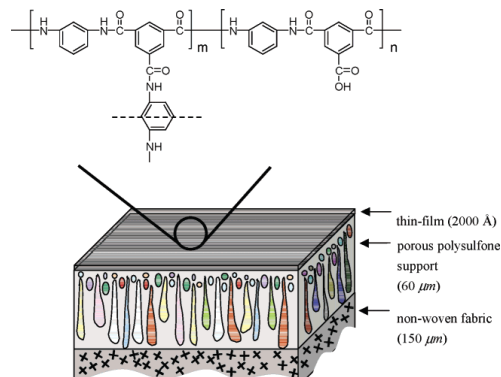


Figure 2-5: Schematic of a thin-film composite (TFC) RO membrane and the chemical structure of an aromatic polyamide thin-film layer (based on [127])

Many different polymers have been tested for their suitability for the production of RO membranes. The materials used to produce the skin layer include polyamides from aliphatic or

aromatic diamines [127-132], or their mixtures [126], polysulfonamides [133], poly(aminostyrene) [134, 135], aromatic diols and a combination of diol amides [136], while the cross-linking agents such as trimesoyl chloride (TMC), isophthaloyl chloride (IPC) and terephthaloyl chloride (TPC) are most commonly employed. Other polymers, such as polyurea, polyurea-amide, polyetheramide, etc. [27, 137-140] have been investigated as candidate TFC materials. Among these polymers, the cross-linked aromatic PA obtained via IP of *m*-phenylenediamine (MPD) in aqueous phase and TMC in organic phase is the most successful commercial product [129].

TFC membrane productivity and salt retention efficiency are of equal importance. It may be important in specific applications to increase membrane productivity without any appreciable change in salt retention efficiency; on the other hand, many applications may demand membranes that provide higher salt retention efficiency without adversely affecting membrane productivity [141, 142].

The relationship between membrane performance and the molecular structure of aromatic polyamides has been studied. Masahiko et al. [143] studied the relationship between the surface structure of skin layers of cross-linked aromatic PA RO membranes and their RO performance. Roh et al. [144] proposed that the mechanical strength of the barrier layer should be an important factor in determining its performance. Zhang et al. [42] prepared a composite membrane from piperazine (PIP) and TMC but coated the surface with PVA to improve the hydrophilicity and smoothness.

It is known that the membranes fabricated from the various aromatic polyamides have low water permeability as a result of the rigid cross-linked structure [27]. Incorporation of various polymers such as PVA and polyvinyl phenol to the aromatic polyamides has been studied to mitigate the cross-linked barrier with bulky groups in the polymer backbone or side chain [44, 134]. **Table 2-6** lists details of some of the commercially available PA membranes.

2.6 POLY(VINYL ALCOHOL) / POLYAMIDE MEMBRANES

An insolubilized gel layer of PVA deposited between the support membrane and the PA layer can solve many of the problems that arise in the preparation of the TFC membranes. The PVA gel layer can cover the larger pores and the defects of the support membranes; it can act as an excellent support for the fragile PA layer, and it can enhance the hydrophilicity of the membrane surface [3].

Three composite membranes with significant chlorine resistance, NTR-7250, NTR-729HF and NTR-739HF, have been commercialized by Nitto Denko for use in desalinating low salinity brackish water [110, 142, 145]. These membranes have particularly found use in the final filtration of ultrapure water in semiconductor chip manufacturing, where the claimed chlorine resistance of these membranes was seen as an advantage for system disinfection and sterilization. The development of chlorine-resistant PVA-based RO membranes by Nitto Electric Industrial Co. has been discussed by Kamiyama et al. [146] and Kawada et al. [142]. The NTR-7250 membrane is manufactured in continuous flat sheet form and sold as four and eight inch diameter spiral wound modules. The NTR-7250 membrane is chlorine resistant and exhibits very high flux at low operating pressures.

Thus, Nitto began developing membranes with high salt retention, high product water fluxes and excellent chlorine resistance. Among the new developments were the NTR-739HF and NTR-729HF membranes, which are low-pressure RO membranes that can be applied for brackish water desalination. Both these membranes are TFC in which the PS UF substrates are covered with ultra-thin skin layers, featuring high salt retention at low pressure.

Table 2-6: Composition and RO performance of various polyamide (PA) membranes [2, 3, 27]

Membrane Designation	Active layer	Test conditions	Retention, %	Flux, Lmd	Reference
NS-100 / PA-100	PEI + IPC	35000 ppm NaCl, 10.337 MPa, 25°C	99.3	30.57	[137]
PA-300	Polyepiamine + IPC	35000 ppm NaCl, 10.337 MPa, 25°C	99.4	33.96 – 42.45	[140, 147]
RC-100	Polyepiamine + TDI	35000 ppm NaCl, 10.337 MPa, 25°C	98 – 99		[140, 147, 148]
LP-300	Polyepiamine + IPC	5530 ppm NaCl, 2.58 MPa, 25°C	98.5	33.96	[149]
NTR-9197	Polyurea layer	500 ppm NaCl, 3.87 MPa, 25°C	99.0	67.92	[146, 150]
NTR-9199	Polyurea layer	500 ppm NaCl, 3.87 MPa, 25°C	99.5	33.96	[146, 150]
PIP	PIP + IPC	35000 ppm NaCl, 9.68 MPa, 25°C	98.00	44.15	[45, 151]
NS-300 family	PIP + TMC	35000 ppm NaCl, 10.337 MPa, 25°C	98.00	44.15	[151, 152]
	PIP oligomer + IPC + TMC	35000 ppm SSW, 10.337 MPa, 25°C	99.00	22.07	[151-153]
NF-40	PIP + TMC	Pure water, 1.45 MPa, 25°C		42.45	[154-156]
NTR-7250	PIP + PVA + TMC	500 ppm MgSO ₄ , 1.29 MPa, 25°C	99	50.94	[110, 146]
UTC-20HF	Poly(piperazineamide)	1500 ppm NaCl, 1.47 MPa, 25°C	70	101.88	[157]
ATF-50	Poly(piperazineamide)	2000 ppm NaCl, 1.45 MPa, 25°C	69	101.88	[27]
BR-101	p-phenylenediamine + TMC	35000 ppm NaCl, 3.87 MPa, 25°C	99	11.88	[158]
TTM-20	N-methyl-amino-methyl + IPC + TMC	500 ppm NaCl, 2.58 MPa, 25°C	20	203.77	[158]
TTM-60		500 ppm NaCl, 2.58 MPa, 25°C	60	203.77	[158]
TTM-90		35000 ppm NaCl, 5.16 MPa, 25°C	98.5	50.94	[158]
FT-30	MPD + TMC	35000 ppm SSW, 6.891 MPa, 25°C	99.4	30.56	[129, 139, 155, 159]
TFCL	MPD + TMC		99	1.41	[160]
CPA2 / NTR-759	MPD + IPC / TMC	2000 ppm NaCl, 2.71 MPa, 25°C	99	42.45	[132, 161]
UTC-70	Aromatic polyamide with carboxylate groups	1500 ppm NaCl, 1.45 MPa, 25°C	> 99.5	37.35	[162, 163]
A-15	1,3-benzenediamine + cyclohexane-1,3,5-tricarbonyl chloride	200 ppm NaCl, 2.71 MPa, 25°C	99		[138, 164, 165]
NCM1	Polyamide polymer	1500 ppm NaCl, 1.45 MPa, 25°C	99	50.94	[27]
NS-200	Furfuryl alcohol + sulfuric acid	35000 ppm NaCl, 9.68 MPa, 25°C	99.8 – 99.9	33.96	[166]
PEC-1000	1,3,5-tris(hydroxyl-ethyl) isocyanuric acid + furfuryl alcohol + sulfuric acid	35000 ppm NaCl, 6.45 MPa, 25°C	99.9	20.37	[167, 168]
2N31	Ethylenediamine + TMC	1000 ppm NaCl, 5.513 MPa, 25°C	96.9	543.39	[3]

PEI = Polyethyleneimine TDI = Toluene diisocyanate PIP = Piperazine MPD = m-Phenylenediamine
IPC = Isophthaloyl chloride TMC = Trimesoyl chloride PVA = Poly(vinyl alcohol) SSW = Synthetic seawater

In the Nitto Denko patent [110] a membrane was made by the IP reaction of TMC with an aqueous solution containing 0.25% PIP, 0.25% PVA and 0.5% NaOH, followed by a heat-curing step at 110°C for completion of the cross-linking reaction and insolubilization of the PVA layer. The resulting membrane exhibits about 99% MgSO₄ retention and 50.94 Lmd flux, tested at 1.29 MPa with a 500 ppm feed water. The patent claims a discrete layer of insolubilized PVA resting upon a microporous support, and a polypiperazineamide barrier layer resting upon the PVA layer. The method of making the membrane allows concurrent esterification of PVA by TMC during amide formation, which correlates with an alkaline pH limit of 9 stated for the NTR-7250 [27].

In the Nitto Denko patent applications [106, 110, 114, 115, 169] PVA and difunctional secondary amines were cross-linked with di- and trifunctional acid chlorides on the PS support to form TFC RO membranes. This patent [126] describes procedures for the preparation of a composite membrane of PVA / polypiperazineamide, wherein the membrane is treated by irradiation treatment to increase the degree of cross-linking. The porous PS support was coated with an aqueous solution containing 0.25% PVA, 0.25% N,N'-dimethyl-1,2-ethanediamine and 0.5% NaOH. The support was then dipped into a hexane solution of 1.0% TMC for 1 min. The interfacial polyamide / ester was then heated to 110°C to insolubilize unreacted PVA, followed by 10 Mrad of irradiation with an electron beam. The composition of the membrane barrier layer is believed to comprise of PVA and piperazine trimesoylamide. **Table 2-7** lists some solute retention data of these membranes, compared to CA [8, 9, 15, 27, 142].

Table 2-7: Comparison of solute retention data of NTR-7250HF, NTR-729HF and NTR-739HF membranes with that of cellulose acetate (CA) membranes [27]

Solute	Retention, %			
	NTR-7250HF	NTR-729HF	NTR-739HF	CA
NaCl	60	92	95	97
MgSO ₄	89	> 99	> 99	> 99
Ethanol	20	25	30	9
Isopropanol	-	70	75	45
N-methyl-pyrrolidone	-	86	84	60
Sucrose	99	> 99	> 99	> 99
Test pressure: 1 MPa for NTR membranes, 3 MPa for CA membranes				

Shang and Peng [170] used the IP of PVA, piperazine and terephthaloyl chloride on a PES support membrane to produce a composite UF membrane with a thin hydrophilic layer. Infrared spectra showed that PVA exists in the surface layer and the PA-PVA/PES composite UF membrane has better water flux and antifouling performance against protein and oil, compared to PA / PES composite UF membranes without PVA.

2.7 REFERENCES

- [1] Lonsdale, H.K., U. Merten, and R.L. Riley, *Transport properties of cellulose acetate osmotic membranes*. Journal of Applied Polymer Science, 1965. 9(4): p. 1341-1362.
- [2] Hurndall, M.J., *The chemistry of poly-2-vinylimidazoline reverse osmosis membranes*, PhD. thesis, 1991. University of Stellenbosch; Stellenbosch.
- [3] Bezuidenhout, D., *Polyvinyl alcohol and amine-modified polyvinyl alcohol nanofiltration and reverse osmosis membranes*, MSc. thesis, 1991. University of Stellenbosch; Stellenbosch.

- [4] Mulder, M., *Basic principles of membrane technology*, Kluwer Academic: Dordrecht, 1992.
- [5] Lonsdale, H.K., *The growth of membrane technology*. Journal of Membrane Science, 1982. 10: p. 81-181.
- [6] Baker, R.W., E.L. Cussler, W. Eykamp, W.J. Koros, R.L. Riley, and H. Strathmann, *Membrane separation systems: recent developments and future directions*. First ed., Noyes data corporation: New Jersey, U.S.A., 1991.
- [7] Loeb, S. and S. Sourirajan, *Sea water demineralization by means of an osmotic membrane, in saline water conversion-II*. Advances in Chemistry Series, 1963. 38. p. 15
- [8] Porter, M.C., *Handbook of industrial membrane technology*. First ed., Noyes publications: New Jersey, U.S.A., 1990
- [9] Noble, R.D. and S.A. Stern, *Membrane separations technology: principles and applications*. First ed., Membrane Science and Technology Series, 2, Elsevier: Amsterdam. The Netherlands. 1995
- [10] Bechhold, H., *Kolloidstudien mit der Filtrationsmethode*. Z. Physical Chemistry, 1907. 60: p. 257-318.
- [11] Zsigmondy, R. and W. Bachmann, *Über neue Filter*, Zeitschrift für anorganische und allgemeine Chemie, 1918. 103: p. 119-128.
- [12] Ferry, J.D., *Ultrafilter membranes and ultrafiltration*. Chemical Review, 1936. 18(3): p. 373-455.
- [13] Elford, W.J., *Principles governing the preparation of membranes having graded porosities. The properties of 'gradocol' membranes as ultrafilters*. Transactions of the Faraday Society, 1937. 33: p. 1094-1116.
- [14] Michaels, A.S., *High flow membrane*. United States Patent 3,615,024 (Oct 1971).
- [15] Baker, R.W., *Membrane technology and applications*. Second ed. 2004, California: John Wiley & Sons Inc. p. 237-272.
- [16] Belfort, G., *Desalting experience by hyper-filtration in the U.S.*, in *Synthetic Membrane Processes*, Academic Press: Orlando, 1984. Chapter 7
- [17] Potts, D.E., R.C. Ahlert, and S.S. Wang, *A critical review of fouling of reverse osmosis membranes*. Desalination, 1981. 36(3): p. 235-264.
- [18] Golomb, A. and F. Besik, *Reverse osmosis - a review of its applications to waste treatment, water and seawater*. 1970. p. 81-89.
- [19] Zhang, S.H., X.G. Jian, and Y. Dai, *Preparation of sulfonated poly(phthalazinone ether sulfone ketone) composite nanofiltration membrane*. Journal of Membrane Science, 2005. 246(2): p. 121-126.
- [20] Kim, I.C., H.G. Yoon, and K.H. Lee, *Formation of integrally skinned asymmetric PEI NF membranes by phase inversion process*. Journal of Applied Polymer Science, 2002. 84(6): p. 1300-1307.
- [21] Lin, D.J., C.L. Chang, T.C. Chen, and L.P. Cheng, *Microporous PVDF membrane formation by immersion precipitation from water/TEP/PVDF system*. Desalination, 2002. 145: p. 25-29.
- [22] Kastelan-Kunst, L., V. Dananic, B. Kunst, and K. Kosutic, *Preparation and porosity of cellulose triacetate reverse osmosis membranes*. Journal of Membrane Science, 1996. 109: p. 223-230.

- [23] McHugh, A.J. and D.C. Miller, *The dynamics of diffusion and gel growth during nonsolvent-induced phase inversion of polyethersulfone*. Journal of Membrane Science, 1995. 105: p. 121-136.
- [24] Osmonics Inc., *Preparation of polyethersulfone membranes*. United States Patent 6,056,903 (2000).
- [25] Witte, P. Van de, P.J. Dijkstra, J.W.A. Van den Berg, and J. Feijen, *Phase separation processes in polymer solutions in relation to membrane formation*. Journal of Membrane Science, 1996. 117: p. 1-31.
- [26] Gelman Sciences Inc., *Hydrophilic membranes prepared from polyethersulfone / poly-2-oxazoline / polyvinylpyrrolidone blend*. European Patent WO / 1993 / 005871 (1993).
- [27] Petersen, R.J., *Composite reverse osmosis and nanofiltration membranes*. Journal of Membrane Science, 1993. 83: p. 81-150.
- [28] Barth, C. and B.A. Wolf, *Evidence of ternary interaction parameters for polymer solutions in mixed solvents from headspace-gas chromatography*. Polymer, 2000. 41: p. 8587-8596.
- [29] Barton, B.F., J.L. Reeve, and A.J. McHugh, *Observations on the dynamics of nonsolvent-induced phase inversion*. Journal of Polymer Science B : Polymer Physics, 1997. 35: p. 569-585.
- [30] Han, M.J., P.M. Bummer, M. Jay, and D. Bhattacharyya, *Phase transitions of polysulfone solution during coagulation*. Polymer, 1995. 36(24): p. 4711-4714.
- [31] Han, M.J. and D. Bhattacharyya, *Morphology and transport study of phase inversion polysulfone membranes*. Chemical Engineering Communications, 1994. 128: p. 197-209.
- [32] Tkacik, G. and L. Zeman, *Component mobility analysis in the membrane-forming system water/N-methyl-2-pyrrolidone / polyethersulfone*. Journal of Membrane Science, 1987. 31: p. 273-288.
- [33] Mosqueda-Jiminez, D.B., R.M. Narbaitz, and T. Matsuura, *Manufacturing conditions of surface-modified membranes: effects on ultrafiltration performance*. Separation and Purification Technology, 2004. 37: p. 51-67.
- [34] Barth, C., M.C. Goncalves, A.T.N. Pires, J. Roeder, and B.A. Wolf, *Asymmetric polysulfone and polyethersulfone membranes: Effects of thermodynamic conditions during formation on their performance*. Journal of Membrane Science, 2000. 169(2): p. 287-299.
- [35] Marchese, J., M. Ponce, N.A. Ochoa, P. Pradanos, L. Palacio, and A. Hernandez, *Fouling behaviour of polyethersulfone UF membranes made with different PVP*. Journal of Membrane Science, 2003. 211: p. 1-11.
- [36] Han, M.J. and S.T. Nam, *Thermodynamic and rheological variation in polysulfone solution by PVP and its effect in the preparation of phase inversion membrane*. Journal of Membrane Science, 2002. 202: p. 55-61.
- [37] Kim, J.H. and K.H. Lee, *Effect of PEG additive on membrane formation by phase inversion*. Journal of Membrane Science, 1998. 138: p. 153-163.
- [38] Chaturvedi, B.K., A.K. Ghosh, V. Ramachandhran, M.K. Trivedi, M.S. HanTa, and B.M. Misra, *Preparation, characterization and performance of polyethersulfone ultrafiltration membranes*. Desalination, 2001. 133: p. 31-40.

- [39] Chiellini, E., A. Corti, S. D'Antone, and R. Solaro, *Biodegradation of poly(vinyl alcohol) based materials*. Progress in Polymer Science 2003. 28(6): p. 963-1014.
- [40] Finch, C.A., *Polyvinyl alcohol: properties and applications*, John Wiley and Sons: New York, 1973.
- [41] Finch, C.A., *Polyvinyl alcohol-developments*, John Wiley and Sons: New York, 1992.
- [42] Zhang, W., G. He, P. Gao, and G. Chen, *Development and characterization of composite nanofiltration membranes and their application in concentration of antibiotics*. Separation and Purification Technology, 2003. 30 p. 27-35.
- [43] Reid, C.E. and H.G. Spencer, *Ultrafiltration of salt solutions by ion-excluding and ion-selective membranes*. Journal of Applied Polymer Science, 1960. 4(12): p. 354-361.
- [44] Jian, S. and S.X. Ming, *Cross-linked PVA-PS thin-film composite membrane for reverse osmosis*. Desalination, 1987. 62: p. 395-403.
- [45] Cadotte, J.E., K.E. Cobian, R.H. Forrster, and R.J. Petersen. *Continued evaluation of in-situ-formed condensation polymers for reverse osmosis membranes*. NTIS Report No. PB-253193, (1976).
- [46] Fujimaki, H., M. Kurihara, and T. Uemura. Japan Kokai, Tokyo Koho Japan 60,183,009 (Chemical Abstract 104:21033u) (1990)
- [47] Himeshima, Y. and T. Uemura. Japan Kokai, Tokyo Koho Japan 01,254,203 (Chemical Abstract 112: 1409148) (11 Oct 1989).
- [48] Cadotte, J.E., *Alkali resistant hyper-filtration membrane*. United States Patent 4,895,661 (1990).
- [49] Saunders, K.J., *Organic polymer chemistry*. 1973: London, Chapman and Hall Ltd.
- [50] Mark, H.F., N.M. Bikales, C.G. Overberger, and G. Menges, in *Encyclopedia of polymer science and engineering*, New York: W. Interscience, 1985.
- [51] Brandrup, J. and E.H. Immergut, *Polymer handbook*. Second ed., New York: Wiley Interscience, 1975.
- [52] Sweeting, O.J., *The science and technology of polymer films*. New York: Wiley Interscience, 1971.
- [53] Lang, K., S. Sourirajan, T. Matsuura, and G. Chowdhury, *A study on the preparation of polyvinyl alcohol thin-film composite membranes and reverse osmosis testing*. Desalination, 1996. 104: p. 185-196.
- [54] Li, R.H. and T.A. Barbari, *Performance of poly(vinyl alcohol) thin-gel composite ultrafiltration membranes*. Journal of Membrane Science, 1995. 105 p. 71-78.
- [55] Na, L., L. Zhongzhou, and X. Shuguang, *Dynamically formed poly(vinyl alcohol) ultrafiltration membranes with good anti-fouling characteristics*. Journal of Membrane Science, 2000. 169 p. 17-28.
- [56] Jegal, J., N.-W. Oh, and K.-H. Lee, *Preparation and characterization of PVA/SA composite nanofiltration membranes*. Journal of Applied Polymer Science, 2000. 77: p. 347-354.
- [57] Peter, S. and R. Stefan, in. *Synthetic Membranes*, ACS Symposium Series, 154, American Chemical Society, Washington, DC, 1981. Volume 2: p. 281.
- [58] Wojciak, W. and A. Voelkel, *Polimery (Warsaw)*, 1983. 28(5): p. 153 [Chemical Abstract 99 159341c (1983)].

- [59] Chen, C.T., Y.J. Chang, M.C. Chen, and A.V. Tobolsky, *Formalized poly(vinyl alcohol) membranes for reverse osmosis*. Journal of Applied Polymer Science, 1973. 17(3): p. 789-796.
- [60] Chang, H.N., *Reverse osmosis separation of inorganic salts using poly(vinyl alcohol) membranes*. Desalination, 1982. 42(1): p. 63-77.
- [61] Peter, S. and R. Stefan, Ger. Offen. 2,730,528, 1979.
- [62] Dick, R. and L. Nicolas, *Membranes composites prepare a partir d'alcool polyvinylique et de diisocyanate de toluylene destinees a l'osmose inverse*. Desalination, 1975. 17(3): p. 239-255.
- [63] Shang, Y. and Y. Peng, *UF membrane of PVA modified with TDI*. Desalination, 2008. 221: p. 324-330.
- [64] Immelman, E., D. Bezuidenhout, R.D. Sanderson, E.P. Jacobs, and A.J. Van Reenen, *Poly(vinyl alcohol) gel sub-layers for reverse osmosis membranes. III. Insolubilization by cross-linking with potassium peroxydisulphate*. Desalination, 1993. 94(2): p. 115-132.
- [65] Sanderson, R.D., E. Immelman, D. Bezuidenhout, E.P. Jacobs, and A.J. Van Reenen, *Polyvinyl alcohol and modified polyvinyl alcohol reverse osmosis membranes*. Desalination, 1993. 90 (1-3): p. 15-29.
- [66] Peppas, N.A. and E.W. Merrill, *Poly(vinyl alcohol) hydrogels: Reinforcement of radiation-cross-linked networks by crystallization*. Journal of Polymer Science B. 14(2): p. 441-457.
- [67] Peppas, N.A., *Development of cross-linked PVA biomembranes*, American Chemical Society, Polymer Preprints., 1977. 18(1): p. 794-797.
- [68] Wesslein, M., A. Heintz, and R.N. Lichtenthaler, *Pervaporation of liquid mixtures through poly(vinyl alcohol) (PVA) membranes. I. Study of water containing binary systems with complete and partial miscibility*. Journal of Membrane Science. 51(1-2): p. 169-179.
- [69] Wydeven, T., *Method for the preparation of thin-skinned asymmetric reverse osmosis membranes and products thereof*. United States Patent 4,456,708 (1984).
- [70] Miura, M. European Patent Application EP 302,650 (1987).
- [71] Katz, M.G. and T. Wydeven, in. *Synthetic Membranes*, ACS Symposium Series, 153, American Chemical Society, Washington, DC, 1981. Volume 1: p. 383.
- [72] Katz, M.G. and T. Wydeven, *Selective permeability of PVA membranes. II. Heat-treated membranes*. Journal of Applied Polymer Science, 1982. 27(1): p. 79-87.
- [73] Koyama, K., M. Okada, and M. Nishimura, *An interpolymer anionic composite reverse osmosis membrane derived from poly(vinyl alcohol) and poly(styrene sulfonic acid)*. Journal of Applied Polymer Science, 1982. 27(8): p. 2783-2789.
- [74] Koyama, K., T. Nishi, I. Hashida, and M. Nishimura, *The rejection of polar organic solutes in aqueous solution by an interpolymer anionic composite reverse osmosis membrane*. Journal of Applied Polymer Science, 1982. 27(8): p. 2845-2855.
- [75] Koyama, K., E. Kimura, I. Hashida, and M. Nishimura, *Rejection of phenolic derivatives in aqueous solution by an interpolymer anionic composite reverse osmosis membrane*. Journal of Applied Polymer Science, 1984. 29(9): p. 2929-2936.
- [76] Chiang, W.-Y. and C.-M. Hu, *Modelling the free radical solution and bulk polymerization of methyl methacrylate*. Journal of Applied Polymer Science, 1985. 30(10): p. 3985-4012.

- [77] Immelman, E., R.D. Sanderson, E.P. Jacobs, and A.J. Van Reenen, *Poly(vinyl alcohol) gel sub-layers for reverse osmosis membranes. II. Insolubilization by cross-linking with poly(methyl vinyl ether-alt-maleic anhydride)*. *Desalination*, 1993. 94(1): p. 37-54.
- [78] Nitto Electrical Industrial Co. Ltd. Japan Kokai, Tokkyo Koho Japan 59 69,107 (1984).
- [79] Immelman, E., R.D. Sanderson, E.P. Jacobs, and A.J. Van Reenen, *Poly(vinyl alcohol) gel sub-layers for reverse osmosis membranes. I. Insolubilization by acid-catalyzed dehydration*. *Journal of Applied Polymer Science*, 1993. 50(6): p. 1013-1034.
- [80] Tsuchihara, T., Y. Ohmura, and H. Ohya, Maku, 1982. 7(2): p. 123 [Chemical Abstract 96 223839p (1982)].
- [81] Ichimura, K. and S. Watanabe, *Preparation and characteristics of photocrosslinkable poly(vinyl alcohol)*. *Journal of Polymer Science*, 1982. 20(6): p. 1419-1432.
- [82] Hirotsu, T., K. Ichimura, K. Mizoguchi, and E. Nakamura. Japan. Kokai, Tokkyo Koho Japan 62,129,107 (1987).
- [83] Brannon, M.L. and N.A. Peppas, *Solute diffusion in swollen membranes: Part VIII. Characterization of and diffusion in asymmetric membranes*. *Journal of Membrane Science*, 1987. 32(2-3): p. 125-138.
- [84] Peter, S., N. Hese, and R. Stefan, *Phenol-selective, highly resistant RO-membranes made from PVA for the purification of toxic industrial wastes*. *Desalination*, 1976. 19(1-3): p. 161-167.
- [85] Gryte, C.C., *1,1,1-Tris(hydroxymethyl)propane-cross-linked poly(vinyl alcohol)-poly(styrene sodium sulfonate) interpolymer membranes*. *Journal of Applied Polymer Science*, 1978. 22(8): p. 2401-2402.
- [86] Wydeven, T. and M.G. Katz. United States Patent 392,092 (1983).
- [87] Ochiai, H., Y. Kurita, and I. Murakami, *Viscosity behaviour of the polyelectrolyte poly(vinyl alcohol) having some intrachain cross-links*. *Die Makromolekulare Chemie*, 1984. 185(1): p. 167-172.
- [88] Sinton, S.W., *Complexation chemistry of sodium borate with poly(vinyl alcohol) and small diols. A ¹¹B NMR study*. *Macromolecules*, 1987. 20(10): p. 2430-2441.
- [89] Shibayama, M., M. Adachi, F. Ikkai, H. Kurokawa, S. Sakurai, and S. Nomura, *Gelation of poly(vinyl alcohol)-vanadate aqueous solutions*. *Macromolecules*, 1993. 26(4): p. 623-627.
- [90] Ikkai, F., M. Shibayama, S. Nomura, and C.C. Han, *Complexation of poly(vinyl alcohol)-congo red aqueous solutions. 3. Dynamic light scattering study*. *Journal of Polymer Science*, 1996. 34(5): p. 939-945.
- [91] Tsujimoto, M. and M. Shibayama, *Dynamic light scattering study on reentrant sol-gel transition of poly(vinyl alcohol)-congo red complex in aqueous media*. *Macromolecules*, 2002. 35(4): p. 1342-1347.
- [92] Pezron, E., L. Leibler, A. Ricard, F. Lafuma, and R. Audebert, *Complex formation in polymer-ion solution. 1. Polymer concentration effects*. *Macromolecules*, 1989. 22(3): p. 1169-1174.
- [93] Pezron, E., A. Ricard, F. Lafuma, and R. Audebert, *Reversible gel formation induced by ion complexation. 1. Borax-galactomannan interactions*. *Macromolecules*, 1988. 21(4): p. 1121-1125.

- [94] Pezron, E., L. Leibler, A. Ricard, and R. Audebert, *Reversible gel formation induced by ion complexation. 2. Phase diagrams*. *Macromolecules*, 1988. 21(4): p. 1126-1131.
- [95] Keita, G., A. Ricard, R. Audebertt, E. Pezron, and L. Leibler, *The poly(vinyl alcohol)-borate system: influence of polyelectrolyte effects on phase diagrams*. *Polymer*, 1995. 36(1): p. 49-54.
- [96] Kurokawa, H., M. Shibayama, T. Ishimaru, S. Nomura, and W.I. Wu, *Phase behaviour and sol-gel transition of poly(vinyl alcohol)-borate complex in aqueous solution*. *Polymer*, 1992. 33(10): p. 2182-2188.
- [97] Leibler, L., E. Pezron, and P.A. Pincus, *Viscosity behaviour of polymer solutions in the presence of complexing ions*. *Polymer*, 1988. 29(6): p. 1105-1109.
- [98] Wise, E.T. and S.G. Weber, *A simple partitioning model for reversibly cross-linked polymers and application to the poly(vinyl alcohol) / borate system ("slime")*. *Macromolecules*, 1995. 28: p. 8321-8327.
- [99] Robb, I.D. and J.B.A.F. Smeulders, *The rheological properties of weak gels of poly(vinyl alcohol) and sodium borate*. *Polymer*, 1997. 38(9): p. 2165-2169.
- [100] Shibayama, M., H. Kurokawa, S. Nomura, M. Muthukumar, R.S. Stein, and S. Roy, *Small-angle neutron scattering from poly(vinyl alcohol)-borate gels*. *Polymer*, 1992. 33(14): p. 2883-2890.
- [101] Chen, J.Y. and W. Pusch, *Solute-membrane interactions in hyper-filtration*. *Journal of Applied Polymer Science*, 1987. 33(5): p. 1809-1822.
- [102] Nozawa, Y. and F. Higashide, *Journal of Polymer Science B*, 1975. 13: p. 433.
- [103] Uragami, T. and M. Sugihara, *Studies on syntheses and permeabilities of special polymer membranes. III. Permeation of aqueous alcohol solutions and binary organic liquid mixtures through alkali bridged poly(vinyl alcohol) membranes*, *Angewandte Makromolekulare Chemie*, 1977. 57: p. 123-137.
- [104] Uragami, T. and M. Sugihara, *Studies on syntheses and permeabilities of special polymer membranes. X. Effects of conditions of membrane preparation on permeation characteristics of cellulose acetate membranes in separation of aqueous polymer solutions*, *Angewandte Makromolekulare Chemie*, 1978. 70: p. 119-134.
- [105] Peter, S. and R. Stefan, *Proc. 6 Intern. Symp., Fresh Water from the Sea*, 1978. 6(3): p. 239-246.
- [106] Kamiyama, Y., N. Yoshioka, and K. Nakagome, *Ger. Offen. DE 3,129,702*, 1982.
- [107] Katz, M.G. and T. Wydeven, *Selective permeability of PVA membranes. I. Radiation-cross-linked membranes*. *Journal of Applied Polymer Science*, 1981. 26(9): p. 2935-2946.
- [108] Kormeyer, R.w. and N.A. Peppas, *Effect of the morphology of hydrophilic polymeric matrices on the diffusion and release of water soluble drugs*. *Journal of Membrane Science*, 1981. 9: p. 211-227.
- [109] Ying, W., *Desalination by the use of dynamically formed PVA membranes*. *Desalination*, 1983. 46(1-3): p. 335-342.
- [110] Kazuse, N., T. Shintani, and A. Iwama. *Japan Kokai, Tokyo Koho Japan 61,93,806 (Chemical Abstract 105:174043t), (1986)*.

- [111] Gebben, B., H.W.A.v.d. Berg, D. Bargeman, and C.A. Smolders, *Intermolecular cross-linking of poly(vinyl alcohol)*. *Polymer*, 1985. 26(11): p. 1737-1740.
- [112] Uragami, T., T. Wada, and M. Sugihara, *Studies on syntheses and permeabilities of special polymer membranes. 62. Active transport of alkali metal ions through poly(vinyl alcohol) membranes cross-linked with glutaraldehyde*, *Die Angewandte Makromolekulare Chemie*, 1986. 138: p. 173-183.
- [113] Higuchi, A. and T. Iijima, *Permeation of solutes in water-swollen poly(vinyl alcohol-co-itaconic acid) membranes*. *Journal of Applied Polymer Science*, 1986. 32(1): p. 3229-3237.
- [114] Kamiyama, Y., N. Yoshioka, and K. Nakagome. *Composite semipermeable membrane*, United States Patent 4,619,767 (1986).
- [115] Kazuse, Y., A. Iwama, and T. Shintani. European Patent Application EP 228,248 (Chemical Abstract 107:199859T), (July. 8, 1987).
- [116] Cheng, A.T.Y. and F. Rodriguez, *Mechanical properties of borate cross-linked poly(vinyl alcohol) gels*. *Journal of Applied Polymer Science*, 1981. 26(11): p. 3895-3908.
- [117] Murakami, I., Y. Fujino, R. Ishikawa, H. Ochiai, and Y. Tadokoro, *Temperature dependence of the viscosity of aqueous poly(vinyl alcohol)-borax solutions*. *Journal of Polymer Science*, 1980. 18(10): p. 2149-2153.
- [118] Finch, C.A., *Some properties of polyvinyl alcohol and their possible applications*, in *Chemistry and Technology of Water-Soluble Polymers*, C.A. Finch, Editor. 1983, Plenum Press: New York. p. 304.
- [119] Ochiai, H., S. Fukushima, M. Fujikawa, and H. Yamamura, *Mechanical and thermal properties of poly(vinyl alcohol) cross-linked by borax*. *Polymer*, 1976. 8: p. 131-133.
- [120] Ma, X., Y. Su, Q. Sun, Y. Wang, and Z. Jiang, *Enhancing the antifouling property of polyethersulfone ultrafiltration membranes through surface adsorption-cross-linking of poly(vinyl alcohol)*. *Journal of Membrane Science*, 2007. 300: p. 71-78.
- [121] Morgan, P.W., *Condensation polymers: by interfacial and solution methods*, John Wiley & Sons: New York. 1965.
- [122] Cadotte, J.E., *Synthetic Membranes*. ACS Symposium Series 153, ed. A.F. Turbak., American Chemical Society: Washington, D.C. 1981. p. 305-326.
- [123] Wamser, C.C., R.R. Bard, and V. Senthilathipan, *Synthesis and photoactivity of chemically asymmetric polymeric porphyrin films made by interfacial polymerization*. *Journal of the American Chemical Society*, 1989. 111: p. 8485-8491.
- [124] Wittbecker, E.L. and P.W. Morgan, *Interfacial polycondensation*. *Journal of Polymer Science*, 1996. 34(4): p. 521-529.
- [125] Morgan, P.W. and S.L. Kwolek, *Interfacial polycondensation. II. Fundamentals of polymer formation at liquid interfaces*. *Journal of Polymer Science*, 1996. 34(4): p. 531-559.
- [126] Ahmad, A.L., B.S. Ooi, and J.P. Choudhury, *Preparation and characterization of co-polyamide thin-film composite membrane from piperazine and 3,5-diaminobenzoic acid*. *Desalination*, 2003. 158: p. 101-108.
- [127] Kim, S.H., S.-Y. Kwak, and T. Suzuki, *Positron annihilation spectroscopic evidence to demonstrate the flux-enhancement mechanism in morphology-controlled thin-film-composite (TFC) membrane*. *Environmental Science & Technology*, 2005. 39: p. 1764-1770.

- [128] Cadotte, J.E., *Evolution of composite reverse osmosis membranes*, in *Materials Science of Synthetic Membranes*, D.R. Lloyd, Editor. American Chemical Society: Washington D.C., 1985.
- [129] Cadotte, J.E., *Interfacially synthesized reverse osmosis membrane*. United States Patent 4,277,344 (1981).
- [130] Sundet, S.A., *Production of composite membranes*. United States Patent 4,520,044 (1985).
- [131] Fibiger, R.F., J.Y. Koo, D.J. Fogach, R.J. Petersen, D.L. Schmidt, R.A. Wessling, and T.F. Stocker, *Novel polyamide reverse osmosis membranes*. United States Patent 4,769,148 (1988).
- [132] Tomaschke, J.E., *Interfacially synthesized reverse osmosis membrane containing an amine salt and processes for preparing the same*. United States Patent 4,872,984 (1989).
- [133] Trushinski, B.J., J.M. Dickson, T. Smyth, R.F. Childs, and B.E. McCarry, *Polysulfonamide thin-film composite reverse osmosis membranes*. *Journal of Membrane Science*, 1998. 143: p. 181-188.
- [134] Roh, I.J., J.J. Kim, S.Y. Park, and C.K. Kim, *Effects of the polyamide molecular structure on the performance of reverse osmosis membranes*. *Journal of Polymer Science*, 1998. 36: p. 1821-1830.
- [135] Kim, C.K., J.H. Kim, I.J. Roh, and J.J. Kim, *The changes of membrane performance with polyamide molecular structure in the reverse osmosis process*. *Journal of Membrane Science*, 2000. 165: p. 189-199.
- [136] Jayarani, M.M. and S.S. Kulkarni, *Thin-film composite poly(esteramide)-based membranes*. *Desalination*, 2000. 30(1): p. 17-30.
- [137] Cadotte, J.E., *Reverse osmosis membrane*. United States Patent 4,039,440 (1977).
- [138] Sundet, S.A., *Multilayer reverse osmosis membrane of polyamide-urea*. United States Patent 5,019,264 (1991).
- [139] Cadotte, J.E., R.J. Petersen, R.E. Larson, and E.E. Erickson, *A new thin-film composite sea water reverse osmosis membrane*. *Desalination*, 1980. 32: p. 25-31.
- [140] Riley, R.L., R.L. Fox, C.R. Lyons, C.E. Milstead, M.W. Seroy, and M. Tagami, *Spiral-wound poly(ether amide) thin-film composite membrane systems*. *Desalination*, 1976. 19: p. 113-126.
- [141] Naaktgeboren, A.J., G.J. Sniijders, and J. Gons, *Characterization of a new reverse osmosis composite membrane for industrial application*. *Desalination*, 1988. 68: p. 223-242.
- [142] Kawada, I., K. Inoue, Y. Kazuse, H. Ito, T. Shintani, and Y. Kamiyama, *New thin-film composite low pressure reverse osmosis membrane and spiral wound modules*. *Desalination*, 1987. 64: p. 387-401.
- [143] Masahiko, H., I. Hiroki, and K. Yoshiyasu, *Effect of skin layer surface structures on the flux behaviour of RO membranes*. *Journal of Membrane Science*, 1996. 121(2): p. 209-215.
- [144] Roh, I.J., J.J. Kim, and S.Y. Park, *Mechanical properties and reverse osmosis performance of interfacially polymerized polyamide thin-films*. *Journal of Membrane Science*, 2002. 197(1-2): p. 199-210.
- [145] Kazuse, Y., T. Shintani, I. Kawada, K. Inoue, and A. Iwama, *A new composite membrane for low pressure RO use with chlorine resistance*, in *Abstract of the International Congress on Membranes and Membrane Processes*, 1987: Tokyo. p. 6-19.

- [146] Kamiyama, Y., N. Yoshioka, K. Matsui, and K. Nakagome, *New thin-film composite reverse osmosis membranes and spiral wound modules*. Desalination, 1984. 51: p. 79-92.
- [147] Wrasidlo, W.J., *Semipermeable membranes and the method for the preparation thereof*. United States Patent 4,005,012 (Jan 25, 1977).
- [148] Riley, R.L., C.E. Milstead, A.L. Lloyd, M.W. Seroy, and M. Tagami, *Spiral-wound thin-film composite membrane systems for brackish and seawater desalination by reverse osmosis*. Desalination, 1977. 23: p. 331-355.
- [149] Milstead, C.E. and R.L. Riley. *Low pressure brackish water reverse osmosis membrane development*, NTIS Report no. PB 80-153539 , (Feb 1980).
- [150] Kimura, S., S. Nakao, S. Tanimura, and T. Nomura, *A comparison of different classes of spiral-wound membrane elements at low concentration feeds*. Ultrapure Water, 1990. 7(3): p. 18-25.
- [151] Cadotte, J.E., M.J. Steuck, and R.J. Petersen, *Research on in-situ-formed condensation polymers for reverse osmosis membranes*. NTIS Report No. PB-288387 (March 1978).
- [152] Cadotte, J.E., *Reverse osmosis membrane*. United States Patent 4,259,183 (Mar 31, 1981).
- [153] Cadotte, J.E., R.S. King, and N.A. Newkumet, *Advanced poly(piperazineamide) reverse osmosis membranes*. NTIS Report No. PB 80-127574 (Sep 1979).
- [154] Simpson, A.E., C.A. Kerr, and C.A. Buckley, *The effect of pH on the nanofiltration of the carbonate system in solution*. Desalination, 1987. 64: p. 305-319.
- [155] Eriksson, P., *Water and salt transport through two types of polyamide composite membranes*. Journal of Membrane Science, 1988. 36: p. 297-313.
- [156] Bindoff, A., C.J. Davies, C.A. Kerr, and C.A. Buckley, *The nanofiltration and reuse of effluent from the caustic extraction stage of wood pulping*. Desalination, 1987. 67: p. 455-465.
- [157] Kurihara, M., T. Uemura, Y. Nakagawa, and T. Tonomura, *The thin-film composite low pressure reverse osmosis membranes*. Desalination, 1985. 54: p. 75-88.
- [158] McCray, S.B., D.T. Friesen, and R. Ray, *Novel reverse-osmosis membranes made by interfacial polymerization*, Paper presented at 5th Annual Meeting of the North American Membrane Society. May 17-20, 1992: Lexington.
- [159] Larson, R.E., J.E. Cadotte, and R.J. Petersen, *The FT-30 seawater reverse osmosis membrane-element test results*. Desalination, 1981. 38: p. 473-483.
- [160] Light, W.G., H.C. Chu, and C.N. Tran, *Reverse osmosis TFC magnum elements for chlorinated / dechlorinated feed water processing*. Desalination, 1987. 64: p. 411-421.
- [161] Tomaschke, J.E., *Dry high flux semipermeable membranes*. United States Patent 4,983,291 (Aug 14, 1990).
- [162] Uemura, T., Y. Himeshima, and M. Kurihara, *Interfacially synthesized reverse osmosis membrane*. United States Patent 4,761,234 (Aug 2, 1988).
- [163] Kurihara, M. and Y. Himeshima, *The major developments of the evolving reverse osmosis membranes and ultrafiltration membranes*. Polymer, 1991. 23: p. 513-520.
- [164] Sundet, S.A., S.D. Arthur, D. Campos, T.J. Eckman, and R.G. Brown, *Aromatic / cycloaliphatic polyamide membrane*. Desalination, 1987. 64: p. 259-269.
- [165] Arthur, S.D., *Structure-property relationship in a thin-film composite reverse osmosis membrane*. Journal of Membrane Science, 1989. 46: p. 243-260.

- [166] Cadotte, J.E., *Reverse osmosis membrane*. United States Patent 3,926,798 (16 Dec, 1975).
- [167] Kurihara, M., N. Kanamaru, N. Harumiya, K. Yoshimura, and S. Hagiwara, *Spiral-wound new thin-film composite membrane for a single-stage seawater desalination by reverse osmosis*. *Desalination*, 1980. 32: p. 13-23.
- [168] Kurihara, M., N. Harumiya, N. Kanamaru, T. Tonomura, and M. Nakasatomi, *Development of PEC-1000 composite membrane for single-stage seawater desalination and the concentration of dilute aqueous solutions containing valuable materials*. *Desalination*, 1981. 38: p. 449-460.
- [169] Kamiyama, Y. and K. Nakagome. Japan Kokai, Tokyo Koho Japan 61,129,004 (Chemical Abstract 106: 22824f) (9 May 1987).
- [170] Shang, Y. and Y. Peng, *Research of a PVA composite ultrafiltration membrane used in oil-in-water*. *Desalination*, 2007. 204: p. 322-327.

Chapter 3

MEMBRANE FABRICATION, CHARACTERIZATION AND EVALUATION

3.1 INTRODUCTION

The thin-film composite (TFC) membranes prepared in this study can be divided into two groups, according to their respective compositions and preparation methods. The first group (code: PVA-SB) was prepared by cross-linking poly(vinyl alcohol) (PVA) using sodium tetraborate (SB). The second group (code: PVA-SB-PA) was prepared by depositing a polyamide (PA) layer over the cross-linked PVA-SB membrane to form a composite PA membrane with a PVA gel sub-layer. **Table 3-1** tabulates the two membrane groups and the materials used in the fabrication of the respective membranes, including the type of amine and acid chloride used in the preparation of the PA. Many membranes of each group were prepared in efforts to determine their optimum fabrication conditions. Only the basic fabrication techniques used to fabricate the two respective groups of membranes will be described in this chapter. Details of the fabrication conditions will be given, together with membrane performance results, in Chapter 4.

3.2 CHARACTERIZATION OF POLYETHERSULFONE ULTRAFILTRATION MEMBRANES

3.2.1 MATERIALS

Polyethersulfone (PES) ultrafiltration (UF) membranes were used as support membranes in the fabrication of all the membranes. The PES-UF membranes were supplied by Koch Membrane Systems (USA). They comprise an asymmetric PES membrane, cast onto a polyester backing material, using the phase inversion technique. All the substrate membranes were stored in water to prevent deterioration due to drying and pore tightening. **Table 3-2** summarizes the specifications of the Koch 4312 PES-UF membrane used as porous substrate in the preparation of the TFC membranes. This support has good mechanical properties, chemical stability, and a symmetrical pore structure [1]. De-ionized (DI) water with a conductivity of 2 μ s/cm was used for permeation experiments.

3.2.2 THE EFFECT OF HEATING AND DRYING ON POLYETHERSULFONE ULTRAFILTRATION (PES-UF) MEMBRANES

Table 3-3 tabulates the experimental conditions used to study the effect of drying and heating on the substrate PES-UF membrane.

3.2.2.1 Drying

The membrane samples were dried at room temperature for various periods of times (1 and 3 hours). They were coded as PES-UF1H and PES-UF3H.

3.2.2.2 Heating

PES-UF flat sheet membranes were washed with DI water for 24 hours at room temperature. The membrane were cut into pieces (15 cm x 20 cm) and then placed in an oven, and heated with air circulated at various temperatures (30 – 80°C) for 10 minutes. They were cooled to room temperature before being tested. The PES-UF membrane samples so prepared were coded as PES-UF30, PES-UF40, PES-UF50, PES-UF60, PES-UF70 and PES-UF80, respectively.

3.2.2.3 Morphology

In order to study the effect of heating and drying on the morphology of the PES-UF membrane, samples of selected membranes were taken before and after heating and drying and then prepared for scanning electronic microscopy (SEM) analysis (See **Appendix D**).

Table 3-1: Classification of membranes prepared in this study

Membrane group	Membrane code	Chemicals used in membrane preparation			
		PVA	SB	Amine	Acid Chloride
PVA-SB	PVA-SB	Yes	Yes	No	No
PVA-SB-PA	PVA-SB-MPD-TMC	Yes	Yes	MPD	TMC
	PVA-SB-DAP-TMC	Yes	Yes	DAP	TMC
	PVA-SB-MPD-FC	Yes	Yes	MPD	FC
	PVA-SB-DAP-FC	Yes	Yes	DAP	FC
MPD = m-phenylenediamine TMC = Trimesoyl chloride		DAP = 2,6-diaminopyridine FC = 2,5-furanyol chloride			

Table 3-2: Polyethersulfone ultrafiltration (PES-UF) membrane properties [1]

Identity	Polyethersulfone, 4321PES-UF
Source	Koch
Nature	Microporous
Property	Hydrophobic
Molecular weight cut-off	6,000 – 10,000
Maximum operating temperature	50°C
Allowable pH	2 – 10
Maximum feed turbidity	1 NTU
Maximum feed SDI (15 minute)	5
Gross thickness, μm	170
Free PES thickness, μm	50

Table 3-3: Experimental conditions used to study the effect of drying and heating of the polyethersulfone ultrafiltration (PES-UF) membrane

Series	1	2	3
Drying	Yes	No	Yes
Temperature, °C	Room	-	Room
Period, h	a.s. ^a	-	10 min
Heating	No	Yes	Yes
Temperature, °C	-	a.s. ^a	50
Period, min	-	10	10

^aAs specified in **Figures 4-2 to 4-4** in Chapter 4

3.3 POLY(VINYL ALCOHOL)-SODIUM TETRABORATE (PVA-SB) MEMBRANES

3.3.1 MATERIALS

PVA of various molecular weights and degrees of hydrolysis were used, as shown in **Table 3-4** (the PVA samples were labeled as H, M or L to indicate high, medium and low molecular weights). All chemicals were analytical grade, and used as received without further purification.

3.3.2 EXPERIMENTAL PROCEDURES

Typical conditions used to prepare PVA-SB membranes are tabulated in **Table 4-1**, Section 4.3.

Table 3-4: Materials used in the fabrication of poly(vinyl alcohol)-sodium tetraborate (PVA-SB) membranes

Material	Type / Grade	Supplier	Catalogue number
Poly(vinyl alcohol) (PVA)	Low molecular weight (11,000 – 31,000), 98 – 99% hydrolyzed (L)	Industrial Analytical (Pty) Ltd.	41241
	Medium molecular weight (31,000 – 50,000), 98 – 99% hydrolyzed (M)	Sigma-Aldrich	363138-25G
	High molecular weight (88,000 – 97,000), 98 – 99% hydrolyzed (H)	Industrial Analytical (Pty) Ltd.	41243
Sodium tetraborate (Na ₂ B ₄ O ₇ ·10H ₂ O)	Decahydrate GR	Merck	5825680
Water	De-ionized (DI)	In house	
Sodium hydroxide (NaOH)	AR	Saarchem	5823160
PES-UF support	UF membranes (Section 3.2.1)	Koch Membrane Systems	4321PES-UF

3.3.2.1 Solution preparation

Aqueous PVA solution was prepared by dissolving PVA in DI water under constant stirring for at least 6 h in an oil bath at 90°C. The PVA solution was cooled to room temperature once the PVA was completely dissolved. The cross-linking solutions were obtained by dissolving SB and 0.001 wt% NaOH in DI water. The solutions were then filtered to remove any impurities and other undissolved particles.

3.3.2.2 Membrane fabrication

The standard cross-linking method [2] used to prepare a PVA-SB membrane involves the following steps (see also **Figure 3-1**): The PES-UF support membrane was washed and rinsed with DI water for 30 min. The membrane was clamped between two Teflon frames (height 0.8 cm and inner cavity 15 cm x 20 cm) and dried in air at room temperature for 10 min. PVA solution was poured on the top surface of the PES-UF membrane to soak it. After 10 min the membrane was rinsed and air-dried at room temperature for 10 min. SB solution was poured onto the PVA, and soaked for another 10 min. The membrane was then rinsed and air-dried at room temperature for 10 min. This completed the cross-linking cycle. The resultant cross-linked PVA-SB membrane was washed with an excess volume of water and stored in DI water for a day, to remove any unreacted material remaining on the membrane.

Some PVA-SB membranes were prepared under slightly modified conditions. This was done in an effort to optimize the fabrication conditions of the PVA-SB membranes. The membrane fabrication conditions such as PVA molecular weight, PVA concentration, SB concentration, cross-linking reaction time, number of coatings, and mode of coating were investigated (see Sections 4.1.2.1 to 4.1.2.7).

3.4 POLY(VINYL ALCOHOL) / POLYAMIDE (PVA-SB-PA) MEMBRANES

3.4.1 MATERIALS

Table 3-5 lists the materials used in the fabrication of PVA-SB-PA membranes. All chemicals were commercial analytical grade and were used as received without further purification.

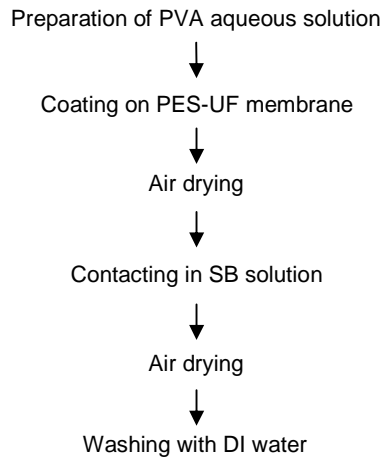


Figure 3-1: Schematic describing the cross-linking process used to prepare poly(vinyl alcohol)-sodium (PVB-SB) membranes

Table 3-5: Materials used in the fabrication of poly(vinyl alcohol)-sodium tetraborate-polyamide (PVA-SB-PA) membranes

Material	Grade	Supplier	Catalogue number
Hexane	99%	Aldrich	15671-1L
Water	DI	In house	
Sodium dodecyl sulfate (SLS)	99%	Sigma-Aldrich	L 4509
Triethylamine (TEA)	99%	Sigma-Aldrich	T 0886
(±)-Camphor-10-sulfonic acid (β) (CSA)	98%	Fluka	21370-500G-F
m-phenylenediamine (MPD)	99%	Aldrich	P23954-100G
2,6-diaminopyridine (DAP)	98%	Aldrich	D24404-100G
Trimesoyl chloride (TMC)	98%	Aldrich	147532-25G
2,5-Furanoyl chloride (FC)	98%	Prepared in house	

3.4.2 EXPERIMENTAL PROCEDURES

Typical conditions used to prepare PVA-SB-PA membranes are tabulated in **Table 4-2** and **Table 4-3**, Section 4.4.

3.4.2.1 Solution preparation

Two solutions were required for the formation of the PA membrane, first, the aqueous solution containing the diamine (MPD or DAP), surfactant (SLS), suitable acid scavenger (TEA) and CSA used to adjusted pH at 10, and second, the organic phase solution of the acid chloride (TMC or FC) in hexane. Both solutions were prepared in Schott bottles, using a magnetic stirrer.

3.4.2.2 Membrane fabrication

The fabrication of these membranes involved the creation of a polyamide layer on the top surface of the cross-linked PVA-SB membrane. This was done in an attempt to improve the salt retention properties of the PVA-SB membrane. The active skin layer of the composite membrane was prepared using interfacial polymerization (IP) technology [3]. The aqueous solution of diamine was poured onto a PVA-SB membrane and allowed to soak for 5 min. Excess solution was drained and the membrane air-dried at room temperature until no liquid remained. The organic phase solution was then poured

onto the membrane surface and allowed to soak for 1 min, to form the PA layer at the interface of the two immiscible solvents. After drainage of the second solution, the membrane was cured at elevated temperature in a vacuum oven to complete the IP reaction. These membranes were thoroughly rinsed with DI water to remove any unreacted materials on the surface. All the above operations were performed in an assembly room.

3.5 MEMBRANE CHARACTERIZATION

3.5.1 FOURIER TRANSFORM INFRARED (FT-IR) SPECTROSCOPY

FT-IR is a very useful analytical technique used for analyzing the surface of materials. FT-IR is widely used as an analytical technique in the coating and membrane industries. In this study, FT-IR spectra for the top surfaces of the membranes were recorded. Photoacoustics (PAS) is based on a principle that involves the absorption of radiation by a sample, causing an increase in the temperature of the surface. This then leads to the formation of thermal waves that cause variations in the pressure of the surrounding gas in the sample cabinet which, in turn, are transmitted to a microphone in the form of an acoustic signal, and which, upon Fourier transform, yields infrared spectra.

A spectrum can be analyzed according to the peak absorptions at different characteristic wavelengths, or it can be compared to spectra in an electronic library, which then proposes the chemical composition of the sample. The FT-IR scans were conducted using a Perkin Elmer Paragon 1000 PC FT-IR spectrometer equipped with a Photoacoustic MTEC 300 cell. The instrument was calibrated, using carbon black, at least every 8 h. The samples to be analyzed were placed in the sample holder, which was then placed inside a sealed chamber. A photograph of the sealed chamber is shown in **Figure 3-2**. The reason for placing the sample in a sealed chamber is to prevent the acoustic waves from escaping. The chamber was then flushed with an inert gas, such as helium, in order to promote these acoustic waves. The instrument resolution was 8 cm^{-1} and the number of scans 128, with a mirror speed of 0.15 cm/s .



Figure 3-2: Photograph of the sealed chamber used in photoacoustic (PAS) cell

- Sample preparation for Fourier transform infrared analysis

Membrane samples were dried in vacuum at 25°C overnight: Samples were cut to size, to fit inside the PAS chamber. Forceps were used to place a sample in a sample holder. Spectra were recorded in the range $450 - 4000\text{ cm}^{-1}$.

3.5.2 SCANNING ELECTRON MICROSCOPY (SEM)

A Leo 1430VP scanning electron microscope fitted with backscatter, cathodoluminescence, variable pressure and energy dispersive detectors, as well as a Link EDS system, and software for microanalysis and qualitative work, was used. The system is designed to produce high-resolution imaging, and quantitative analyses, with errors ranging from 0.2 – 0.5 wt% on the major elements as well as imaging of soft biological samples under variable pressure conditions. The morphologies of membrane cross sections and top surfaces were characterized by SEM after minimal gold coating.

- Sample preparation for SEM analysis

A membrane sample (15 mm x 10 mm) was cut with scissors to fit on the aluminium stub (sample platform). The membrane sample was fixed to the stub for the surface view with silver paint. For cross-section images, membrane samples were obtained by fracturing the membrane in liquid nitrogen. The membrane samples, held with a forceps, were immersed into liquid nitrogen for 5 min. The sample was then removed from the liquid nitrogen, and a nick was made at the edge of the membrane sample with a razor blade. The membrane sample was immersed into liquid nitrogen again for 5 min. After the membrane was removed from the liquid nitrogen, a second pair of forceps was used to pull apart the sample where the nick was made. Since the sample was flimsy, the fractured sample (supported by a small toothpick) was glued on the stub with epoxy, so that the fractured edge of the membrane sample could be positioned face up to obtain the required angle to the detector. A light microscope with 10 times magnification was used to visually confirm that the required position of the sample was obtained. If only SEM was performed on the sample, the fractured edge was grounded to the stub by silver paint.

The mounted samples were placed in a desiccator under low vacuum and samples were sputter coated with a minimum of 15 – 20 nm thick layer of gold. The resolution of the SEM instrument was about 2 – 10 μm . The operating voltage of the electron beam was 1 – 30 kV (to prevent deterioration of the sample).

3.5.3 CONTACT ANGLE MEASUREMENT

Contact angle measurement (CAM) is a simple-to-adopt method for surface analysis related to surface energy and tension. The contact angle is the angle at which a liquid / vapour interface meets a solid surface. Most often the concept describes the shape of a small liquid droplet resting on a flat horizontal solid surface. When drawing a tangent line from the droplet to the touch of the solid surface, the contact angle is the angle between the tangent line and the solid surface.

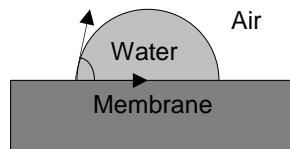
CAM can be used to detect the presence of films, coating, or contaminants with a surface energy different from that of the underlying substrate. CAM helps chemists to determine the properties of detergents, surfactants, coatings, adhesives, etc. CAM measurement has been broadly accepted for use in material surface analysis related to wetting, adhesion and absorption, because of its simplicity.

Consider a liquid drop on a solid surface. If the liquid is very strongly attracted to the solid surface the droplet will completely spread out on the solid surface and the contact angle will be close to 0°. Less strongly hydrophilic solids will have a contact angle of up to 90°. On many highly hydrophilic surfaces, water droplets will exhibit contact angles of 0° to 30°. If the solid surface is

hydrophobic, the contact angle will be larger than 90° . On highly hydrophobic surfaces the surfaces have water contact angles as high as 150° , or even nearly 180° . The contact angle thus directly provides information on the interaction energy between the surface and the liquid.

When a liquid droplet is applied on a membrane surface the droplet will take a specific shape, resulting in a specific contact angle with the membrane, as illustrated in **Figure 3-3 (a)**. The value of the contact angle theoretically ranges from 0° to 180° . The higher the affinity between the water droplet and the membrane surface the smaller is the contact angle and the higher is the degree of wetting. Contact angles measured with water are used to study the degree of hydrophilicity / hydrophobicity: hydrophilic surfaces show a small value for the contact angle, whereas hydrophobic surfaces show a large contact angle.

CAMs were performed with a Nikon MSZ-2T apparatus, as shown in **Figure 3-3 (b)**, in a three-phase system consisting of the membrane surface, air and water droplets of $1\ \mu\text{L}$. CAM utilizes a sample stage to hold the substrate, a syringe to apply a droplet of liquid, a light source to illuminate the droplet, and a set of optics for magnifying the image for observation. Modern contact angle systems, however, adopt precision optics and charge-couple device cameras with image processing hardware and software to enhance the performance of contact angle analysis, making it easier, quicker, and more precise.



(a)



(b)

Figure 3-3: Contact angle measurements: (a) principle, (b) experimental setup

- Sample preparation for contact angle measurement

A membrane sample was dried for 2 h and then placed on the sample stage. A droplet of water ($1\ \mu\text{L}$) is dispensed onto the membrane surface. A charge-couple camera reveals the profile of the droplet on the computer screen. Afterwards, a photograph of the droplet of water on the membrane surface is taken. Software calculates the tangent to the droplet shape and the contact angle. Data and the image are collected, analyzed, and saved on computer. Each contact angle was measured 15 times and an average value was calculated. The sessile drop method was chosen and the contact angle was measured in an equilibrium mode: a droplet of water is placed on the membrane surface, after which the contact angle between the droplet and the membrane surface is calculated.

3.6 MEMBRANE EVALUATION

3.6.1 MATERIALS

Table 3-6 lists the materials used in the evaluation of the membranes that were prepared in this study. All chemicals were commercial analytical grade and were used as received without further purification.

Table 3-6: Materials used in the evaluation of membranes

Material	Grade	Supplier	Catalogue Number
Water	RO	In house	
NaCl	EM	Saarchem	5822300
MgSO ₄	EM	Merck	4123940
NaOH	EM	Saarchem	5823160
HCl	Concentration, 32%	Merck	3063040

3.6.2 EQUIPMENT

3.6.2.1 Flat sheet test cells plant

A schematic representation of the flat sheet test cells plant used for the evaluation of membranes is shown in **Figure 3-4**. The system was constructed to provide the same operating conditions for eight oval-shaped flat sheet test cells arranged in parallel. Each cell has an active cross-sectional area of 22.068 cm². The feed solution for these cells was contained in a 50 L plastic tank, with a thermostat coupled to a digital thermometer (25°C). The feed tank temperature was kept constant by cold water flowing through the cooling coil. The flow of the cooling water was controlled by a temperature controller (TC) coupled to a solenoid valve and a thermocouple in the feed tank. The feed solution was circulated through the membranes by a Hydracell D10 diaphragm pump before being returned to the feed tank. The volumetric flow rate was measured using a rotameter, whilst the inlet and outlet pressures were recorded on the pressure gauges P₁ and P₂ respectively. A by-pass loop enabled the operator to control the pressure and flow rate in the test sections by the manipulation of control valves V₁ and V₂. Both retentate and permeate were recirculated to the feed tank to maintain a constant feed concentration during the permeation experiments. The plant has a pure water feed tank of 20 L, containing pure water to rinse the system thoroughly [4].

3.6.2.2 Experimental procedures

The membrane samples were checked carefully under a fluorescent lamp before testing to avoid using samples with any obvious defects. Membrane samples were placed in the test cells with the active layer facing the incoming feed. After washing and rinsing the system, a feed solution was prepared by adding a concentrated feed solution to the water in the feed tank; the feed tank was filled with a suitable feed solution that had been prepared. All permeation experiments were carried out at 25°C and a recirculating flow of 45 – 50 L/h. The retention and water flux were determined at different operating pressures (0.45 – 2.5 MPa). The permeate flow rate was determined volumetrically using a stop-watch and 20 mL volumetric flasks. Salt concentrations were determined using a CyberScan Con 500 Bench conductivity metre. Eight membrane samples were cut from a prepared membrane sheet. The data presented are the average of these measurements.

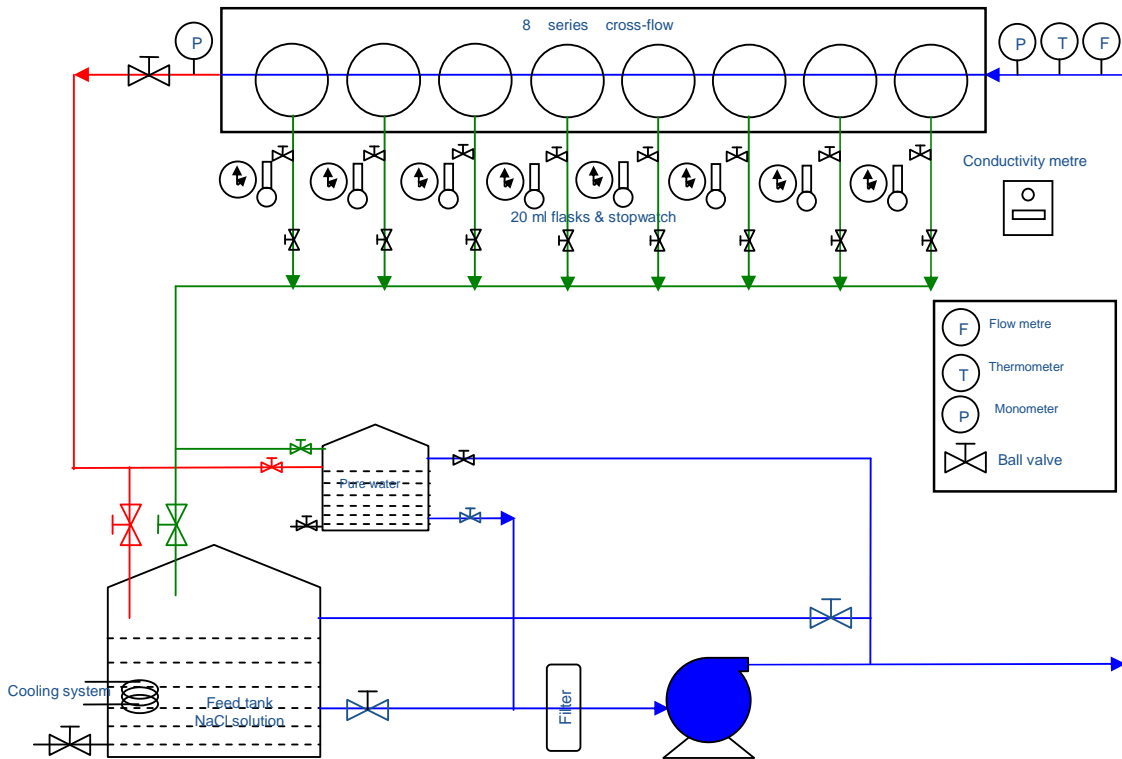


Figure 3-4: Diagram of a flat sheet test cell plant

3.6.3 EVALUATION CRITERIA

The permeation flux of the membrane, J , was calculated according to

$$J = \frac{V}{S \Delta t} \quad (3.1)$$

where V is the total volume of the permeate collected; S represents the membrane area; and Δt denotes the collection time. The pure water permeation rate (PWP, $L/m^2 \cdot h$) in the absence of the solute in the feed and the retention, R , was calculated according to

$$R = 1 - \frac{C_P}{C_F} \quad (3.2)$$

where C_P and C_F are permeate concentration and feed concentration, respectively.

3.7 REFERENCES

- [1] Koch membrane systems. [cited; Available from: web site: www.koch.com], 2008.
- [2] Ma, X., Y. Su, Q. Sun, Y. Wang, and Z. Jiang, *Enhancing the antifouling property of polyethersulfone ultrafiltration membranes through surface adsorption-cross-linking of poly(vinyl alcohol)*. Journal of Membrane Science, 2007. 300: p. 71-78.
- [3] Petersen, R.J., *Composite reverse osmosis and nanofiltration membranes*. Journal of Membrane Science, 1993. 83: p. 81-150.
- [4] Jacobs, E.P., *Statistical and numerical techniques in the optimization of membrane fabrication variables*. PhD Thesis, University of Stellenbosch, 1988.

Chapter 4

RESULTS AND DISCUSSION OF INITIAL INVESTIGATION

4.1 INTRODUCTION

The results of the evaluation and characterization of the various membranes are reported in this chapter. Details of the conditions used for the preparation of the respective membranes are included to facilitate the comparison of membrane performances based on the effects of fabrication conditions. In efforts to determine the effects of the membrane fabrication parameters on membrane performance parameters were varied one at a time.

4.2 CHARACTERIZATION OF POLYETHERSULFONE ULTRAFILTRATION MEMBRANES

The polyethersulfone (PES) ultrafiltration (UF) membrane was first characterized by determining their pure water permeation (PWP) rate, and the retention and flux using feed solutions of sodium chloride (NaCl) and magnesium sulfate (MgSO_4). The PWP rate of PES-UF was $400 \text{ L/m}^2\cdot\text{h}$. **Figure 4-1** shows the retention and flux of solutes of NaCl and MgSO_4 through the PES-UF support at different operating pressures. The flux increased slightly as the pressure increased. The retention of MgSO_4 was higher than NaCl. The retention increased only slightly as the operating pressure increased.

It is expected that the permeability of the poly(vinyl alcohol)-sodium tetraborate (PVA-SB) membranes will be lower than those of the PES-UF membranes that is used as the porous substrate because the PES-UF membrane is covered with a cross-linked PVA layer. However, the heating and drying processes involved in the preparation of the PVA-SB and poly(vinyl alcohol)-sodium tetraborate-polyamide (PVA-SB-PA) membranes may also be the cause of some unexpected effects on membrane performance and therefore the effects of drying and heating on the PES-UF support alone were first studied in more detail.

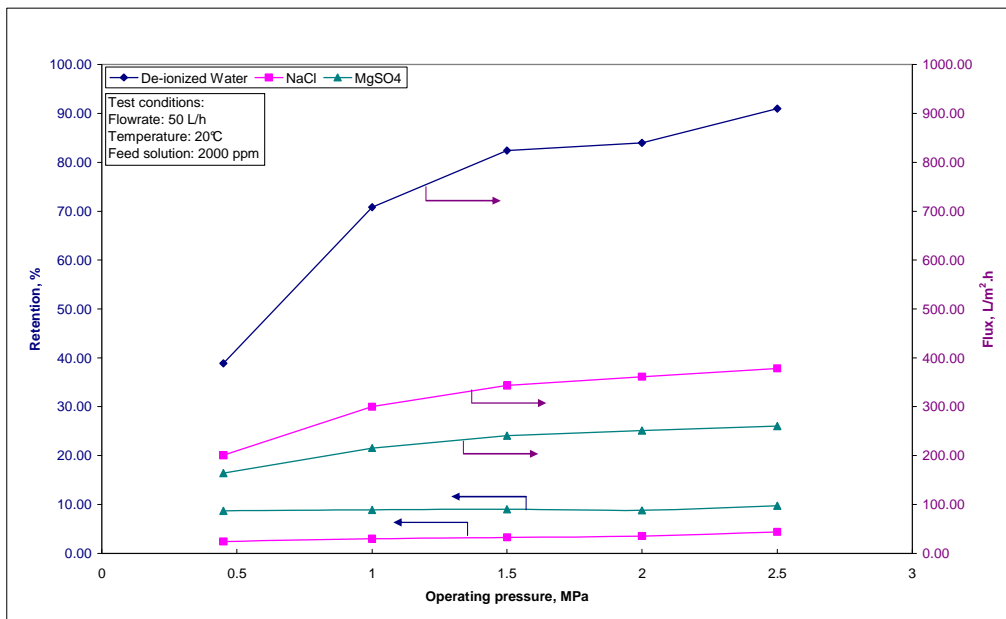


Figure 4-1: Effect of operating pressure on the RO performance of polyethersulfone ultrafiltration (PES-UF) support

4.2.1 EFFECT OF DRYING ON THE PURE WATER PERMEATION (PWP) RATE OF THE POLYETHERSULFONE (PES-UF) SUPPORT

The effect of drying on the porous PES-UF support was studied by treating it under the experimental conditions in **Table 3-3** (Section 3.2.2, series 1). **Figure 4-2** shows that the PWP rate decreased sharply when the membrane was dried.

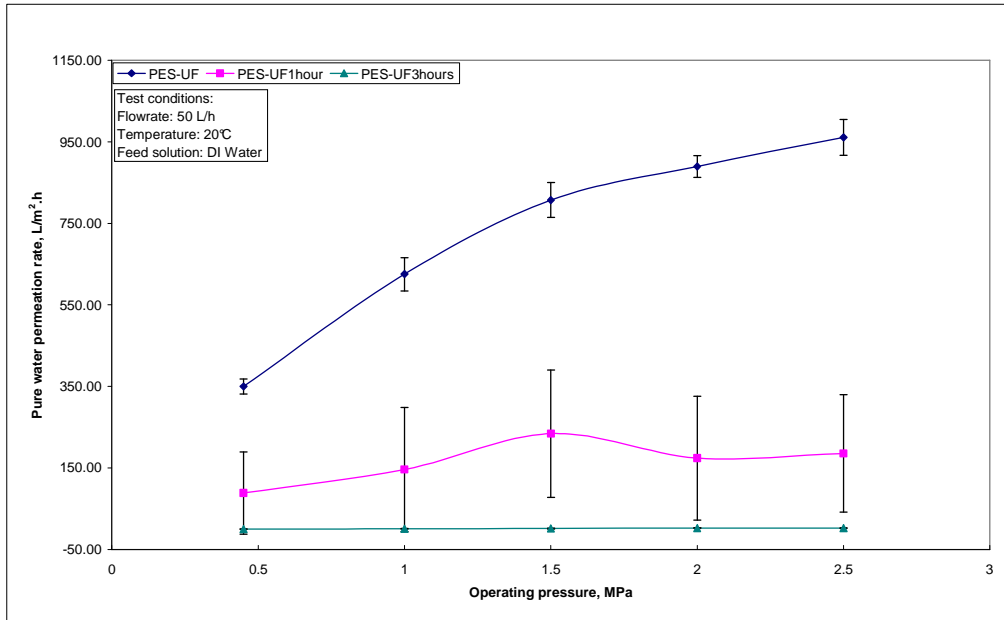


Figure 4-2: Effect of drying time on the pure water permeation rate of the polyethersulfone ultrafiltration (PES-UF) support

4.2.2 EFFECT OF HEATING ON THE PURE WATER PERMEATION (PWP) RATE OF THE POLYETHERSULFONE (PES-UF) SUPPORT

Heating causes a reduction in pore size and densification of the PES layer, thus resulting in decreased PWP rate for the PES-UF support. The effect of heating on the porous PES-UF support was studied by treating it under the conditions specified in **Table 3-3** (Section 3.2.2, series 2). The results of the PWP rate, under different operating pressures, after heating the membranes at various temperatures are presented in **Figure 4-3**. The PWP rate decreased with an increase in heating temperature from 50 to 80°C. As the heating temperature increased from 30 to 60°C, the PWP decreased slightly from 400 to 250 L/m²·h. The PWP rate decreased drastically when the membrane was heated to 70°C, and the PWP rate decreased significantly further at 80°C. The effect of heating is clearly observed upon comparison of the PES-UF support heated at various temperatures and an untreated PES-UF support in term of PWP rate, as shown in **Figure 4-3**. The PES-UF support showed the lowest PWP rate at a heating temperature 80°C.

4.2.3 EFFECT OF DRYING AND HEATING ON THE PURE WATER PERMEATION (PWP) RATE OF THE POLYETHERSULFONE (PES-UF) SUPPORT

The effect of drying and heating on the porous PES-UF support was studied by treating the membrane under the conditions specified in **Table 3-3** (Section 3.2.2, series 3). The PES-UF support was dried at

room temperature for 10 min, and then heating for 10 min at 50°. **Figure 4-4** shows that the PWP rate decreased significantly.

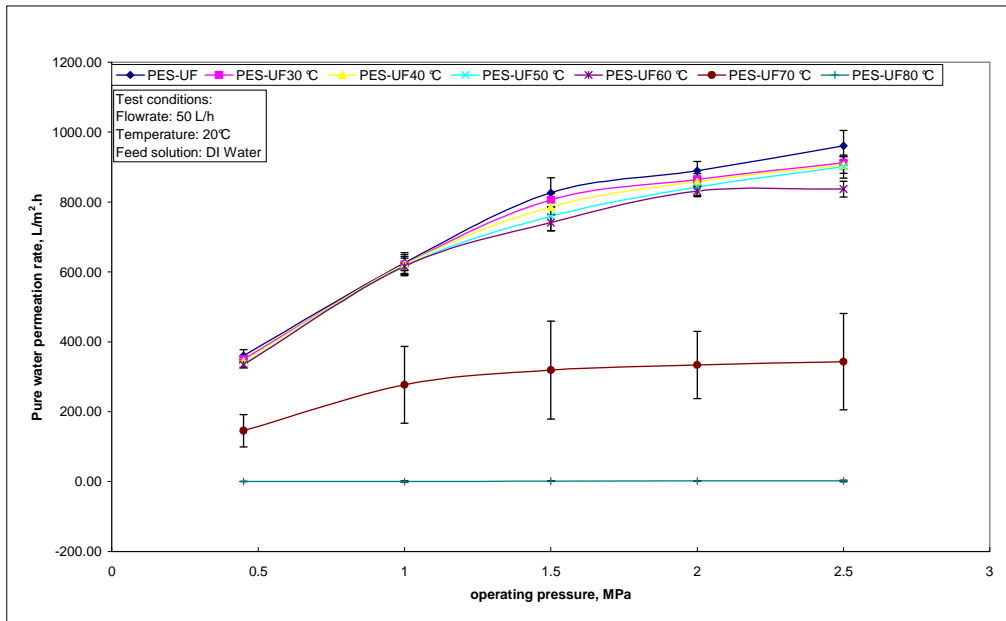


Figure 4-3: Effect of heating on the pure water permeation rate of the polyethersulfone ultrafiltration (PES-UF) support

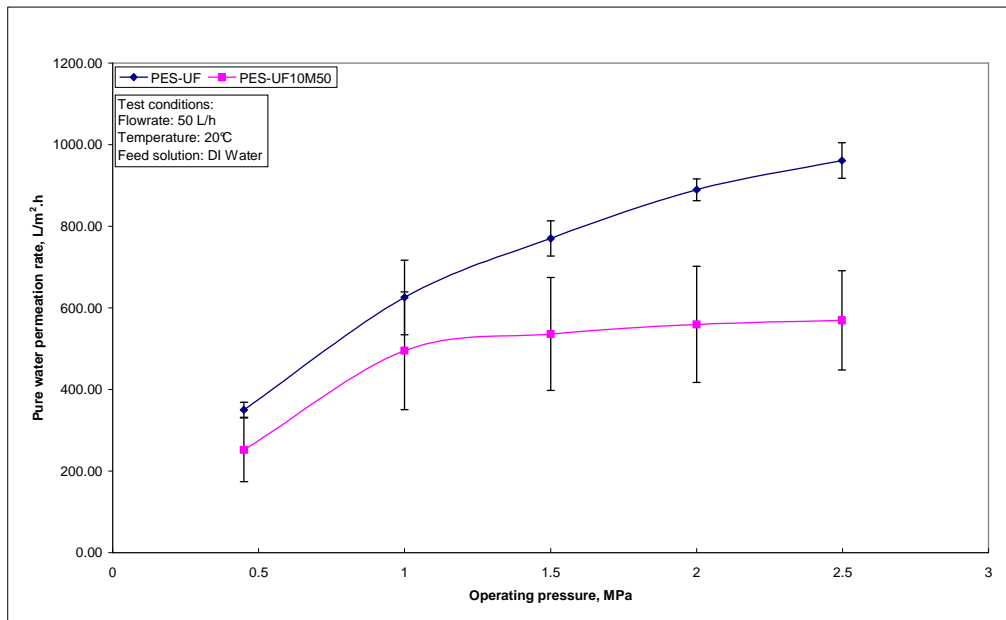


Figure 4-4: Effect of drying and heating on the pure water permeation rate of the polyethersulfone ultrafiltration (PES-UF) support

The pores of the PES-UF membranes are shrunk by the drying and heating. The PWP rate decreased as the temperature of the heat treatment increased. A drastic decrease in PWP rate was observed as the heat temperature approached 70°C. After studying the effect of drying and heating, it was concluded that the combination of 50°C for 10 min would produce the best results.

4.3 EVALUATION OF POLY(VINYL ALCOHOL)-SODIUM TETRABORATE (PVA-SB) MEMBRANES

A desirable membrane should have a high permeate flux and good selectivity. Although the choice of a suitable polymer is essential for preparing good membranes, factors involved in membrane preparation greatly influence the membrane structure and performance. The general fabrication method used in the preparation of these membranes is described in Chapter 3, Section 3.3.2. In this study the following membrane preparation factors were investigated:

- PVA layer without cross-linking
- PVA molecular weight
- PVA concentrations
- SB concentrations
- Cross-linking reaction time
- Number of coatings
- Mode of coating

Different grades of PVA, 98 – 99% hydrolyzed (H), were used in the preparation of the PVA-SB type membranes. Typical preparation conditions used to prepare the PVA-SB membranes are tabulated in **Table 4-1**. These were used throughout except when mentioned otherwise.

Table 4-1: Typical conditions used to fabricate poly(vinyl alcohol)-sodium tetraborate (PVA-SB) membranes

Step	Parameter	unit	Value
1	Wash PES-UF with DI water	min	30
2	Pre-drain	min	10
3	Concentration of PVA solution	%	1.5
4	Soak time	min	10
5	Drain time	min	10
6	Concentration of SB solution	%	0.5
7	Soak time	min	10
8	Drain time	min	10

4.3.1 EFFECT OF POLY(VINYL ALCOHOL) LAYER WITHOUT CROSS-LINKING

As a blank, the PES-UF support was investigated by coating with a 1.5 wt% aqueous solution of PVA, without cross-linking, and then the membrane was dried at room temperature for 10 mins as described in **Table 4-1**. **Figure 4-5** shows the results of the PES-PVA membranes in terms of flux and retention of NaCl solution. It shows that the flux of the membrane decreased, whereas the retention increased with a PVA layer without cross-linking.

Similar results were observed by Cadotte et al [1]. Before the above mentioned experiment was conducted it was hypothesised that the loss in the PWP rate could occur during the PVA solution coating, by blocking the PES pores with PVA molecules. However, it was revealed by the above mentioned experiment (**Figures 4-2 to 4-5**) that the penetration of large PVA molecules into the pore is impossible since even small water molecules cannot enter the pore unless a sufficiently high pressure is applied [2].

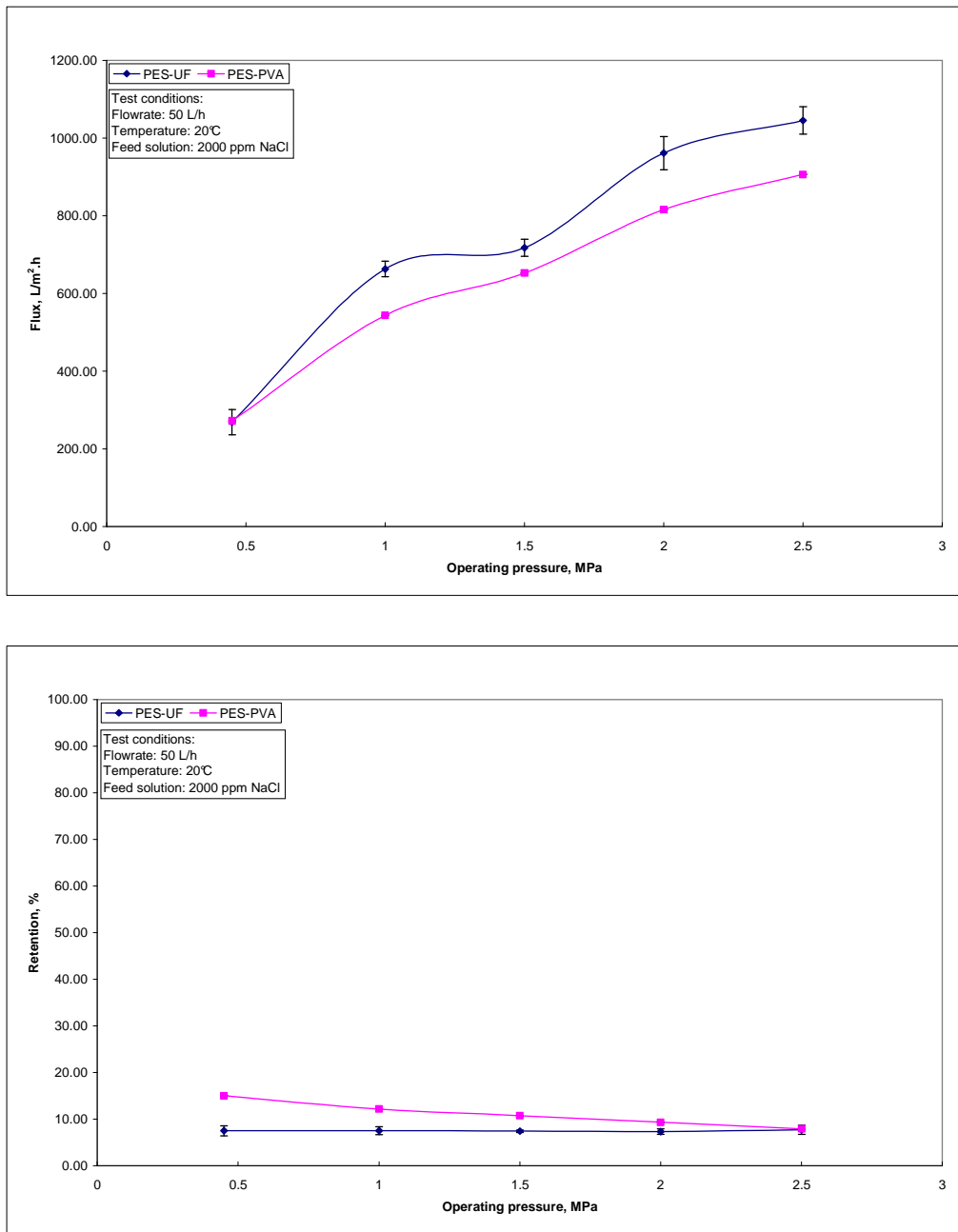


Figure 4-5: Effect of the poly(vinyl alcohol) coating layer on the performance of polyethersulfone ultrafiltration (PES-UF) support: (a) Flux, (b) Retention

4.3.2 EFFECT OF POLY(VINYL ALCOHOL) MOLECULAR WEIGHT

Three types of PVA-SB membranes were prepared with PVA of different molecular weights, with similar degrees of hydrolysis (98.99%). PVA-SB-L, PVA-SB-M and PVA-SB-H (indicating low, medium and high molecular weight PVA, respectively) (see **Table 3-4**). One percent aqueous solutions of PVA of different PVA molecular weights were used to fabricate membranes. The other conditions were as specified in **Table 4-1**. The effect of PVA molecular weight on the flux and the retention of these membranes was studied at different operating pressures. Results are shown in **Figure 4-6**. Retention increased while flux decreased when PVA of increasing molecular weight was used.

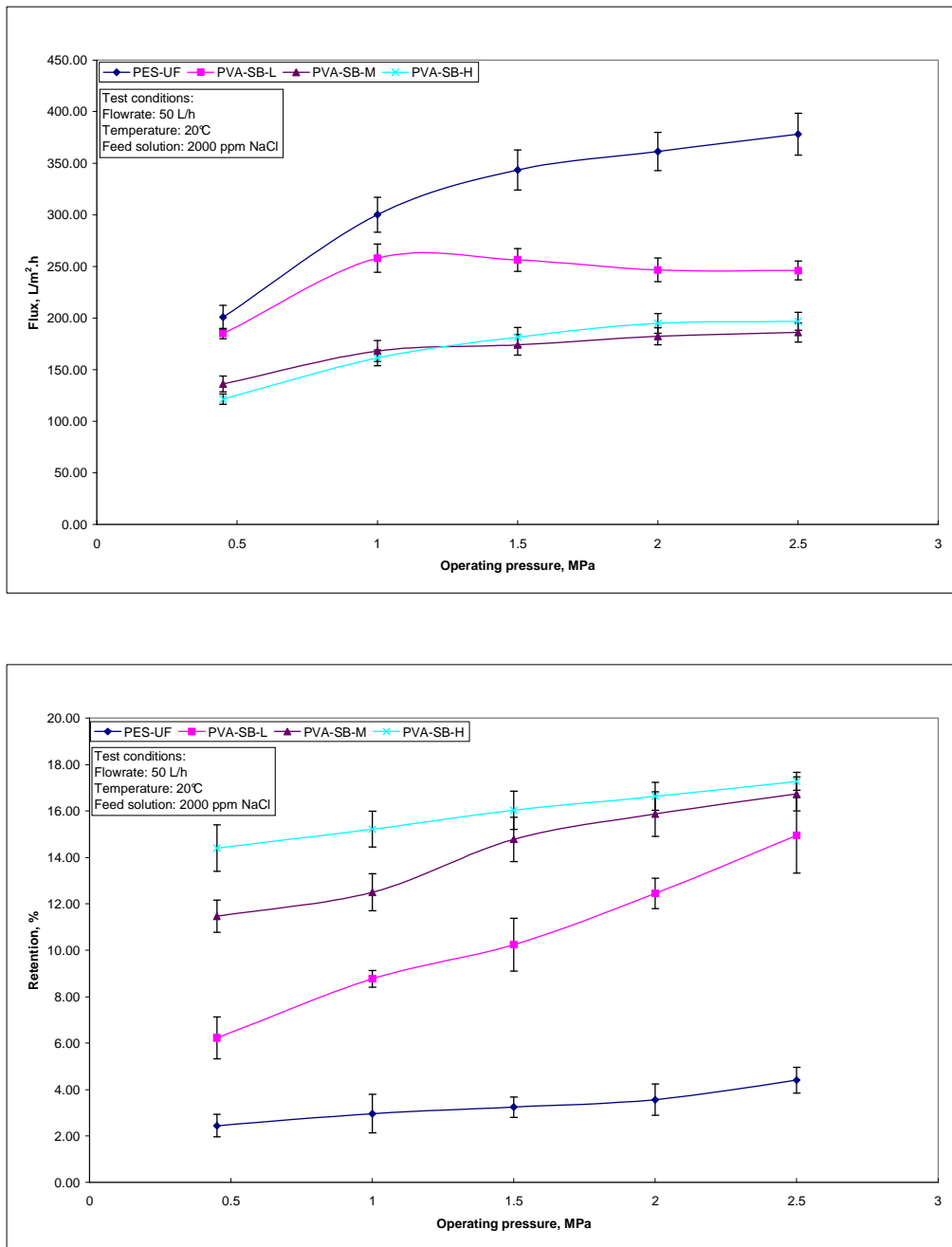


Figure 4-6: Effect of poly(vinyl alcohol) molecular weight on the performance of poly(vinyl alcohol)-sodium tetraborate (PVA-SB) membranes: (a) Flux, (b) Retention

The PVA-SB membranes prepared from high molecular weight PVA exhibited the highest retention and lowest flux. It could be explained that the length of the PVA polymer chain on the PES-UF membrane surface increases with increasing the PVA molecular weight, and the long chains of PVA become more stable than a short chain of PVA on the membrane surface. The SB has more opportunity to react with OH group in a PVA polymer chain and create a dense layer. The flux and retention differences between high and medium molecular weight membranes are very small. The film ought also to be thicker as the higher molecular weight ought to increase viscosity and related density with respect to shorter chains.

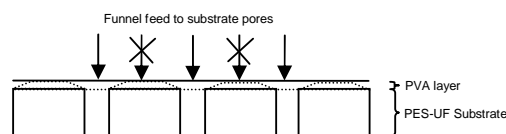
4.3.3 EFFECT OF POLY(VINYL ALCOHOL) CONCENTRATION

It is necessary to choose a suitable PVA solution concentration. The viscosity of the PVA solution is also related to its concentration, and a solution that is not too dilute or too concentrated is required for the preparation of PVA-SB membranes. A series of PVA-SB membranes was prepared from PVA solutions ranging from 0.25% to 2.0% to investigate the effect of the PVA concentration on the membranes performance. The other membrane fabrication factors were kept constant. The membranes were prepared from the following of the PVA solutions: 0.25%, 0.5%, 1.0%, 1.5% and 2.0%. **Figure 4-7** shows the effect of the PVA concentration on the flux and salt retention under different operating pressures, respectively. There was an unexpected increase in flux with an increase in the PVA concentration. The flux of the membrane prepared with 2% PVA is approximately twice as high as that of the membrane prepared with 0.25% PVA. As expected, the retention increased with an increase in PVA concentration due to an increased cross-linking density of the PVA layer.

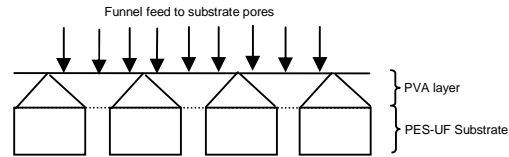
This phenomenon could be explained as follows: the PVA-SB membranes made with low PVA concentrations means thinner films and therefore easier exposure to SB, which means the film can be made more cross-linked and glassy, and this can continue until a concentration of 1.0%, by only becoming thicker and with less defects; therefore flux decreases and retention increases. At still higher concentrations the SB can not penetrate sufficiently and a post treatment rearrangement of the PVA cross-linked structure in the presence of Na^+ ions in the feed, which can complex the liganded SB and make it charged and less functional and therefore can give a less cross-linked, thicker, higher flux, lower retention, membrane. **Figure 4-7** shows the flux was highest at the PVA concentration of 1.6 – 1.7% than at any other concentration used and the retention was higher at the PVA concentration of 1% than at any other concentration used.

These experiments were repeated to determine reproducibility and to try to explain the irregularities present (see **Figure 4-8**). The same PVA concentrations were used and two further concentrations were added: 2.5% and 3%. **Figure 4-8** shows that the flux increased and the retention was almost constant with an increase in PVA concentration. It is known that the retention of a membrane is defined by its chemical structure and not by its thickness [3]. Yet it is obvious that use of a higher concentration of PVA in the coating solution leads to a thicker layer. The premise is, therefore, that the PES-UF membrane has pores of variable sizes, and that a thicker gel layer seals imperfections arising from the larger pores.

Figure 4-7 and **Figure 4-8** do not show the expected decrease in permeate flux with an increase in the PVA concentration, as the membrane thickness increases. It must be remembered that a PES-UF membrane has only about 2% of its surface covered by pores. If it is accepted that PVA at low concentrations gives a thin layer and PVA at high concentration leads to thick layer then the following will apply. When the substrate is covered with a thin layer of PVA not all of the coating is active, as much of it lies over a non-porous area of the substrate, and then the situation arises as is sketched below:



In the case of a thick layer, the following sketch would be more applicable:



The thicker layer is sometimes referred to as a bucket layer, as it channels water to pores in the substrate. As in the solution-diffusion model described in Chapter 2, the flux of the PVA-SB membranes increases linearly with increase in pressure, whereas the retention increases asymptotically toward an upper limit. The variation in the repeat experiments was the average of eight membranes, so the trends were similar but the obvious differences are difficult to explain, which means more experimental factor dependence measurements are necessary.

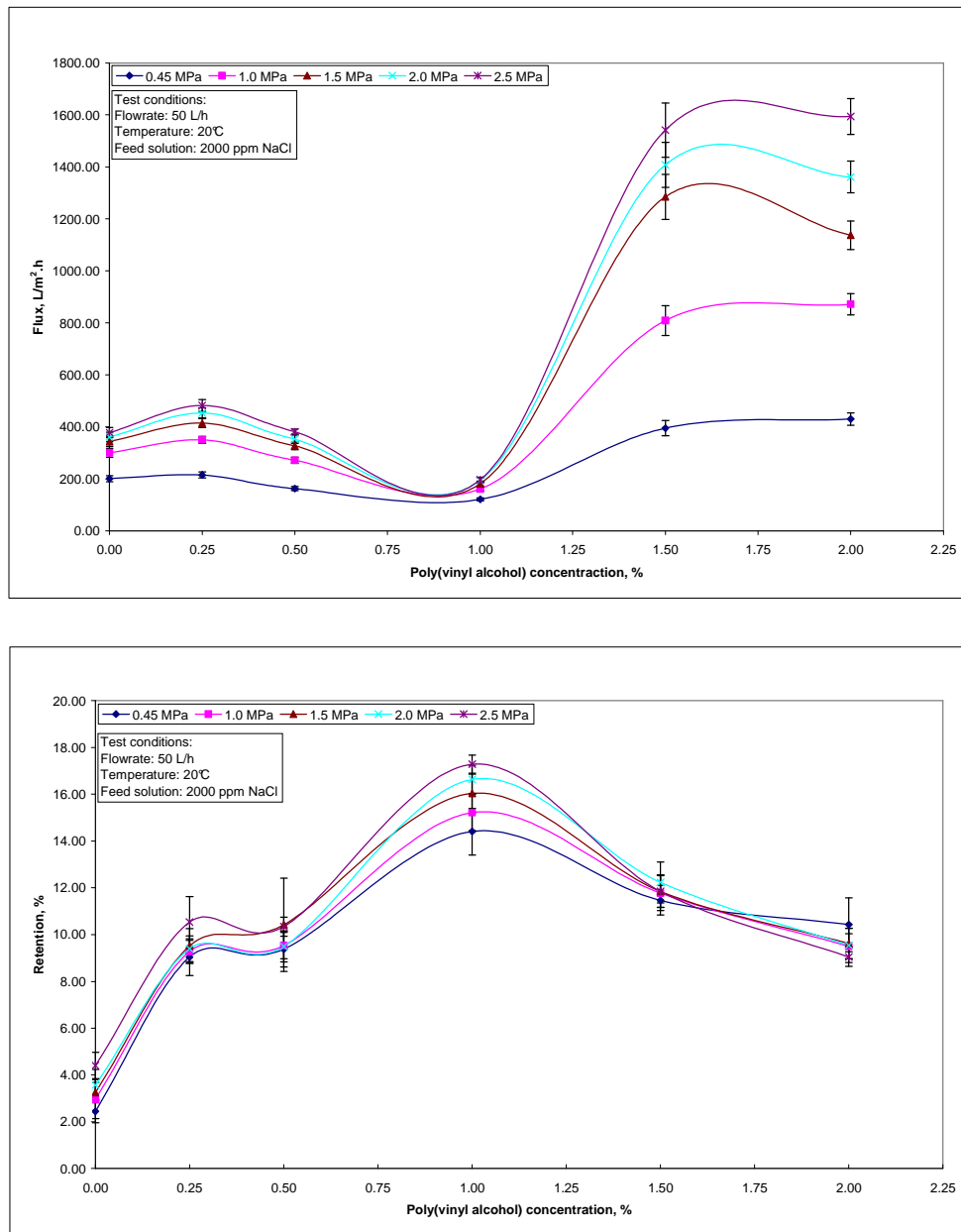


Figure 4-7: Effect of poly(vinyl alcohol) concentration on the performance of poly(vinyl alcohol)-sodium tetraborate (PVA-SB) membranes: (a) Flux, (b) Retention (first trial)

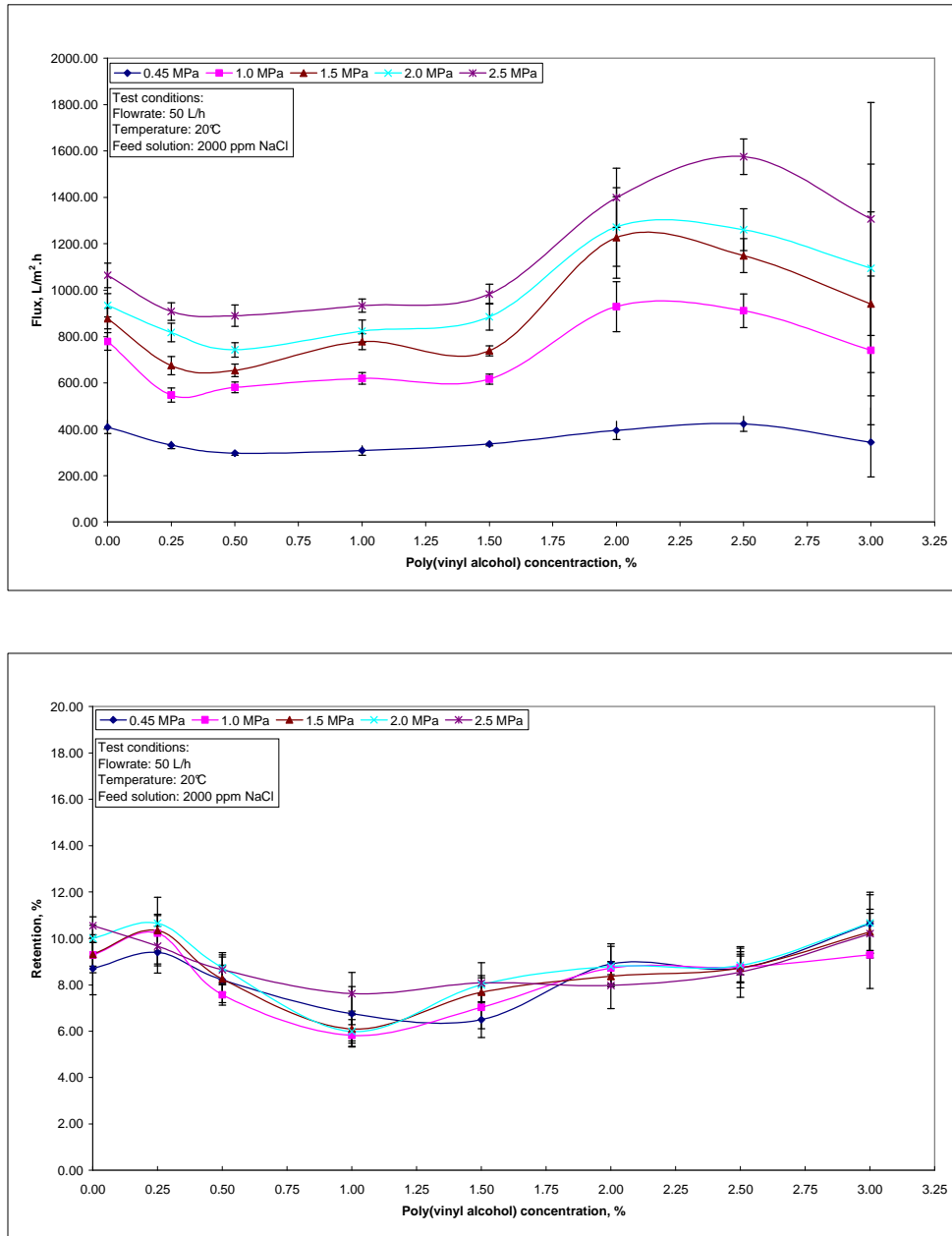


Figure 4-8: Effect of poly(vinyl alcohol) concentration on the performance of poly(vinyl alcohol)-sodium tetraborate (PVA-SB) membranes: (a) Flux, (b) Retention (second trial)

4.3.4 EFFECT OF SODIUM TETRABORATE CONCENTRATION

SB was selected as the cross-linking reagent for the following reasons: first, it can react with the hydroxyl groups in PVA to form a polymeric gel; second, the introduction of hydroxyl groups from the SB, can increase the hydrophilicity of the membrane if monocomplex formed; and, finally, it can react with PVA at room temperature. To investigate the effect of the SB concentration on the membrane performance, a series of PVA-SB membranes were prepared using SB concentrations ranging from 0.05 to 1.0%. The results are shown in **Figure 4-9**. As the SB concentration was increased from 0.05 to 0.25%, the flux increased. However, when the SB concentration exceeded 0.25% the flux began to decrease and the retention continued to show a negligible change.

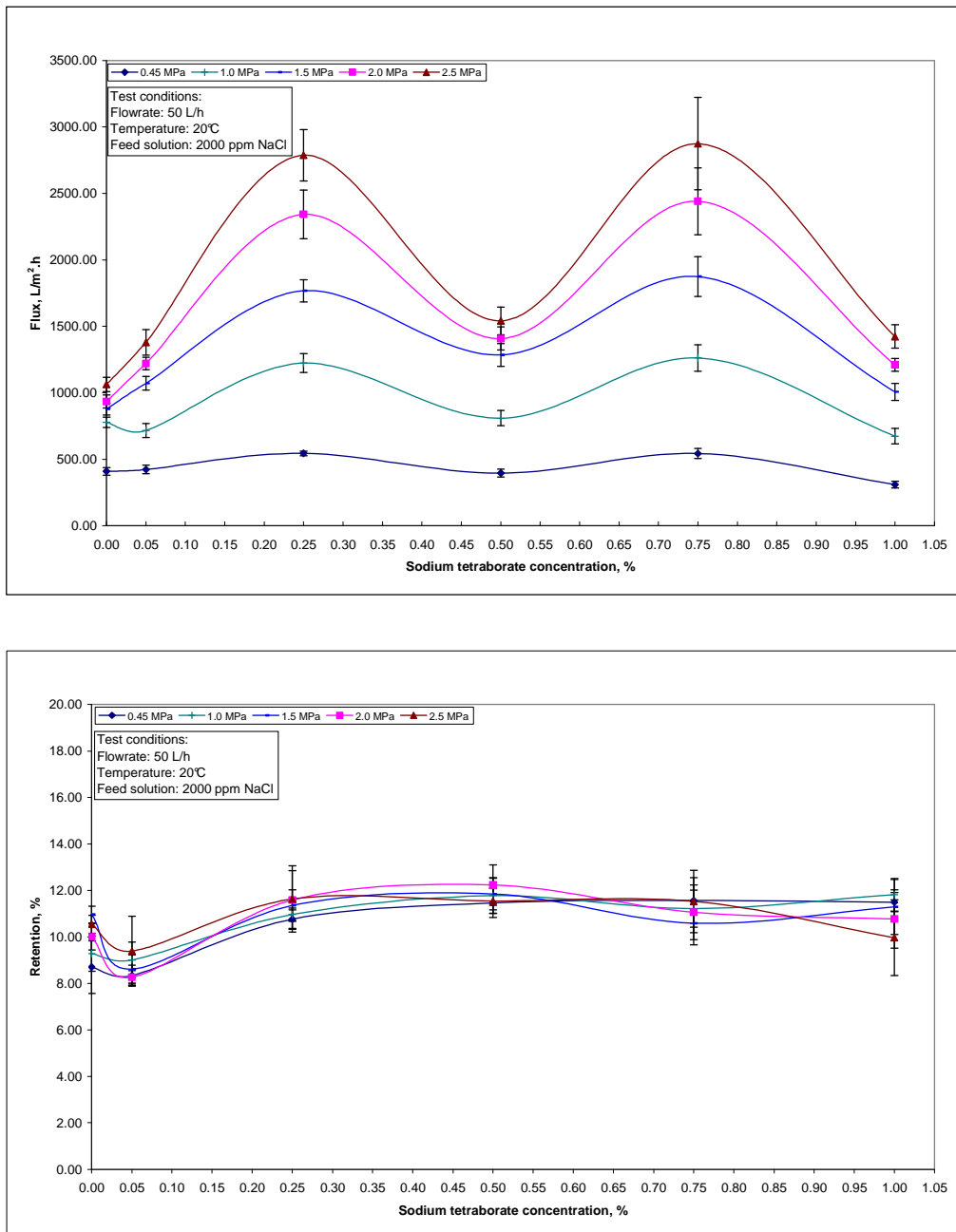


Figure 4-9: Effect of sodium tetraborate concentration on the performance of poly(vinyl alcohol)-sodium tetraborate (PVA-SB) membranes: (a) Flux, (b) Retention

When the concentration was 0.5% the retention was at its highest value and the flux was at its lowest value. This could be explained by postulating that the reaction was intensified between SB and the surface of the membrane and resulted in a compact surface. The cross-linking reaction tends to be complete, which makes the membrane surface less permeable. Thus, the flux decreased and the retention hardly changed. The low point at 0.5% concentration can be the result of improved cross-linking as the concentration increases, but the further increase in flux at higher concentrations has only one further explanation, i.e. more diol structures are formed with excess SB in the monocomplex and less cross-linked tetrads.

4.3.5 EFFECT OF CROSS-LINKING REACTION TIME

A series of PVA-SB membranes was prepared using different cross-linking reaction times of 5 – 15 min. **Figure 4-10** shows that the retention increases with an increase in cross-linking time until 10 min. This results from an increase in the degree of cross-linking. When the cross-linking time was longer than 10 min the retention begins to decrease due to a decrease in the degree of cross-linking. The optimum cross-linking reaction time of 10 min is proposed. **Figure 4-10** six mins could gives high flux. The same explanation as for SB concentrations applies. The layer becomes more cross-linked and later changes to more diols and fewer cross-links at longer time. (see OH peak area in **Figure A-2** in **Appendix A**).

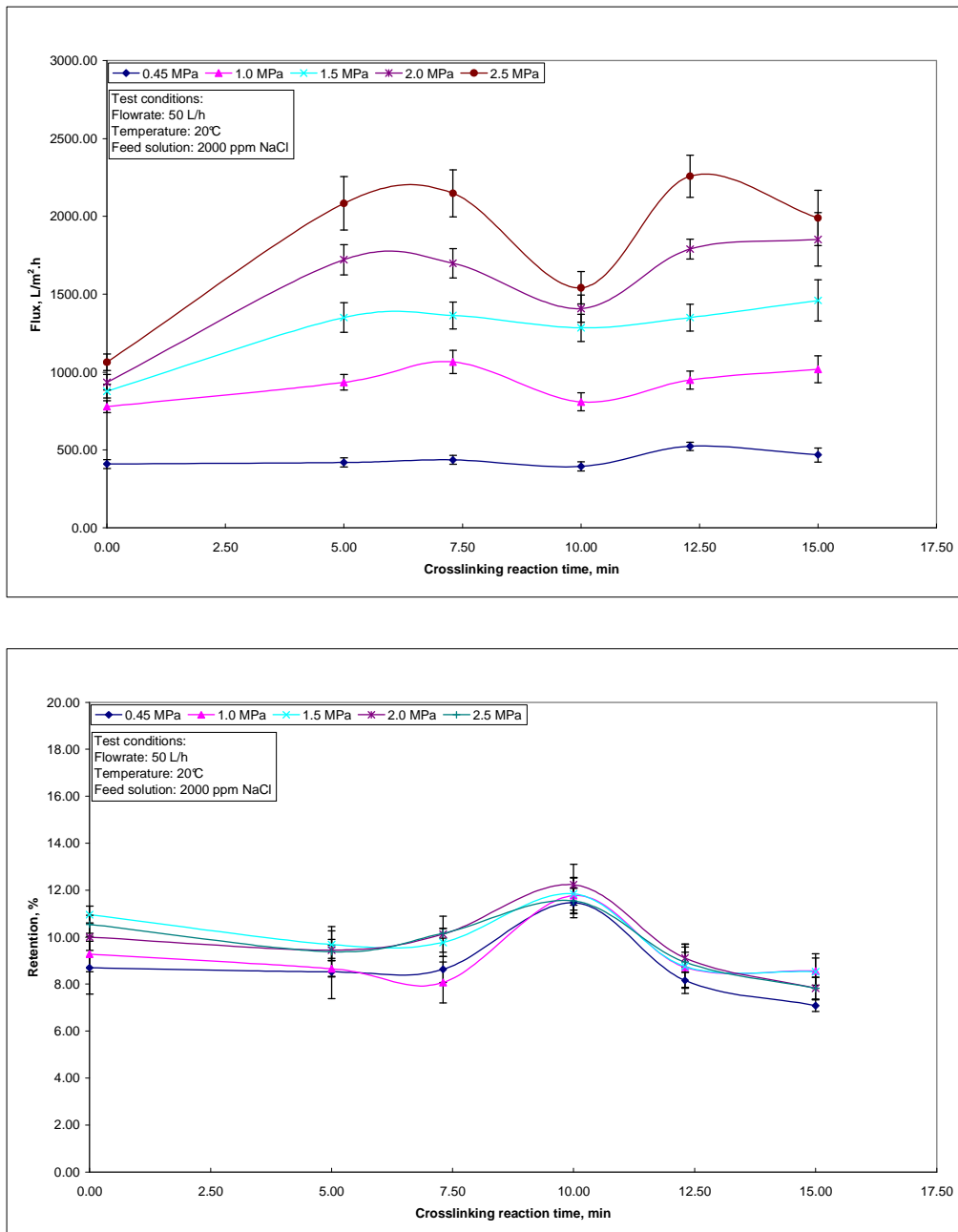


Figure 4-10: Effect of cross-linking reaction time on the performance of poly(vinyl alcohol)-sodium tetraborate (PVA-SB) membranes: (a) Flux, (b) Retention

4.3.6 EFFECT OF THE NUMBER OF COATINGS

The effect of the number of coatings on the PVA-SB membrane performance was investigated by repeatedly coating a PES-UF membrane. A series of PVA-SB membranes was prepared by repeatedly coating a PES-UF membrane with PVA and SB from 1 to 4 times. Results showed that the retention and flux increased as the increasing number of coatings (**Figure 4-11**). This may be explained as follows: an increase in the number of coatings makes the surface of the membrane slightly more dense due to cross-linking, and hence the retention increases slightly. However, the increase in thickness eventually compensates for the resistance flow due to cross-linking because of an improved bucket effect with the number of coatings, thereby the flux increases pressures. Higher pressure / higher flux therefore needs a stronger bucket effect.

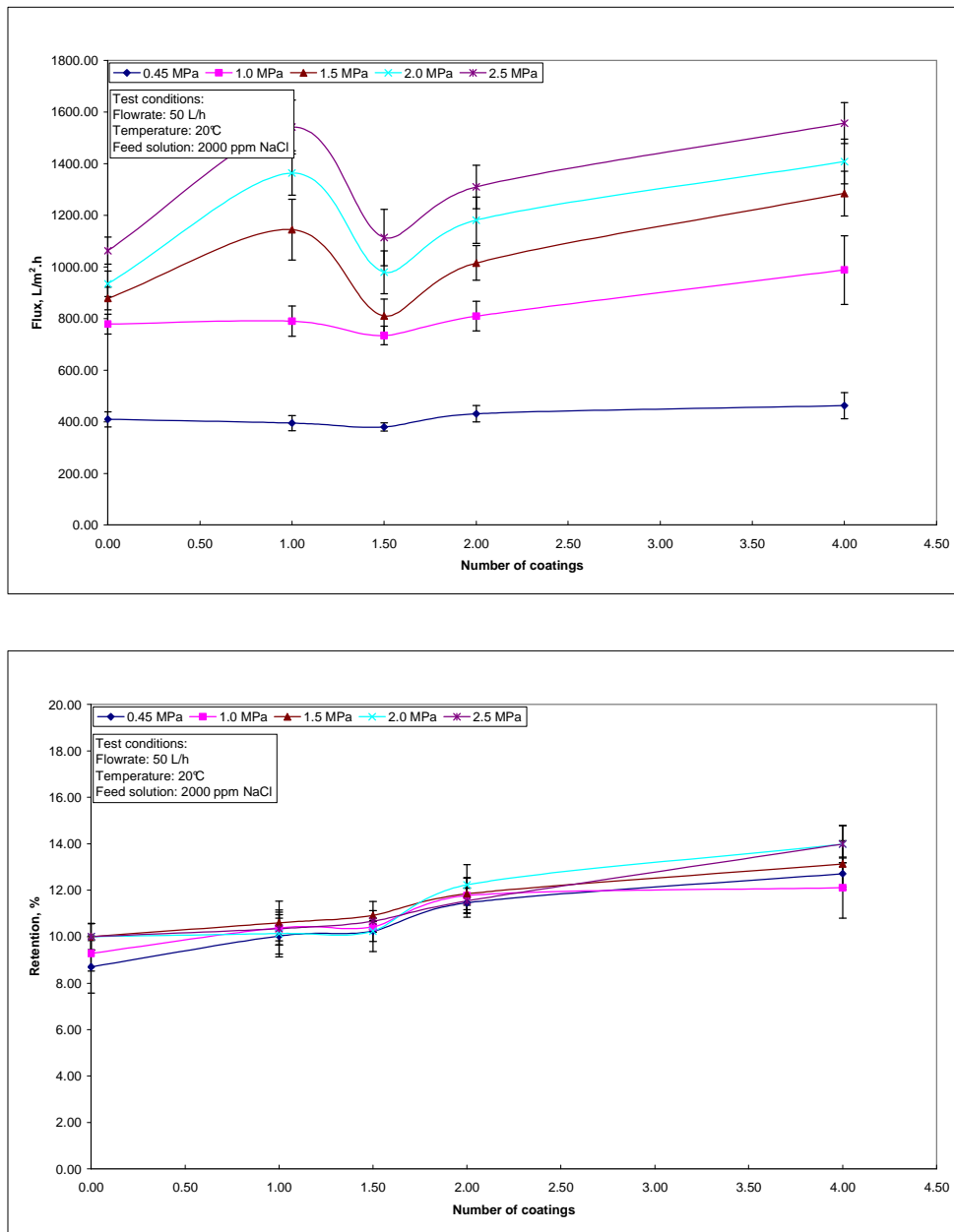


Figure 4-11: Effect of the number of coatings on the performance of poly(vinyl alcohol)-sodium tetraborate (PVA-SB) membranes: (a) Flux, (b) Retention

4.3.7 EFFECT OF THE MODE OF COATING

Two PVA-SB membranes were prepared by changing the steps of the standard coating procedures. **Figure 4-12** shows the effect of the mode of coating on the membrane performance. The PVA-SB-way-1 membrane was prepared according to the basic standard procedure. The PVA-SB-way-2 membrane was prepared by coating the PES-UF support with SB solution first and then coating with the PVA solution. Changing the mode of coating had a significant influence on the performance of the PVA-SB membranes. This could be a result of inverting the degree of cross-linking profile from the almost interfacial reaction (same solvent not two phases), with the most of the cross-linking now closer to the membrane surface.

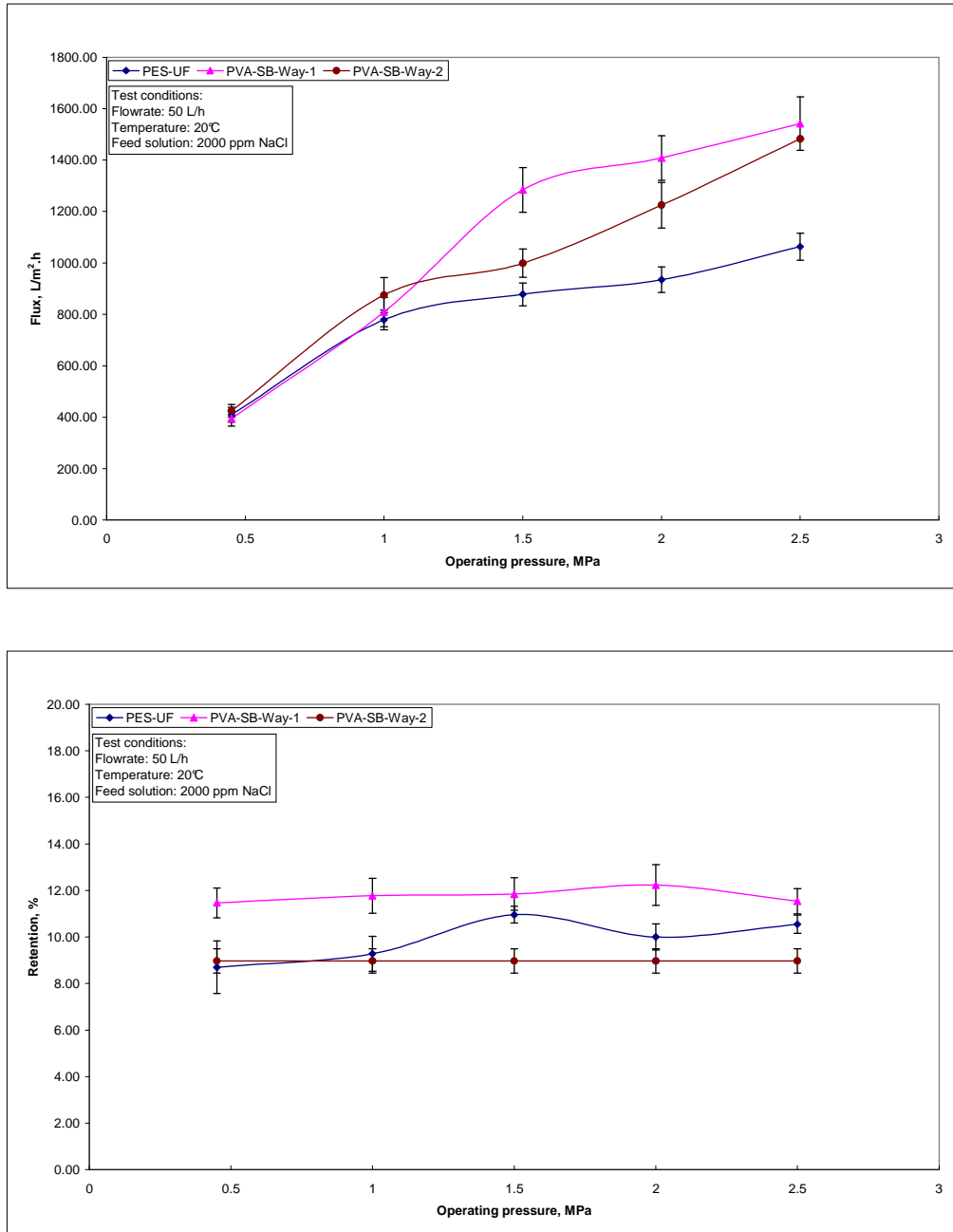


Figure 4-12: Effect of the mode of coating on the performance of poly(vinyl alcohol)-sodium tetraborate (PVA-SB) membranes: (a) Flux, (b) Retention

4.4 EVALUATION OF POLY(VINYL ALCOHOL) / POLYAMIDE (PVA-SB-PA) MEMBRANES

The parameters expected to influence the performance of the PVA-SB-PA membranes are:

- PVA concentration
- PVA dip time
- PVA drain time
- SB concentration
- SB dip time
- SB drain time
- Amine concentration
- Scavenger concentration
- Surfactant concentration
- pH of the aqueous solution
- Amine dip time
- Amine drain time
- Acid chloride concentration
- Acid chloride dip time
- Acid chloride drain time
- Curing temperature
- Curing time

Experiments were carried out with a new acid chloride, 2,5-furanoyl chloride (FC), which was produced in-house, by a colleague [4] (NMR spectra, see **Appendix E**). FC was used to prepare PVA-SB-PA membranes and their results of RO performance compare to those of PVA-SB-PA membranes, prepared with trimesoyl chloride (TMC) as acid chloride. Various aqueous and organic solutions were prepared according as tabulated in **Table 4-2**. The amine concentration was changed from 2% to 1% when FC was used as acid chloride. The membranes were fabricated according to the conditions given in **Table 4-3**. The aqueous solution consisted of either m-phenylene diamine (MPD) or 2,6-diaminopyridine (DAP) as amine and the organic solution consisted of either TMC or FC in hexane as acid chloride.

Sodium dodecyl sulphate (SLS) was used to reduce the surface tension of the aqueous solution, to facilitate uniform transport of the amine to the interface between the water and the organic phases, resulting in a thin and integrated surface layer.

Table 4-2: Aqueous and organic solutions used for the fabrication of PVA-SB-PA membranes

Aqueous solution			Organic solution		
Code	Content	Value	Code	Contents	Value
MPD	MPD	2%	TMC	TMC	0.25%
	SLS	0.1%		Hexane	99.75%
	TEA	1%			
	pH	10			
DAP	DAP	2%	FC	FC	0.25%
	SLS	2%		Hexane	99.75%
	TEA	0.1%			
	pH	10			

Four different types of membranes were prepared from all the possible combinations of reagents. They were coded according to the chemicals used to prepare them, for example: PVA-SB-MPD-TMC refers to a membrane made from PVA-SB plus solutions of MPD and of TMC. Eight membranes were prepared for each of the membrane types.

Table 4-3: Basic conditions used in the fabrication of PVA-SB-PA membranes

Step	Parameters	Unit	Value
1	Wash PES-UF support with DI water	min	30
2	Pre-drain	min	10
3	Soak time of PVA solution	min	10
4	Post drain	min	10
5	Soak time of SB solution	min	10
6	Air dry	min	10
7	Repeat steps 3 to 5		
8	Air dry	min	20
9	Soak time of aqueous solution	min	5
10	Air dry	min	10
11	Soak time of organic solution	min	1
12	Curing temperature	°C	50
13	Curing time	min	10

4.4.1 EFFECT OF THE USE OF TRIMESOYL CHLORIDE WITH TWO DIFFERENT DIAMINES

The molecular structure of the DAP differs from that of MPD. DAP has a nitrogen atom in the ring (DAP was selected as it could show ionic interaction with the boron ion). Two composite membranes (PVA-SB-MPD-TMC and PVA-SB-DAP-TMC) were fabricated by an IP of MPD or DAP, with TMC, separately. Their performances were evaluated and their surface morphologies determined. The two composite membranes that were prepared from TMC with MPD or DAP gave high salt retention and very low flux. The retention and flux of these two membranes were determined at different operating pressures using a 2000 ppm NaCl solution at 25°C.

Figure 4-13 shows the effect of using TMC with MPD or DAP on the RO performance of the PVA-SB-PA membranes that included the polyamide MPD / TMC or polyamide DAP / TMC. The salt retention increased and flux decreased when the PA layer was created on the PVA-SB membrane surface. The PVA-SB-MPD-TMC membranes had 96.23% salt retention and 12.23 L/m².h flux, while the PVA-SB-DAP-TMC membranes had 89.25% salt retention and 32.09 L/m².h flux. As shown in **Figure 4-13**, PVA-SB-PA membranes that included MPD displayed higher salt retention than those that included DAP, in the order of PVA-SB-MPD-TMC > PVA-SB-DAP-TMC, whereas the order of the water flux was PVA-SB-DAP-TMC > PVA-SB-MPD-TMC.

4.4.2 EFFECT OF THE USE OF 2,5-FURANOYL CHLORIDE WITH TWO DIFFERENT DIAMINES

The interfacial polymerizations (IP) of the difunctional acid chloride with MPD and with DAP were examined to determine the best conditions for producing the PVA-SB-PA membrane in terms of the membrane performance and morphology of the thin-film. The PVA-SB membranes were coated with an aqueous solution (1.0%) of MPD or DAP and then reacted with an organic solution containing (0.25%) of difunctional acid chloride. The membranes were tested with feed solutions containing 2000 ppm NaCl and MgSO₄.

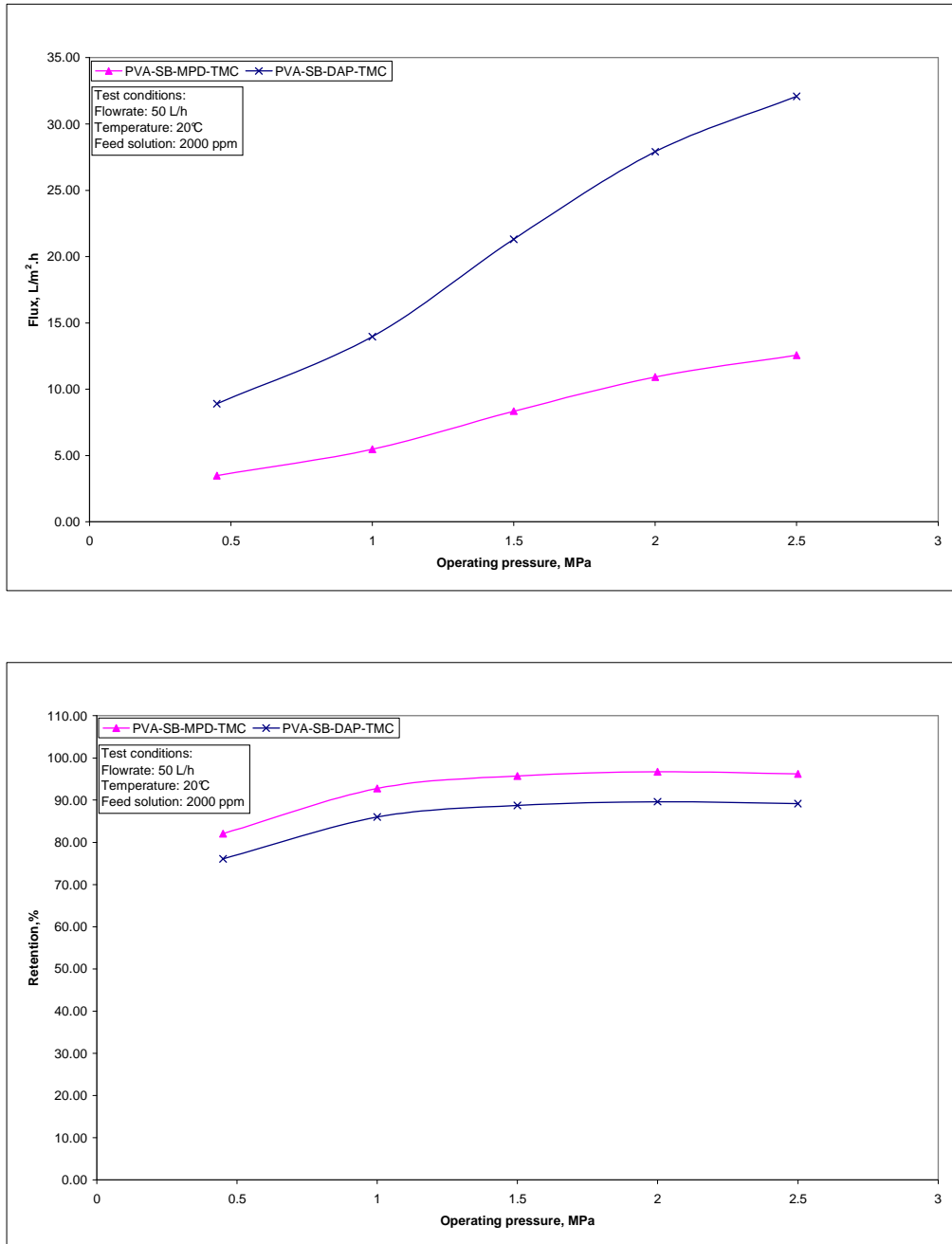


Figure 4-13: Effect of using trimesoyl chloride with different diamines on the performance of poly(vinyl alcohol-sodium tetraborate-polyamide (PVA-SB-PA) membranes: (a) Flux, (b) Retention

Figure 4-14 shows the effect of FC with the two respective diamines on the performance of the PVA-BS-PA membranes. The polyamide layer had a significant effect on the salt retention and flux. The NaCl retention of the PVA-SB-DAP-FC membranes was higher than that of the PVA-SB-MPD-FC membranes, whereas the flux of the PVA-SB-MPD-TMC membranes was higher than that of the PVA-SB-DAP-FC membranes. The MgSO₄ retention followed the same basic trends as that of the NaCl, but the effect was not as pronounced. The PVA-SB-DAP-FC membranes showed a higher salt

retention to divalent anions than to monovalent anions. Salt retention of NaCl is (59.01% and MgSO₄ 74.94%), as well as a higher flux (NaCl 72.68 L/m².h and MgSO₄ 80.31 L/m².h).

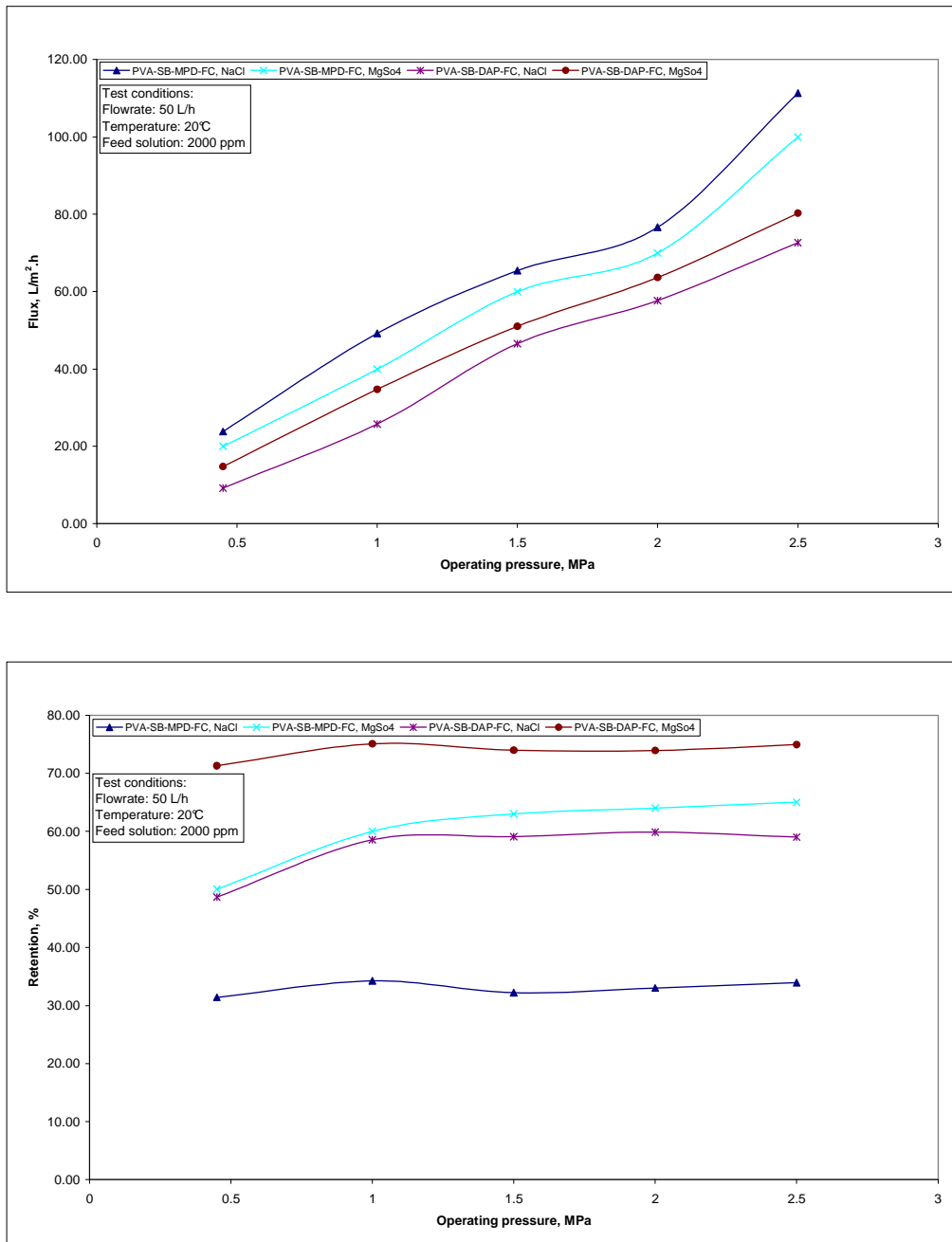


Figure 4-14: Effect of using 2,5-furanoyl chloride with different diamines on the performance of poly(vinyl alcohol-sodium tetraborate-polyamide (PVA-SB-PA) membranes: (a) Flux, (b) Retention

The PVA-SB-MPD-FC membranes showed relatively similar values of water flux for the respective salt solutions: 111.3 L/m².h for NaCl and 100.0 L/m².h for MgSO₄. On the other hand, PVA-SB-MPD-FC membranes have a lower retention to NaCl and MgSO₄. The MgSO₄ retention increased from 65% to 75% when the diamine was changed from MPD to DAP. The composite membranes prepared by reaction of FC have a higher flux compared to the other membranes prepared with TMC.

The lower retention of the monovalent salt, NaCl, is an advantage because the NF membranes are often used as pre-treatment before RO. In the RO step the monovalent salts are totally removed. Partial removal of NaCl in the NF step has consequently resulted in the need for higher transmembrane pressures, which has an impact on operation costs.

4.5 MEMBRANE CHARACTERIZATION

4.5.1 CONTACT ANGLE ANALYSIS

Hydrophilicity or wettability of the membranes can be determined by the contact angle between the membrane and water, which is a well-known method to study the tendency for the water to wet the membrane surface. Salt and water permeate membranes according to the solution-diffusion transport mechanism, so the capability of water sorption at the feed water / membrane interface is an important factor for the water flux. The lower contact angle means the surface is more hydrophilic and it can be more easily wetted by water. Water contact angle was employed to evaluate the effect of the PVA layer and the PA layer on the membrane surface hydrophilicity.

The results of contact angle measurement are presented in **Figure 4-15** to **4-20** and shows the PES-UF membrane has the highest contact angle of 73.24°, corresponding to the lowest surface hydrophilicity, while the PVA-SB membranes has the most hydrophilic surface. As shown in **Figure 4-15**, the value was decreased with an increase PVA molecular weight and the high molecular weight gives the lowest value.

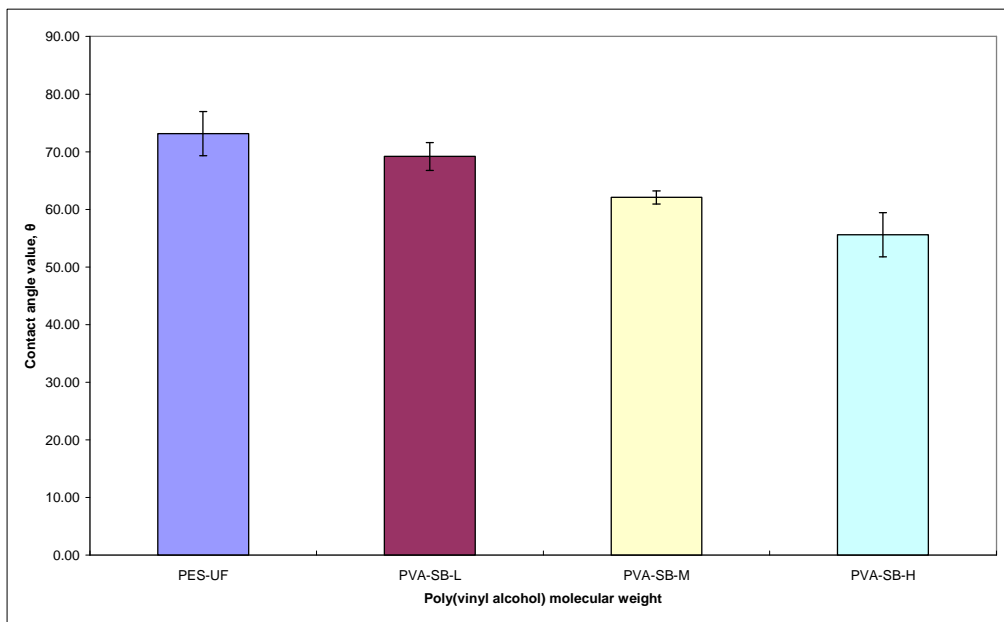


Figure 4-15: Contact angle values of polyethersulfone (PES-UF) support modified with poly(vinyl alcohol) of different molecular weights

The contact angle decreases to 55.01° when the PVA concentration was between 1.0% and 2.0% as shown in **Figure 4-16**. However, the contact angle decreased slightly with low or high PVA concentration. It could be explained that the more of the OH group reacts with SB when the PVA concentration was low or high. The proper PVA concentration should be between 1.0% and 2.0%.

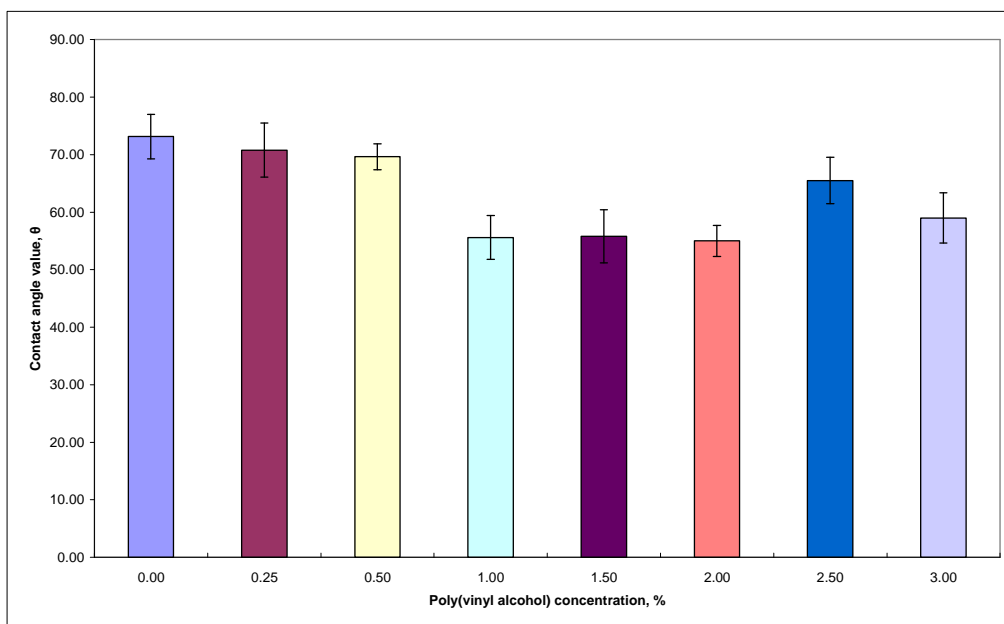


Figure 4-16: Contact angle values of polyethersulfone (PES-UF) support modified with poly(vinyl alcohol) of different concentrations

The results of the effect of SB concentration are showed in **Figure 4-17**, it can be readily seen that, as the SB content in the membrane increases the hydrophilicity increases and contact angle value decreases. The highest hydrophilicity, which includes both hydroxyl groups and the charge carried by the boron in the complex, matches the improvement in retention and the drop in flux.

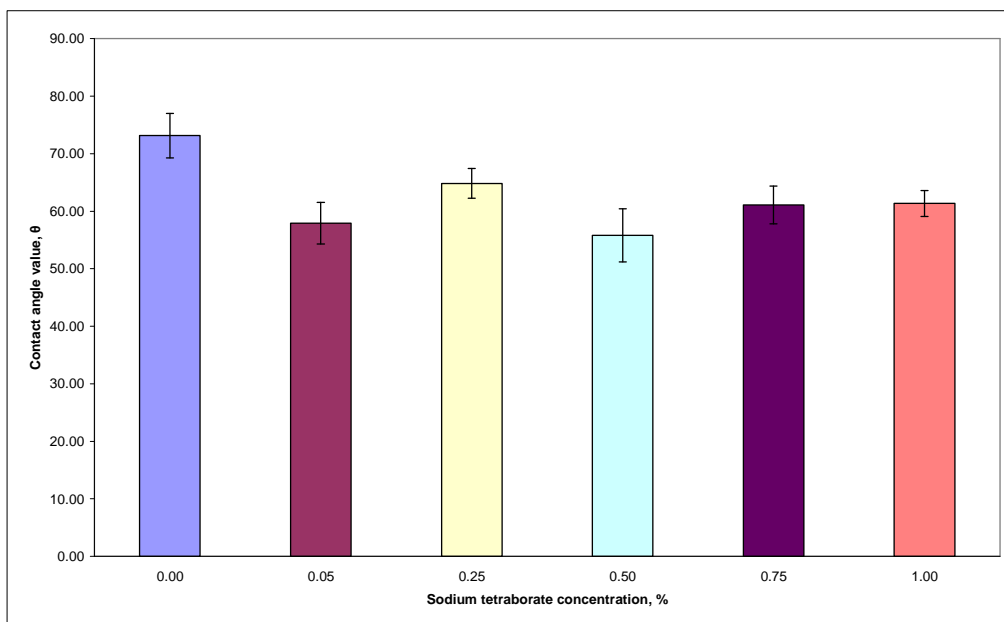


Figure 4-17: Contact angle values of polyethersulfone (PES-UF) support modified with sodium tetraborate of different concentrations

Figure 4-18 shows the effect of the changing of the cross-linking reaction time. Even this, the results may indicate that the PVA-SB membranes have a comparable hydrophilicity with the PES-UF membrane. Here, again the small but maximum retention is found at 10 mins cross-linking time, and which corresponds to the most hydrophilic surface.

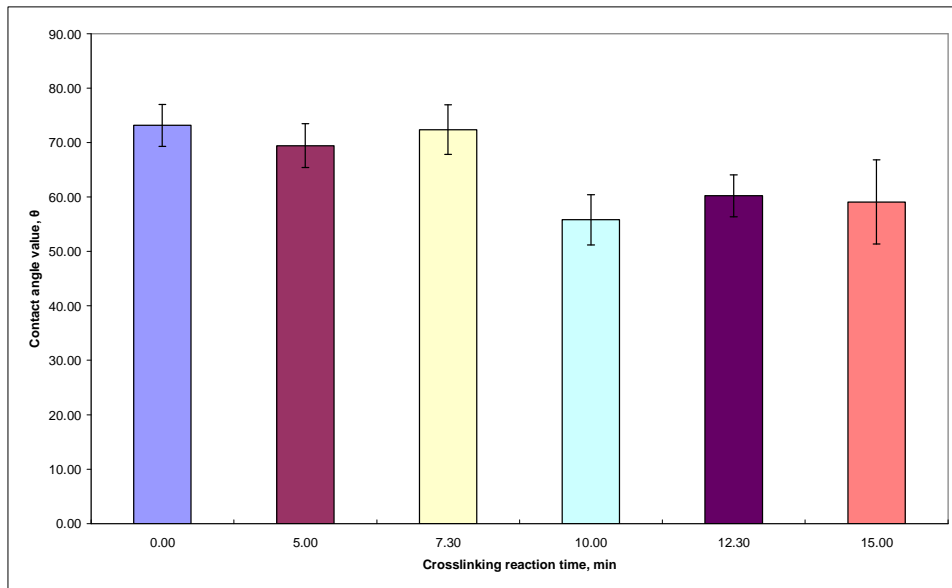


Figure 4-18: Contact angle values of polyethersulfone (PES-UF) support modified using different cross-linking reaction times

Figure 4-19 shows the effect of number of coating on the contact angle measurements, whereas the membrane coated four times has contact angle of 39.87° and the surface of the membrane became more hydrophilic. It was thus concluded that number of coating could effectively enhance the surface hydrophilicity of PES-UF membrane. At high transfer membrane pressure the flux increased with four coating again agreeing with the influence of the hydrophilicity on retention and flux.

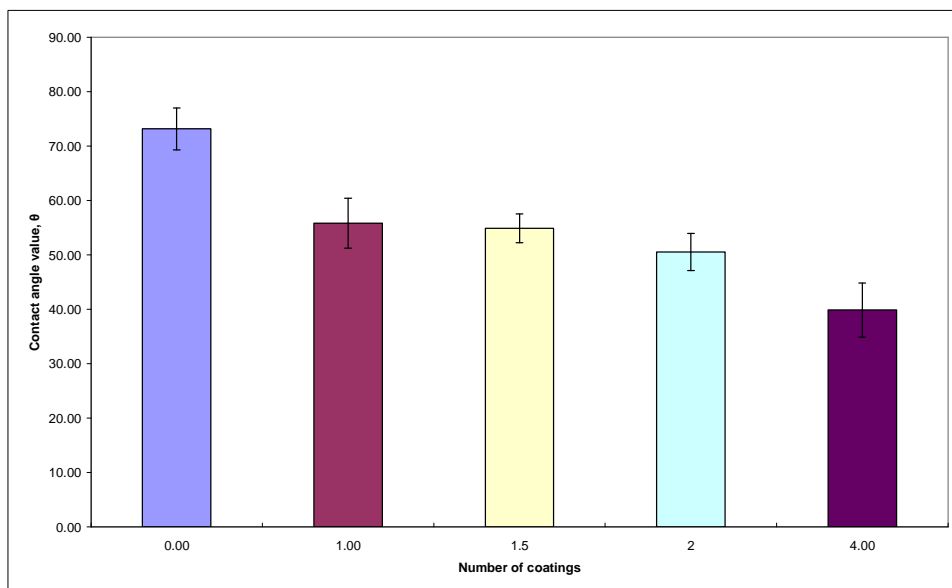


Figure 4-19: Contact angle values of polyethersulfone (PES-UF) support modified using different number of coatings

Figure 4-20 shows there was only a small influence on the contact angle value when the mode of coating was changed. This was expected as now the cross-linking is closer to the membrane surface and the upper surface is less cross-linked, and has more hydrogel groups.

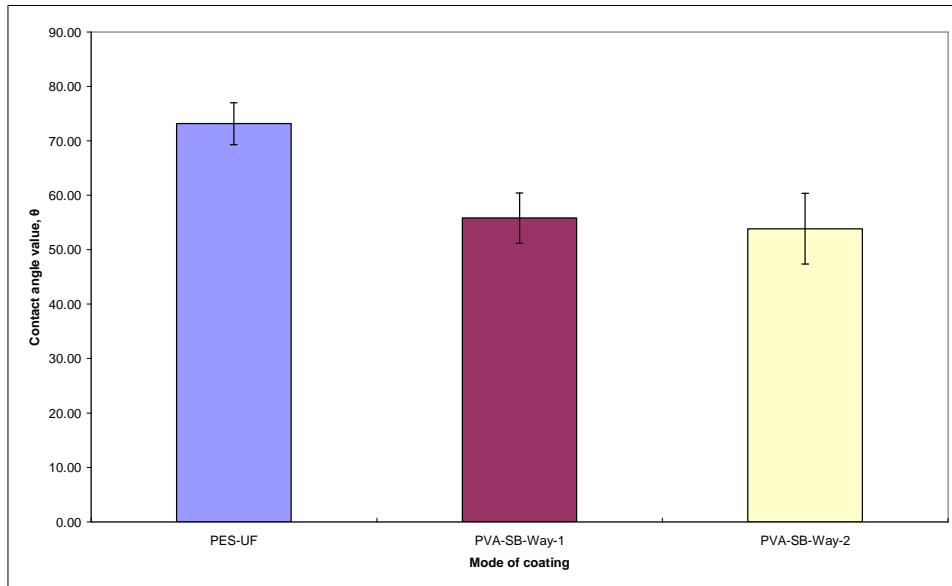


Figure 4-20: Contact angle values of polyethersulfone (PES-UF) support modified with different of modes of coating

The hydrophobic / hydrophilic character of the polymer obtained by IP is naturally influenced by the hydrophobic / hydrophilic character of the monomers. Since all the membranes prepared used the same acid chloride, only the hydrophobic / hydrophilic character of the amines should influence the differences of hydrophobic / hydrophilic character of the resulting polymer. **Figure 4-21** and **Figure 4-22** show the influence of the polyamide layer on the membrane surface.

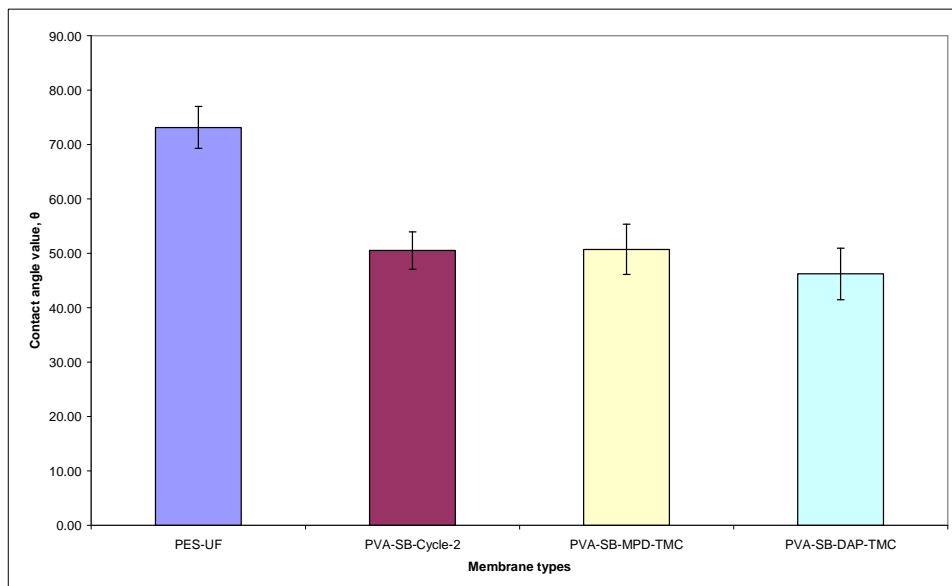


Figure 4-21: Contact angle values of poly(vinyl alcohol)-sodium tetraborate (PVA-SB) membranes modified with trimesoyl chloride (TMC)

The results in **Figure 4-21** show that the PVA-SB-DAP-TMC membranes have low values, when compared with the other modified membrane and unmodified membrane, which is an indication of a more hydrophilic character. As shown in **Figure 4-22**, the membranes made from DAP with FC became more hydrophilic than the membrane made from MPD with FC.

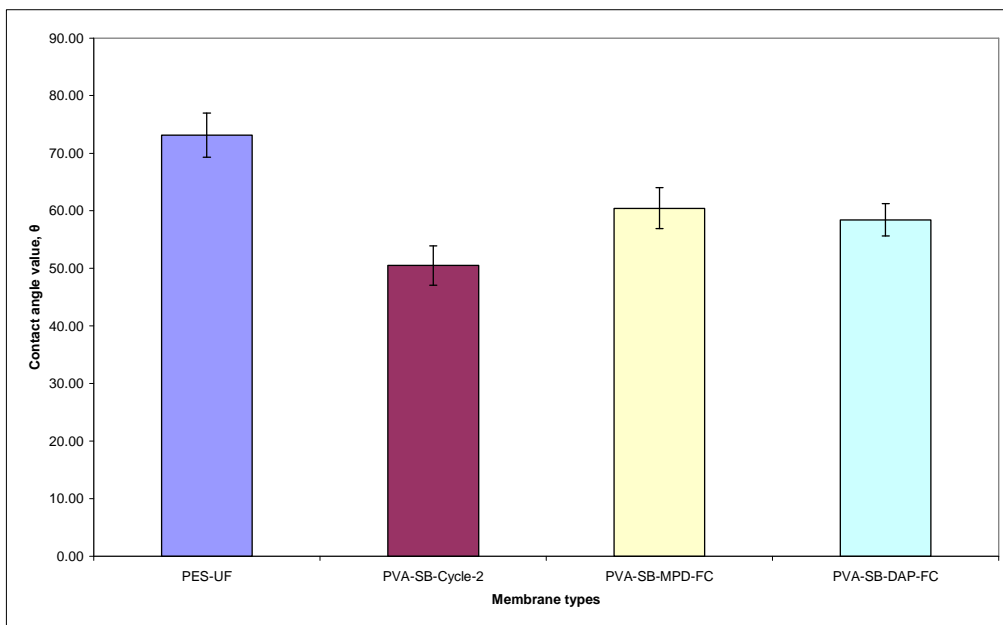


Figure 4-22: Contact angle values of PVA-SB poly(vinyl alcohol)-sodium tetraborate membranes modified with 2,5-furanoyl chloride (FC)

From this data it seems that the aromatic ring versus pyridine ring has less influence than the triacid versus the cyclic ether containing difunctional acid, which tends to be more hydrophobic. The answer must lie in unreacted carbonyl groups on the surface of the membrane. **Figure 4-21** and **Figure 4-22** show that DAP gives membranes with a more hydrophilic surface than MPD, and also the TMC gives membranes with a more hydrophilic surface than FC.

4.5.2 FOURIER TRANSFORM INFRARED (FT-IR) ANALYSIS

The active layer of a composite membrane is a very thin-film that bridges and overcoats the surface pores of the PES-UF membranes. FT-IR analysis can be used to identify the functional groups present in the barrier layer, after reaction of the amine species with the cross-linking agent. The FT-IR spectra of the four membranes: PES-UF, PVA-SB, PVA-SB-MPD-TMC and PVA-SB-DAP-TMC are presented in **Figure 4-23**. There are significant differences between these spectra, which indicate that there are significant differences in the structures of the composite layer.

Table 4-4 tabulates probable assignments of FT-IR absorbance for the PES-PVA-PA composite membrane. For example, in the spectrum of PVA-SB-DAP-TMC the band at 1680 cm^{-1} , which is characteristic of the amide I (C=O stretch), the 1547 cm^{-1} band is due to amide II (C-N stretch), the 1609 cm^{-1} band is due to polyamide aromatic ring breathing. The near surface region of the membrane contains amide (-NHCO-) groups and aromatic groups. The 950 cm^{-1} band is ascribed to amide V. These bands are clearly distinguishable from bands of the PES-UF FT-IR.

There is no absorption maximum at 3400 cm^{-1} for the PES-UF membrane, indicating that there were no hydroxyl groups (-OH) of PVA on the membrane surface. The strong band observed at 3400 cm^{-1} is a characteristic of the -OH of PVA on the surface of PVA-SB and PVA-SB-PA composite membranes. FT-IR spectra are presented in **Appendix A**.

Table 4-4: Possible assignments of IR peaks in the spectra of the polyethersulfone (PES-UF), poly(vinyl alcohol)-sodium tetraborate (PVA-SB) and poly(vinyl alcohol)-sodium tetraborate-polyamide (PVA-SB-PA) membranes

Spectra assignments	Wave number (cm^{-1})			
	PES	PVA-SB	PVA-SB-MPD-TMC	PVA-SB-DAP-TMC
O-H stretching	Nil	~3400 (broad)	~3474 (broad)	~3466 (broad)
C-H aromatic stretching	3070 – 3096	3068 – 3096	3068 – 3096	3068 – 3096
C-H aliphatic stretching	2872, 2928	2874, 2928	2856, 2928	2856, 2928
C=O stretching (acid)	Nil	Nil	1774	1782
C=O stretching (polyamide)	Nil	Nil	1680	1680
Aromatic ring breathing (polyamide)	Nil	Nil	1609	1609
C=C aromatic ring stretching	1580	1580	1582	1580
C-N stretching (polyamide)	Nil	Nil	1547	1532
C=C aromatic ring stretching	1502	1502	1502 (shoulder)	1502 (shoulder)
CH ₂ -C-CH ₃ stretching	1488	1488	1488	1488
OH deformation band (acid)	Nil	Nil	Nil	1454
C=C aromatic ring stretching	1410	1410	1410	1410
CH ₂ -C-CH ₃ symmetric deformation	1372	1372	1372	1376
C-SO ₂ -C asymmetric stretching	1324	1324	1324	1324
S=O stretching	1298	1298	1298	1298
C-O-C stretching	1246	1246	1246	1246
C-SO ₂ -C symmetric stretching	Nil	Nil	1156	1156
Skeletal aliphatic C-C/aromatic hydrogen bending, rocking	1156, 1108, 1074, 1012, 872	1154, 1108, 1074, 1012, 872	1106, 1080, 1015, 873	1108, 1074, 1012, 872
Aliphatic C-H rocking	836, 796, 718, 702	836, 796, 718, 702	854, 834, 740, 716	872, 836, 796, 718
Amide (polyamide)	Nil	Nil	950	950

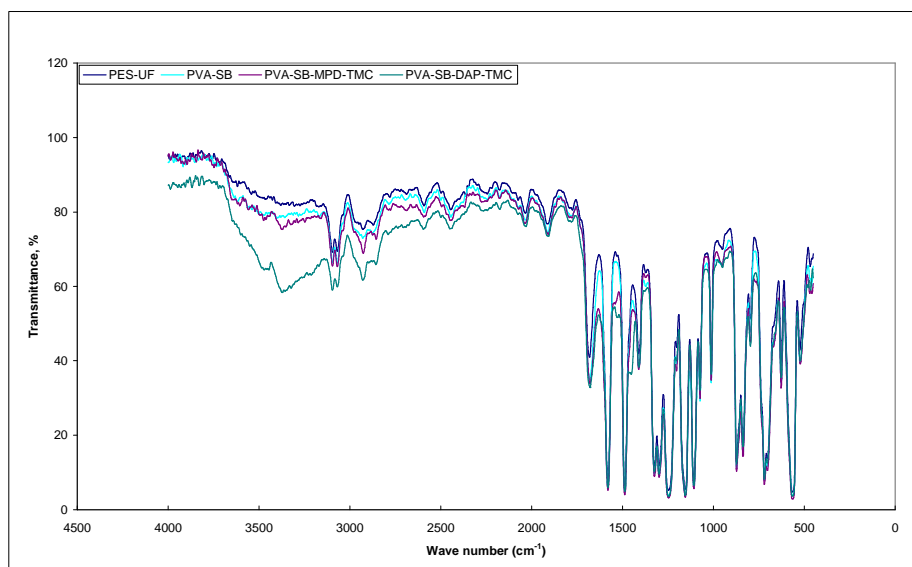


Figure 4-23: FT-IR spectra of polyethersulfone (PES-UF), poly(vinyl alcohol)-sodium tetraborate (PVA-SB) and poly(vinyl alcohol)-sodium tetraborate-polyamide (PVA-SB-PA) membranes

The following conclusions can be drawn from the above experimental results. The PVA-SB composite UF membrane prepared under the following conditions: high molecular weight of PVA, 1.5 wt% PVA solution, drained for 10 min at room temperature, cross-linked at room temperature with 0.5 wt% SB in aqueous solution for 10 min, and coated twice, showed better properties than the PES-UF membrane.

The PVA-SB-DAP-FC composite membrane from 2.0 wt% DAP solution, drained at room temperature for 10 min, then cross-linked with FC solution for 1 min at room temperature, then heated at 50 °C for 10 min will be used to carry out further experiments in the next chapter.

4.6 REFERENCES

- [1] Cadotte, J.E., *Synthetic Membranes*. ACS Symposium Series 153, ed. A.F. Turbak, American Chemical Society: Washington, D.C., 1981. p. 305-326.
- [2] Lang, K., S. Sourirajan, T. Matsuura, and G. Chowdhury, *A study on the preparation of polyvinyl alcohol thin-film composite membranes and reverse osmosis testing*. Desalination, 1996. 104: p. 185-196.
- [3] Bezuidenhout, D., *Polyvinyl alcohol and amine-modified polyvinyl alcohol nanofiltration and reverse osmosis membranes*, M.Sc. thesis, 1991, University of Stellenbosch: Stellenbosch.
- [4] Nielek, S., and T. Lesiak, *The synthesis of 2,5-diisocyanatofuran*. Journal fuer Praktische Chemie (Leipzig), 1988. 330 (5): p. 825-829.

Chapter 5

*OPTIMIZATION OF THE FABRICATION CONDITIONS
FOR NANOFILTRATION MEMBRANES USING
RESPONSE SURFACE METHODOLOGY*

Abstract

This chapter describes the response surface methodology (RSM) used to optimize the preparation conditions that had the largest effects on the performance of the poly(vinyl alcohol) PVA / polyamide (PA) composite membranes. Good membrane performance could be realized through manipulating three variables: 2,6-diaminopyridine (DAP) concentration, 2,5-furanyl chloride (FC) concentration and polymerization time (PT). The regression equations between the preparation variables and the reverse osmosis (RO) performance of the composite membranes were established. Main effects, quadratic effects and interactions of these variables on the composite membrane performance were investigated. According to the results of this study the DAP concentration was the most significant variable that influenced the permeate flux and the retention. The experimental results were in good agreement with those predicted by the proposed regression models. One can expect to apply the regression equations in the preparation of composite membranes and reasonably predict and optimize the performance of the composite membranes. The analysis of variance (ANOVA) was performed to validate the developed regression models. Furthermore, the response surface plots were drawn for spatial representation of the regression equations.

Keywords: Thin-film composite membrane, Polyamide, Response surface, Factorial design

5.1 INTRODUCTION

The thin-film composite (TFC) membranes have become commercially important because of their excellent performance. They are widely used, for a number of applications, such as in the desalination of brackish water or seawater [1, 2]. The TFC RO membranes consists of two layers of dissimilar materials bonded together to form a single membrane. This layered construction permits the use of material combinations that optimize the performance and durability of the membrane. The two phases involved in the interfacial polymerization (IP) process include the aqueous phase and the organic phase to form the active layer having semipermeability. Both the type of material and the molecular structure of polymer in the two phases influenced the permeation properties of membrane performance [3].

The reactants and conditions used in IP have been recognized as the primary factors determining the separation performance of RO membranes [4-6]. Kim et al. [4] investigated the relationship between PT versus membrane performance. They observed that salt retention and water flux of the TFC membrane did not change when the reaction time was longer than 1 min. Rao et al. [7] studied the effects of the concentration of reactants, reaction time, curing time and curing temperature of the IP reaction on the RO performance. Additionally, post treatment plays an important role in determining the membrane flux and retention. On the other hand, Rao et al. [6] believe that the changes in the coating conditions influence the membrane structure of the interfacial polymerized surface film and subsequently the membrane performance.

Preparation conditions can determine the membrane structure and performance. Thus, a composite membrane with good performance can be obtained by manipulating preparation conditions. Most of the early research on membranes involved the use of changing one factor at a time to improve membrane performance. This experimental approach is not only time consuming and costly but also ignores the interaction effect between the considered factors, and leads to low efficiency in process optimization [8]. Use of the statistical design of experimental techniques in membrane science has

been increasing. The data collected is analyzed using statistical methods, resulting in a valid and objective conclusions [8]. RSM can be applied to avoid the limitations of the conventional method. It involves the following major steps: (1) statistical design of experiments in which all factors are varied simultaneously over a set of experimental runs; (2) estimation of the coefficients in the mathematical model based on experimental design; (3) checking the adequacy of the developed model; (4) prediction of the response and optimization of experimental conditions using the valid model [8, 9].

Although the traditional orthogonal method is capable of considering a few factors at the same time, and it can develop a functional expression between the factors and response values, it is difficult to determine optimal factor combinations and optimal response values in the whole area. In membrane studies, Idris et al. [10] have used the Taguchi method, which is a statistical design of experiment technique, to determine the significant factors affecting the spinning process and the optimal spinning parameter. Chau et al. [11] has studied phase inversion factors influencing polysulfone (PS) ultrafiltration (UF) hollow fiber membrane fabrication in a systematic manner using the orthogonal array method, while Pesek and Koros [12] studied the influence of four factors in the production of gas separation membranes using the complete 2^k factorial method.

RSM is a statistical method that uses quantitative data from appropriate experiments to determine multiple regression equations between the factors and experimental results [9]. In recent years RSM has played an important role in biotechnology. However, there have been few investigations of the function of RSM in the membrane field. Ismail and Lai [13] studied the preparation of defect-free asymmetric PS membranes for gas separation through the manipulation of membrane fabrication variables using RSM. Idris et al. [14] used RSM to investigate the composition effect of the aqueous phase on the IP of RO membranes. Xiangli et al. [15] used RSM to optimize the preparation conditions that had great effects on the performance of polydimethylsiloxane / ceramic composite membranes for pervaporation. To date, there is no report available on using RSM to optimize the preparation conditions of PVA / PA TFC membranes.

As described in Chapter 4, high flux of PVA / PA composite membranes was prepared. Upon investigating the effects of the operating pressure on the membrane performance, it was found that the preparation conditions affected the performance of composite membranes. The detailed relationship between the preparation conditions and the performance was not investigated. Therefore, in order to elucidate this relationship, the PA layer on the top of PVA-SB asymmetric support was prepared and the preparation conditions were optimized by using RSM. The regression equations between the preparation parameters and the performances of the composite membranes were established. The following were considered as dominant preparation parameters in controlling the membrane performance: DAP concentration, FC concentration and PT. Main effects, quadratic effects and interactions of the three variables on the flux and the selectivity of composite membrane were investigated.

5.2 RESPONSE SURFACE METHODOLOGY

RSM is a statistical and mathematical method that offers an effective practical means for design optimization and that can be used for studying the effect of several factors at different levels and their influence on each other [9]. Furthermore, it helps to obtain the surface contour that provides a good means of visualizing the parameter interaction [16]. Two goals of RSM are to find an approximating

function for predicting future response and to determine factor values that optimize the response function.

A RSM study begins with a definition of the problem for which a response is to be measured, how it is to be measured, and which variables are to be explored. The experimental plan is then designed. When the behaviour (response) (y), which should be taken into consideration for the design, is determined as a function of multiple variables (x), the behaviour of the response surface is expressed by a polynomial $y = f(x)$ on the basis of observation data. In the case of a quadratic response function, with a multiple linear regression model, it is expressed by equation 5.1:

$$y = \beta_0 + \sum_i^p \beta_i x_i + \sum_i^p \beta_{ii} x_i^2 + \sum_{i < j}^p \beta_{ij} x_i x_j + \dots + \varepsilon \quad (5.1)$$

where x_1, x_2, \dots, x_i are the variables that influence the response y , β_0 is the constant coefficient, β_i are the linear coefficients, β_{ii} are the quadratic coefficients, β_{ij} are the second-order interaction coefficients, and ε is the approximation error. In developing the regression equation the test variables were coded according to the following equation:

$$x_i = \frac{(X_i - X_i^*)}{\Delta X_i} \quad (5.2)$$

where x_i is the coded value of the i th independent variable, X_i is the uncoded value of the i th independent variable, X_i^* is the uncoded i th independent variable at the centre point, and ΔX_i is the step change value.

Response surfaces and contour plots are developed using the fitted quadratic polynomial equations obtained from the response surface regression analysis. The fitted surface may have a maximum, a minimum, or a saddle point in the region. At an optimal point, the rates of change $\partial y / \partial x_i$ are equal to 0. Central composite designs are response surface designs that can fit a full quadratic model. The general form of a central composite design is composed of NC cube points, NA axial points and NO centre points for a total of $N = NC + NA + NO$ experimental units.

The 2^3 full factorial design for three independent variables, each at five levels with eight cube points, six axial points and six replicates at the centre points, was employed to fit a second order polynomial model, which indicated that 20 experiments were required. The Design Expert Version 7.0 software [17] was used to develop the experimental plan for RSM. This software was also used to analyze the data collected by performing ANOVA. If the model looks good, then the three-dimensional graphs and contour plots would be plotted for interpretation. In brief, a good model must be significant and the lack-of-fit must be insignificant. The various coefficients of determination, R^2 values, should be close to 1. The diagnostic plots should exhibit trends associated with a good model and these will be elaborated.

5.3 EXPERIMENTAL

5.3.1 MATERIALS

The polyethersulfone (PES) ultrafiltration (UF) membranes were used as support membranes (see Section 3.1.1). All chemicals were commercial analytical grade and were used as received without further purification (see **Table 3-4** and **Table 3-5**).

5.3.2 MEMBRANE FABRICATION

PVA solution (1.5%) and sodium tetraborate (SB) solution (0.5%) were prepared. The aqueous solutions were prepared according to the experimental plan using DAP as a monomer in the presence of triethylamine (TEA) as a catalyst, sodium dodecyl sulfate (SLS) as surfactant, and camphor sulfonic acid (CSA) to adjust the pH to 10. The organic solutions were prepared according to the experimental plan using FC as dicarboxylic acid chloride and dissolved in hexane.

The PES-UF support was first washed with pure water and then dried at room temperature for 10 min. The PES-UF support was coated twice with a PVA gel sub-layer, as described in Chapter 4, Section 4.4, **Table 4-3**. The PVA-SB surface was then exposed to the aqueous solution of DAP for 5 min and the excess solution was drained for 10 min. The membrane surface was again immersed into FC dissolved in hexane according to the experimental plan. Finally, the membrane was cured for 10 min at 50°C.

5.3.3 MEMBRANE EVALUATION

The composite membrane performance was determined using a flat sheet permeation cell using an applied pressure of 1 MPa (see Section 3.5). A feed solution of 2000 ppm Na₂SO₄ solution was used. The flux (J) in the presence of solute for the membranes is obtained by:

$$J = \frac{V}{S \cdot \Delta t} \quad (5.3)$$

where V is volume of permeate (L), S is membrane surface area (m²) and Δt is the permeation time (hour). A minimum of eight membrane samples were tested and the tabulated results are the averaged values. The retention of the membrane is given by:

$$R = \left[1 - \left(\frac{C_p}{C_f} \right) \right] \times 100 \quad (5.4)$$

where C_p is the solute concentration in the permeate stream and C_f is the solute concentration in the feed stream. C_p and C_f were determined using a CyberScan Con 500 Bench conductivity metre.

5.3.4 EXPERIMENTAL DESIGN

Central composite design (CCD) is widely used in statistical modelling to obtain response surface models that set the mathematical relationships between response and factors. In this study the experimental design was based on the CCD. 2³ full factorial experimental designs were used to optimize the three independent variables according to Myers and Montgomery [9]. The processing variables involved in the study are shown in **Table 5-1**. The variables investigated were DAP concentration (A), FC concentration (B) and PT (C). The response variables measured were the flux (J) and the retention (R). Hence, the central composite experimental design of orthogonal type was employed as it is shown in **Table 5-2**.

The CCD selected a range of a high (+1) level and a low (-1) level based on results of preliminary experiments, and used an axial spacing (± 1.682). The experimental design of $N = 8 + 6 + 6 = 20$ experimental units and the RO performance results are presented in **Table 5-2**. The Design-Expert Software 7.0 [17] was utilized to analyze the experimental designs in **Table 5-2**. Design-Expert is a comprehensive, integrated data analysis, graphics, and database management software. It can

provide the widest selection of predictive modelling and the most comprehensive array of data analysis.

Table 5-1: The variable factors investigated and levels in the experimental design

Factors	Levels				
	-1.682	-1	0	+1	+1.682
(A) DAP concentration, %	0.66	1	1.5	2	2.34
(B) FC concentration, %	0.26	0.4	0.6	0.8	0.94
(C) PT, sec	26.36	40	60	80	93.64

Table 5-2: Design layout and experimental results

Experiment	Run	Type	Factors			Response variables	
			A	B	C	Flux, L/m ² .h	Retention, %
1	12	Fact	-1.000	-1.000	-1.000	69.9	63.7
2	2	Fact	1.000	-1.000	-1.000	41.7	71.0
3	19	Fact	-1.000	1.000	-1.000	55.6	71.1
4	13	Fact	1.000	1.000	-1.000	43.8	73.2
5	4	Fact	-1.000	-1.000	1.000	65.9	34.6
6	15	Fact	1.000	-1.000	1.000	32.5	70.2
7	8	Fact	-1.000	1.000	1.000	56.7	47.4
8	9	Fact	1.000	1.000	1.000	40.3	73.9
9	7	Axial	-1.682	0.000	0.000	69.8	41.8
10	16	Axial	1.682	0.000	0.000	52.6	81.4
11	20	Axial	0.000	-1.682	0.000	52.1	44.6
12	18	Axial	0.000	1.682	0.000	41.5	72.6
13	10	Axial	0.000	0.000	-1.682	67.0	67.8
14	3	Axial	0.000	0.000	1.682	43.7	48.6
15	6	Centre	0.000	0.000	0.000	69.4	51.9
16	1	Centre	0.000	0.000	0.000	65.3	52.8
17	11	Centre	0.000	0.000	0.000	74.1	52.5
18	17	Centre	0.000	0.000	0.000	72.6	45.2
19	14	Centre	0.000	0.000	0.000	68.1	48.4
20	5	Centre	0.000	0.000	0.000	75.2	50.7

5.4 RESULTS AND DISCUSSION

The results of the performance evaluation of the TFC membranes produced as per the experimental plan are showed in **Table 5-2**. The retention and flux rate results were input into the Design Expert software for further analysis. Examination of the Fit Summary output revealed that the Multiple Linear Regressions (MLR) model is statistically significant for the flux and the retention. Therefore, this model was used to represent each of the responses for further analysis.

5.4.1 ANALYSIS OF VARIANCE

In order to ensure a good model, a test for significance of the regression model, a test for significance on individual model coefficients and a test for lack-of-fit needed to be performed. An ANOVA table is commonly used to summarize the results of the tests performed. Based on the multiple linear regressions model, 10 coefficients (3 main effects, 3 quadratic effects, 3 interactions, 1 constant) and coefficient of determination (R^2) were estimated.

Table 5-3 and **Table 5-4** show the ANOVA analysis for the flux and the retention. Parameters at the 95% confidence level were considered as significant. According to **Table 5-3**, the coefficient of determination ($R^2 = 0.91$) was close to 1, which is acceptable. It indicates that only 9% of the variations in the observed data could not be explained by the model. The value of the adjusted R^2 was equal to 0.83, which is also a very high significance for a model [9]. The predicted R^2 square is in reasonable agreement with the adjusted R^2 . Adequate precision compares the range of the predicted values at the design points to the average prediction error. Ratios greater than 4 indicate adequate model discrimination. In this case the value is well above 4.

According to **Table 5-4**, the R^2 value for retention is 0.94, which is close to 1, which is desirable. This means that the regression model explained 94% of the variations. Also, the predicted R^2 is in agreement with the adjusted coefficient of determination R^2 . The adequate precision value is well above 4. The p -value for the model in **Table 5-3** and **Table 5-4** is less than 0.05, which indicates that the model is adequate. All these statistical estimators reveal that the response model is acceptable from a statistical point of view for the prediction of the response in the considered range of factors (valid region).

The effects of DAP concentration (A , A^2), FC concentration (B^2), and PT (C , C^2) have statistical significance with respect to flux within the limits of the operating levels. The DAP concentration and FC concentration are the most significant factors for the flux. The main effects of FC concentration (B) and its interaction (AB , BC), and interaction (AC), are less significant than the other effects (A , A^2 , B^2 , C , and C^2) with respect to the flux. However, the importance of FC concentration (B) and its interaction (AB , BC), and interaction (AC), can not be neglected. The insignificance of effects does not mean that these factors are unimportant; it simply implies little influence on response. These insignificant terms can be removed and may result in an improved model. The lack-of-fit can also be said to be insignificant. This is desirable as we require a model that fits. The significant factors could be ranked based on F -value or p -value. Thus, in this study, the ranking is as follows: $B^2 > A > C^2 > A^2 > C$ for the flux in **Table 5-3**.

The same procedures were applied to the other response variable, i.e. retention, and the resulting ANOVA table for the quadratic model is shown in **Table 5-4**. The significant model terms are DAP concentration (A , A^2), FC concentration (B , B^2), PT (C , C^2), the interaction of DAP concentration and PT (AC). The DAP concentration and FC concentration are the most significant factors associated with retention because they control the thickness of the selective layer. However, the importance of interaction effects could not be neglected. Note that the insignificance of interaction effects did not necessarily mean that these particular factors were unimportant, but just implied that interactions among them had little influence on response. The larger the magnitude of the F -value and correspondingly the smaller the $\text{prob} > F$ value, the more significant is the corresponding coefficient [18]. It was concluded that the significant effects were in the order of $A > B > C > AC > A^2 > B^2 > C^2$ for the retention in **Table 5-4**.

The application of RSM allowed two empirical models between the responses and the coded variables to be obtained, as follows:

- Flux, J: $\text{Flux} = +70.90 - 8.69 * A - 4.02 * C - 3.96 * A^2 - 9.05 * B^2 - 6.03 * C^2$ (5.5)

- Retention, %:

$$\text{Retention} = +50.14 + 10.12 * A + 5.37 * B - 6.24 * C + 6.60 * A * C + 4.67 * A^2 + 3.62 * B^2 + 3.48 * C^2 \quad (5.6)$$

In terms of actual factors the final empirical models are as follows:

- Flux, J: $\text{Flux} = -16.65 + 12.53 * \text{DAP} + 1.59 * \text{PT} - 15.86 * \text{DAP}^2 - 226.31 * \text{FC}^2 - 0.02 * \text{PT}^2$ (5.7)

- Retention, %:

$$\text{Retention} = +79.47 - 64.61 * \text{DAP} - 68.00 * \text{FC} - 2.48 * \text{PT} + 0.66 * \text{DAP} * \text{PT} + 18.67 * \text{DAP}^2 + 90.46 * \text{FC}^2 + 0.0087 * \text{PT}^2$$
 (5.8)

Table 5-3: Analysis of variance of the regression model for flux

Source	Sum of squares	dF	Mean squares	F-value	Prob > F	Coefficient
Model	3154.00	9	350.44	11.31	0.0004 significant	70.90
A	1031.08	1	1031.08	33.27	0.0002	-8.69
B	72.94	1	72.94	2.35	0.1560	-2.31
C	220.97	1	220.97	7.13	0.0235	-4.02
AB	139.31	1	139.31	4.49	0.0600	4.17
AC	12.09	1	12.09	0.39	0.5463	-1.23
BC	14.85	1	14.85	0.48	0.5045	1.36
A ²	226.46	1	226.46	7.31	0.0222	-3.96
B ²	1180.93	1	1180.93	38.10	0.0001	-9.05
C ²	523.14	1	523.14	16.88	0.0021	-6.03
Residual	309.92	10	30.99			
Lack of fit	237.70	5	47.54	3.29	0.1085 not significant	
Pure error	72.21	5	14.44			
Correct total	3463.91	19				
<hr/>						
Standard deviation		5.57	R-Squared R^2		0.9105	
Mean		57.90	Adjusted R-squared R^2		0.8300	
Coefficient of Variation, C.V. %		9.62	Predicted R-squared R^2		0.4490	
PRESS		1908.68	Adequate precision		10.062	

Table 5-4: Analysis of variance of the regression model for retention

Source	Sum of squares	dF	Mean squares	F-value	Prob > F	Coefficient
Model	3273.03	9	363.67	19.15	< 0.0001 significant	50.14
A	1397.88	1	1397.88	73.62	< 0.0001	10.12
B	394.34	1	394.34	20.77	0.0010	5.37
C	532.20	1	532.20	28.03	0.0004	-6.24
AB	25.72	1	25.72	1.35	0.2715	-1.79
AC	348.16	1	348.16	18.34	0.0016	6.60
BC	6.20	1	6.20	0.33	0.5803	0.88
A ²	314.11	1	314.11	16.54	0.0023	4.67
B ²	188.70	1	188.70	9.94	0.0103	3.62
C ²	174.60	1	174.60	9.20	0.0126	3.48
Residual	189.88	10	18.99			
Lack of fit	145.92	5	29.18	3.32	0.1070 not significant	
Pure error	43.96	5	8.79			
Correct total	3462.90	19				
<hr/>						
Standard deviation		4.36	R-Squared R^2		0.9452	
Mean		58.18	Adjusted R-squared R^2		0.8958	
Coefficient of Variation, C.V. %		7.49	Predicted R-squared R^2		0.6613	
PRESS		1172.95	Adequate precision		16.051	

Therefore, one can take advantage of the above mentioned effects to obtain a membrane with good performance. In terms of a quadratic response function with a multiple variables model, the flux and retention can be predicted within the limits of the experiment.

The normal probability plot of the residuals and the plot of the residuals versus the predicted response for both the retention and flux are shown in **Figure 5-1** and **Figure 5-2**. A check on the plot in **Figure 5-1** revealed that the residuals generally fall on a straight line, implying that errors are distributed normally, and thus support the adequacy of the least square fit. **Figure 5-2** revealed that it has no obvious pattern and unusual structure. They also show equal scatter above and below the x-axis. This implies that the models proposed are adequate and there is no reason to suspect any violation of the independence or constant variance assumption.

5.4.2 EFFECT OF PROCESS VARIABLES ON MEMBRANE PERFORMANCE

An empirical study on the relationship between responses and input variables with a selected range of the operating level was carried out using RSM. The three dimensional surface and contour plots were fitted to give a functional relationship. Interactions among processing parameters, including DAP concentration (A), FC concentration (B) and PT (C), induced substantial effects on membrane structures and performances. By considering two variables simultaneously, while keeping the third one at the middle level, the surface and contour plots of the DAP concentration (A), FC concentration (B) and PT (C) on the flux and the retention are presented in **Figure 5-3** to **Figure 5-8**.

In **Figure 5-3** the flux decreased when the DAP concentration was 1.0 to 2.0% and the PT was at the middle level (60 sec). The FC concentration had an effect on the flux, which increased from 0.4 to 0.58% and decreased from 0.58 to 0.80%. The decrease in flux was due to an increase in the thickness of the selective layer with the increase in the concentration of the two monomers.

A similar phenomenon is seen in **Figure 5-4**. The flux decreased when the DAP concentration was increased, while keeping the FC concentration at the middle level (0.60%). The flux increased when the PT was increased from 40 to 60 sec, and decreased with an increase in PT from 60 to 80 sec. The flux increased with an increase in PT until 60 sec, which may result from the decrease in the degree of cross-linking. However, when PT exceeds 60 sec, the flux decreased, because tighter cross-linking of bonds leads to less swelling and a decreasing flux [7]. Thus, a polymerization time of 60 sec is the best.

Figure 5-5 shows the effect of FC concentration (B) and PT (C) on the flux. The flux increased when the PT was increased from 40 to 60 sec, and decreased with an increase in PT from 60 and 80 sec, at a fixed DAP concentration (1.5%). The maximum flux of 75.2 L/m².h can be computed by $\partial z/\partial x_i = 0$ when the DAP concentration, FC concentration and PT are 1.5%, 0.6% and 60 sec, respectively, in **Figure 5-3** and **Figure 5-5**.

The response surface and contour plots of the retention response reveal that increasing both DAP concentration and FC concentration leads to an improvement in retention. The effect of the DAP concentration (A) and FC concentration (B), while keeping PT at the middle level (60 sec), is clearly seen in **Figure 5-6**. Retention increases when the DAP concentration changes from 1.0 to 2.0% and the FC concentration increases from 0.4 to 0.8%. The maximum retention of 72.02% is observed when the DAP concentration is 2.0% and the FC concentration is 0.8%. At higher values of the DAP concentration the effect of the FC concentration upon retention is more pronounced than at the lower

DAP concentration. Likewise, the effect of the DAP concentration is more intense at a higher value of the FC concentration.

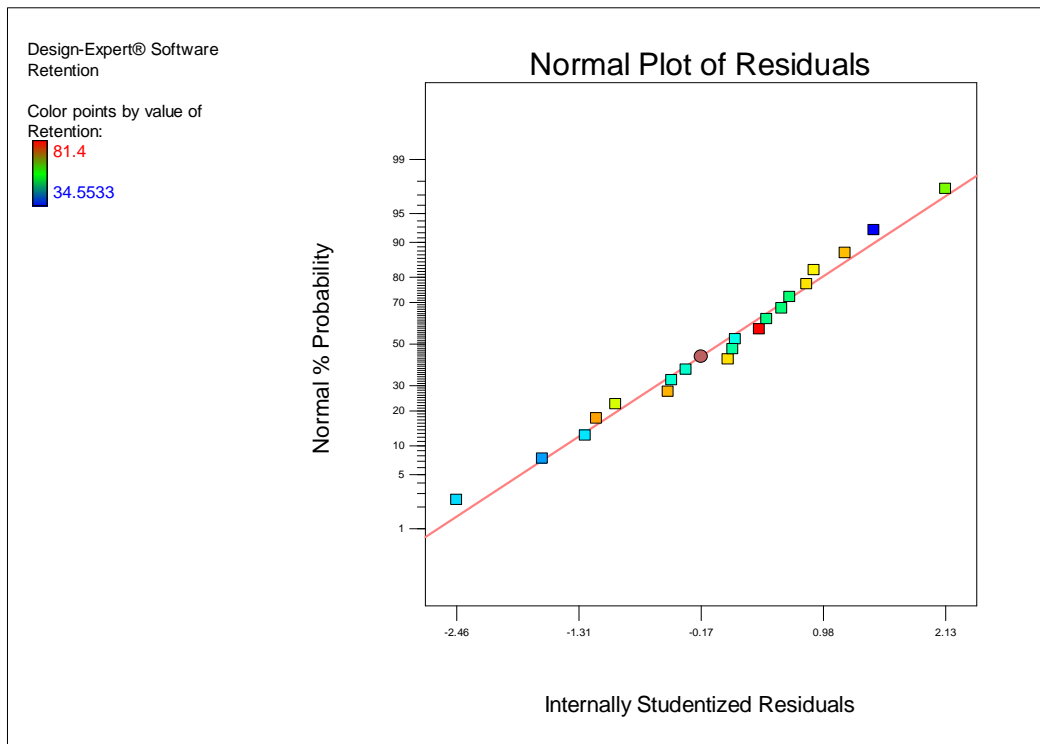
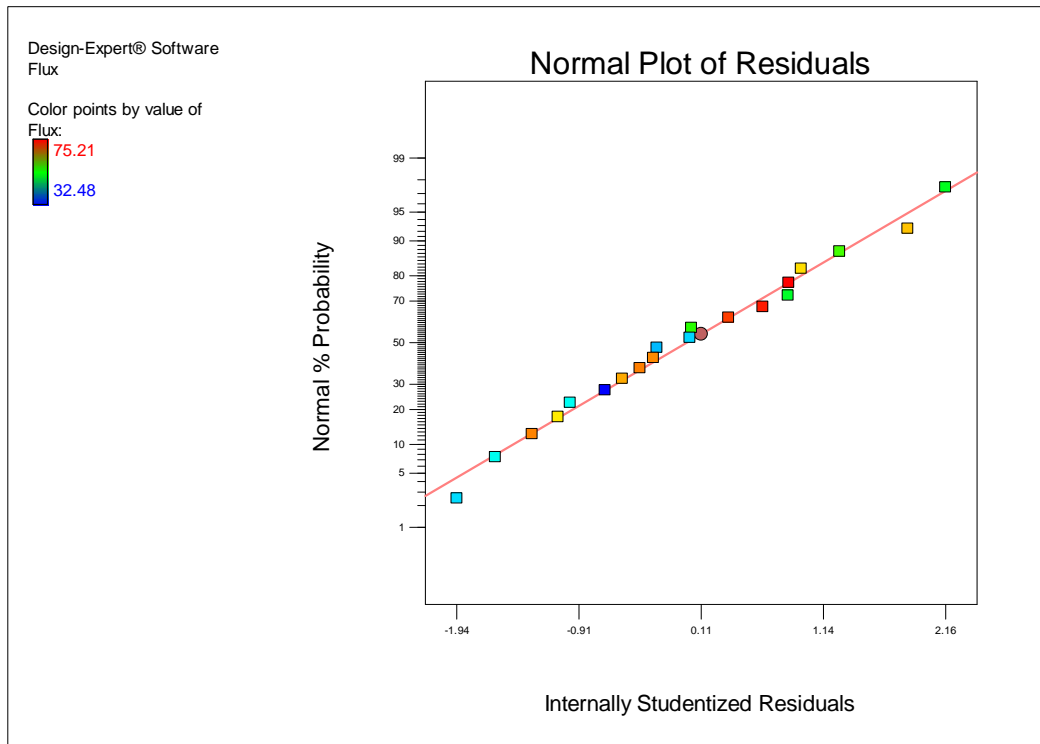


Figure 5-1: Normal probability plot of residual for (a) Flux and (b) Retention

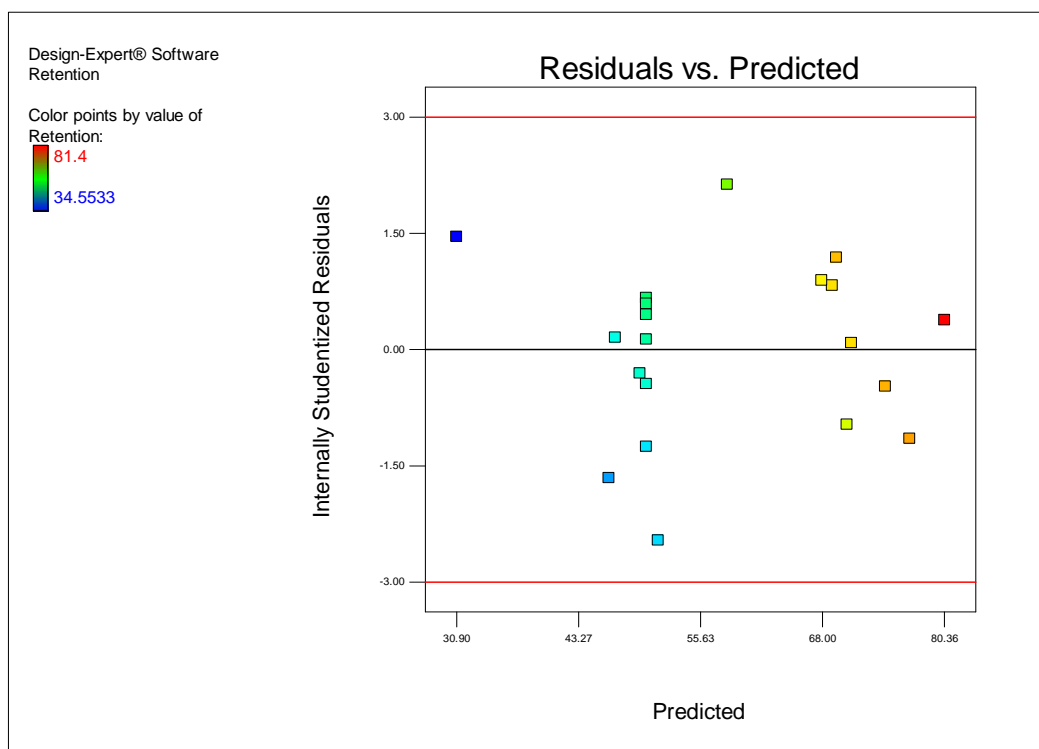
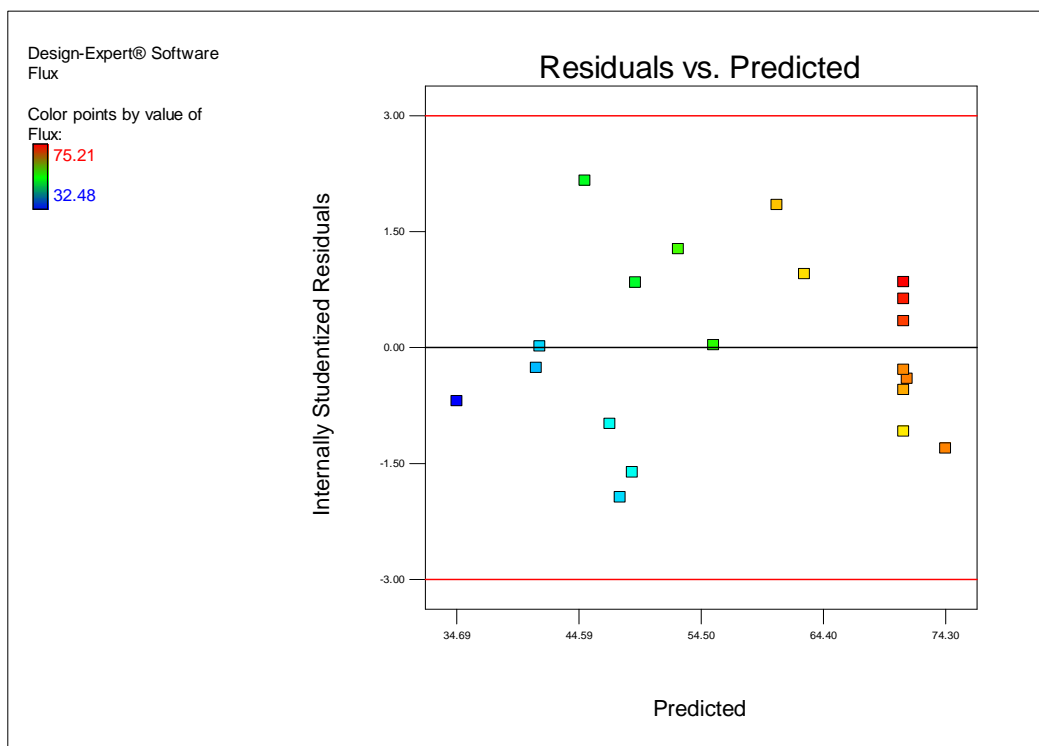


Figure 5-2: Plot of residual vs. predicted response for (a) Flux and (b) Retention

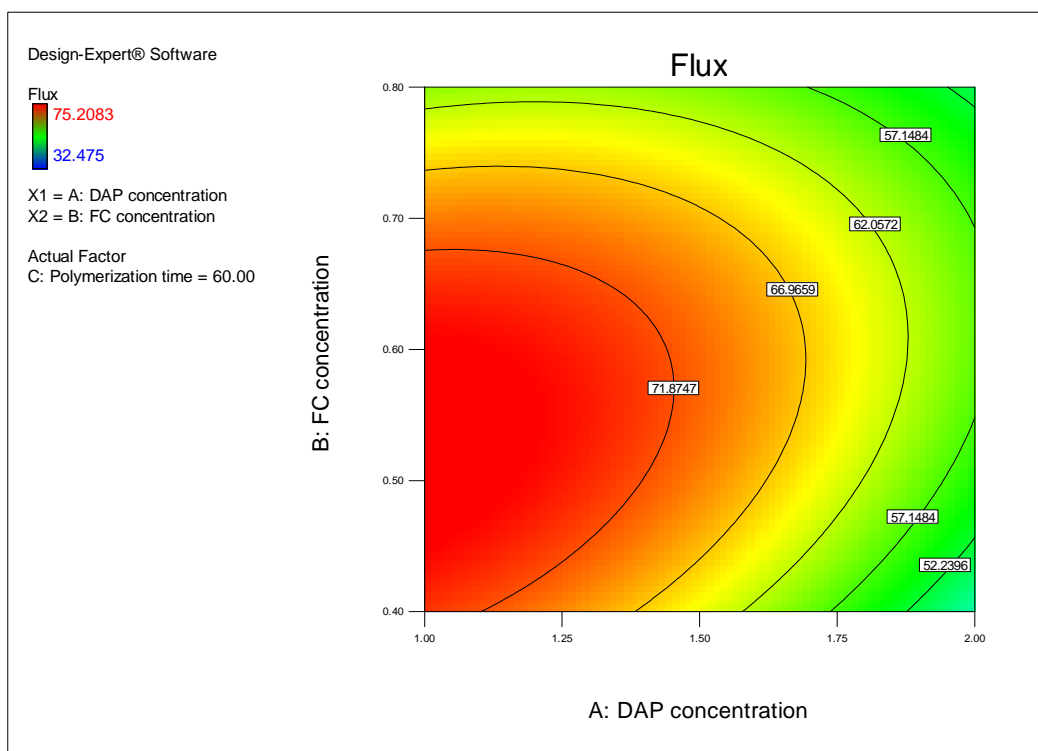
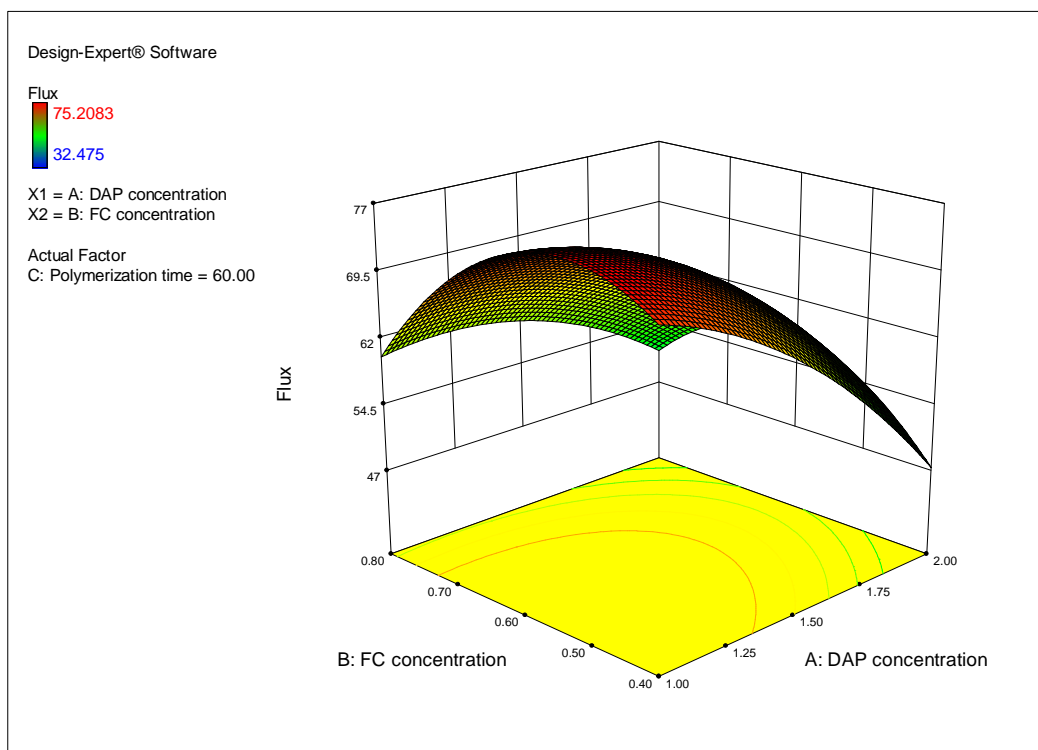


Figure 5-3: Response surface and contour plot indicating the effect of DAP concentration and FC concentration upon flux for a polymerization time 60 sec

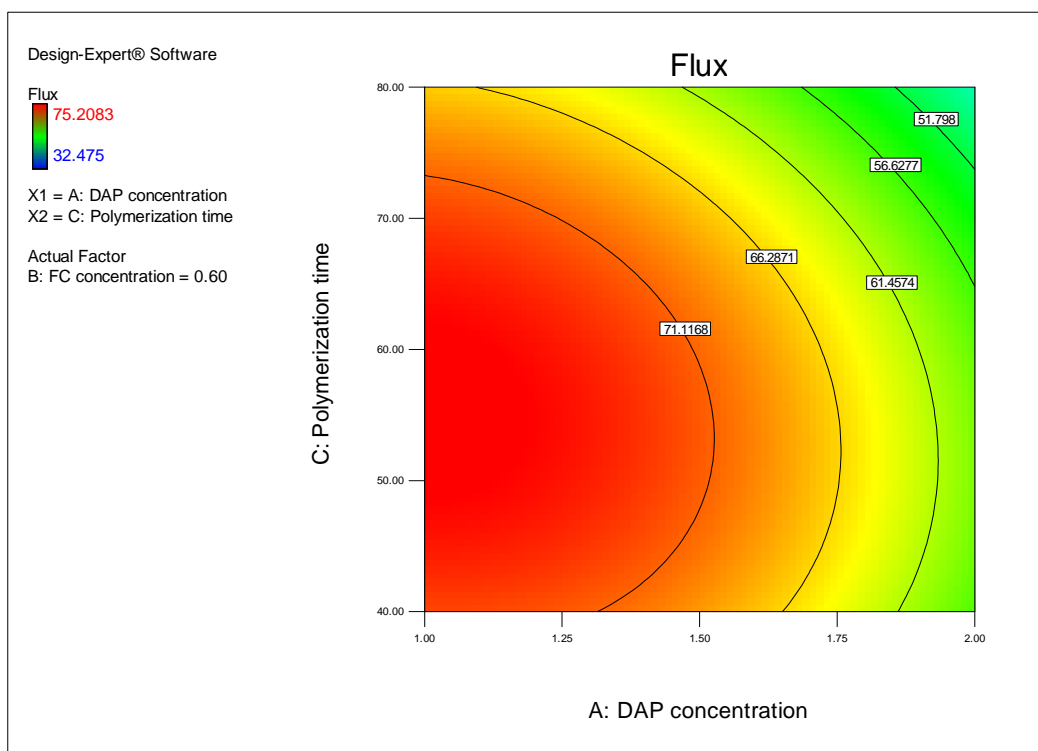
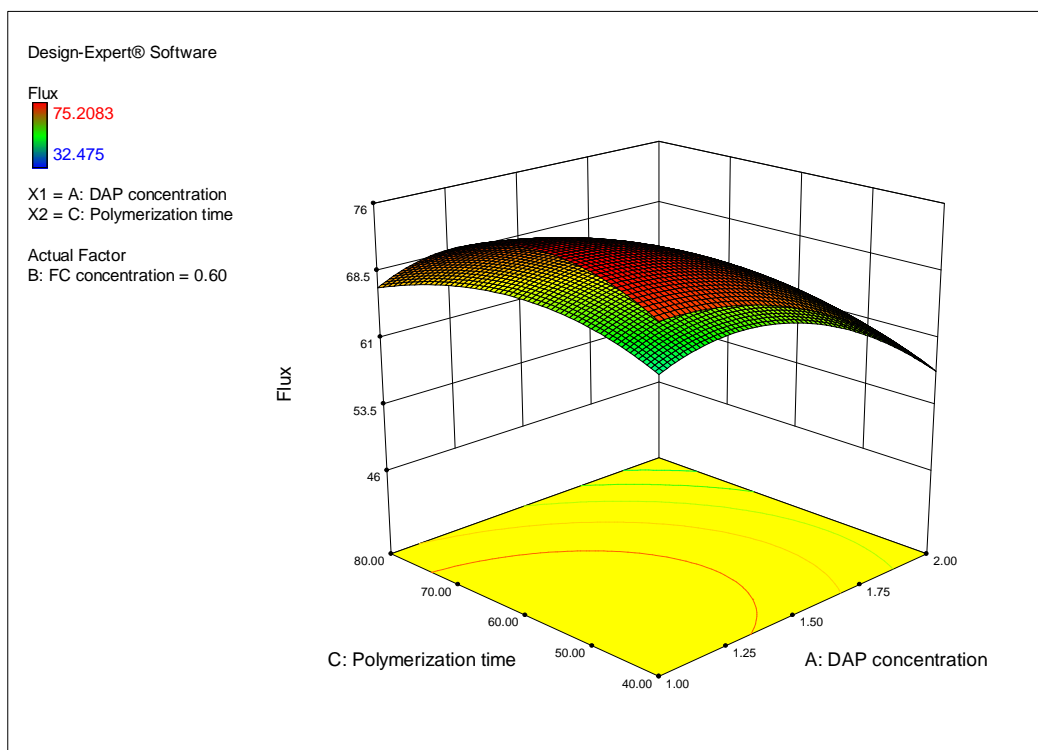


Figure 5-4: Response surface and contour plot indicating the effect of DAP concentration and IP polymerization time upon flux for a FC concentration 0.60%

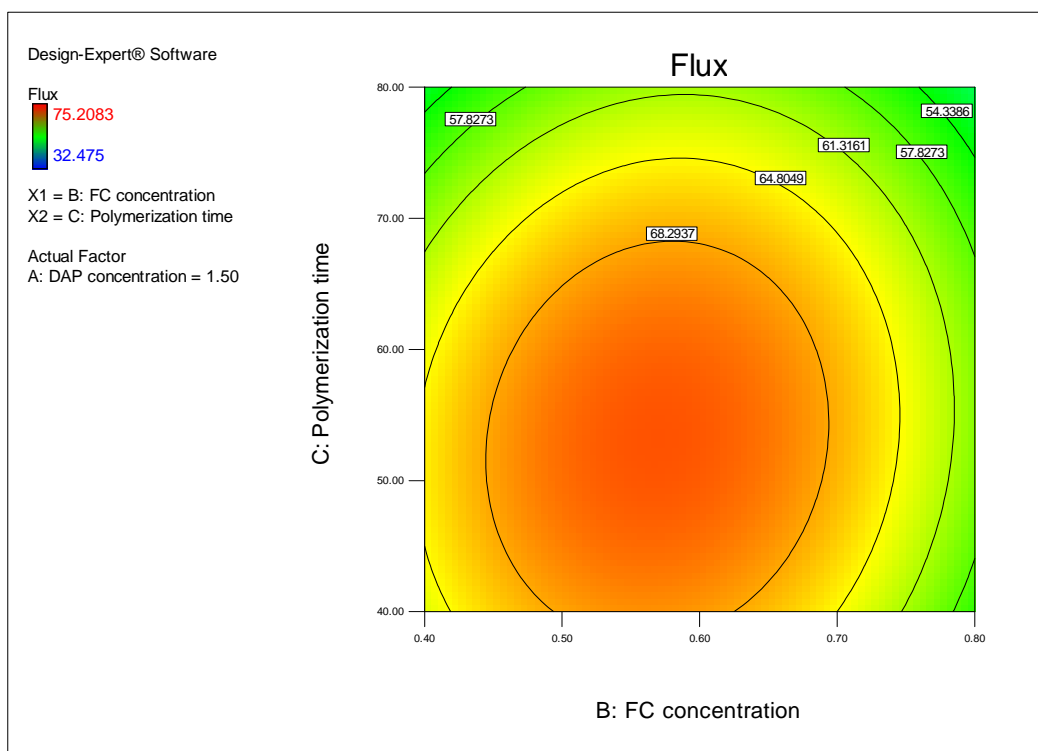
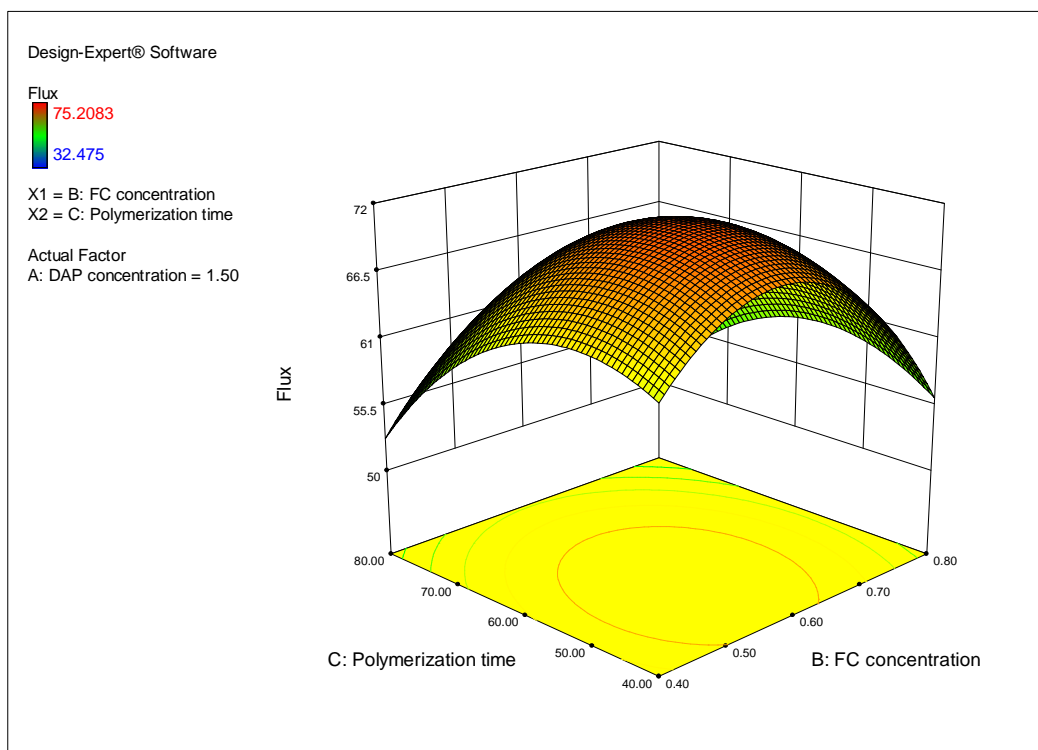


Figure 5-5: Response surface and contour plot indicating the effect of FC concentration and IP polymerization time upon flux for a DAP concentration 1.5%

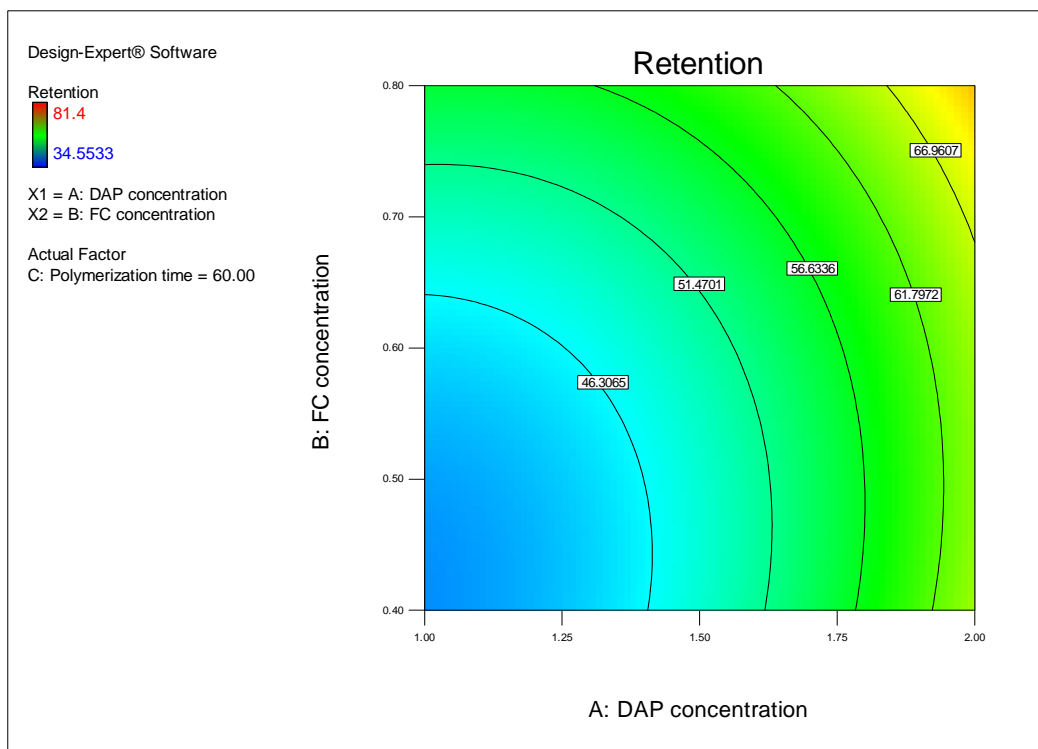
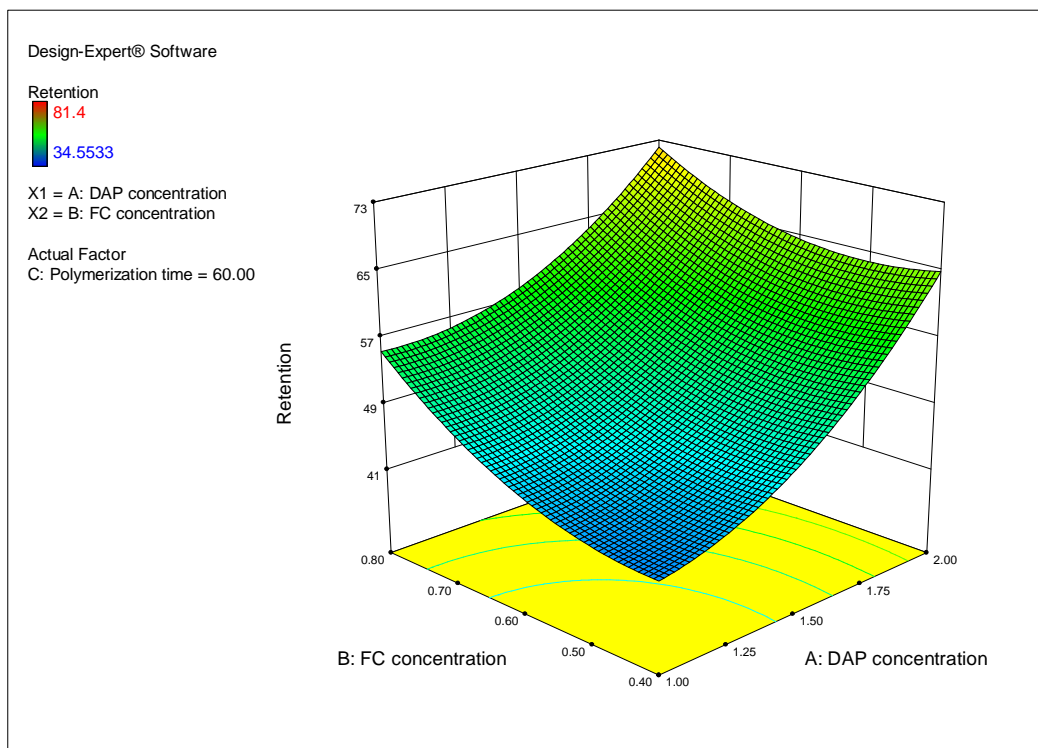


Figure 5-6: Response surface and contour plot indicating the effect of DAP concentration and FC concentration upon retention for a polymerization time 60 sec

The interaction effects between factors DAP and FC concentrations (**Figure 5-6**) show that at higher values of both parameters the retention is more pronounced. The data plot shows that the retention of the composite membranes increases when DAP and FC concentrations are increased. DAP, a polyfunctional amine, reacts with the diacid chloride, forming the thin cross-linked structure. Thus, increasing the amount of polyfunctional amine and acid chloride cause an increase in the retention since there is more than sufficient reactants to react with the acid chloride forming a perfect thin composite layer [19]. However, when the quantity of DAP and FC are decreased, the retention decreases. Thus, the DAP concentration and FC concentration are the most significant factors affecting the retention. Interaction between DAP concentration and FC concentration were not significant. This is expected as stoichiometry is not needed or expected in the IP reaction.

The surface and contour plots of the effect of the DAP concentration and PT at the fixed FC concentration (0.60%) on the retention is represented in **Figure 5-7**. The retention decreased with an increase in the PT, and it increased when the DAP concentration increased. The retention decreased from 69.0% at 2.0% DAP and 80 sec PT to 35.0% at 1.0% DAP and 80 sec PT. This can be explained by the fact that longer polymerization times result in densification of cross-linking bonds, leading to tighter, less swellable structures (with a increasing retention), and if the concentration of one reactant is too low or high it can happen that shorter polymers are formed, incomplete reaction and many end groups unreacted but all of the same reagent cause a decreasing retention. The interaction between the factors DAP concentration and PT (**Figure 5-7**) reveals that the effect of PT is more significant at higher DAP concentration.

The surface and the contour plots of FC concentration (B) versus PT (C) on the retention are presented in **Figure 5-8**. The retention increased when FC concentration increased and PT decreased. The retention increased from 41.0% at B = 0.4%, and C = 80 sec, to 70.8% at B = 2.0%, and C = 40 sec. Interaction between factors FC concentration and PT (**Figure 5-8**) indicates that for increasing the retention the parameters include the short PT and higher FC concentration.

Graphical response surface analysis indicates that increasing of the PT gives lower values for retention. Also, increasing the DAP concentration leads to an increase in the retention, but the effect in this case is similar to the effect of FC concentration.

5.4.3 COMPARISON OF PREDICTED AND ACTUAL EXPERIMENTAL VALUES

The regression equations obtained using the experimental data can be used to predict the flux and the retention at any concentration of DAP, FC concentration and PT within the limits tested. In order to validate the adequacy of the model, twenty experiment runs were performed. The fabrication conditions were taken from the experiments detailed in **Table 5-2**.

Utilizing the point prediction capability of the software enables the prediction of the flux and the retention of the selected experiments complete with the 95% prediction interval. The predicted values and the associated prediction interval are based on the models developed previously. The predicted values and the actual experimental values were compared and the residual and the percentage error for the flux and the retention were calculated. The percentage errors for the flux and the retention are observed to vary from -14.71 to 14.59 and -15.04 to 10.61 in **Table 5-5**.

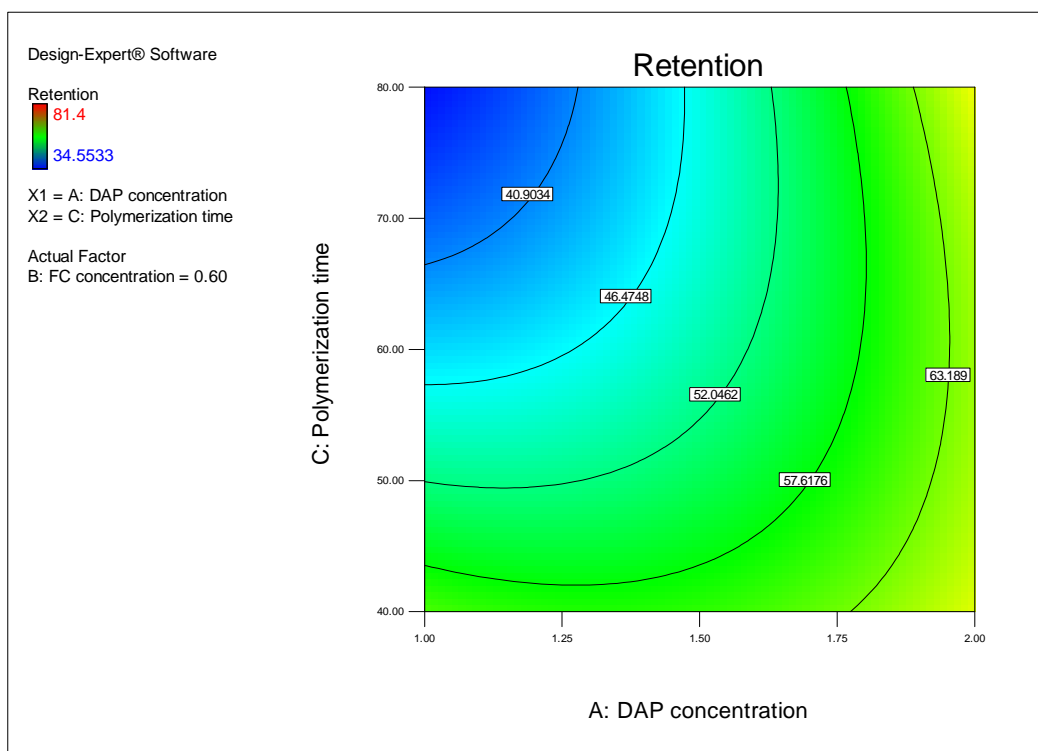
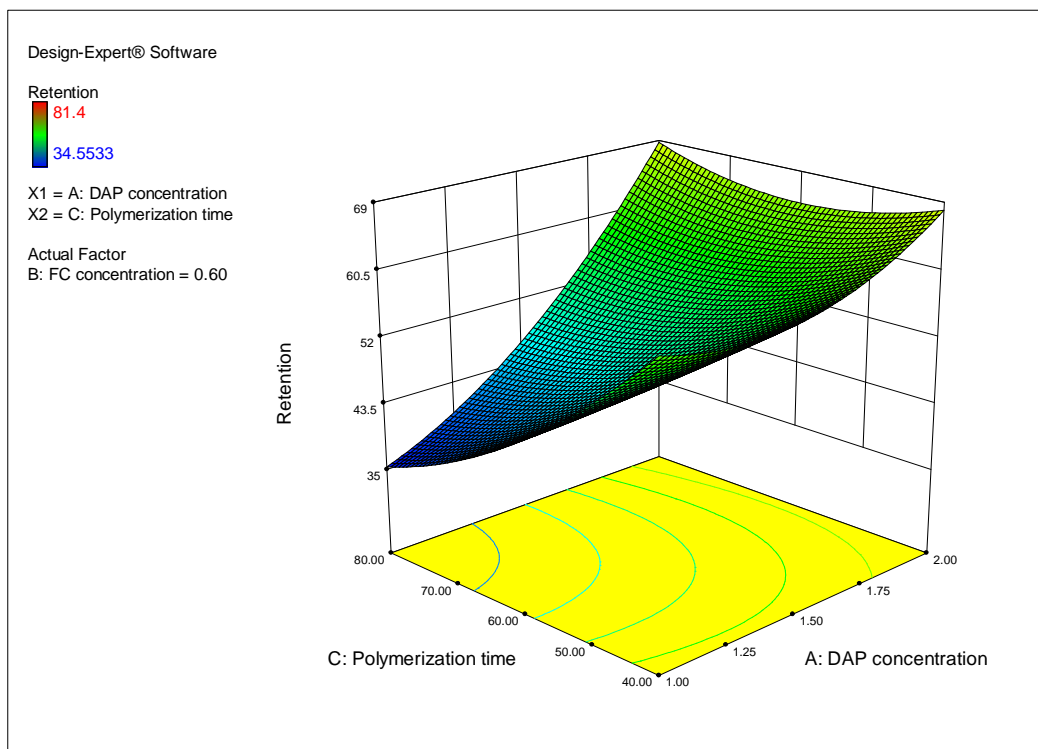


Figure 5-7: Response surface and contour plot indicating the effect of DAP concentration and IP polymerization time upon retention for a FC concentration 0.60%

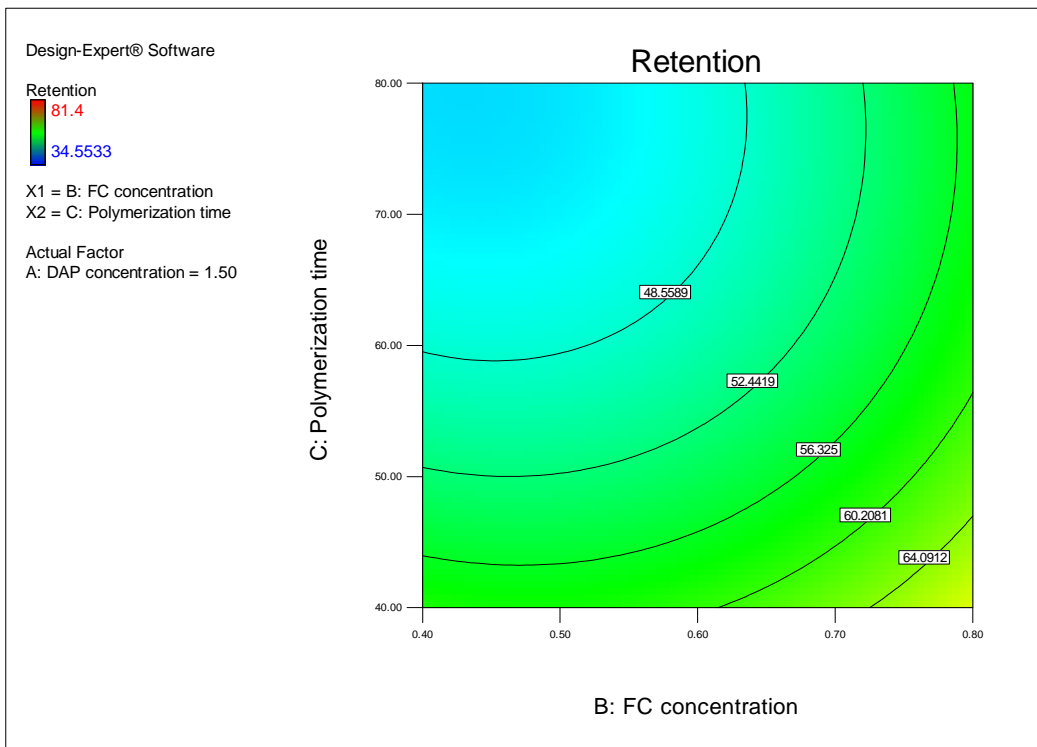
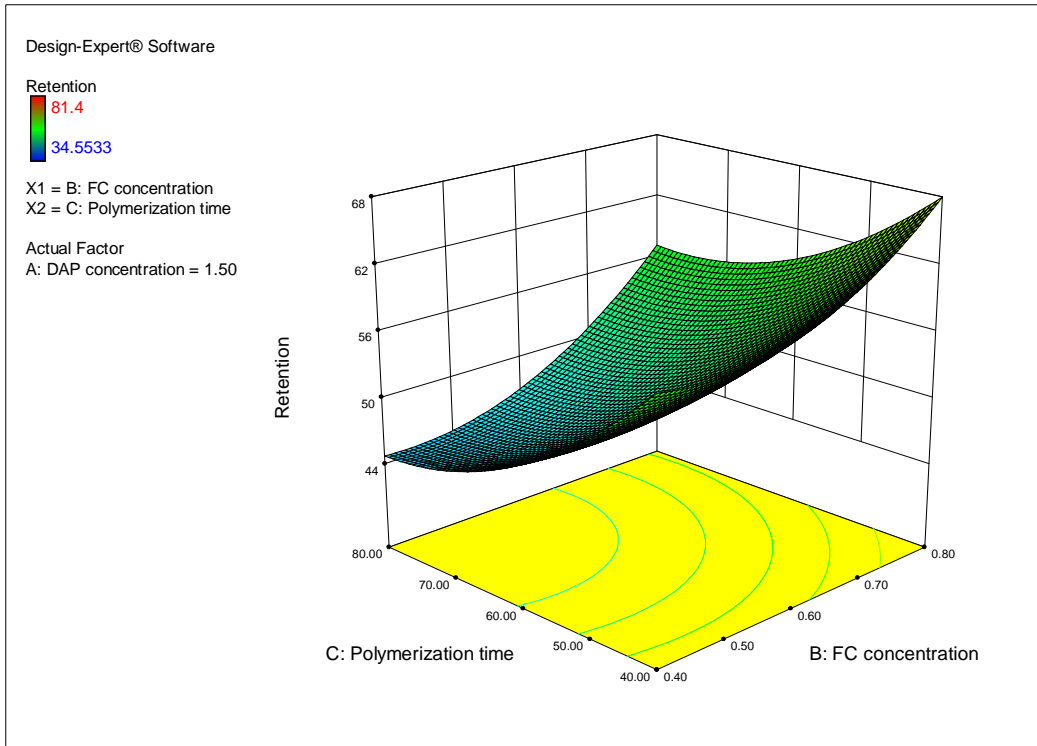


Figure 5-8: Response surface and contour plot indicating the effect of FC concentration and IP polymerization time upon retention for a DAP concentration 1.5%

According to ANOVA analysis in **Table 5-3** and **Table 5-4**, therefore the R^2 value is close to 1, which is desirable. Also the predicted R^2 is in agreement with the adjusted coefficient of determination R^2 adj. All these statistical estimators reveal that the response model is acceptable from a statistical point of view for the prediction of the response in the considered range of factors (valid region). The parity plot of predicted and experimental values of the response is shown in **Figure 5-9** and **Figure 5-10**. According to these figures the response model shows a goodness of fit to the experimental data. Therefore, the model is considered adequate for the prediction (simulation) and optimization.

Thus, it can be thought that the regression models were consistent with the flux and the retention. The regression equation can be expected to apply in the preparation of PVA-PA membranes and can reasonably predict and optimize the performance of the composite membranes. The 95% prediction interval is the range in which one can expect any individual value to fall into the 95% interval most of the time.

Table 5-5: Comparison of the predicted and the actual experimental values

Experiment	Factors			Flux, L/m ² .h				Retention, %			
	A	B	C	Actual	Predicted	Residual	Error,%	Actual	Predicted	Residual	Error,%
1	1.00	0.40	40.00	69.90	71.13	-1.23	-1.75	63.68	58.34	5.34	8.39
2	2.00	0.40	40.00	41.73	47.86	-6.14	-14.71	71.04	68.97	2.08	2.92
3	1.00	0.80	40.00	55.59	55.43	0.16	0.28	71.14	70.91	0.23	0.32
4	2.00	0.80	40.00	43.76	48.86	-5.10	-11.66	73.18	74.36	-1.18	-1.62
5	1.00	0.40	80.00	65.92	62.64	3.28	4.98	34.55	30.89	3.66	10.61
6	2.00	0.40	80.00	32.48	34.46	-1.98	-6.10	70.16	67.90	2.25	3.21
7	1.00	0.80	80.00	56.71	52.39	4.32	7.61	47.39	46.98	0.40	0.85
8	2.00	0.80	80.00	40.31	40.90	-0.59	-1.48	73.96	76.82	-2.86	-3.87
9	0.66	0.60	60.00	69.75	74.17	-4.42	-6.33	41.81	46.32	-4.51	-10.79
10	2.34	0.60	60.00	52.62	44.94	7.68	14.59	81.40	80.35	1.05	1.29
11	1.50	0.26	60.00	52.12	49.05	3.07	5.89	44.62	51.33	-6.71	-15.04
12	1.50	0.94	60.00	41.47	41.27	0.19	0.46	72.65	69.40	3.25	4.48
13	1.50	0.60	26.36	67.06	60.60	6.46	9.64	67.84	70.48	-2.64	-3.89
14	1.50	0.60	93.64	43.65	46.77	-3.12	-7.14	48.65	49.47	-0.82	-1.68
15	1.50	0.60	60.00	69.43	70.77	-1.33	-1.92	51.94	50.13	1.81	3.48
16	1.50	0.60	60.00	65.38	70.77	-5.39	-8.24	52.79	50.13	2.66	5.05
17	1.50	0.60	60.00	74.10	70.77	3.33	4.50	52.50	50.13	2.37	4.51
18	1.50	0.60	60.00	72.64	70.77	1.88	2.58	45.16	50.13	-4.97	-11.01
19	1.50	0.60	60.00	68.12	70.77	-2.65	-3.89	48.38	50.13	-1.75	-3.61
20	1.50	0.60	60.00	75.21	70.77	4.44	5.91	50.67	50.13	0.54	1.06

5.5 CONCLUSIONS

The preparation conditions of TFC membranes were investigated based on the CCD. The results presented here show that good TFC composite membranes can be prepared by optimizing preparation conditions in the membrane formation. Diamine concentration, dicarboxylic acid chloride concentration and polymerization time were identified as dominant fabrication parameters influencing the performance of composite membranes. It was observed that main, quadratic and interaction effects of DAP concentration, FC concentration and polymerization time had important effects on the membrane performance. According to analysis of 2^k factorial designs, main effects of these parameters were more dominant than their interaction effects with respect to both permeability and

retention over a selected range of operating conditions. The optimized parameters obtained in this study were: DAP concentration 1.0 – 2.0%, FC concentration 0.4 – 0.8%, polymerization time 40 – 80 sec.

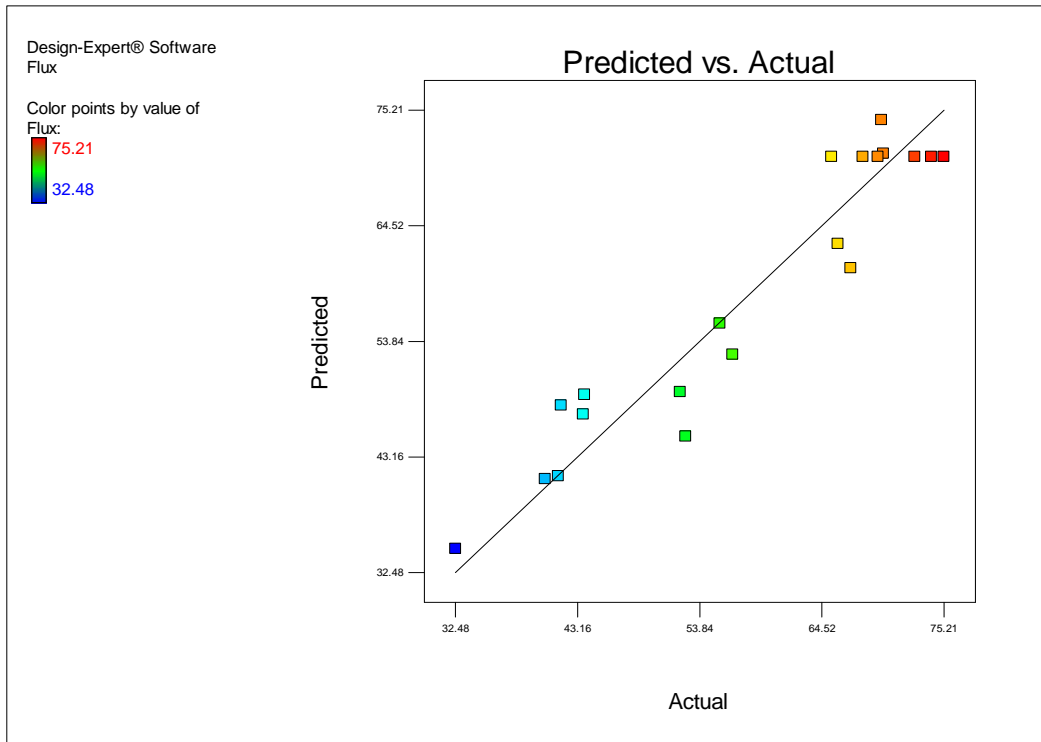


Figure 5-9: Flux, predicted values by response model against the experimental data

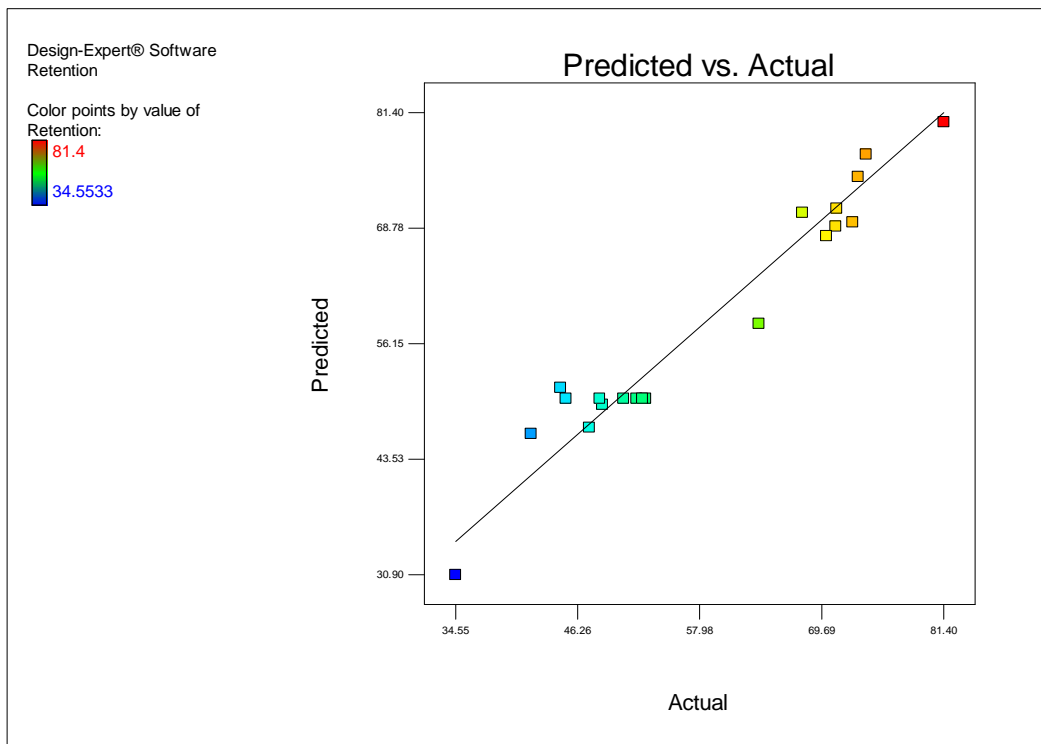


Figure 5-10: Retention, predicted values by response model against the experimental data

The DAP concentration and polymerization time had the strongest influences on flux and retention, while the FC concentration appeared to be a dominant factor responsible for retention. Flux and retention exhibited by these membranes even surpassed the generally recognized intrinsic retention for the corresponding dense film. The regression equations between the preparation variables and the performance of the composite membranes were established by RSM and can be used for prediction within the limits of the factors studied. Additionally, the contour and surface plots are very helpful in visualizing main and interaction effects of the factors.

5.6 REFERENCES

- [1] Cadotte, J.E., R.J. Petersen, R.E. Larson, and E.E. Erickson, *A new thin-film composite sea water reverse osmosis membrane*. *Desalination*, 1980. 32: p. 25-31.
- [2] Lonsdale, H.K., *The growth of membrane technology*. *Journal of Membrane Science*, 1982. 10: p. 81-181.
- [3] Petersen, R.J., *Composite reverse osmosis and nanofiltration membranes*. *Journal of Membrane Science*, 1993. 83: p. 81-150.
- [4] Kim, K.-J., G. Chowdhury, and T. Matsuura, *Low pressure reverse osmosis performance of sulfonated poly(2,6-dimethyl-1,4-phenylene oxide) thin-film composite membranes: effect of coating conditions and molecular weight of polymer*. *Journal of Membrane Science*, 2000. 179: p. 43-52.
- [5] Feng, X. and R.Y.M. Huang, *Preparation and performance of asymmetric polyetherimide membranes for isopropanol dehydration by pervaporation*. *Journal of Membrane Science*, 1996. 109: p. 165-172.
- [6] Rao, A.P., S.V. Joshi, J.J. Trivedi, C.V. Devmurari, and V.J. Shah, *Structure–performance correlation of polyamide thin-film composite membranes: effect of coating conditions on film formation*. *Journal of Membrane Science*, 2003. 211: p. 13-24.
- [7] Rao, A.P., N.V. Desai, and R. Rangarajan, *Interfacially synthesized thin-film composite RO membranes for seawater desalination*. *Journal of Membrane Science*, 1997. 124: p. 263-272.
- [8] Montgomery, D.C., *Design and analysis of experiment*, John Wiley & Sons: New York, 1997.
- [9] Myers, R.H. and D.C. Montgomery, *Response surface methodology: process and product optimization using designed experiments*, John Wiley & Sons: New York, 2002.
- [10] Idris, A., A.F. Ismail, M.Y. Noordin, and S.J. Shilton, *Optimization of cellulose acetate hollow fiber reverse osmosis membrane production using Taguchi method*. *Journal of Membrane Science*, 2002. 205: p. 223-237.
- [11] Chau, J.L., S.S. Wang, and C.L. Guo, *Pilot production of polysulfone hollow fiber for ultrafiltration polyethersulfone hollow fiber membrane*. *Industrial Chemical Res*, 1995. 34: p. 803-919.
- [12] Pesek, S.C. and W.J. Koros, *Aqueous quenched asymmetric polysulfone hollow fiber prepared by dry/wet phase separation*. *Journal of Membrane Science*, 1994. 88: p. 1-19.
- [13] Ismail, A.F. and P.Y. Lai, *Development of defect-free asymmetric polysulfone membranes for gas separation using response surface methodology*. *Separation and Purification Technology*, 2004. 40: p. 191-207.

- [14] Idris, A., F. Kormin, and M.Y. Noordin, *Application of response surface methodology in describing the performance of thin-film composite membrane*. Separation and Purification Technology, 2006. 49: p. 271-280.
- [15] Xiangli, F., W. Wei, Y. Chen, W. Jin, and N. Xu, *Optimization of preparation conditions for polydimethylsiloxane (PDMS)/ceramic composite pervaporation membranes using response surface methodology*. Journal of Membrane Science, 2008. 311: p. 23-33.
- [16] Cochran, W.G. and G.M. Cox, *Experimental Designs*, Second ed., John Wiley & Sons: New York, 1992.
- [17] Helseth, T., N. Vaughn, B. Smith, and H. Anderson, *Design-Expert® version 7.1 software for experiment design*. February 4, 2008, State-Ease statistics made easy.
- [18] Wijmans, J.G. and R.W. Baker, *The solution-diffusion model: a review*. Journal of Membrane Science, 1995. 107: p. 1-12.
- [19] Roh, I.J., J.J. Kim, S.Y. Park, and C.K. Kim, *Effects of the polyamide molecular structure on the performance of reverse osmosis membranes*. Journal of Polymer Science, 1998. 36: p. 1821-1830.

Chapter 6

*MEMBRANE CHARACTERIZATION IN TERMS OF SOLUTE
TRANSPORT USING UV SPECTROPHOTOMETRY AND
GRAVIMETRY METHODS*

Abstract

The performance of asymmetric poly(vinyl alcohol)-sodium tetraborate (PVA-SB) ultrafiltration (UF) flat-sheet membranes is reported in this chapter. The membranes were prepared by coating a polyethersulfone (PES-UF) support membrane with poly(vinyl alcohol) PVA and then cross-linking with sodium tetraborate (SB). The membranes were characterised in terms of their pure water permeation (PWP) rate, molecular weight cut-off (MWCO), solute separation and permeate flux. Mean pore size (μ_p) and standard deviation (σ_p) of the membranes were determined using solute transport data. Results revealed that a PVA-SB membrane has the same PWP rate as PES-UF membranes. The MWCO of the membranes decreased from 19,000 to 13,000 Dalton when the membrane was coated with PVA.

6.1 INTRODUCTION

Membrane technology is an alternative and attractive approach for achieving separation because it is a fast process and does not involve any phase change [1]. The application of membrane technology in ultrafiltration (UF) is growing very rapidly in the pharmaceutical, chemical, paper, semiconductor and dairy industries. The important goal in membrane technology is to control the membrane structure, which affects the membrane performance. Thus extensive research has been conducted in attempts to improve the performance of the membrane. Polyethersulfone (PES) membrane has been used as support due to its excellent chemical resistance, good thermal stability and mechanical properties. PES is more suitable for liquid separation while polysulfone (PS) has advantages in gas separation and can be used at higher pressures [2].

The flux and retention of UF membranes is largely determined by the morphology of the skin layer. The selectivity depends on the pore size while the flux depends on the pore density and the skin layer thickness. It is necessary to know the mean pore size and the pore size distribution to predict the membrane selectivity with significant confidence. Molecular weight cut-off (MWCO) of the membrane requires a solute at which 90% separation can be achieved [3]. There are several techniques that can be used for the determination of pore size and pore size distribution, such as the bubble point technique, the microscopy technique, solute transport, permoporometry, mercury porosimetry, thermoporometry and atomic force microscopy (AFM) [4, 5].

Many studies have been carried out in efforts to obtain information about the pore size distribution of membranes and the relationship between pore size and the solute separation. Michaels [6] found, for a variety of UF membranes (both biological and synthetic membranes), a good fit on a log-normal probability distribution curve for the sieving coefficients and solute size. Kassotis et al. [7] measured the rejection coefficient of polyacrylonitrile (PAN) membranes with dextrans in order to determine the pore size distribution. Aimar et al. [8] used dextrans to measure the retention coefficients of membranes and the data were fitted to a log-normal pore size distribution. Leyboldt [9] presented the mathematical limitation in determining the pore size distribution from the solute separation. Several researchers [8, 10] have suggested that solute separation is dependent on the ratio of the solute's molecular size to the pore size, as was initially suggested by Paine and Scherr [11]. However, in several other studies [6, 12, 13] the dependence of solute separation on the solute size, which results from the steric and the hydrodynamic interactions between the solute and pore, was not considered.

AFM has been applied to studying microfiltration (MF) and UF membranes [14, 15]. AFM can image a non-conducting sample both in air and in liquid. Use of AFM has also eliminated the tedious process of sample preparation that is required for scanning electron microscopy (SEM) and for transmission electron microscopy (TEM). The heavy metal coating required in SEM and TEM might also give some artifacts. High-beam energy as required in SEM for high resolution tends to damage polymeric membranes.

Photometric or colorimetric methods have been used to determine the MWCO of MF and UF membranes. Here the measurement of polyethylene glycol (PEG) concentration relies on the light absorbing properties of either the PEG solution being analyzed or a chemical derivative of the PEG. The light absorbing properties are measured with a device called a spectrophotometer or colorimeter.

PES-UF and PVA-SB membranes have also been characterized by solute transport data, where a sieving curve is obtained by plotting solute retention versus molar mass for the UF membranes. There are two methods to determine the sieving curve [16]. The first method involves successive permeation of several solutions, each of which contains a single solute; whilst the second method involves using solutions containing mixtures of solutes, each having a different molar mass. The advantage is that a single separation experiment is needed to determine the sieving curve. Other researchers advise that the MWCO obtained from using a mixture of solutes should be interpreted with caution [17].

In the present study membranes were characterized using solute transport data, involving the first method mentioned above. The first task was to prepare the respective PEG stock solutions (of eight different molecular weight) to give a series of solutions of different, known concentrations, then the PEG standard solutions were used to construct a standard curve. Finally, the PEG concentration in a real sample (feed and permeate of ultrafiltration experiments) was determined, using a standard curve.

6.2 THEORETICAL BACKGROUND

6.2.1 MEMBRANE CHARACTERIZATION BASED ON SOLUTE TRANSPORT DATA

UF membranes can be characterized by their mean pore size and the pore size distribution obtained from solute transport experiments. According to the method, the size of the solutes used for the UF experiments should be known. Characterization of the mean pore size and pore size distribution of UF membranes by solute separation (f), in percentage, is determined using the following equation:

$$f = \left(1 - \frac{C_p}{C_f} \right) \times 100 \quad (6.1)$$

where C_p and C_f are the solute concentrations in the permeate and in the bulk of the feed, respectively. It should be noted that the effect of concentration polarization on separation is not taken into consideration in equation 6.1. Michaels [6] reports that solute separation can be expressed by a log-normal probability function of solute size, for both biological and synthetic membranes, as expressed by the following equation:

$$f = \text{erf}(Z) = \frac{1}{\sqrt{2\pi}} \int_{-\infty}^Z e^{-\frac{u^2}{2}} du \quad (6.2)$$

where

$$Z = \frac{\ln d_s - \ln \mu_s}{\ln \sigma_g} \quad (6.3)$$

and d_s is the solute diameter, μ_s is the geometric mean diameter of solute, and σ_g is the geometric standard deviation about the mean diameter. According to equations (6.2) and (6.3), a straight line in the form of equation (6.4) will yield f (solute diameter, in percent) and d_s (solute diameter) on a log-normal probability paper.

$$F(f) = A_0 + A_1(\ln d_s) \quad (6.4)$$

where A_0 and A_1 are the intercept and the slope, from this log-normal plot the μ_s can be calculated as d_s corresponding to $f = 50\%$. The value of σ_g can be determined from the ratio of d_s at $f = 84.13\%$ and at $f = 50\%$. By ignoring the dependence of the solute separation on the steric and hydrodynamic interaction between solute and pore size [6, 12, 13] the mean pore size (μ_p) and the geometric standard deviation (σ_p) of the membrane can be considered to be the same as the μ_s and σ_g of the solute. From the values of μ_p and σ_p the pore size distribution of an UF membrane can be expressed by the following probability density function:

$$\frac{df(d_p)}{dd_p} = \frac{1}{d_p \ln \sigma_p \sqrt{2\pi}} \exp \left[-\frac{(\ln d_p - \ln \mu_p)^2}{2(\ln \sigma_p)^2} \right] \quad (6.5)$$

where d_p is the pore size. Furthermore, the MWCO of the membranes, defined as the molecular weight of solutes at the point where the retention of membranes reaches 90%, can be determined from the plot of equation (6.4).

6.2.2 STOKES RADIUS OF POLYETHYLENE GLYCOL (PEG)

The Stokes radius is used to describe the dimension of a solute. The Stokes radius of a macromolecule can be obtained from its diffusivity in a solution by using the Stokes-Einstein equation [6]

$$D_{AB} = \frac{kT}{6\pi\eta a} \quad (6.6)$$

where D_{AB} is the diffusivity of macromolecules in a solution (m^2/s), k is Boltzmann's constant, η is the solvent viscosity (Pa.s) and a is the Stokes radius of a solute (m). The diffusivity can also be calculated using the following equation [18]

$$D_{AB} = \frac{2.54 \cdot 10^6 kT}{\eta (MW[\eta])^{1/3}} \quad (6.7)$$

where MW and $[\eta]$ are the molecular weight (kg/mol) and the intrinsic viscosity of the polymer (m^3/kg), respectively. By combining equations (6.6) and (6.7), the following equation (6.8) is obtained

$$a = 2.122 \cdot 10^{-10} (MW[\eta])^{1/3} \quad (6.8)$$

Because the solvent viscosity and the intrinsic viscosity depend on the solvent, the intrinsic viscosity of PEG of known molecular weight can be calculated from the empirical Mark-Houwink equation [19] as follows:

$$[\eta] = 4.94 \cdot 10^{-4} MW^{0.672} \quad (6.9)$$

Intrinsic viscosities of PEG of various molecular weights calculated from the empirical equation (6.9) are in very good agreement with the values determined experimentally [18, 20]. The intrinsic viscosities of some PEG molecules are given by Bessieres et al. [21], and they are also in very good

agreement with the values calculated from the empirical equation (6.9). By substituting the expression for $[\eta]$ into equation (6.8), equation (6.10) is obtained:

$$a = 16.73 \times 10^{-12} MW^{0.557} \quad (6.10)$$

Solute diameter d_s is given by:

$$d_s = 2a \quad (6.11)$$

6.3 EXPERIMENTAL

6.3.1 MATERIALS

PES-UF membranes were supplied by Koch System Membrane (USA). The PVA-SB membranes were fabricated in-house. PEG samples of different molecular weights, ranging from (1,550 – 35,000) Daltons, were purchased from Fluka (USA) and used as solutes. De-ionized (DI) water with a conductivity 2 $\mu\text{s}/\text{cm}$ was used for permeation experiments. Other chemicals used were potassium iodide (KI) (Holpro Analytics, 77204), barium chloride (BaCl_2) (Pal Chemicals, 00382), iodine (I_2) (Aldrich) and hydrochloric acid (HCl) (Merck, 3063040).

6.3.2 CREATION OF CALIBRATION CURVES (CONCENTRATION VS. ABSORBANCE) OF POLYETHYLENE GLYCOL (PEG) OF DIFFERENT MOLECULAR WEIGHTS

The following procedure was followed to create a standard curve for the concentration versus absorbance of PEG:

1. Prepare the following solutions:
Solution A: Dissolve 5 g BaCl_2 in 100 mL 1 N HCl.
Solution B: Dissolve 2 g KI in 100 mL DI water. Dilute 10 times. Add 1.27 g I_2 to the solution and stir until all solids have dissolved.
Store the two solutions in tightly capped glass bottles at room temperature. These reagents are stable for approximately one month.
2. Prepare a PEG stock solution: Dissolve 0.2 g PEG in 50 mL DI water and dilute to a total volume of 100 mL with DI water (final concentration 2000 ppm).
3. Prepare standard solutions: Dilute the PEG 2000 solution to obtain solutions of 1000, 500, 250, 125, 62.5, 31.25, 15.63, 7.81 and 3.91 ppm by adding appropriate volume of water. The total volume of each should be 100 mL.
4. Prepare "unknown" solutions: These solutions are not true "unknowns", rather, they will be used to demonstrate the capability / suitability of the scan method. "Unknown" solutions were prepared by dissolving 0.16 g PEG in 50 mL DI water and then diluting the resulting stock solution to 100 mL total volume with DI water (concentration 1600 ppm), followed by further dilutions, by adding the appropriate volumes of water, to obtain solutions with the following PEG concentrations: 800, 400, 200, 100, 50, 25, 12.5, 6.25 and 3.125 ppm. The total volume of each solution was 100 mL. The absorbance values of unknown solutions were measured in triplicate.
5. Pipette 1 mL of solution A and 1 mL of solution B into each test tube.
6. Prepare a reagent series by adding 4 mL of each of the PEG standards to ten separate test tubes filled with reagent. Prepare a reagent blank by adding 4 mL DI water to an eleventh different test

- tube filled with reagent. Prepare the serum unknown by adding 4 mL of each of the unknown solutions to ten separate test tubes filled with reagent.
- Allow the cuvettes to stand at room temperature for 15 min to develop the colour.
 - Using the reagent blank, zero the spectrophotometer at 535 nm and measure the absorbance of the reagent series. Mix the contents of the cuvettes well, by inversion, before recording ultraviolet (UV) measurements.
 - Using the reagent blank, re-zero the spectrophotometer and measure the absorbance of the blank series, including the serum unknown. Mix the contents of the cuvettes well, by inversion, before recording UV measurements.
 - Conduct a blank subtraction by subtracting the absorbance of the blank series from its reagent series counterpart. Plot the new absorbance vs. concentration, perform a least square fit to the standard curve and determine the concentration of the unknown.

Repeat the above procedure (steps 2 – 10) for each PEG of the respective different molecular weights (1,550 – 35,000) Daltons. The above procedure is shown schematically in **Figure 6-1**

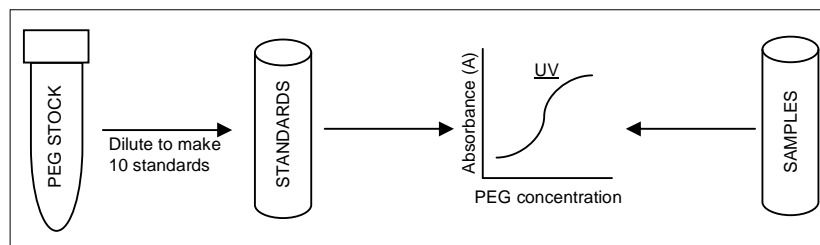


Figure 6-1: Schematic representation of the creation of calibration curves (Concentration vs. Absorbance) of PEG of different molecular weights

6.3.3 ULTRAFILTRATION MEMBRANE EVALUATION

Membrane samples to be evaluated were first carefully checked under a fluorescent lamp to avoid selecting samples that had any obvious defects. All permeation experiments were carried out at 345 kPa and 25°C, using a cycling flow of 45 – 50 L/h. The feed flow velocity was so high that the concentration change in the feed could be ignored. UF experiments were conducted using laboratory test cells, each with an effective area of 22.082 cm² (details of which are described in Chapter 3, Section 3.6.2.1). Each membrane was compacted at 550 kPa (0.51 MPa) for 24 h prior to taking any measurements.

In separate experiments, PEG of different molecular weights (1,550 – 35,000) Daltons was used as solutes in the aqueous feed solutions. The solute concentration was kept at 50 ppm. PEG separation experiments were conducted starting with the lower molecular weight solute. The volume of permeate was collected and measured. The concentrations of the feed and permeate solutions were determined. In order to ensure reproducibility of results a minimum of eight samples were tested for each feed solution. The test system was thoroughly flushed with DI water between runs of the different molecular weight solutes of PEG.

The PES-UF and PVA-SB membranes were first characterized by determining their PWP rate, as calculated from the following equation:

$$PWP = \frac{Q}{S \Delta t} \quad (6.12)$$

where Q is the volume of the permeate (L), s is the membrane surface area (m^2) and Δt is the permeation time (h). The flux (J) of the UF membrane in the presence of solute is obtained from:

$$J = \frac{V}{S \times \Delta t} \quad (6.13)$$

where V is the volume of permeate (L), s is the membrane surface area (m^2) and Δt is the permeation time (h). The solute separation of the membrane is given by:

$$f = \left(1 - \frac{C_p}{C_f}\right) \times 100 \quad (6.14)$$

where C_p is the solute concentration in the permeate stream and C_f is the solute concentration in the feed stream. The values of C_p and C_f were determined using UV spectrophotometry and the gravimetry methods. The procedures followed in these two different analytical methods for determining C_p and C_f are given below.

6.3.3.1 Procedure for the UV spectrophotometry method

The following typical procedure was followed for UV analyses of PEG samples:

A sample solution of 4 mL was added to 1 mL 5% (w/v) $BaCl_2$ in 1N HCl. To this mixture was added 1 mL of a solution of 1.27g I_2 in 100 mL 2% KI (w/v), which had been further diluted 10 times. Colour was allowed to develop over 15 min at room temperature. The absorption was read using a spectrophotometer at 535 nm, against a blank.

6.3.3.2 Procedure for the gravimetry method

- An analytical balance (with 4 decimal point accuracy) was used to measure the weight of dried samples. The weighing pan was cleaned with a soft brush.
- Preheat a 20 mL evaporating glass dish at $100 \pm 5^\circ C$ for 1 h, cool in a drying oven or in the open air (protected from dust) for 15 – 20 min, allow to cool further to room temperature in a desiccator, and then weigh. Repeat this procedure until a constant weight is achieved.
- Measure 10 mL of permeate sample and evaporate to dryness in a drying oven set at $45^\circ C$, then cool in a desiccator, and weigh. As always, the sample should be re-heated and re-weighed, to achieve a constant weight.
- The sample weight is determined by:

$$W_s = W_2 - W_1 \quad (6.15)$$

where W_1 and W_2 are the weights of the empty glass dish and the glass dish plus sample, respectively.

6.4 RESULTS AND DISCUSSION

6.4.1 CALIBRATION CURVES OF POLYETHYLENE GLYCOL (PEG) OF DIFFERENT MOLECULAR WEIGHTS

PEG solutions of different molecular weights (1,550 – 35,000) Daltons and different concentrations (0.0 – 2000 ppm) were analyzed by UV spectrophotometry (to determine the effect of PEG concentration on the absorbance value). It was found that the absorbance decreased when the PEG concentration was more than 50 ppm (see **Appendix B, Figure B-1 to Figure B-8**). It was therefore

decided that a low concentration of PEG (50 ppm) should be used for the feed solution for the UF experiments. Furthermore, a low concentration of PEG would not contribute much to the creation of a cake layer on the membrane surface that would give incorrect membrane retention. It could reveal sensitivity of the UV or gravimetry methods.

In analytical spectrophotometry, the molar absorbance of the unknown compound may not be known. It is therefore common practice to generate a calibration curve. A calibration curve is constructed by measuring the absorbance of a series of samples for which the concentration is known. Then, since the Lambert-Beer' law shows a linear relationship between absorbance and concentration, a squares fit of the calibration curve will yield a mathematical relationship between the absorbance and concentration. This relationship can be used to calculate the concentration of the unknown sample. **Appendix C (Figure C-1 to Figure C-8)** shows the calibration curves of PEG of different molecular weights, which were used to determine the PEG concentration in feed and permeate samples. A regression line was drawn with a high correlation coefficient ($R^2 \geq 0.94$).

6.4.2 MEMBRANE CHARACTERIZATION BASED ON THE ULTRAVIOLET (UV) SPECTROPHOTOMETRY METHOD

6.4.2.1 Pure water permeation (PWP) rate

Figure 6-2 clearly shows that the PWP rate is partly affected by the PVA layer. Here a PES-UF membrane exhibits a PWP rate of 234.85 L/m².h and a PVA-SB membrane a PWP rate of 206.1 L/m².h at the low pressure of 345 kPa. Flux changes considerably at higher pressures (see Section 4.3.3). Apparently, the result indicates that addition of PVA layer onto the surface of PES-UF membrane influences the formation of pore size of the membranes. UF membrane permeability is conceptually related to its pores [22].

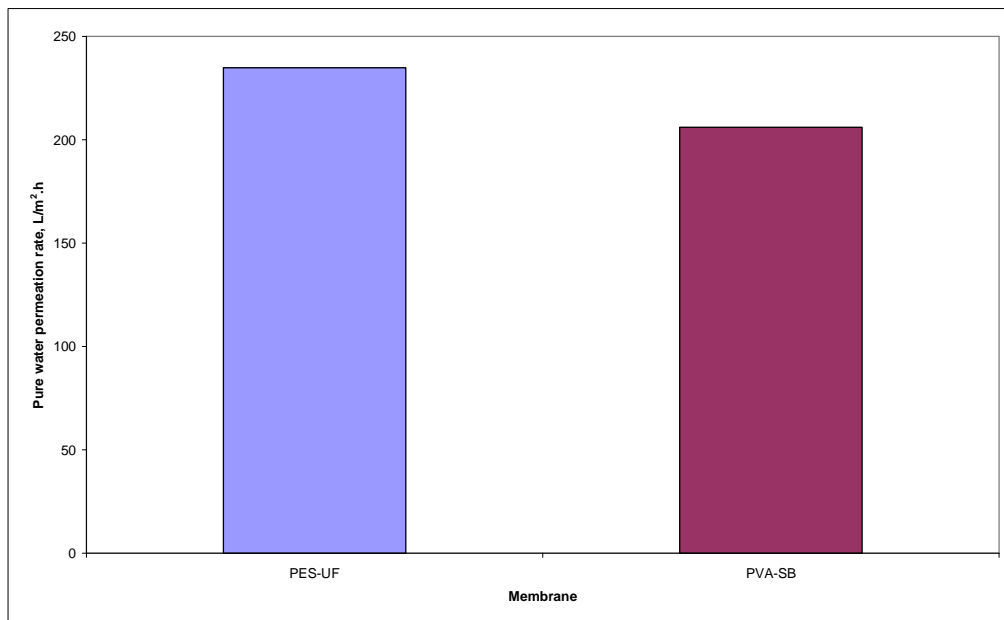


Figure 6-2: Pure water permeation (PWP) rate of polyethersulfone (PES-UF) and poly(vinyl alcohol)-sodium tetraborate (PVA-SB) membranes

6.4.2.2 Molecular weight cut-off (MWCO) profiles

The solute separation versus solute molecular weight relationship for PES-UF and PVA-SB membranes is presented in **Figure 6-3**. The solute separation increases with an increase in molecular weight of solutes. By definition, MWCO is the molecular weight that is 90% rejected by the membrane [23]. **Figure 6-3** shows that PES-UF membranes exhibit higher MWCO values than the PVA-SB membranes.

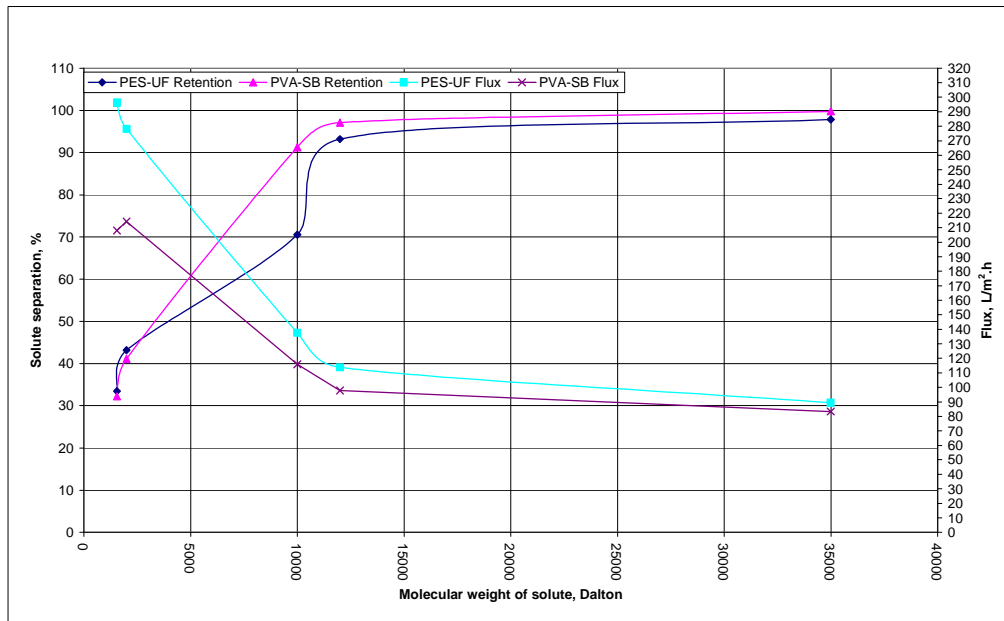


Figure 6-3: Molecular weight cut-off (MWCO) profile of polyethersulfone (PES-UF) and poly(vinyl alcohol)-sodium tetraborate (PVA-SB) membranes using ultraviolet (UV) method

6.4.2.3 Mean pore size and pore size distribution

Membrane pore sizes and their distributions were calculated from the transport data obtained using PEG solutes of various molecular weights. PEG did not significantly foul the membranes as the permeate flux of the membranes, when PEG was present in the feed, was very close to that of the PWP rate. Log-normal plots of solute separation versus solute diameter for PES-UF and PVA-SB membranes are presented in **Figure 6-4**. A regression line was drawn with a high correlation coefficient ($R^2 \geq 0.92$). The Stokes diameter (d_s) can be determined using equation (6.11). The value of the mean pore size (μ_p), standard deviation (σ_p) and MWCO of the PES-UF and PVA-SB membranes were calculated from solute separation curves, as described in the Section 6.2, and the results are tabulated in **Table 6-1**. The mean pore size is the pore diameter when solute separation is 50%. A PES-UF membrane exhibited 19,00 Da MWCO and 2.84 nm μ_p , while a PVA-SB membrane exhibited 14,000 Da MWCO and 2.68 nm μ_p . Results showed that standard deviations decreased from 2.44 to 2.21. There was not much difference between PES-UF and PVA-SB membranes in terms of their μ_p and σ_p . It should be noted that the PWP rate (**Figure 6-2**) and MWCO (**Table 6-1**) of these membranes were also very similar.

Table 6-1: Mean pore size (μ_p), standard deviation (σ_p) and molecular weight cut-off (MWCO) of polyethersulfone (PES-UF) and poly(vinyl alcohol)-sodium tetraborate (PVA-SB) membranes calculated from the solute separation curve using ultraviolet (UV) method

Membrane	Molecular weight cut-off, MWCO, (Da)	Mean pore size, μ_p , (nm)	Standard deviation, σ_p
PES-UF	19003.71	2.84	2.44
PVA-SB	13923.15	2.68	2.21

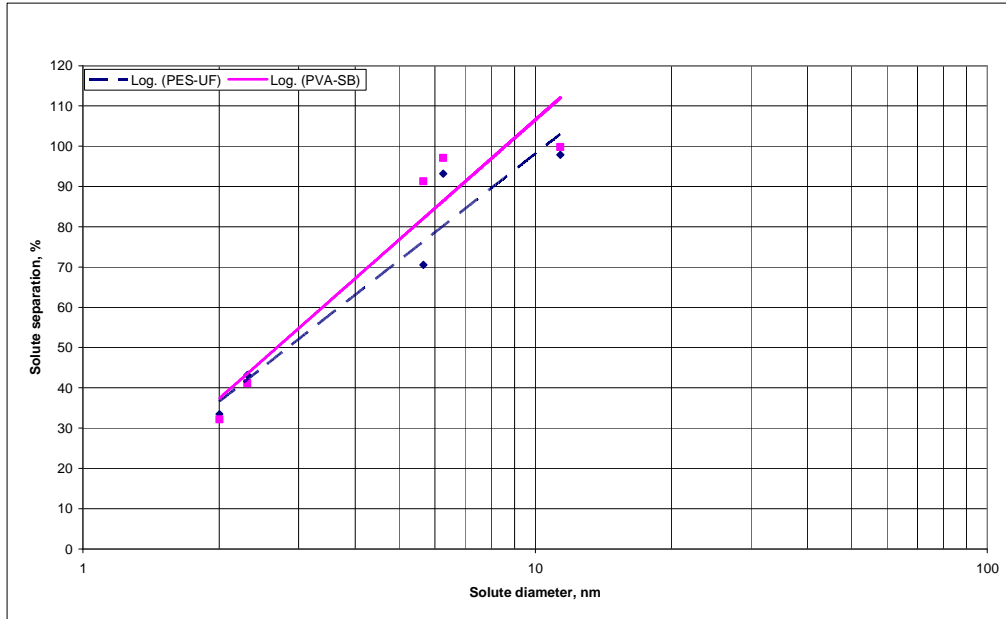


Figure 6-4: Solute separation curve of polyethersulfone (PES-UF) and poly(vinyl alcohol)-sodium tetraborate (PVA-SB) membranes using ultraviolet (UV) method

The results revealed that the membrane with high MWCO has the largest pore radius, which explains the increase in PWP rate. MWCO acts as a guide for pore sizes of the membranes, where large MWCO implies large pore size of the membrane. Thus, this revealed that the PVA layer increased the solute separation and slightly decreased the flux rate. The PVA-SB membrane has a very good flux. PVA-SB membrane is suitable for separation of proteins such as in dairy industries. It is suitable for use in the separation of oil/water emulsions and biological suspensions. Besides, the membranes can be used for waste treatment in separation of colloids and pyrogens.

The cumulative pore size distributions for PES-UF and PVA-SB membranes are shown in **Figure 6-5**. It is evident that there is no significant difference in pore size distributions. For PES-UF and PVA-SB membranes about 50% of the pores were less than 2.86 nm in diameter. Probability and density function curves were also generated from equation (6.5) by using the values of mean pore size and standard deviation for the membranes under consideration.

Michaels [6] found that σ_p values of the different UF membranes, both biological and synthetic, are very close to each other (1.20 – 1.66). On this basis, it was claimed that virtually all the membranes for UF, irrespective of their origin, are quite similar in their microstructure.

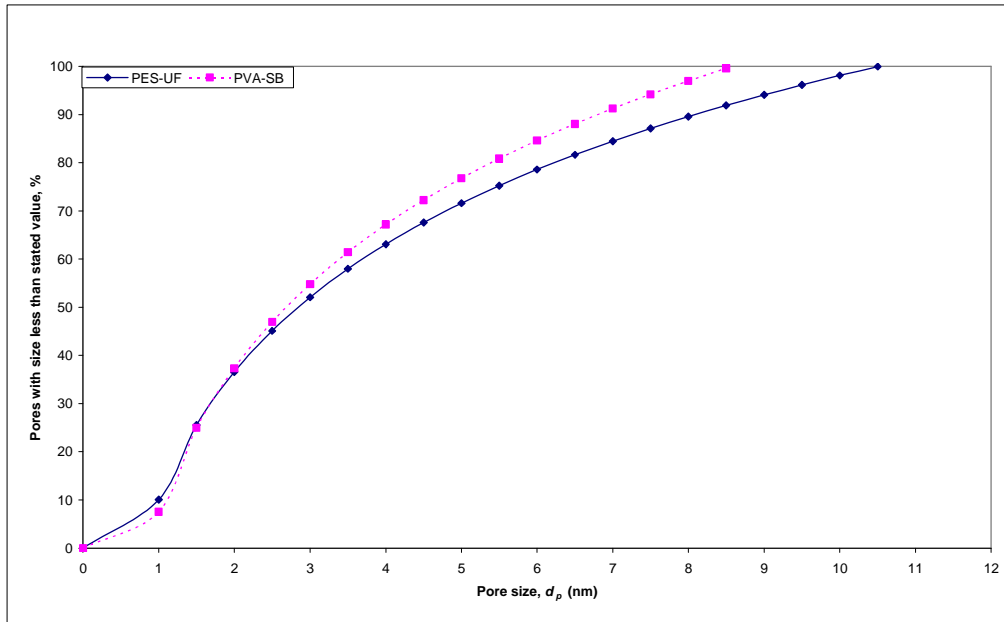


Figure 6-5: Cumulative pore size distribution of polyethersulfone (PES-UF) and poly(vinyl alcohol)-sodium tetraborate (PVA-SB) membranes using ultraviolet (UV) method

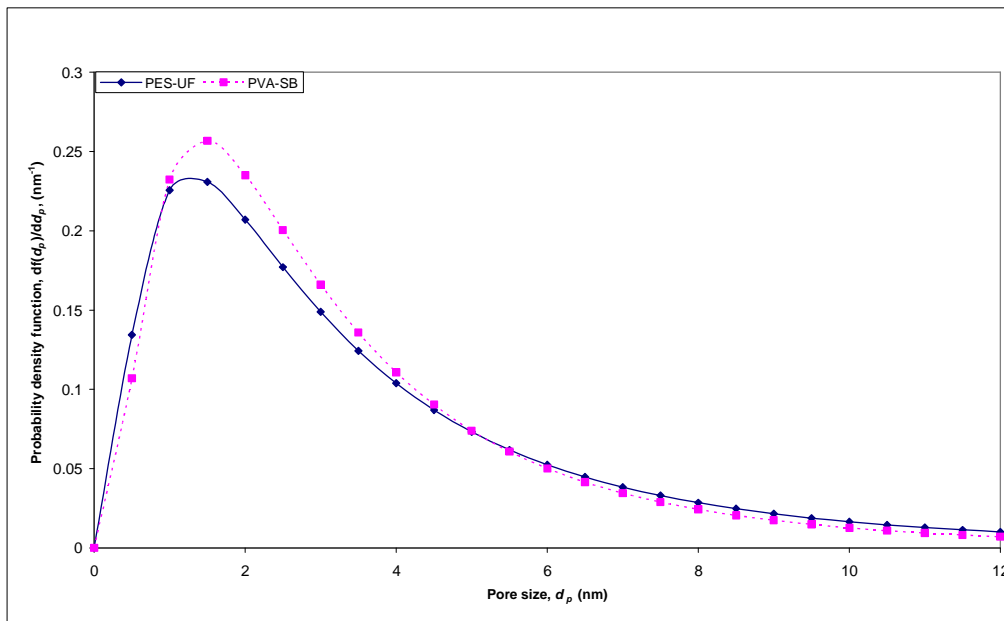


Figure 6-6: Probability density function curve of polyethersulfone (PES-UF) and poly(vinyl alcohol)-sodium tetraborate (PVA-SB) membranes using ultraviolet (UV) method

6.4.3 MEMBRANE CHARACTERIZATION BASED ON THE GRAVIMETRY METHOD

6.4.3.1 Molecular weight cut-off (MWCO) profiles

Figure 6-7 shows that the solute separation for a particular solute increases when a PES-UF membrane is modified with a PVA layer.

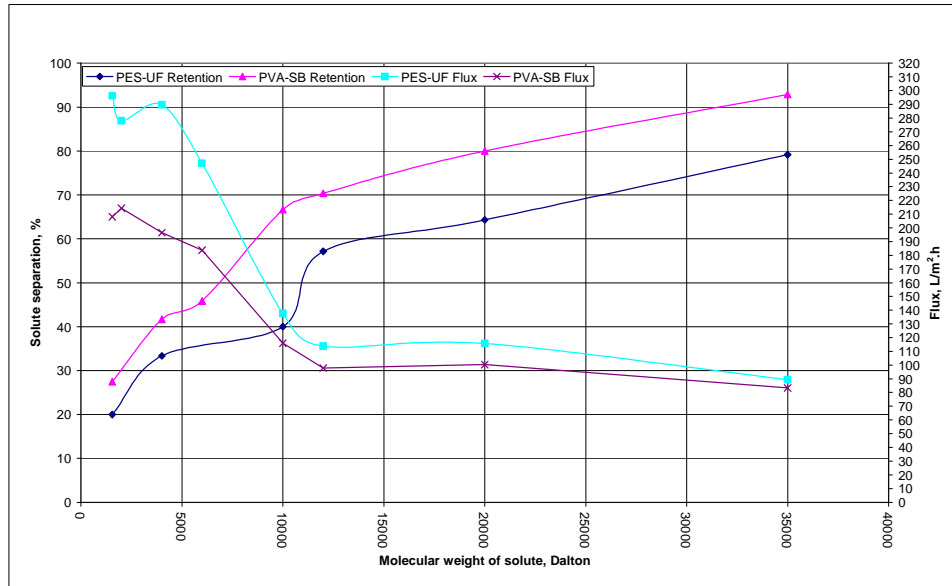


Figure 6-7: Molecular weight cut-off (MWCO) profile of polyethersulfone (PES-UF) and poly(vinyl alcohol)-sodium tetraborate (PVA-SB) membranes using gravimetry method

6.4.3.2 Mean pore size and pore size distribution

Log-normal plots of solute separation versus solute diameter are shown in **Figure 6-8** for PES-UF and PVA-SB membranes. Straight lines fit the data, with a reasonably high correlation coefficient ($R^2 \geq 0.97$). The mean pore size (μ_p) and standard deviation (σ_p) were obtained according to the method described in the Section 6.2 and results are tabulated in **Table 6-2**. The table includes MWCO values: the molecular weight of a solute at which 90% separation can be achieved for a certain membrane. The Stokes diameter of the solute that achieves 90% separation can be obtained from **Figure 6-8**, and the corresponding MWCO can be calculated from equation 6.10.

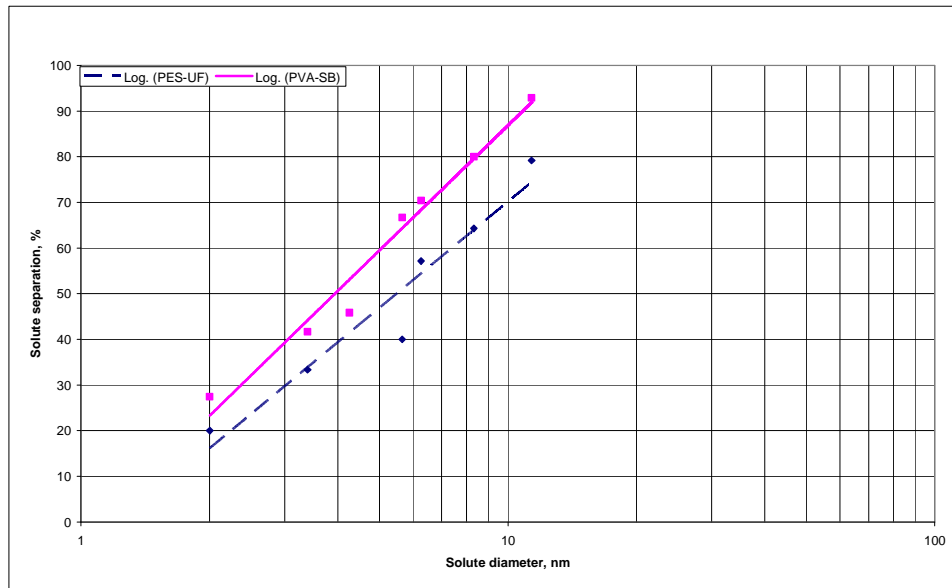


Figure 6-8: Solute separation curve of polyethersulfone (PES-UF) and poly(vinyl alcohol)-sodium tetraborate (PVA-SB) membranes using gravimetry method

The cumulative pore size distributions of the membranes and the probability density function curves are given in **Figure 6-9** and **Figure 6-10**, which were generated from the values of the mean pore size and standard deviation. From **Table 6-2**, it seems that the PVA-SB membrane has a lower mean pore size and standard deviation compared to the PES-UF membrane.

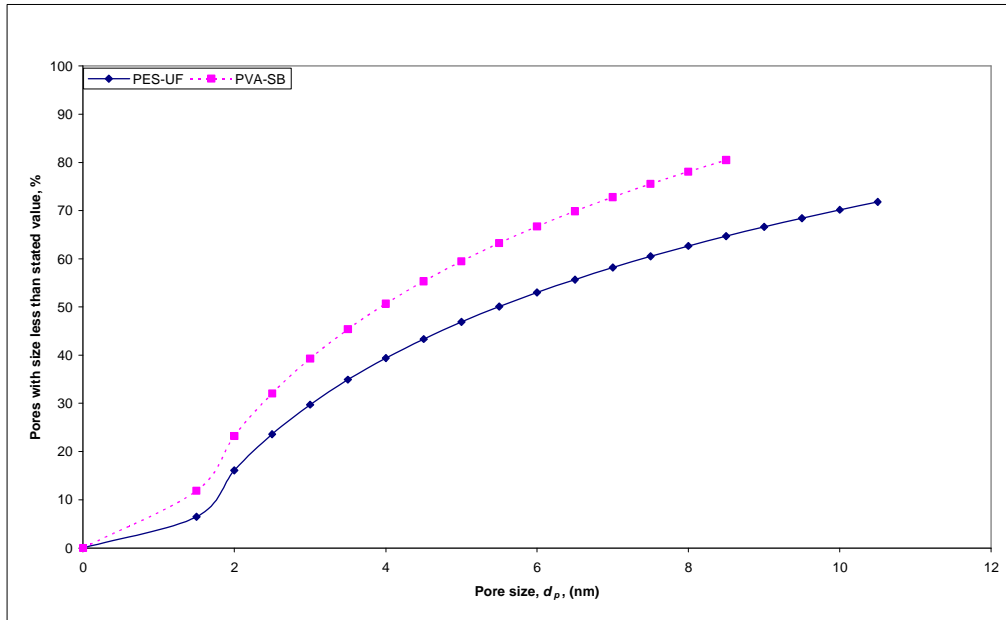


Figure 6-9: Cumulative pore size distribution of polyethersulfone (PES-UF) and poly(vinyl alcohol)-sodium tetraborate (PVA-SB) membranes using gravimetry method

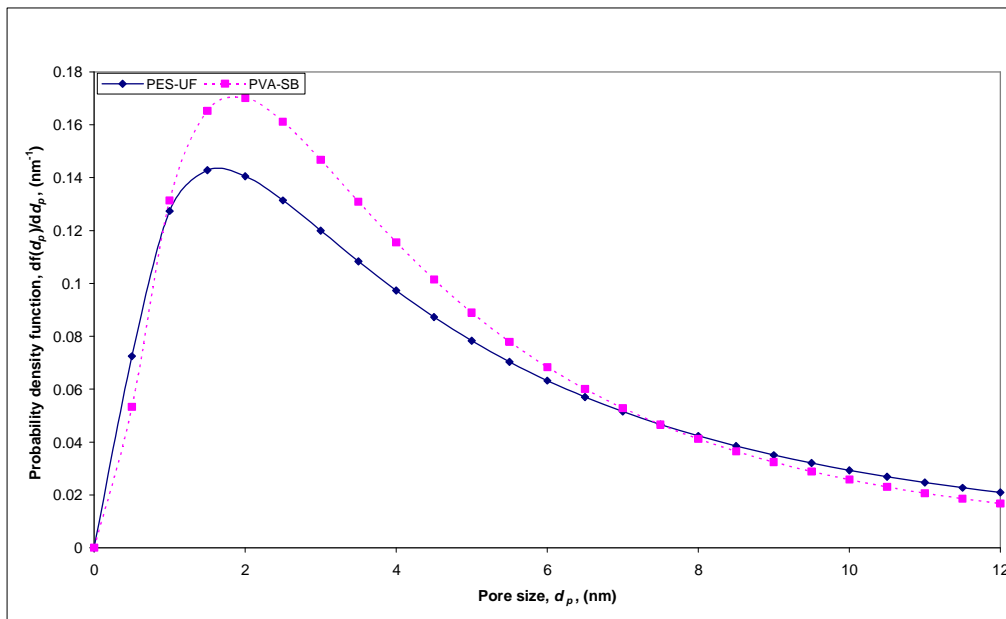


Figure 6-10: Probability density function curve of polyethersulfone (PES-UF) and poly(vinyl alcohol)-sodium tetraborate (PVA-SB) membranes using gravimetry method

Table 6-2: Mean pore size (μ_p), standard deviation (σ_p) and molecular weight cut-off (MWCO) of polyethersulfone (PES-UF) and poly(vinyl alcohol)-sodium tetraborate (PVA-SB) membranes calculated from the solute separation curve using gravimetry method

Membrane	Molecular weight cut-off, MWCO, (Da)	Mean pore size, μ_p , (nm)	Standard deviation, σ_p
PES-UF	80452.01	5.49	2.76
PVA-SB	32043.99	3.93	2.37

6.5 CONCLUSIONS

Membranes were characterized by solute transport using a UV method and a gravimetry method. Comparisons of the results obtained from these two techniques were made. It was found the UV spectrophotometry method is more convenient, sensitive and versatile than the gravimetry method. The log normal distribution was very appropriate for describing the membrane pore size distribution both from UV and gravimetry methods. There was no significant difference between the PES-UF and PVA-SB membranes in terms of their mean pore size and standard deviation as determined using the UV method. Mean pore sizes determined using the gravimetry method were about 4.2 times larger than those calculated from the UV method due to the low concentration of PEG. When the PES-UF membrane was modified to include a PVA layer the mean pore size was reduced but the membrane still had a high flux.

6.6 REFERENCES

- [1] Weatherley, L.R., *Engineering processes for bio-separation*. Butterworth-Heinemann: Northern Ireland. 1994.
- [2] Barth, C., M.C. Goncalves, A.T.N. Pires, J. Roeder, and B.A. Wolf, *Asymmetric polysulfone and polyethersulfone membranes: effects of thermodynamic conditions during formation on their performance*. Journal of Membrane Science, 2003. 169(2): p. 287-299.
- [3] Mulder, M., *Basic principles of membrane technology*, Kluwer Academic: The Netherlands. 1996.
- [4] Nakao, S., *Determination of pore size and pore size distribution. 3. filtration membranes*. Journal of Membrane Science 1994. 96: p. 131-165.
- [5] Singh, S., K.C. Khulbe, T. Matsuura, and P. Ramamurthy, *Membrane characterization by solute transport and atomic force microscopy*. Journal of Membrane Science, 1998. 142: p. 111-127.
- [6] Michaels, A.S., *Analysis and prediction of sieving curves for ultrafiltration membrane: A universal correlation?* Separation Science Technology, 1980. 15: p. 1305-1322.
- [7] Kassotis, J., J. Schmidt, L.T. Hodgins, and H.P. Gregor, *Modelling of the pore size distribution of ultrafiltration membranes*. Journal of Membrane Science, 1985. 22: p. 61-76.
- [8] Aimar, P., M. Meireles, and V. Sanchez, *A contribution to the translation of retention curves into pore size distribution for sieving membranes*. Journal of Membrane Science, 1990. 31: p. 289-305.
- [9] Leyboldt, J., *Determining pore size distributions of ultrafiltration membranes by solute sieving-mathematical limitations*. Journal of Membrane Science, 1987. 31: p. 289-305.
- [10] Zeman, L. and M. Wales, *Steric rejection of polymeric solutes by membranes with uniform pore size distribution*. Separation Science Technology, 1981. 16: p. 275-290.

- [11] Paine, P.L. and P. Scherr, *Drag coefficient for the movement of rigid spheres through liquid-filled cylindrical pores*. Biophysical Journal, 1975. 15 (10): p. 1087-1091.
- [12] Cooper, A.R. and D.S.V. Derveer, *Characterization of ultrafiltration membranes by polymer transport measurement*. Separation Science Technology, 1979. 14: p. 551-556.
- [13] Ishiguro, M., T. Matsuura, and C. Detelie, *A study on the solute separation and the pore size distribution of a montmorillonite membrane*. Separation Science Technology, 1996. 31: p. 545-556.
- [14] Fritzsche, A.K., A.R. Arevalo, A.F. Connolly, M.D. Moore, V. Elings, and C.M. Wu, *The structure and morphology of skin of polyethersulfone ultrafiltration membranes: A comparative atomic force microscope and scanning electron microscope study*. Journal of Applied Polymer Science, 1992. 45: p. 1945-1956.
- [15] Bottino, A., G. Capanneli, A. Grosso, O. Monticelli, O. Cavalleri, R. Rolandi, and R. Soria, *Surface characterization of ceramic membranes by atomic force microscopy*. Journal of Membrane Science, 1994. 95: p. 289-296.
- [16] Platt, S., M. Nyström, A. Bottino, and G. Capanneli, *Stability of NF membranes under extreme acidic conditions*. Journal of Membrane Science, 2004. 239(1): p. 91-103.
- [17] Tram, C.M. and A.Y. Tremblay, *Membrane pore characterization-comparison between single and multicomponent solute probe techniques*. Journal of Membrane Science, 1991. 57(2-3): p. 271-287.
- [18] Hsieh, F.U., T. Matsuura, and S. Sourirajan, *Reverse osmosis separations of polyethylene glycols in dilute aqueous solutions using porous cellulose acetate membranes*. Journal of Applied Polymer Science, 1979. 23: p. 561-573.
- [19] Meireles, M., A. Bessieres, I. Rogissart, P. Aimar, and V. Sanchez, *An appropriate molecular size parameter for porous membranes calibration*. Journal of Membrane Science, 1995. 103: p. 105-115.
- [20] Hsieh, F.H., T. Matsuura, and S. Sourirajan, *Analysis of reverse osmosis data for the system polyethylene glycol-water-cellulose acetate membrane at low operating pressures*. Industrial & Engineering Chemistry Design Process and Development, 1979. 18(3): p. 414-423.
- [21] Bessieres, A., M. Meireles, R. Coratger, J. Beauvillain, and V. Sanchez, *Investigations of surface properties of polymeric membranes by near field microscopy*. Journal of Membrane Science, 1996. 109: p. 271-284.
- [22] Mosqueda-Jimenez, D.B., R.M. Narbaitz, T. Matsuura, G. Chowdhury, G. Pleizer, and J.P. Santerre, *Influence of processing conditions on the properties of ultrafiltration membranes*. Journal of Membrane Science, 2004. 231(1-2): p. 209-224.
- [23] Causserand, C., P. Aimar, C. Vilani, and T. Zambelli, *Study of the effects of defects in ultrafiltration membranes on the water flux and the molecular weight cut-off*, Desalination, 2002. 149: p. 485-491.

Chapter 7

*CONCLUSIONS AND
RECOMMENDATIONS*

7.1 CONCLUSIONS

This study has resulted in an overall appreciation of the many variables pertaining to the formation of thin-film composite (TFC) membranes from poly(vinyl alcohol) (PVA) and polyamide (PA).

1. The first objective was to characterize the polyethersulfone (PES) ultrafiltration (UF) membranes used as support layer and to investigate the effect of heating and drying on the permeability rate of PES-UF membranes. It was found that the drying and heating decreased the pure water permeation (PWP) rate of PES-UF membranes. The heating is the most serious cause of PWP rate decline. Scanning electron microscopy (SEM) observations showed that the surface of the membrane changed and there was a reduction in porosity after drying and heating.
2. The second objective was to fabricate membranes from PVA, using sodium tetraborate (SB) as the cross-linking agent. The effects of numerous fabrication variables such as PVA molecular weight, PVA concentration, SB concentration, cross-linking reaction time, number of coatings, and mode of coating on membrane performance were investigated. The most important findings in this regard were that PVA-SB membranes made by the insolubilization of PVA with SB gave the following typical membrane performance:

Membranes	Flux, L/m ² .h	Retention, %
PVA-SB	431.30	11.46
Test conditions: 2000 ppm MgSO ₄ ; 0.45 MPa; 25°C; 45 – 50 L/h		

3. A composite UF membrane with high flux was prepared from 1.5% PVA solution, draining time 10 min, cross-linked with 0.5% of SB solution at room temperature for 10 min. The stability of the formed PVA layer was validated by water contact angle and FT-IR measurements. The hydrophilicity of the PVA-SB membranes was increased by increasing the PVA concentration in the coating solution and increasing the number of coatings. The effect of the number of coatings was more important than the PVA concentration.
4. The water flux of a PVA-SB membrane remained at 400 L/m².h after the cross-linking process. Due to the covalent cross-linking and the irreversible adsorption, PVA chains could stably exist on the PES-UF membrane surface. All the experiments demonstrated that the cross-linking process was quite promising for the modification of the porous surface of PES-UF membranes.
5. Two amines (m-phenylenediamine (MPD) or 2,6-diaminopyridine (DAP)) and two acid chlorides (trimesoyl chloride (TMC) or 2,5-furanoyl chloride (FC)) were used to create the PA layer by interfacial polymerization (IP) reaction. The deposition of an ultra-thin PA skin on the surface of an insolubilized PVA sub-layer resulted in increased salt retention, but not without adverse effects on the permeate flux. Typical values of the PVA-SB-PA membranes were the following:

PVA-SB-PA membranes	Sodium chloride, NaCl*		Magnesium sulfate, MgSO ₄ **	
	Flux, L/m ² .h	Retention, %	Flux, L/m ² .h	Retention, %
PVA-SB-MPD-TMC	10.93	96.71	-	-
PVA-SB-DAP-TMC	27.91	89.65	-	-
PVA-SB-MPD-FC	49.21	34.22	40.0	60.0
PVA-SB-DAP-FC	25.80	58.54	34.75	75.08
*Test conditions: 2000 ppm NaCl; 2 MPa; 25°C; 45 – 50 L/h				
**Test conditions: 2000 ppm MgSO ₄ ; 1 MPa; 25°C; 45 – 50 L/h				

Membranes prepared with TMC had the highest retentions for 2000 ppm NaCl solution, but the fluxes were low. Therefore, they were suitable for reverse osmosis (RO) membranes, while, the membranes prepared with FC were suitable for brackish water membranes. The PVA-SB-PA membranes have a high retention to divalent salts and could be used in wastewater treatment.

6. The preparation conditions of TFC membranes were modified based on the central composite design (CCD). According to analysis of 2^k factorial designs, main effects of these fabrication parameters were more dominant than their interaction effects with respect to both permeability and retention of membranes over a selected range of operating conditions. DAP concentration, FC concentration, and polymerization time were identified as dominant fabrication parameters which influenced the performance of composite membranes.

The main effects of DAP concentration and polymerization time had the strongest influence on flux and retention, while the main effect of FC concentration appeared to be a dominant factor responsible for retention.

The regression equations between the preparation variables and the performance of the composite membranes were established by response surface methodology (RSM) and can be used for prediction within the limits of factors studied. Additionally, the contour and surface plots are very helpful in visualizing main and interaction effects of the factors.

7. Membranes were characterized by solute transport using an ultraviolet spectrophotometry (UV) method and a gravimetry method. It was found that the UV spectrophotometry method is more convenient, sensitive and versatile than the gravimetry method. The log normal distribution was very appropriate for describing the membrane pore size distribution both from UV and gravimetry methods. There was no significant difference between the PES-UF and PVA-UF membranes in terms of their mean pore size and standard deviation as determined using the UV method. Mean pore sizes determined using the gravimetry method were about 4.2 times larger than those calculated from the UV method due to the low concentration of PEG. When the PES-UF membrane was modified to include a PVA layer the mean pore size was reduced but the membrane still had a good high flux. The MWCO of the surface modified membranes was lower than that of the unmodified membrane. The analysis of solute transport data allowed fine structural details to be proposed and explained concerning the performance versus fabrication and chemistry of PES-UF and PVA-UF membranes.

7.2 RECOMMENDATIONS FOR FUTURE RESEARCH

1. During this study the effects of the degree of hydrolysis of PVA, the temperature of heat treatment, as well as use of an alcohol such as glycerol used for the post-treatment on the RO performance of the membrane have not been investigated. It is therefore necessary to study these variables so that the RO performance of the PVA-SB membranes can be optimized.
2. The reaction of SB and PVA should be further investigated, under the conditions specified with the use of solid state NMR, FT-IR, and viscosity measurements.
3. Mixing the PVA and SB and dynamically applying the mixture to the PES-UF substrate needs to be investigated.

4. Only TMC and FC were used as cross-linking agents. Here the use of other cross-linking agents and, there of mixtures, for example, isophthaloyl chloride, terephthaloyl chloride should still be investigated.
5. PVA / PA membranes should be made by the IP reaction of a mixture of PVA and amine as aqueous solution and cross-linking with FC and compared to those made with or without PVA gel sub-layer.
6. Tolerance and chemical stability tests on membranes should be investigated.
7. It is important to evaluate the resultant membranes on synthetic and real effluents to investigate their performance and fouling characteristics.

APPENDIXES

Appendix A: FOURIER TRANSFORM INFRARED (FT-IR) SPECTRA

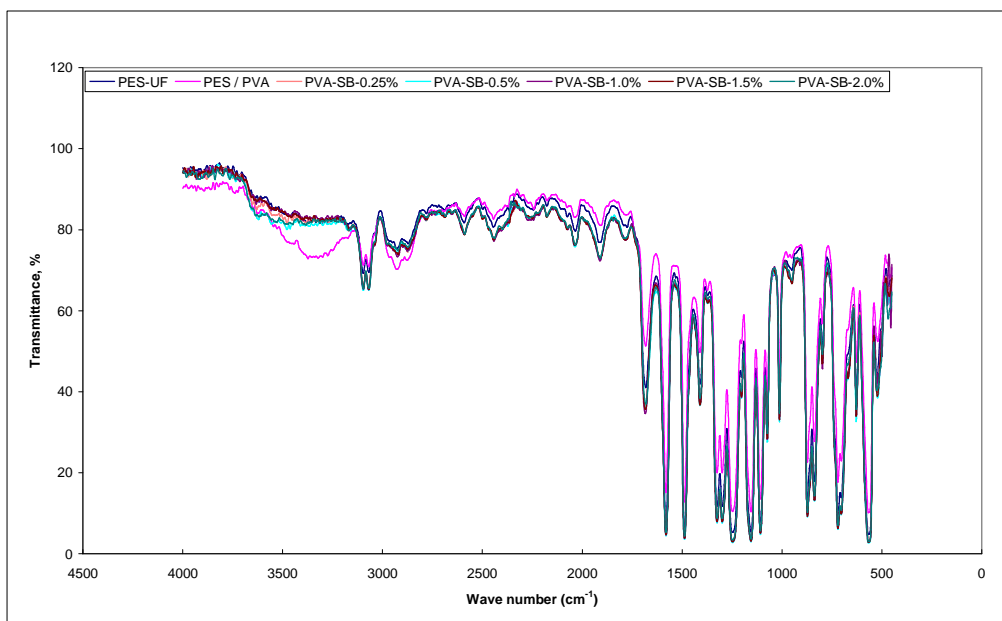


Figure A-1: FT-IR spectra of polyethersulfone (PES-UF), polyethersulfone / poly(vinyl alcohol) (PES / PVA), poly(vinyl alcohol)-sodium tetraborate (PVA-SB) membranes modified with poly(vinyl alcohol) (PVA) of different concentrations

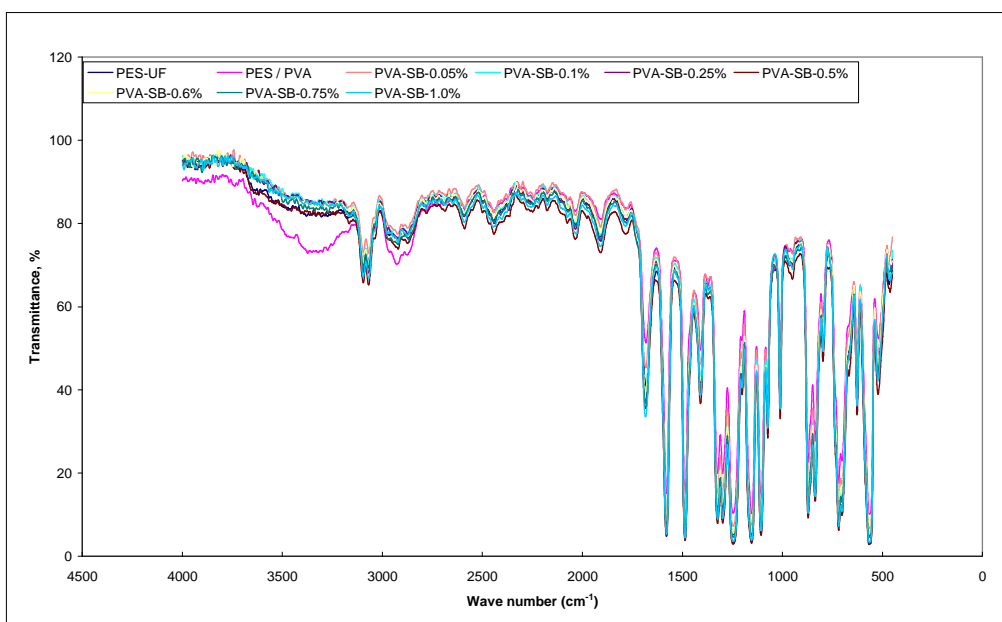


Figure A-2: FT-IR spectra of polyethersulfone (PES-UF), polyethersulfone / poly(vinyl alcohol) (PES / PVA), poly(vinyl alcohol)-sodium tetraborate (PVA-SB) membranes modified with sodium tetraborate (SB) of different concentrations

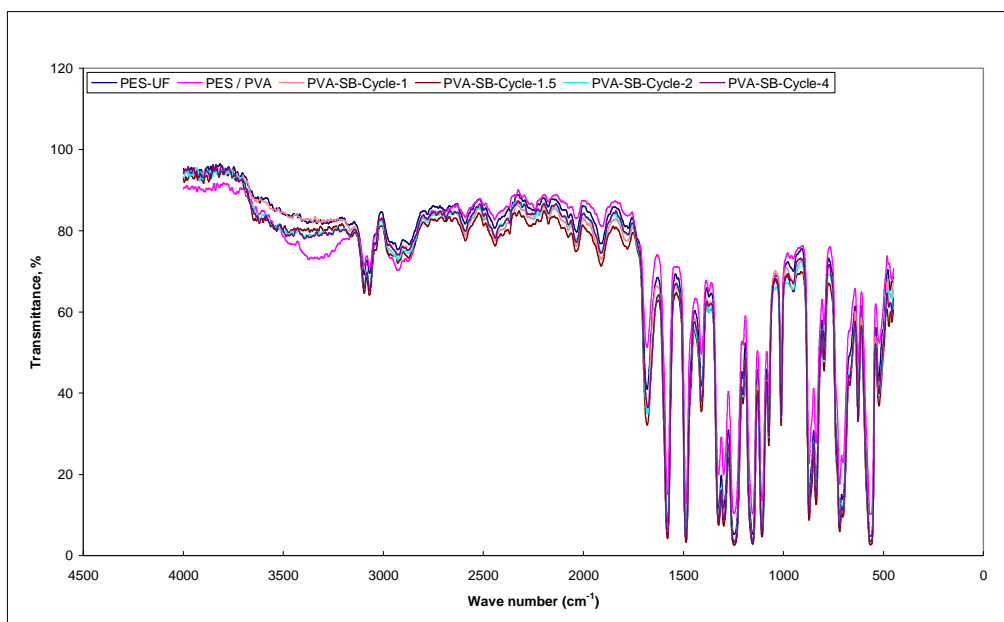


Figure A-3: FT-IR spectra of polyethersulfone (PES-UF), polyethersulfone / poly(vinyl alcohol) (PES / PVA), poly(vinyl alcohol)-sodium tetraborate (PVA-SB) membranes modified with a different number of coatings

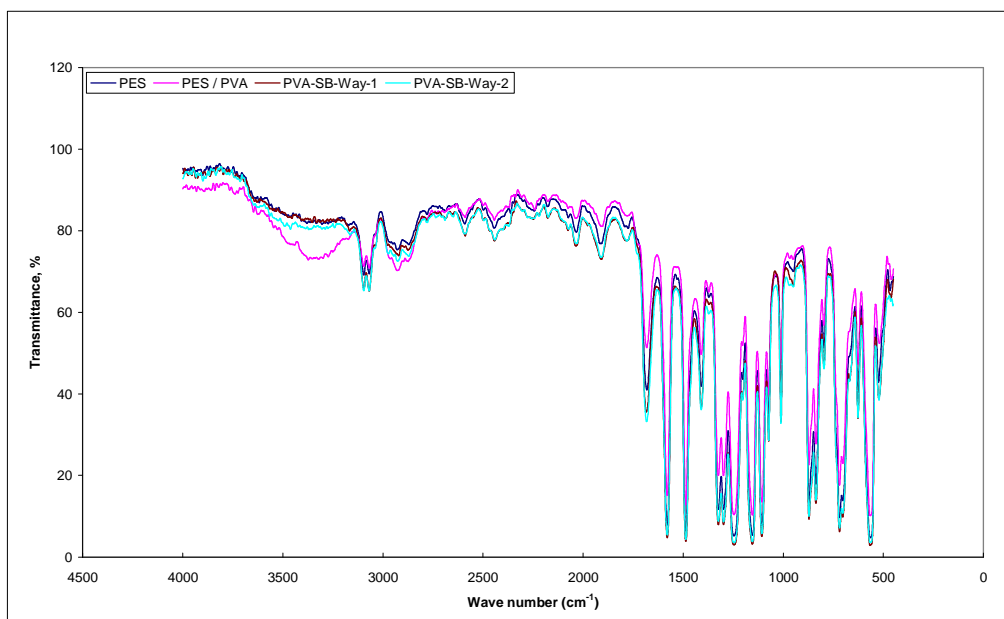


Figure A-4: FT-IR spectra of polyethersulfone (PES-UF), polyethersulfone / poly(vinyl alcohol) (PES / PVA), poly(vinyl alcohol)-sodium tetraborate (PVA-SB) membranes modified with different mode of coating

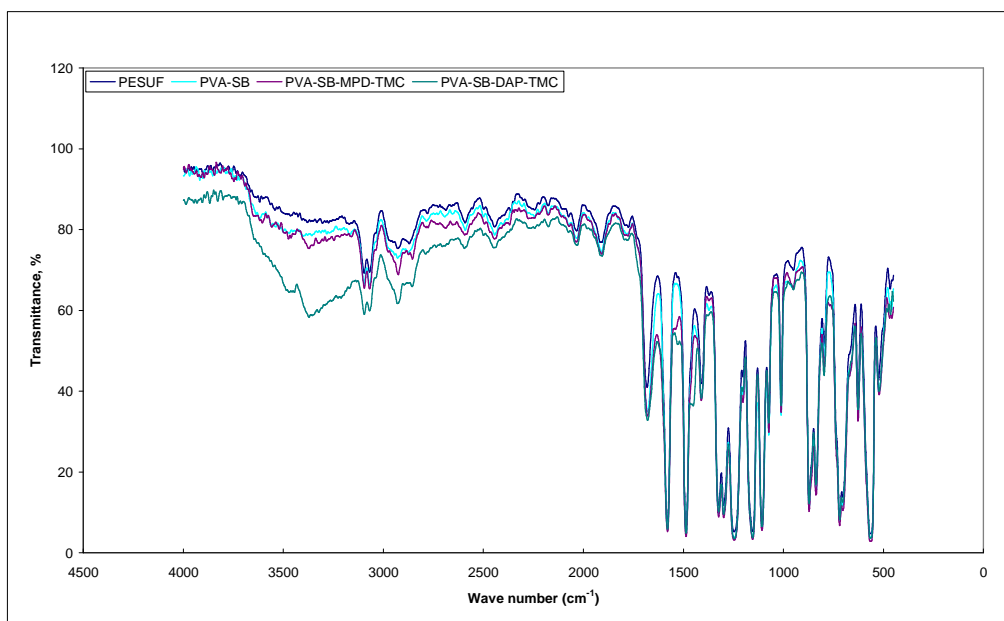


Figure A-5: FT-IR spectra of polyethersulfone (PES-UF), poly(vinyl alcohol)-sodium tetraborate (PVA-SB), poly(vinyl alcohol)-sodium tetraborate-m-phenylene diamine-trimesoyl chloride (PVA-SB-MPD-TMC) and poly(vinyl alcohol)-sodium tetraborate-2,6-diaminopyridine-trimesoyl chloride (PVA-SB-DAP-TMC) membranes

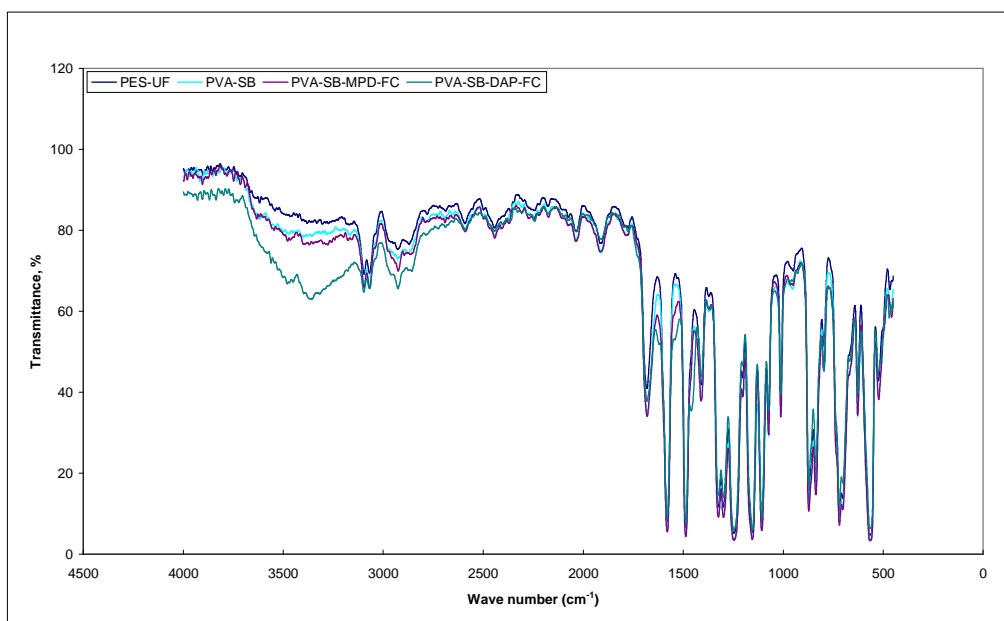
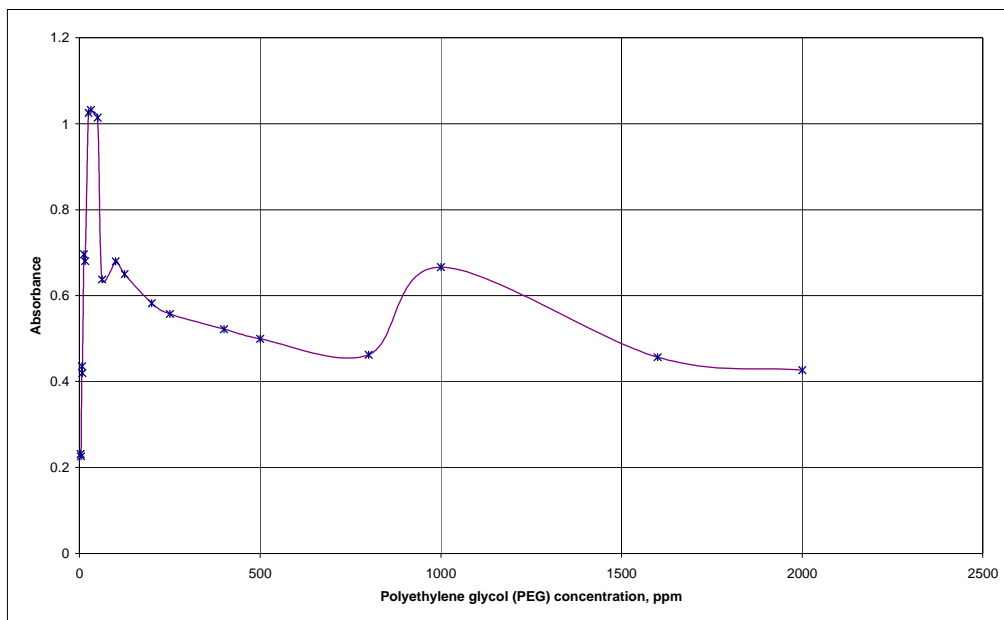
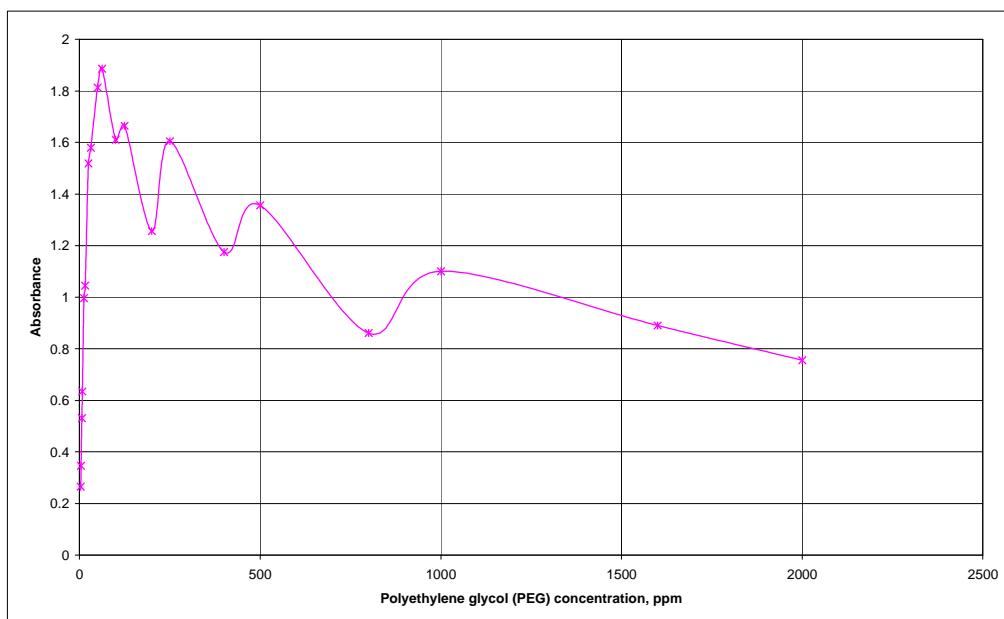


Figure A-6: FT-IR spectra of polyethersulfone (PES-UF), poly(vinyl alcohol)-sodium tetraborate (PVA-SB), poly(vinyl alcohol)-sodium tetraborate-m-phenylene diamine-2,5-furanoyl chloride (PVA-SB-MPD-FC) and poly(vinyl alcohol)-sodium tetraborate-2,6-diaminopyridine-furanoyl chloride (PVA-SB-DAP-FC) membranes

Appendix B: ULTRAVIOLET SPECTRA OF POLYETHYLENE GLYCOL (PEG) OF DIFFERENT MOLECULAR WEIGHTS**Figure B-1: Ultraviolet spectra of polyethylene glycol (PEG-1550)****Figure B-2: Ultraviolet spectra of polyethylene glycol (PEG-2000)**

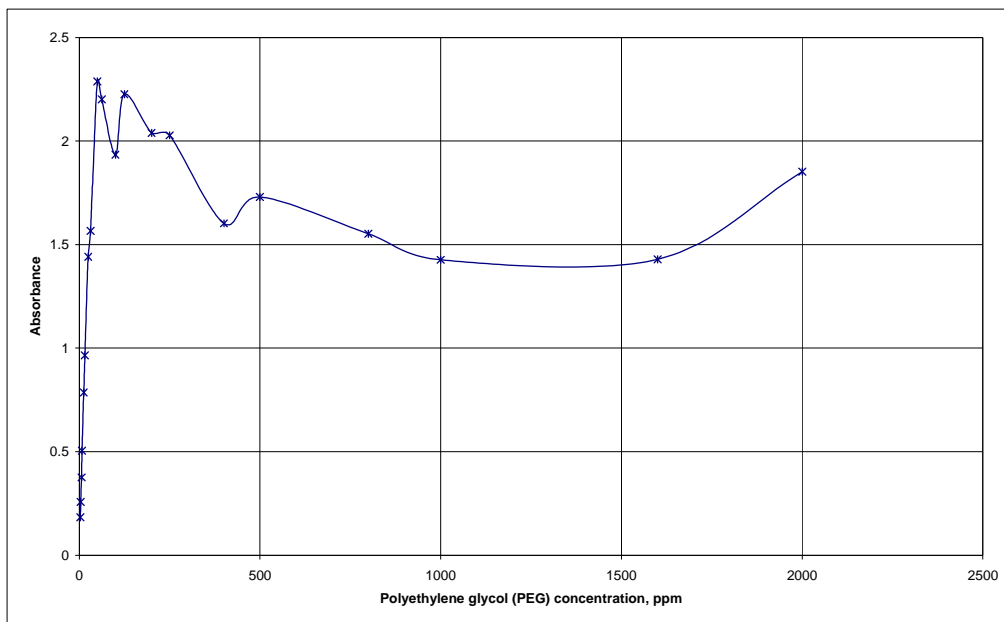


Figure B-3: Ultraviolet spectra of polyethylene glycol (PEG-4000)

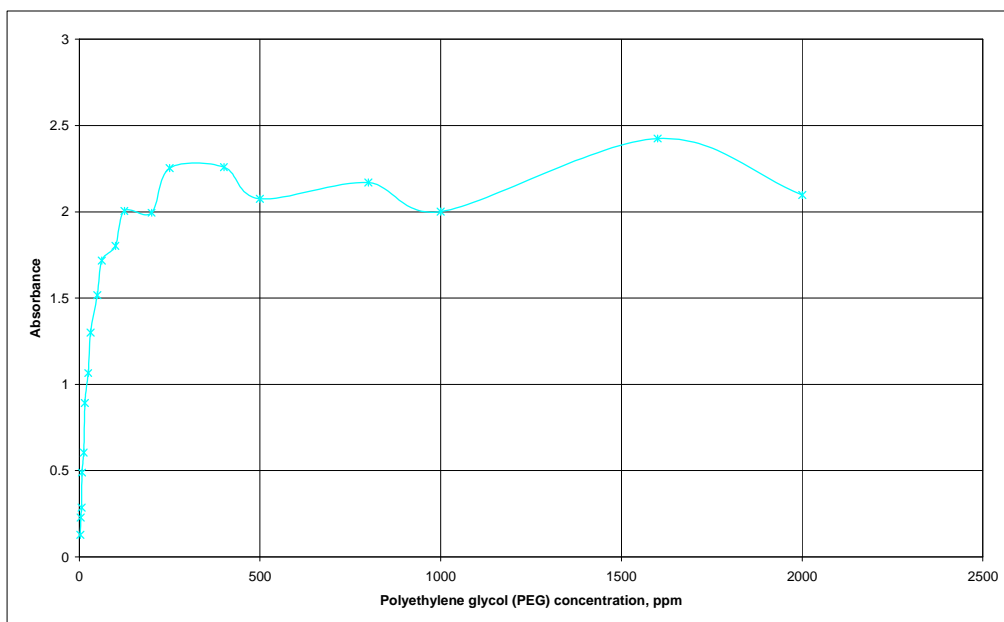


Figure B-4: Ultraviolet spectra of polyethylene glycol (PEG-6000)

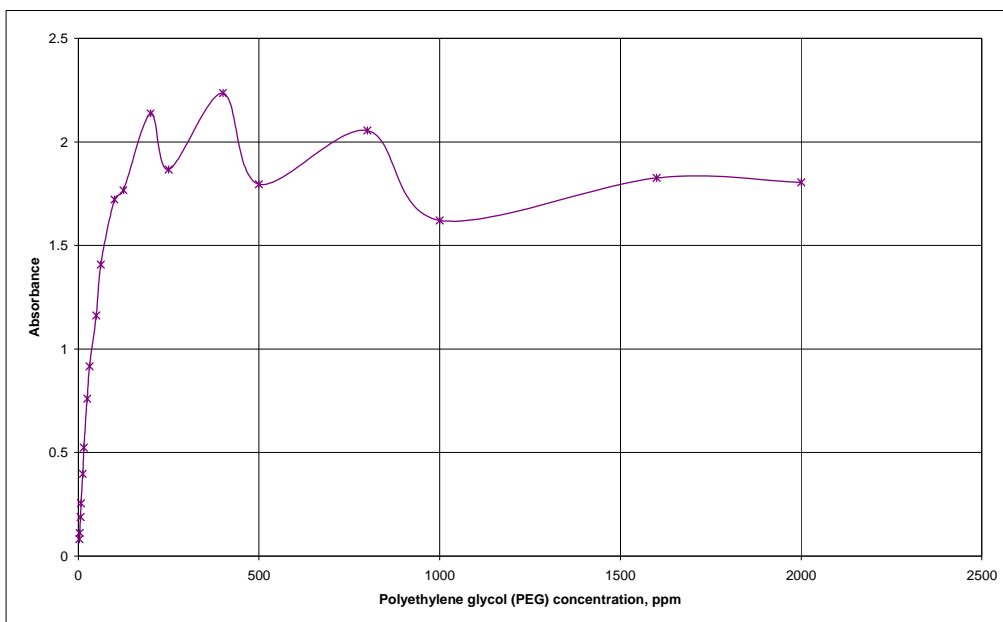


Figure B-5: Ultraviolet spectra of polyethylene glycol (PEG-10000)

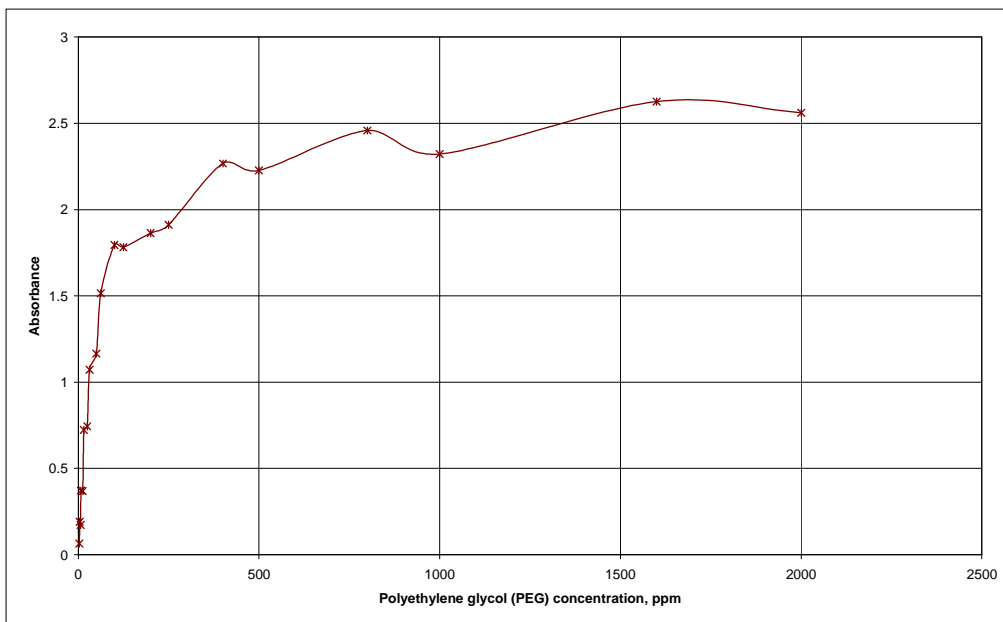


Figure B-6: Ultraviolet spectra of polyethylene glycol (PEG-12000)

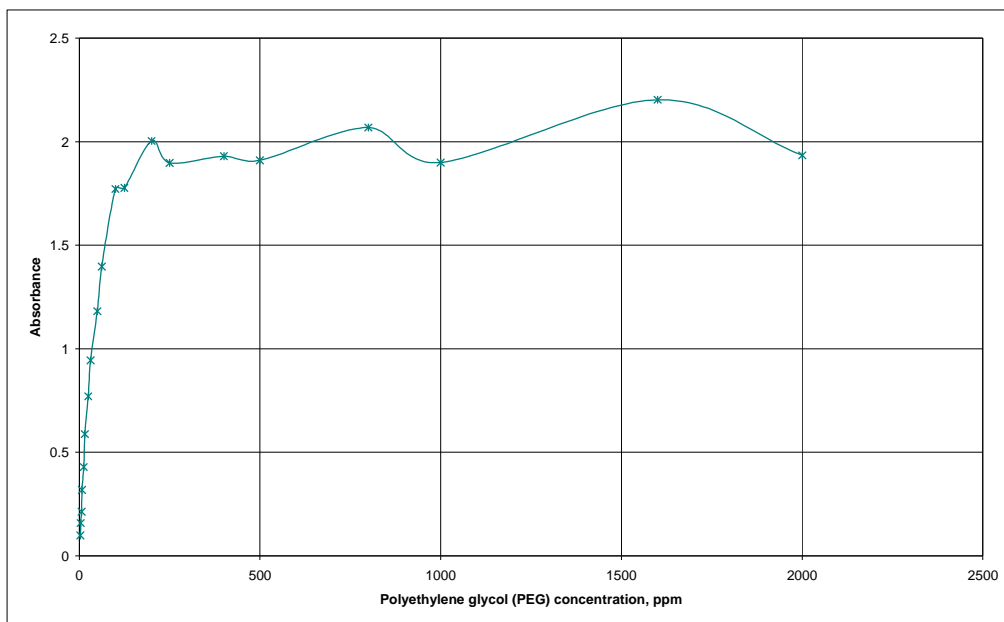


Figure B-7: Ultraviolet spectra of polyethylene glycol (PEG-20000)

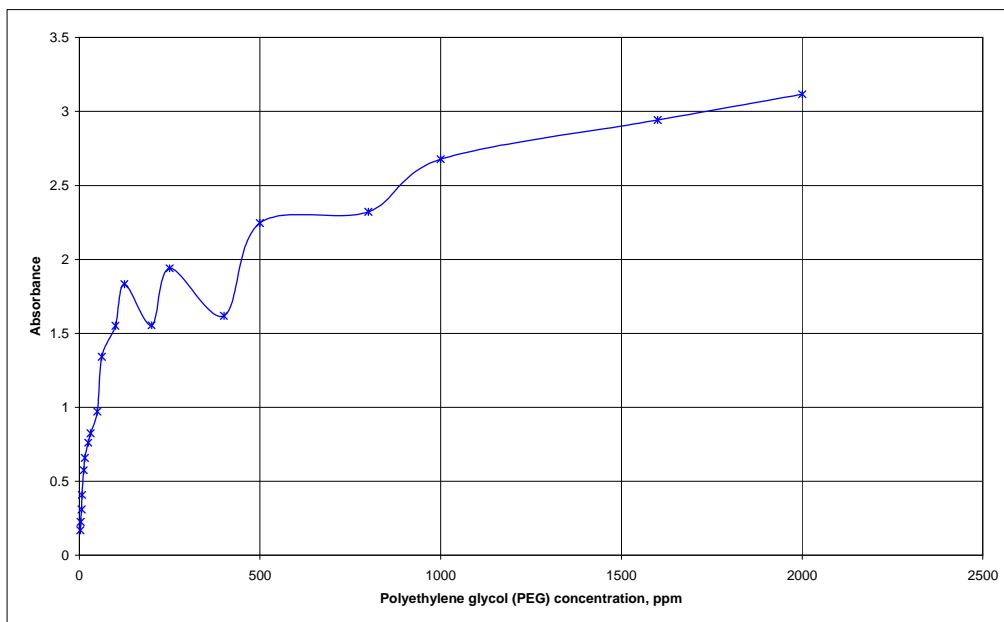


Figure B-8: Ultraviolet spectra of polyethylene glycol (PEG-35000)

Appendix C: CALIBRATION CURVES OF POLYETHYLENE GLYCOL (PEG)

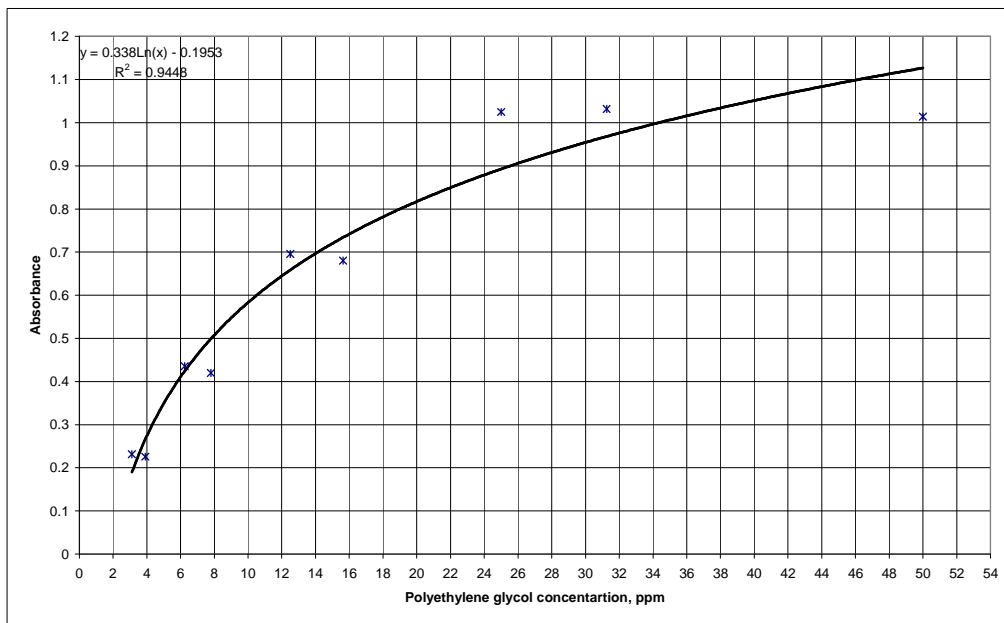


Figure C-1: Calibration curve of polyethylene glycol (PEG-1550)

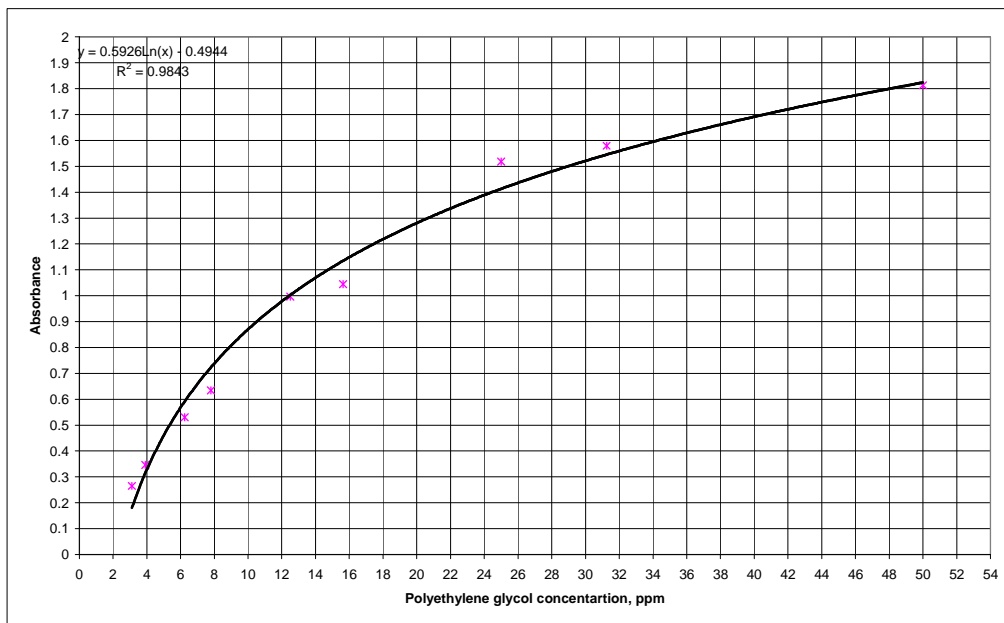


Figure C-2: Calibration curve of polyethylene glycol (PEG-2000)

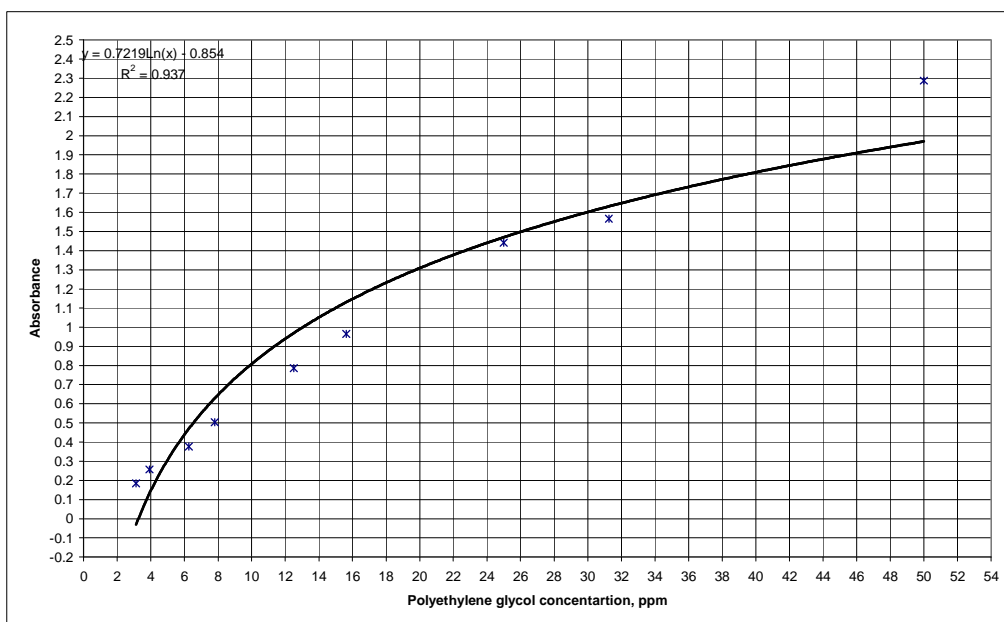


Figure C-3: Calibration curve of polyethylene glycol (PEG-4000)

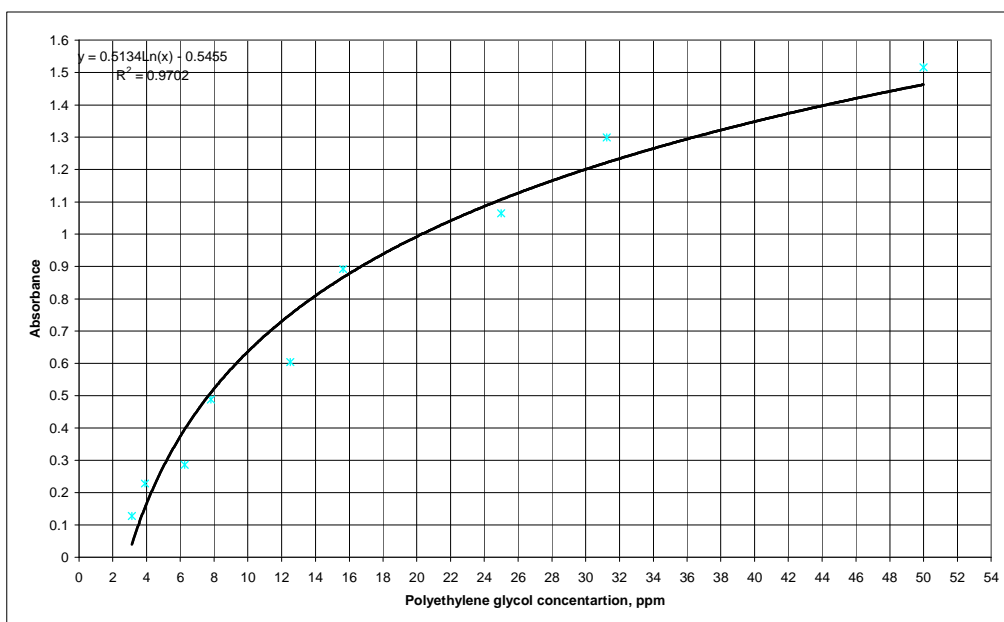


Figure C-4: Calibration curve of polyethylene glycol (PEG-6000)

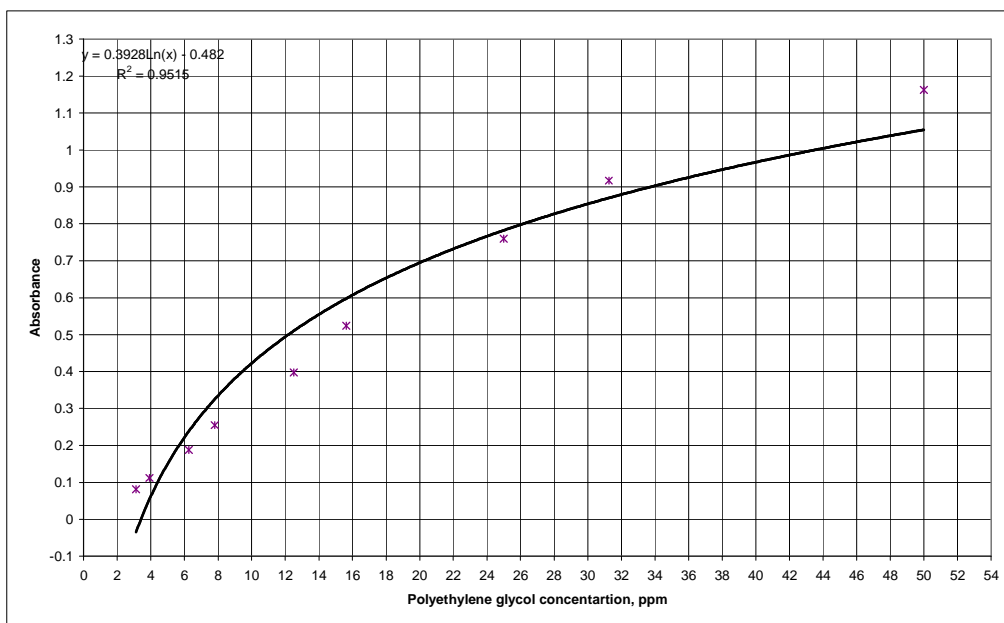


Figure C-5: Calibration curve of polyethylene glycol (PEG-10000)

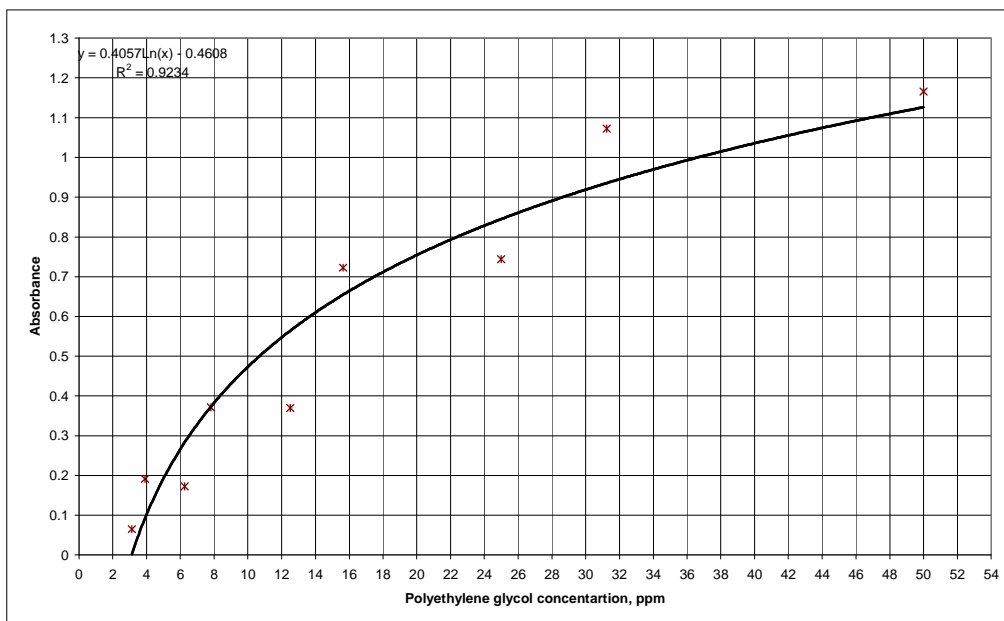


Figure C-6: Calibration curve of polyethylene glycol (PEG-12000)

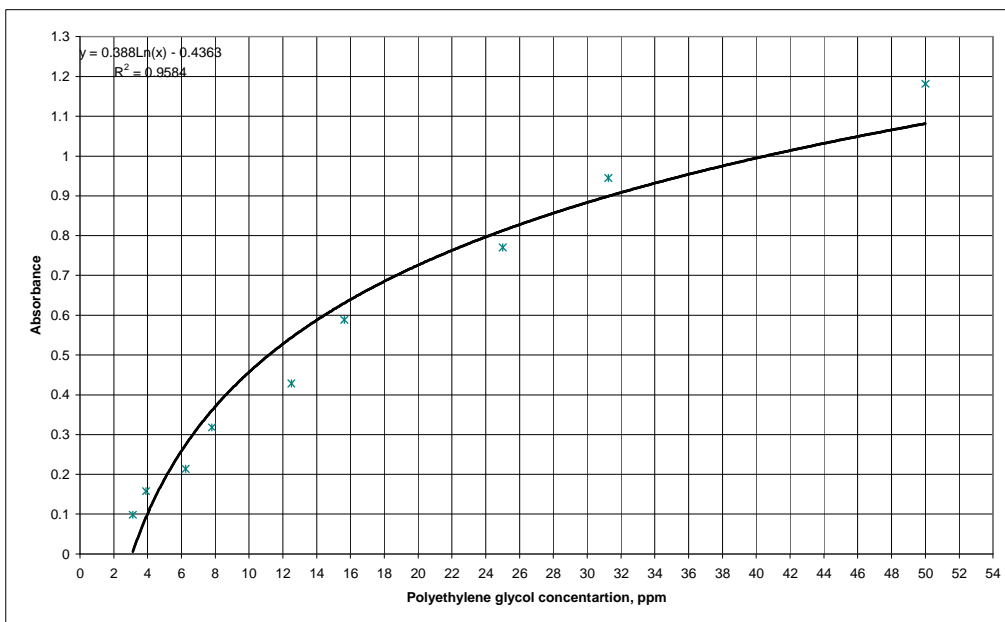


Figure C-7: Calibration curve of polyethylene glycol (PEG-20000)

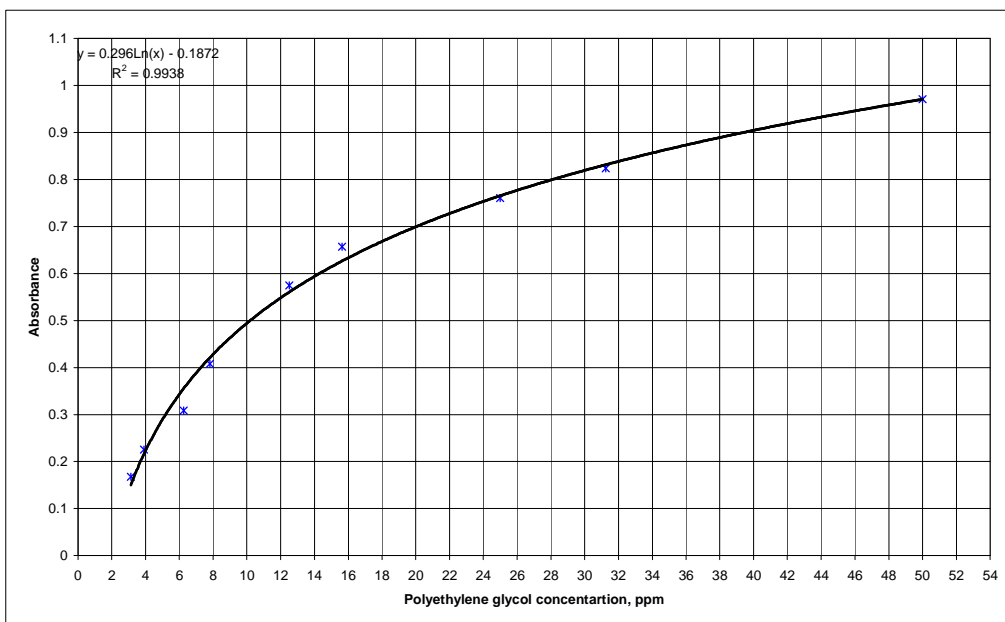


Figure C-8: Calibration curve of polyethylene glycol (PEG-35000)

Appendix D: MEMBRANE MORPHOLOGY

It is important to investigate whether any morphological changes occurred after drying and heating. The scanning electron microscopy (SEM) images of the cross-section of the PES-UF membranes before and after drying and heating at different temperatures are presented in **Figure D-1**. There seemed to be a reduction in the pore and macrovoids sizes though not too distinct for membrane heated at 30°C and 50°C and dried for one hour, as shown in **Figure D-1** (b, c & e) compared to untreated PES-UF membrane. The difference is very much visible for the membranes heated at 80°C or dried for three hours as shown in **Figure D-1** (d & e), where the macrovoids for the membranes heated at 80°C or dried for three hours seem to be narrower and smaller compared to those untreated, dried for one hour and heated at 30°C and 50°C. The results seem to be in line with previous work on a PES-UF membrane where heating implies a reduction in porosity due to heat treatment. The results are also in line with work done by Barzin et al. [1], where the finger like structure of PES hollow fiber membrane becomes narrower after being heated at 150°C, compared to membrane without heating.

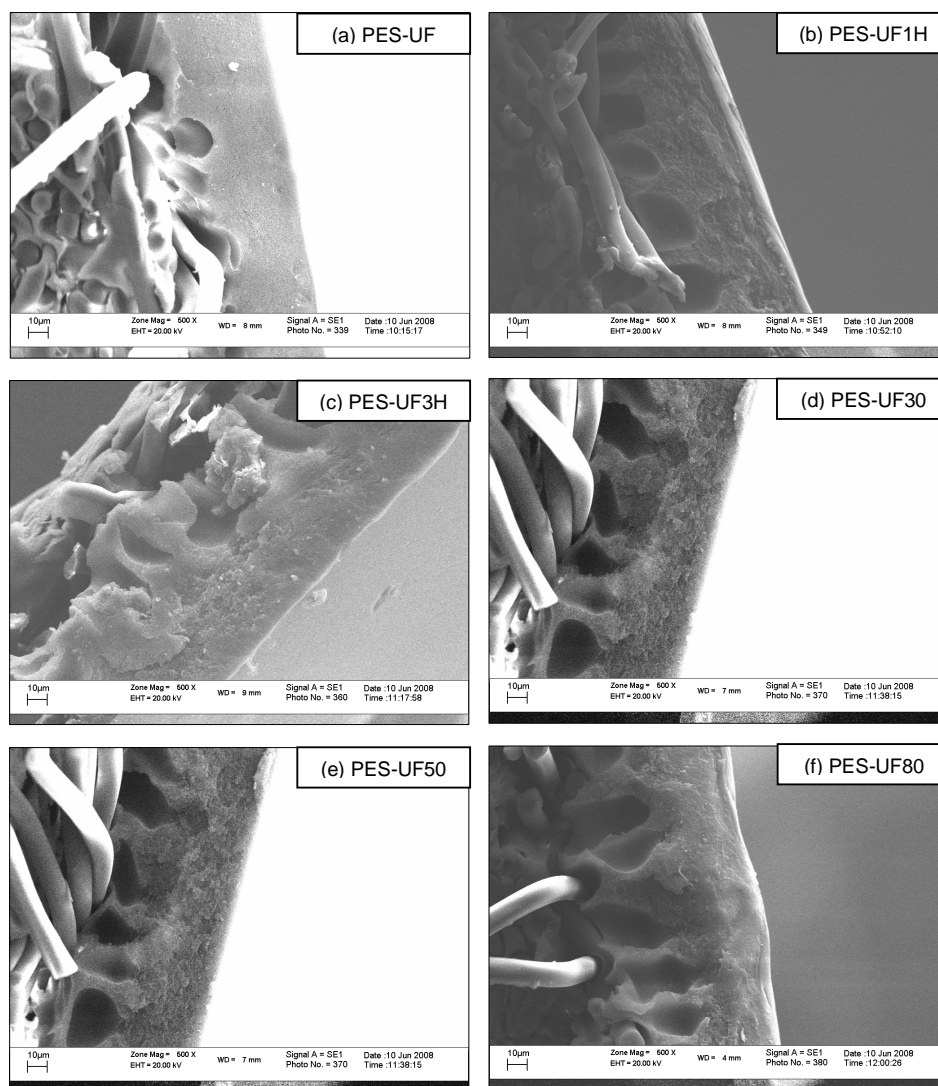


Figure D-1: Scanning electron microscopy (SEM) images of cross-section of polyethersulfone (PES-UF) membrane before and after drying and heating

Further analysis was performed by investigating the surface of the membrane for changes after heating at different temperatures. **Figure D-2** shows the SEM images of membrane surfaces. It is clearly observed that the surface of the membrane changed with different heating temperatures and different drying periods at room temperature. Previous work by researchers indicated that the membrane surface of PES hollow fiber membrane containing PVP-10000 as additive becomes rougher with increased heating temperature from 180 to 210°C.

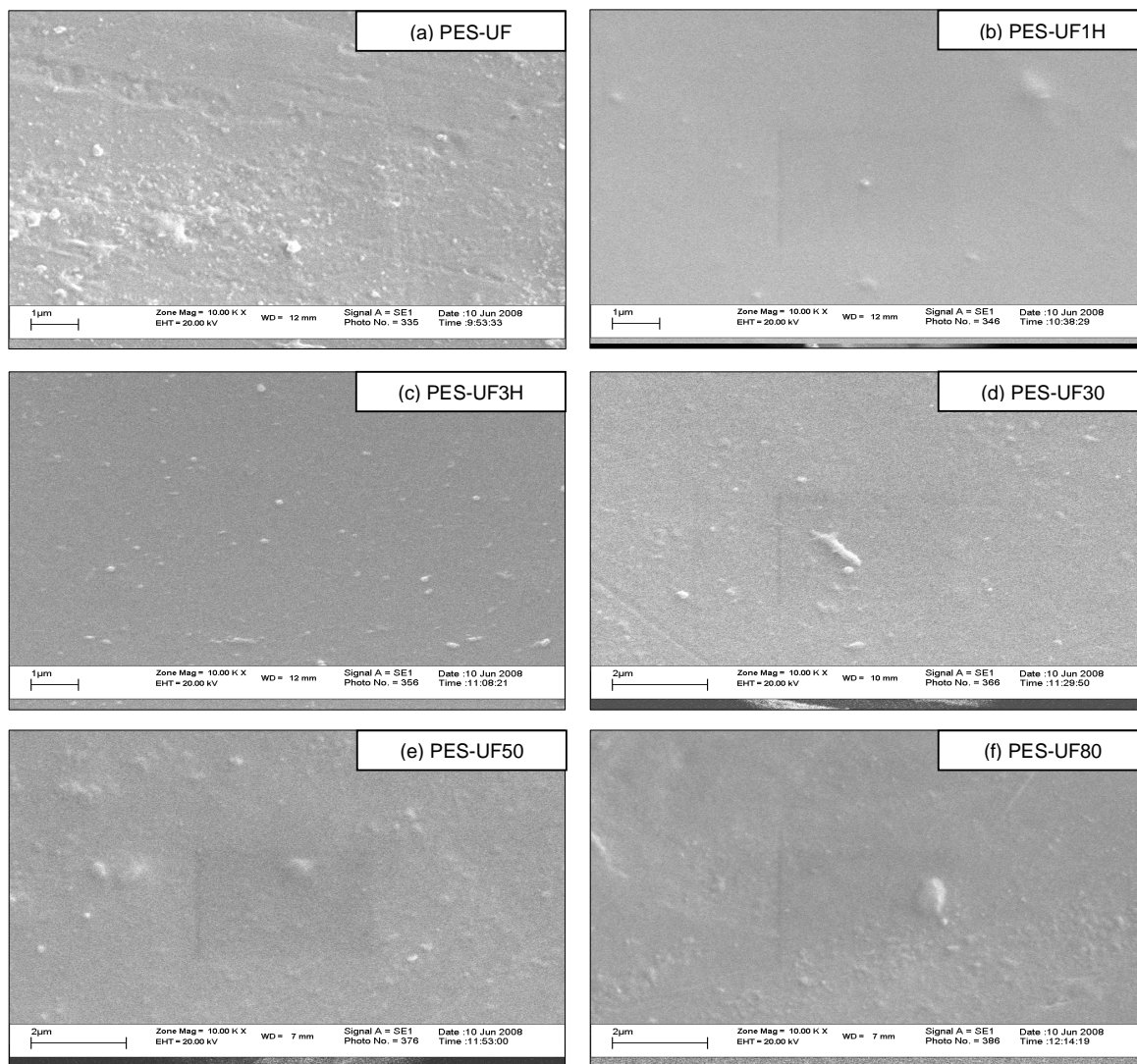
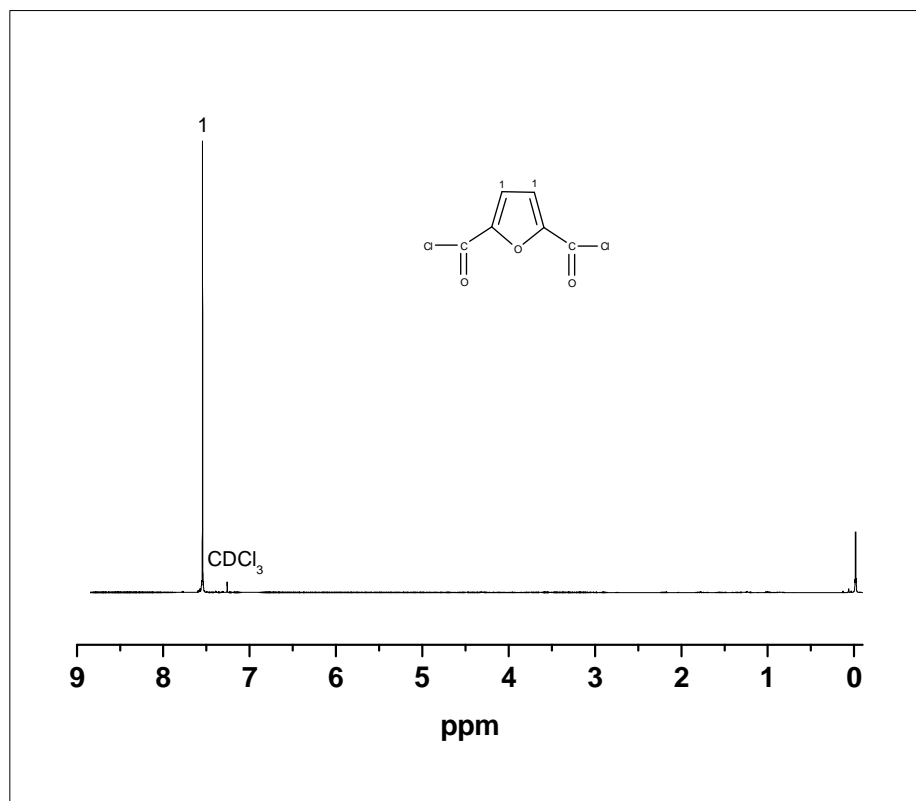
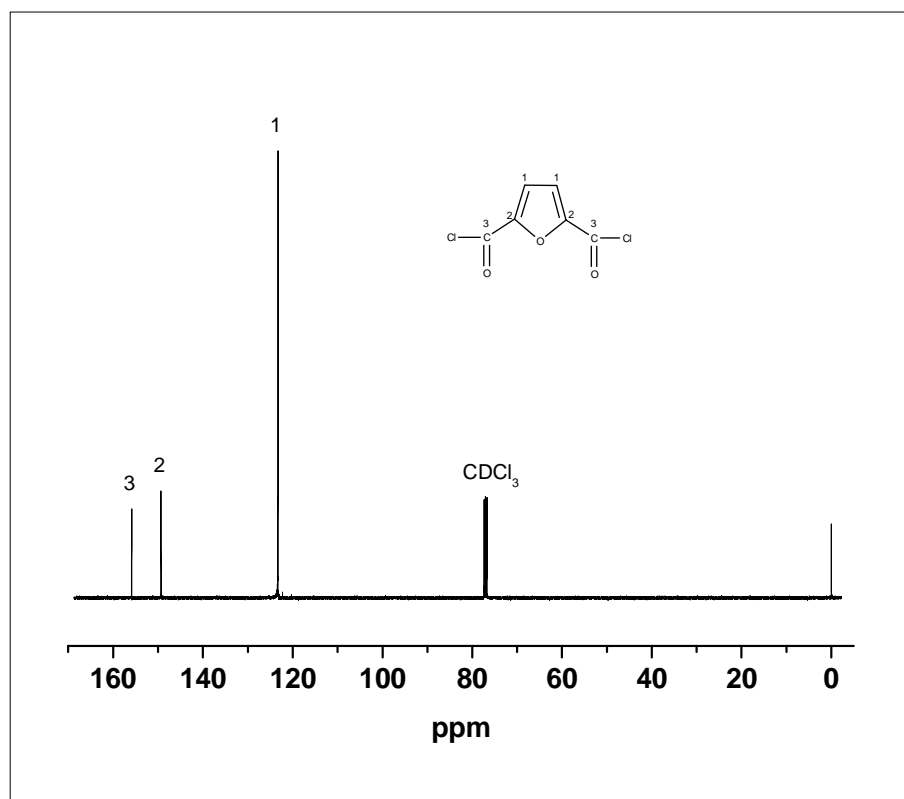


Figure D-2: Scanning electron microscopy (SEM) images of the surface of a polyethersulfone (PES-UF) membrane before and after drying and heating

[1] Barzin, J., C. Feng, K. C. Khulbe, T. Matsuura, S. S. Madeni, and H. Mirzadeh, *Characterization of Polyethersulfone Homodialysis Membrane by Ultrafiltration and Atomic Force Microscopy*, *Journal of Membrane Science*, 2004, 237: P. 77–85.

Appendix E: UNCLER MAGNETIC RESONANCE (NMR) SPECTRA

Figure E-1: ^1H NMR spectrum of 2,5-furanyl chloride in CDCl_3 Figure E-2: ^{13}C NMR spectrum of 2,5-furanyl chloride in CDCl_3